



Bacterial quorum sensing chemistry : From acyl homoserine lactone analogs in *Vibrio fischeri* to carbohydrate phosphodiester in *Agrobacterium*

Qiang Zhang

► To cite this version:

Qiang Zhang. Bacterial quorum sensing chemistry : From acyl homoserine lactone analogs in *Vibrio fischeri* to carbohydrate phosphodiester in *Agrobacterium*. Agricultural sciences. Université de Lyon, 2021. English. NNT : 2021LYSEI015 . tel-03219205

HAL Id: tel-03219205

<https://theses.hal.science/tel-03219205>

Submitted on 6 May 2021

HAL is a multi-disciplinary open access archive for the deposit and dissemination of scientific research documents, whether they are published or not. The documents may come from teaching and research institutions in France or abroad, or from public or private research centers.

L'archive ouverte pluridisciplinaire **HAL**, est destinée au dépôt et à la diffusion de documents scientifiques de niveau recherche, publiés ou non, émanant des établissements d'enseignement et de recherche français ou étrangers, des laboratoires publics ou privés.



N°d'ordre NNT : 2021LYSEI015

THESE de DOCTORAT DE L'UNIVERSITE DE LYON

opérée au sein de
(L'INSA LYON)

**Ecole Doctorale N° ED206
(Ecole Doctorale de Chimie de Lyon)**

Spécialité de doctorat : Chimie

Soutenue publiquement le 23/02/2021, par :
(Qiang ZHANG)

Chimie du quorum sensing bactérien: des analogues d'acyl homosérine lactones chez *Vibrio fischeri* aux phosphodiesteres de carbohydrates chez *Agrobacterium*.

Bacterial quorum sensing chemistry: from acyl homoserine lactone analogs in *Vibrio fischeri* to carbohydrate phosphodiesteres in *Agrobacterium*.

Devant le jury composé de :

Mme Florence Djedaini-Pilard, Professeure, Université de Picardie
M. Yves Blache, Professeur, Université de Toulon
Mme Florence Popowycz, Professeure, INSA de Lyon
M. Sébastien Fort, DR CNRS, Université de Grenoble Alpes
M. Yves Queneau, DR CNRS, Université de Lyon
M. Laurent Soullère, Maître de conférence HDR, INSA de Lyon
M. Mohammed Ahmar, CR CNRS, Université de Lyon

Rapporteure
Rapporteur
Examinatrice
Examineur
Directeur de thèse
Co-directeur de thèse
Membre Invité

Département FEDORA – INSA Lyon - Ecoles Doctorales – Quinquennal 2016-2020

SIGLE	ECOLE DOCTORALE	NOM ET COORDONNEES DU RESPONSABLE
CHIMIE	CHIMIE DE LYON http://www.edchimie-lyon.fr Sec. : Renée EL MELHEM Bât. Blaise PASCAL, 3e étage secretariat@edchimie-lyon.fr INSA : R. GOURDON	M. Stéphane DANIELE Institut de recherches sur la catalyse et l'environnement de Lyon IRCELYON-UMR 5256 Équipe CDFA 2 Avenue Albert EINSTEIN 69 626 Villeurbanne CEDEX directeur@edchimie-lyon.fr
E.E.A.	ÉLECTRONIQUE, ÉLECTROTECHNIQUE, AUTOMATIQUE http://edeea.ec-lyon.fr Sec. : M.C. HAVGOUDOUKIAN ecole-doctorale.eea@ec-lyon.fr	M. Gérard SCORLETTI École Centrale de Lyon 36 Avenue Guy DE COLLONGUE 69 134 Écully Tél : 04.72.18.60.97 Fax 04.78.43.37.17 gerard.scorletti@ec-lyon.fr
E2M2	ÉVOLUTION, ÉCOSYSTÈME, MICROBIOLOGIE, MODÉLISATION http://e2m2.universite-lyon.fr Sec. : Sylvie ROBERJOT Bât. Atrium, UCB Lyon 1 Tél : 04.72.44.83.62 INSA : H. CHARLES secretariat.e2m2@univ-lyon1.fr	M. Philippe NORMAND UMR 5557 Lab. d'Ecologie Microbienne Université Claude Bernard Lyon 1 Bâtiment Mendel 43, boulevard du 11 Novembre 1918 69 622 Villeurbanne CEDEX philippe.normand@univ-lyon1.fr
EDISS	INTERDISCIPLINAIRE SCIENCES-SANTÉ http://www.ediss-lyon.fr Sec. : Sylvie ROBERJOT Bât. Atrium, UCB Lyon 1 Tél : 04.72.44.83.62 INSA : M. LAGARDE secretariat.ediss@univ-lyon1.fr	Mme Sylvie RICARD-BLUM Institut de Chimie et Biochimie Moléculaires et Supramoléculaires (ICBMS) - UMR 5246 CNRS - Université Lyon 1 Bâtiment Curien - 3ème étage Nord 43 Boulevard du 11 novembre 1918 69622 Villeurbanne Cedex Tel : +33(0)4 72 44 82 32 sylvie.ricard-blum@univ-lyon1.fr
INFOMATHS	INFORMATIQUE ET MATHÉMATIQUES http://edinfomaths.universite-lyon.fr Sec. : Renée EL MELHEM Bât. Blaise PASCAL, 3e étage Tél : 04.72.43.80.46 infomaths@univ-lyon1.fr	M. Hamamache KHEDDOUCI Bât. Nautibus 43, Boulevard du 11 novembre 1918 69 622 Villeurbanne Cedex France Tel : 04.72.44.83.69 hamamache.kheddouci@univ-lyon1.fr
Matériaux	MATÉRIAUX DE LYON http://ed34.universite-lyon.fr Sec. : Stéphanie CAUVIN Tél : 04.72.43.71.70 Bât. Direction ed.materiaux@insa-lyon.fr	M. Jean-Yves BUFFIÈRE INSA de Lyon MATEIS - Bât. Saint-Exupéry 7 Avenue Jean CAPELLE 69 621 Villeurbanne CEDEX Tél : 04.72.43.71.70 Fax : 04.72.43.85.28 jean-yves.buffiere@insa-lyon.fr
MEGA	MÉCANIQUE, ÉNERGÉTIQUE, GÉNIE CIVIL, ACOUSTIQUE http://edmega.universite-lyon.fr Sec. : Stéphanie CAUVIN Tél : 04.72.43.71.70 Bât. Direction mega@insa-lyon.fr	M. Jocelyn BONJOUR INSA de Lyon Laboratoire CETHIL Bâtiment Sadi-Carnot 9, rue de la Physique 69 621 Villeurbanne CEDEX jocelyn.bonjour@insa-lyon.fr
ScSo	ScSo* http://ed483.univ-lyon2.fr Sec. : Véronique GUICHARD INSA : J.Y. TOUSSAINT Tél : 04.78.69.72.76 veronique.cervantes@univ-lyon2.fr	M. Christian MONTES Université Lyon 2 86 Rue Pasteur 69 365 Lyon CEDEX 07 christian.montes@univ-lyon2.fr

Acknowledgement

Being curious about scientific research, I chose to be a PhD student four years ago. Time flies quickly, and I will complete my PhD research soon to reach an important stage.

First of all, I would like to appreciate my supervisor, Prof. Yves Queneau, for a lot of support when I have been studying for my PhD. Under the serious and considerate guidance of my supervisors, I can complete my scientific research. My supervisors have a very deep theoretical foundation, so I always get useful and technical advice when I am confused about scientific problems. Looking at the past 42 months, I improved a lot, either the scientific skills or the English level.

Secondly, I would like to thank my co-supervisor, Dr. Laurent Soullère, who is very friendly and helpful. My co-supervisor always encourages me to do better than before. He gave many detailed instructions about the experiments, paper writing. Also, he is very knowledgeable and patient. I learned a lot from him.

Thirdly, I would like to give my appreciation to Dr. Ahmar Mohammed who gave me encouragement in my study and daily life. When I encountered any small difficulties in my life, he is always glad to help me. I remember I once had my severe toothache at one time, then he told me that I had to go to the emergency room. Thanks to his nice reminder, I recovered soon.

Finally, I would like to give my acknowledgment to all my colleagues in the group COB and the lab ICBMS. Thanks to Prof. Florence Popowycz, Dr. Sylvie Moebs-sanchez, Dr. Maïwenn Jacolot, Dr. Stéphane Chambert and Mrs. Lucie Grand. They are so friendly that I could adapt to the new environment soon. I would like to thank Dr. Anne Baudouin, Dr. Elodie Fromentin for help with NMR and MS analyses. I also thank the China Scholarship Council (CSC) for a scholarship to study abroad.

Abbreviations

Ac	Acetyl
A2P	Arabinose-2-phosphate
Acc	Agrocinopine catabolism operon
AccR	Agrocinopine catabolic regulator
AHL	Acyl homoserine lactones
AI	Autoinducer
BHL	Butyl-L-homoserine lactone
Bn	Benzyl
Boc	<i>tert</i> -Butyloxycarbonyl
Bz	Benzoyl
CAN	Ammonium cerium nitrate
COSY	Correlation spectroscopy
DBH	1,3-Dibromo-5,5-dimethylhydantoin
DBU	1,8-Diazabicyclo[5.4.0]undec-7-ene
DCC	<i>N,N'</i> -Dicyclohexylcarbodiimide
DCM	Dichloromethane
DEPC	Diethyl phosphorocyanidate
DIPEA (DIEA)	Diisopropylethylamine
DIPA	Diisopropylamine
DMAP	4-Dimethylaminopyridine
DMF	Dimethylformamide
DMP	Dimethoxypropane
DMSO	Dimethyl sulfoxide
DPD	Dihydroxypentanedione
EC ₅₀	The half-maximal effective concentration
EDC	1-(3-Dimethylaminopropyl)-3-ethyl carbodiimide
G1P	Glucose-1-phosphates

G2P	Glucose-2-phosphates
G6P	Glucose-6-phosphates
G2LP	Glucose-2-phosphate lactic acid ester
GCP	Glucose-1,2-phosphates
GFP	Green fluorescent protein
HMBC	Heteronuclear multiple-bond correlation
HMPA	Hexamethylphosphoramide
HSL	Homoserine lactone
HSQC	Heteronuclear single-quantum correlation spectroscopy
IC ₅₀	The half-maximal inhibitory concentration
LDA	Lithium diisopropylamide
LiHMDS	Lithium bis(trimethylsilyl)amide
MSNT	1-Methylenesulfonic acid (3-nitro-1,2,4-triazolide)
NMR	Nuclear magnetic resonance
OdDHL	3-oxo-dodecanoyl-L-homoserine lactone
OHHL	3-oxo-hexanoyl-L-homoserine lactone
QS	Quorum sensing
SAM	S-Adenosylmethionine
TBS	<i>tert</i> -Butyldimethylsilyl
TBAF	<i>tert</i> -n-Butylammonium fluoride
TBABr	<i>tert</i> -n-Butylammonium bromide
TFA	Trifluoroacetic acid
THF	Tetrahydrofuran
Ti	Tumor inducing
TIBAL	Triisobutylaluminium
TLC	Thin layer chromatography
<i>p</i> -TsOH	<i>p</i> -Toluenesulfuric acid

Abstract

The process used by bacteria to coordinate their behavior as a function of their population density, by communicating through small chemical signals (synthesis and sensing), is known as bacterial quorum sensing. This pathway exists in many bacteria, including pathogenic ones. Quorum sensing regulates various gene expressions, including growth, virulence and toxin production. Therefore, the inhibition of quorum sensing is regarded as a promising strategy for preventing bacterial infection. Considering the necessity to diversify antibacterial strategies for facing the issue of antibiotic resistance of bacteria, targeting the QS can propose a complementary approach to existing biological pathways. Focusing on the chemistry of bacterial quorum sensing, this thesis has investigated two different aspects. On one hand, looking for novel QS signals mimics, we discovered new analogs of acyl homoserine lactones (AHLs), able to modulate quorum sensing in Gram-negative bacteria such as *Vibrio fischeri*. On the other hand, studying carbohydrate phosphodiesterases involved in the pathogenicity of *Agrobacterium fabrum* C58, we developed an efficient method to synthesize a natural agrocinopine as well as some analogs.

In the first part, we designed and synthesized novel AHLs analogues including hydrazide, carbamate or thiocarbamate functions, as well as 2-OH AHLs and other analogues based on heterocyclic scaffolds such as imidazole and triazole. We found that AHLs analogues with a carbamate or a thiocarbamate function displayed antagonistic activity whereas the hydrazide analogues were inactive. In the series having a 2-OH function, 2-hydroxy hexanoyl HSL or 2-hydroxy octanoyl HSL were found very active, with opposite activity for each of the two diastereoisomers. In the third set of heterocyclic AHL analogs, it was found that some triazole and imidazole derivatives act as QS antagonists.

In the second part, we developed a flexible synthetic route to access the rare glucose-2-phosphate structures, including the native agrocinopine D. Agrocinopines are capable of activating the pathway of quorum sensing in *Agrobacterium* which in

turn activate the virulence factor. In this study, we used an efficient one-pot method to synthesize the precursor of agrocinopine D. It relies on the coupling reaction of the phosphoramidite with benzyl 3,4,6-tri-*O*-benzyl- β -D-glucopyranoside which is prepared from the commercially available tri-*O*-benzyl-D-glucal. Biological investigations on the binding mode of this synthetic agrocinopine D with some *Agrobacterium* proteins are in progress.

Key words: quorum sensing, AHL analogs, agrocinopines, *Vibrio fischeri*, *Agrobacterium*, G2P, phosphate.

Résumé

Le processus utilisé par les bactéries pour coordonner leur comportement en fonction de leur densité de population en communiquant par de petits signaux chimiques (synthèse et détection) est connu sous le nom de Quorum Sensing (QS). Ce processus existe chez de nombreuses bactéries, y compris les pathogènes. Le QS régule diverses expressions de gènes impliqués dans la croissance, la virulence et la production de toxines. Par conséquent, l'inhibition du QS est considérée comme une stratégie prometteuse pour prévenir l'infection bactérienne. Compte tenu de la nécessité de diversifier les stratégies antibactériennes pour faire face à la problématique de la résistance aux antibiotiques des bactéries, cibler le QS peut être une approche complémentaire aux voies biologiques existantes. En se concentrant sur la chimie du quorum sensing bactérien, les travaux de cette thèse visent à en étudier deux aspects. D'une part, par la recherche de nouveaux mimes de signaux moléculaires du QS, nous avons découvert de nouveaux analogues d'acyl homosérine lactones (AHL) capables de moduler le QS chez les bactéries Gram-négatives telles que *Vibrio fischeri*. D'autre part, en étudiant les phosphodiester de carbohydrates impliqués dans la pathogénicité de la bactérie *Agrobacterium fabrum* C58, nous avons développé une méthode efficace pour synthétiser l'agrocinopine D, une agrocinopine naturelle, ainsi que certains analogues.

Dans la première partie, nous avons conçu et synthétisé une série de nouveaux analogues d'AHL, dont des hydrazides, des carbamates ou des thiocarbamates, des 2-OH AHL et des analogues hétérocycliques dérivés de l'imidazole et du triazole. Nous avons constaté que les analogues d'AHL portant une fonction carbamate ou thiocarbamate présentaient une activité antagoniste alors que les analogues de l'hydrazide étaient inactifs. Dans une autre série ayant une fonction 2-OH, les deux diastéréoisomères de 2-hydroxy hexanoyl HSL ou 2-hydroxy octanoyl HSL se sont avérés exercer une activité forte et opposée. Enfin, dans un nouvel ensemble de systèmes hétérocycliques, il a été trouvé que les analogues triazole et imidazole

d'AHL agissent comme des antagonistes de QS.

Dans la deuxième partie, nous avons développé une voie synthétique flexible pour accéder au rare de glucose-2-phosphate et ses dérivés, dont l'agrocinopine D. Les agrocinopines sont capables d'activer la voie du quorum sensing chez *Agrobacterium* qui à son tour active le facteur de virulence. Dans cette étude, nous avons utilisé une méthode efficace en un seul pot pour synthétiser le précurseur de l'agrocinopine D. Elle repose sur la réaction de couplage du phosphoramidite avec le benzyl 3,4,6-tri-*O*-benzyl- β -D-glucoside qui est préparé à partir de tri-*O*-benzyl-D-glucal disponible dans le commerce. L'agrocinopine D synthétique obtenue fait l'objet d'une étude biologique approfondie sur son mode de liaison avec des protéines d'*Agrobacterium*.

Mots clés: quorum sensing, analogues AHL, agrocinopines, *Vibrio fischeri*, *Agrobacterium*, G2P, phosphate.

List of publications

1. Zhang, Q.; Queneau, Y.; Soulère, L. Biological Evaluation and Docking Studies of New Carbamate, Thiocarbamate, and Hydrazide Analogues of Acyl Homoserine Lactones as *Vibrio fischeri*-Quorum Sensing Modulators. *Biomolecules* **2020**, 10, 455.
2. Qiang Zhang, Erwann Jeanneau, Yves Queneau, Laurent Soulère, (2*R*)- and (2*S*)-2-hydroxy- hexanoyl and octanoyl-L-homoserine lactones: new highly potent quorum sensing modulators with opposite activities, *Bioorganic Chemistry*, **2020**, 104, 104307.
3. Zhang, Q.; Li, S.-Z.; Ahmar, M.; Soulère, L.; Queneau, Y. Esters of Glucose-2-Phosphate: Occurrence and Chemistry. *Molecules* **2020**, 25, 2829.
4. Zhang, Q.; Li, S.-Z.; Ahmar, M.; Soulère, L.; Queneau, Y. Synthetic strategies towards agrocinopines, bacterial carbohydrate phosphodiester, and their analogues. (manuscript in preparation)
5. Zhang, Q.; Queneau, Y.; Soulère, L. Synthesis, biological evaluation and docking studies of 1,4- and 1,5- substituted imidazoles and triazoles AHL analogs as QS modulators in *Vibrio fischeri*. (manuscript in preparation)

Contents

Acknowledgement	- 1 -
Abbreviations.....	- 3 -
Abstract.....	- 5 -
Résumé.....	- 7 -
List of publications	- 9 -
Contents	- 11 -
General introduction	- 13 -
Part I. Synthesis, biological evaluation of quorum sensing signals mimics related to AHLs.....	- 15 -
Chapter 1. Background on quorum sensing and its chemical modulation.....	- 17 -
1.1 Quorum sensing	- 17 -
1.2 Chemical modulation of QS.....	- 19 -
1.3 Focus on the modification of AHLs involving a heterocyclic building block..	- 26 -
Chapter 2. Result and discussion	- 41 -
2.1 Studies of novel carbamate, thiocarbamate and hydrazide analogues of AHLs as <i>Vibrio fischeri</i> quorum sensing modulators	- 43 -
2.1.1 Introduction.....	- 43 -
2.1.2 Synthesis of carbamate, thiocarbamate and hydrazide analogues of AHLs-	44 -
2.1.3 Biological evaluation	- 50 -
2.1.4 Docking study	- 52 -
2.1.5 Conclusions.....	- 55 -
2.2 2-Hydroxy AHL analogs: synthesis and biological evaluation in <i>Vibrio fischeri</i> quorum sensing	- 57 -
2.2.1 Introduction.....	- 57 -
2.2.2 Synthesis of 2-hydroxy AHL analogs	- 58 -
2.2.3 Biological evaluation	- 63 -
2.2.4 Docking study	- 65 -
2.2.5 Conclusions.....	- 67 -
2.3 Studies of new AHL analogs based on imidazole or triazole scaffolds	- 68 -
2.3.1 Introduction.....	- 68 -
2.3.2 Synthesis of AHL analogs based on imidazole or triazole scaffolds	- 68 -
2.3.3 Biological evaluation	- 76 -
2.3.4 Docking study	- 78 -

2.3.5 Conclusions.....	- 80 -
2.4 Alternative route towards AHL analogues by late lactone formation	- 82 -
2.4.1 Introduction.....	- 82 -
2.4.2 Alkylation and cyclization to synthesize lactone	- 84 -
2.4.3 Conclusions.....	- 87 -
References.....	- 88 -
Part II. Synthesis of agrocinopine D and D-glucose-2-phosphodiester involved in the regulation of quorum sensing in <i>Agrobacterium fabrum</i> C58.	- 92 -
Chapter 3. Quorum sensing in <i>Agrobacterium</i> and agrocinopines	- 94 -
3.1 Introduction.....	- 94 -
3.2 Background on the structural and synthetic chemistry of agrocinopines and their analogues.....	- 97 -
3.2.1 Agrocinopine A	- 98 -
3.2.2 Agrocinopine B	- 102 -
3.2.3 Agrocinopine C	- 103 -
3.2.4 Agrocinopine D.....	- 107 -
3.2.5 Arabinose-2-phosphate (A2P) and their derivatives	- 108 -
3.2.6 D-Glucose-2-phosphate (G2P)	- 109 -
3.3 Conclusions.....	- 111 -
Chapter 4. Result and discussion	- 112 -
4.1 Synthesis of agrocinopine D and D-glucose-2-phosphodiester	- 114 -
4.1.1 Introduction.....	- 114 -
4.1.2 Synthesis of the glucose building block bearing 2-OH	- 115 -
4.1.3 Phosphorylation reagent.....	- 116 -
4.1.4 Synthesis of agrocinopine D and D-glucose-2-phosphodiester	- 117 -
4.1.5 Biological studies using agrocinopine D	- 126 -
4.1.6 Conclusions.....	- 126 -
References.....	- 128 -
General conclusion.....	- 130 -
Experimental section.....	- 132 -
Supporting information (I).....	- 134 -
Supporting information (II).....	- 166 -

General introduction

Bacteria communicate through chemical signals according to their population density. This signaling process, referred to as quorum sensing (QS), means that bacteria do not behave like isolated cells but coordinate their behaviors. Among various phenotypes, bacterial quorum sensing regulates the production of virulence factors. This is why it can be considered as a target in antibacterial strategies in human and plant health. Since this phenomenon relies on specific small molecules and their interactions with specific proteins, we can contribute, as organic chemists, to the QS modulation. This is the purpose of this thesis, which addresses QS chemistry from two distinct viewpoints.

The first viewpoint is the search for new molecules that can modulate the bacterial QS. In this aspect, we have designed novel types of AHL analogue aiming at acting as new QS modulators, either as agonists or antagonists. We give first a bibliographic update (chapter 1.3) on the various approaches to QS modulation and more specifically those related on the design of analogs of acyl homoserine lactones (AHL), an important type of natural QS inducer in Gram negative bacteria. Then in the following chapters, we describe our work involving the replacement of the amide function in AHLs with other functions, namely carbamate or thiocarbamate, hydrazide functions, imidazole, and triazole moiety, all this concomitantly with the modulation of acyl chain length. In this part of the work, we also investigated AHLs modified with a 2-hydroxy group. Our work included the design, the synthesis and the biological evaluation of the new QS modulation candidates. In some cases, the structure-properties relationships are also discussed based on docking experiments.

The second viewpoint on the chemistry of QS, presented in the second part of this thesis, concerns carbohydrate phosphodiester named agrocinopines which are involved in the virulence of *Agrobacterium*. Depending on bacterial strains, agrocinopines are built either with arabinose, glucose or sucrose building blocks. In section 2.2, we provide a full bibliographic chapter on the chemistry of agrocinopines

and their analogues. Then, in the following sections, we describe our results on a new synthetic route to access agrocinopine D and other glucose-2-phosphates derivatives.

**Part I. Synthesis, biological evaluation of quorum sensing signals
mimics related to AHLs**

Chapter 1. Background on quorum sensing and its chemical modulation

1.1 Quorum sensing

Bacterial quorum sensing is a cell-cell communication pathway used by bacteria to coordinate their population density. As single cells, bacteria are capable of dealing with multicellular behaviors at high population density due to the QS signaling process. In this process, the molecular chemical signals termed autoinducers play a critical role in the overall communication system. Quorum sensing has become a basic process that is wide-ranging in pathogenic bacteria and is used to regulate their gene expressions including bioluminescence, growth, biofilm formation, virulence, and so on [1,2]. Even if the signals-dependent quorum-sensing system has not been fully understood, it still provides an opportunity to interfere with virulence by modulation of QS through a chemical approach.

The quorum sensing regulatory pathway relies on the production, diffusion and detection of autoinducers. In detail, the overall concentration of autoinducer in the outside environment consists of QS signals produced by each cell. When QS signals accumulate and reach a critical concentration, they can be detected and then activate the transcription of specific genes [3,4]. Quorum sensing message is usually integrated by small RNA (sRNA) [5] which can regulate the expression of some target genes. Therefore, further understanding of the mechanism of quorum sensing can be useful for designing tools able to control pathogenicity in bacteria.

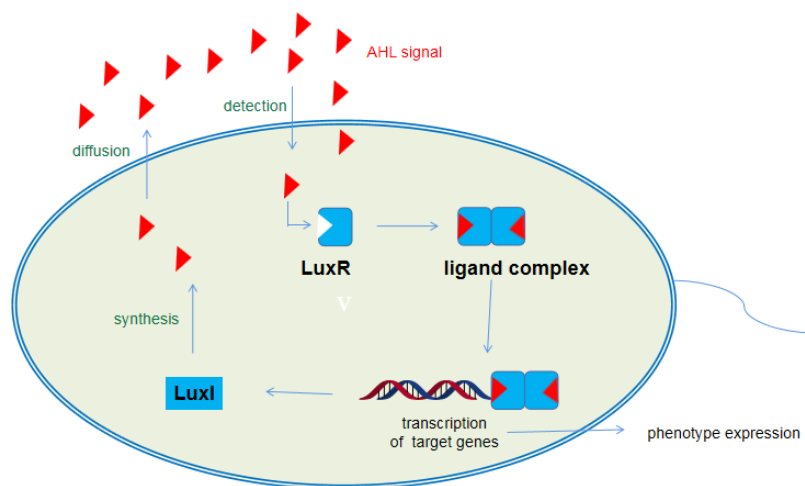


Figure 1. Mechanism of quorum sensing system.

Diffusible autoinducers are produced via an inducer synthase and detected by their cognate receptor. Evolving research on QS has led to the discovery of different kinds of autoinducers. Among them, the AHL-mediated quorum sensing system was used by over 50 species in Gram-negative bacteria, while numerous Gram-positive bacteria utilized cyclic oligopeptide as a chemical signal. Autoinducer-2 (AI-2) originated from dihydroxy-pentanedione (DPD) has been identified both in Gram-negative bacteria and Gram-positive bacteria [6], which is involved in interspecies bacterial communication.

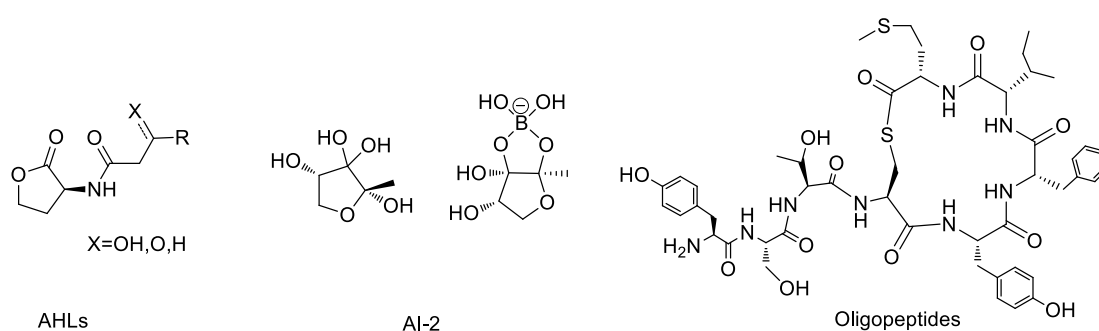


Figure 2. Structures of autoinducers.

If bacteria can exchange information with each other by diffusible signals, it has been found recently that some viruses use the same way to communicate. In 2017, Sorek's group firstly reported that bacteriophages could communicate and cooperate to control

their density by the way of a communication peptide [7]. Recently, biologists discovered that QS autoinducers released by some bacteria could control viruses to make a lysis-lysogeny decision [8]. Their research demonstrates that viruses (bacteriophages) and pathogenic bacteria (*Vibrio cholerae*) count on the same molecular signals to cause the disease.

1.2 Chemical modulation of QS

With the growing development of bacterial resistance, quorum sensing inhibition has attracted much attention as a new target to decrease bacterial virulence. Chemical modulation of quorum sensing provides a route to develop new anti-infection strategies. Up to now, the AHLs-mediated bacterial signaling pathway is the best-understood at the molecular level.

In general, there are three available strategies to interfere with the bacterial quorum sensing process. The first strategy is to prevent the production of the autoinducers by controlling the synthase. This is the most direct way to inhibit the bacterial quorum sensing pathway, as the autoinduction circuit is discontinued without a chemical messenger. The crystal structure of a LasI synthase protein in *Pseudomonas aeruginosa* by X-ray reported [9] in 2004, has been a powerful tool to guide the design of QS modulators targeting the synthase. Blackwell and her colleagues [10] found that some acyl homoserine D-lactones and acyl homocysteine D-thiolactones with a long chain displayed antagonistic activities towards the synthase in *Pseudomonas aeruginosa*. Except for the design of synthase specific modulators, LasI proteins mutants in *P. aeruginosa* is also a forceful manner to decrease or inhibit bacterial group behavior.



Figure 3. QS modulators for synthase RhII protein in *P. aeruginosa*.

The second strategy is to decrease the concentration of autoinducers in the extracellular environment by degradation. A traditional approach is the hydrolysis of natural signals either by basic conditions (increasing the value of pH), enzymes [11,12] (lactonases and amidases) or by their destruction by catalytic antibodies [13], a process named quorum quenching. The expected AHLs hydrolysis product shown in Fig 4 is the ring-opening product (pathway A), which is inactive for QS. In 2005, undocumented hydrolysis product tetramic acid derivative in *P. aeruginosa* was revealed (pathway B) and it was identified as a potent antibacterial agent [14]. More recently, biodegradable molecularly imprinted polymers have been utilized as affinity ligands to breakdown homoserine lactones, which act as an anti-infective by preventing QS [15-17].

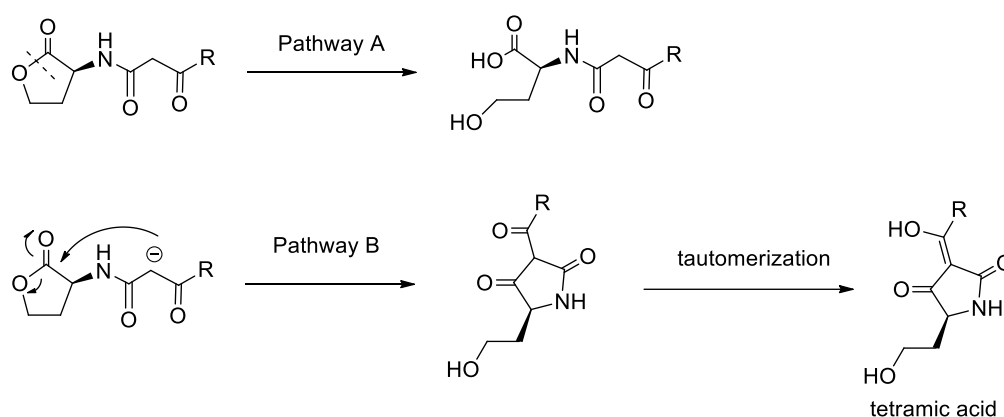


Figure 4. Degradation of 3-oxo-AHLs under basic condition.

The third strategy is to interfere with the ligand-receptor interaction by adding antagonistic analogues that mimic natural ligands. Among the three strategies, this latter has been the most investigated one, with many different kinds of autoinducer inhibitors being reported.

Due to a large amount of reported biochemical data about the protein LuxR, the LuxR-type protein family can be regarded as a useful target for a medicinal chemistry approach to the design of modulators of ligand-receptor interactions. Indeed, some experimental data with LuxR-type protein knockouts indicate a significant decrease in

coordinated QS phenotypes, validating the approach based on the modulation of bacterial QS communication. The availability of the X-ray structure of LuxR-type proteins has also accelerated the researches on QS modulation based on synthetic AHLs analogues. Close to LuxR-type proteins, the LasR receptor consists of two independently folded domains: a small C-terminal DNA binding domain (DBD) and a large N-terminal ligand-binding domain (LBD) [18]. The structural data of LuxR-type proteins opens a door for designing not only agonists of LuxR-type proteins but also antagonists.

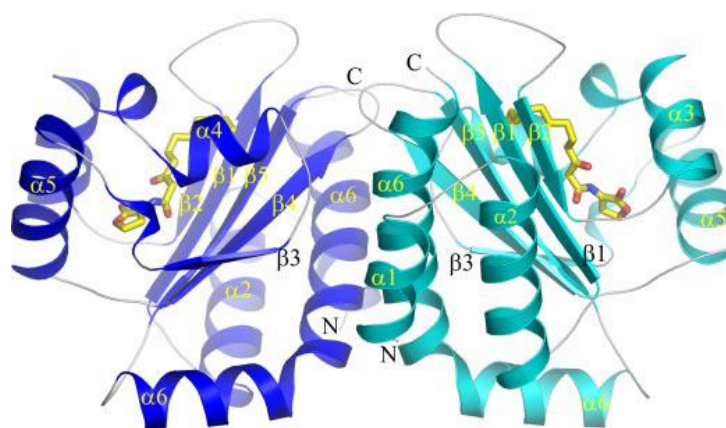
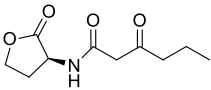
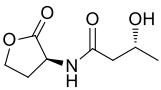
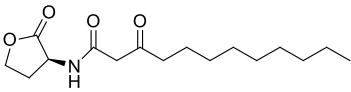
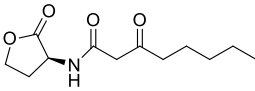
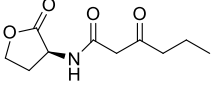
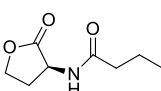


Figure 5. A symmetrical dimer of LasR-LBDs in complex with its natural ligand [18].

1.2.1 AHL-based QS modulation

Two landmark discoveries in the 1980s include: i) the *Vibrio fischeri lux* genes of QS system which is responsible for bioluminescence [19,20]; and ii) the identification of the chemical structure of the autoinducer (3-oxo-C6-HSL) in *Vibrio fischeri* [21]. Further investigations made the mechanism of AHLs-mediated QS system clearer. Different autoinducers and their QS-regulated phenotypes in other bacterial species have been found and well-characterized (Table 1). In principle, different bacteria use different AHL signals. However, it must be noted that some signals can be common to several species (such as *Vibrio fischeri* and *Erwinia carotovora*). It is proposed that this overlap probably affords a way for different bacteria to communicate between different species [22].

Table 1. Representative structures in the AHL system.

Bacteria	AHL signal	LuxI/R	QS phenotype
<i>Vibrio fischeri</i>	 (OHHL)	LuxI/R	luminescence
<i>Vibrio harveyi</i>	 (3-OH-BHL)	LuxM/N	virulence
<i>Pseudomonas aeruginosa</i>	 (OdDHL)	LasI/R; QscR	virulence, biofilm formation
<i>Agrobacterium fabrum</i> C58	 (OOHL)	TraI/R	Ti plasmid transfer
<i>Erwinia carotovora</i>	 (OHHL)	ExpI/R; CarI/R	antibiotic production
<i>Serratia liquefaciens</i>	 (BHL)	SwrI/R	antibiotic production

Many chemical drugs and probes are designed and discovered counting on the natural product [23-29]. As many Gram-negative bacteria use acyl-homoserine L-lactones (AHLs) as autoinducers, these natural ligands are significant starting points of inspiration for discovering QS modulators. In this field, many non-native ligands mimicking natural AHLs have been designed, synthesized, and assessed with respect to their biological activity.

The backbone of AHLs features three areas: the lactone ring which is synthesized from *S*-adenosylmethionine (SAM), the amide function, and the acyl chain. This latter can be functionalized with a 3-oxo group (such as in *Vibrio fischeri* or in *Pseudomonas aeruginosa*) or a (3*R*)-hydroxyl functional group (such as in *Vibrio*

harveyi). In most cases, the specific acyl chain is derived from fatty acid biosynthesis intermediates [30]. The structure of AHLs varies with bacterial strains as shown in Table 1. Natural ligands are equipped with an acyl chain that alternates in carbon number from 4 to 18 carbons. The length of the side chain can influence the stability of the AHL. Also, the acyl chain has a hydrophobic character which is essential for the entry and diffusion of chemical molecules through the cell membranes and within the hydrophobic pocket of the receptor. Meanwhile, the amide function provides hydrogen binding sites that would locate in a polar area of the receptor.

The synthesis of AHLs analogs is based on the structural modifications of AHLs backbone such as the replacement of the amide functional group with bioisosteres, or variations of the lactone part or the side chain. Structural variations of AHLs have been identified to induce or block biological effects.

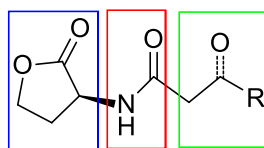


Figure 6. Three components of AHLs backbone.

Table 1 also highlights that AHL-mediated QS systems across different bacterial species share two common areas, the amide function and lactone signature moiety which can be degraded by AHL-degrading enzymes diffused into the outside environment by neighboring bacteria. If the lactone ring is replaced as a heterocycle or carbocycle, the degradation of these analogues by lactonases can be avoided. Several examples of such variations of the lactone have been reported, notably by replacing the ring oxygen atom of the lactone with a methylene [31], a nitrogen atom [32], or a sulfur atom [33,34]. Some other investigations focused on systems bearing an additional substituent on the lactone ring [35,36] while some others modified more drastically the lactone ring by installing a carbocycle [37] or an aromatic ring [38].

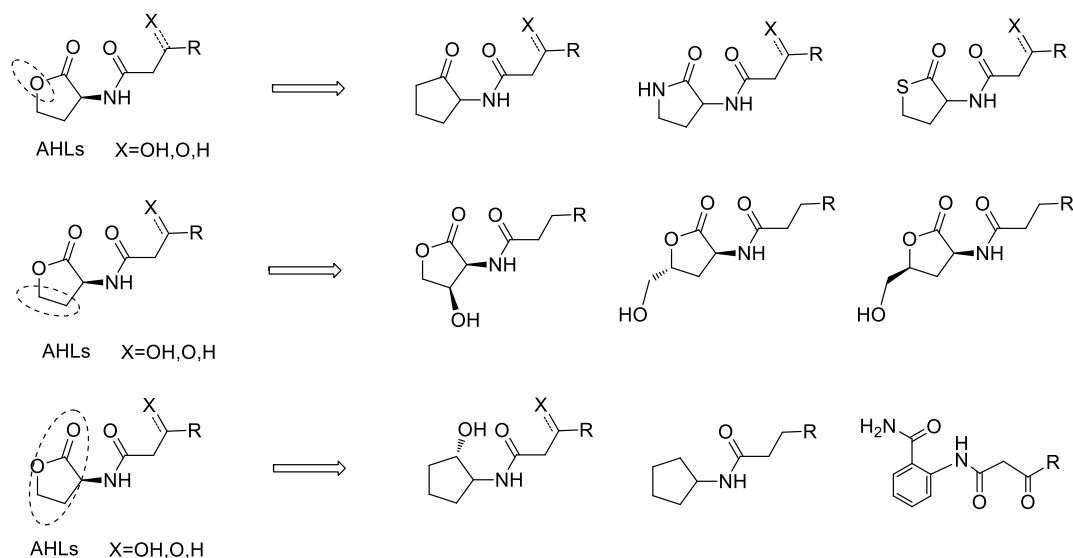


Figure 7. Variations of lactone in AHLs backbone.

The amide function of AHLs is an important H-binding site, and is therefore an indispensable group for the activity of natural autoinducers. In the field of peptides, bioisosteres are used to replace the amide function to design biologically active molecules. Inspired by this approach, our group and others have designed QS modulators based on bioisosteres to replace the amide function, such as sulfonamide [39], urea [40], sulfonylurea [41], reverse amide function [42], triazole [43,44], and tetrazole ring [44]. Most of these AHL analogues have proven to be antagonists against the LuxR receptor. Especially, compounds **1-15** exerted significant inhibitory activity. These results show that the strategy of replacing amide function with bioisosteres is useful to expand the discovery of potent antagonists.

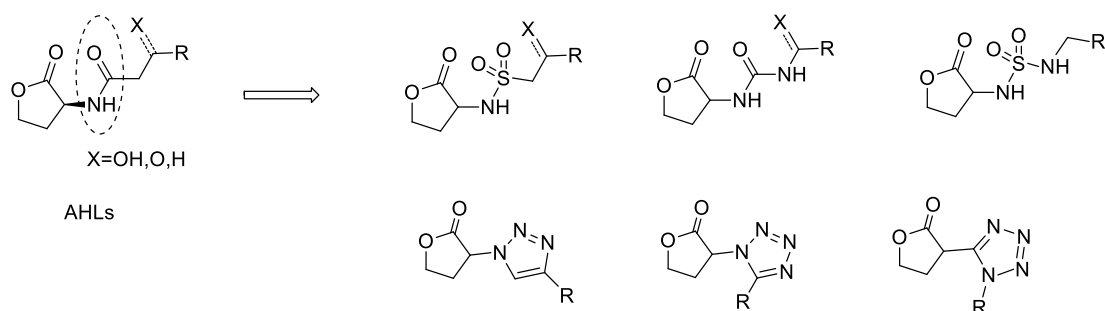


Figure 8. Variations of amide function in AHLs backbone.

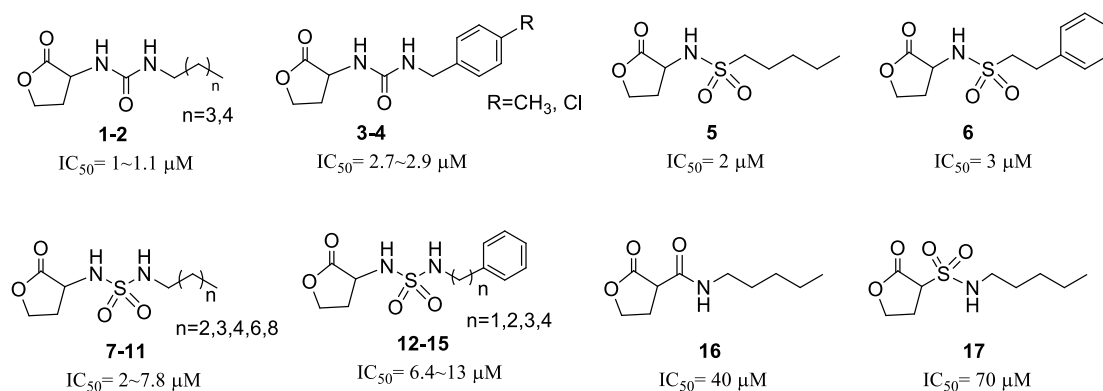


Figure 9. Main examples of variations of amide function in AHLs backbone.

The length of the alkyl chain is a key parameter in the design of AHLs analogues. It provides the necessary lipophilic property important for occupying the hydrophobic pocket of the binding site. A natural autoinducer with a given alkyl chain length can exert an agonistic activity for one species while behaving as an antagonist in another species of bacteria. This is a way some bacteria use to compete with each other. In contrary to the natural ligands, AHLs analog with a long acyl chain often displays antagonistic activity. To develop QS inhibitors, many investigations have focused on altering the acyl chain of natural AHLs, such as the modification of the chain length, the introduction of the phenyl group or the alkene unit.

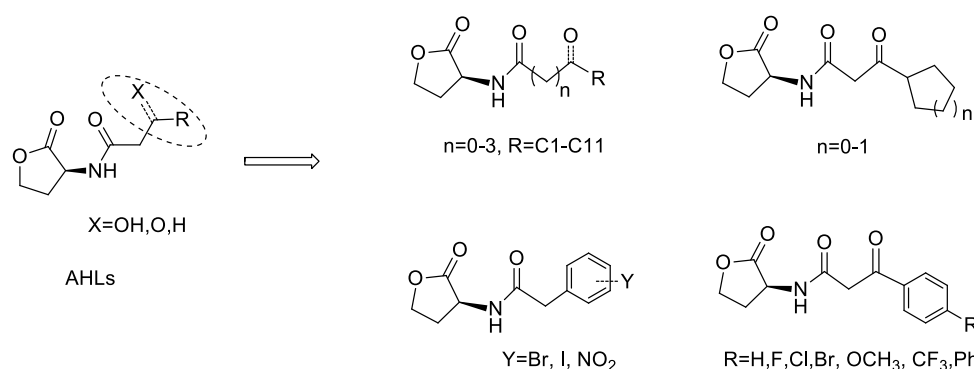


Figure 10. Variations of acyl chain in AHLs backbone.

The oxidation state of C-3 in the side chain is also an interesting point to address when looking for novel QS agonists or antagonists. Many natural AHL autoinducers

bear a 3-oxo or a 3-hydroxyl group in the acyl chain. The influence of the 3-OH stereochemistry of natural AHL ligand in *A. baumannii* on the biological properties was studied [45]. The *R/S* diastereoisomers of 3-hydroxyl C12 homoserine L-lactone were prepared and tested for their ability to activate the receptor. The result showed that the *R* isomer ($EC_{50}=0.7\ \mu\text{M}$) displayed a 40-times higher potency than the *S* isomer ($EC_{50}=29\ \mu\text{M}$). Biological analysis data suggested that (3*R*) isomer was more likely to be the natural ligand.

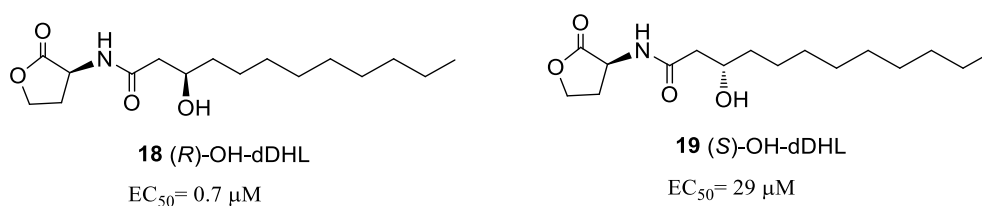


Figure 11. Two diastereoisomers of 3-hydroxyl C12 homoserine L-lactone.

1.3 Focus on the modification of AHLs involving a heterocyclic building block

The modifications based on acyl chain length and the oxidation state (C-3) of AHLs have been well-reviewed in other reports [46,47]. Here, we focus on AHL modifications leading to analogues containing heterocyclic rings. Actually, heterocyclic rings are widespread structural components in a variety of active compounds, particularly in pharmaceuticals. Like for triazoles, these heterocycles can constitute an amide bond bioisosteres in drug design strategies.

1.3.1 Heterocycles as amide bond bioisosteres in AHLs

Generally, any structural variations of natural signals can cause a loss of QS activity. However, synthetic analogues in which the amide function is replaced by a bioisostere function are prone to be better tolerated.

In 2006, Greenberg's group [48] identified a tetrazole with a long alkyl chain named PD12 which was a highly potent inhibitor of LasR in *P. aeruginosa*. Due to the

structural similarity to the natural autoinducer, 3-oxo-C12 HSL, the authors suggested that the inhibitor may bind to the specific region of LasR where the native signal interacted with. In their study, the authors designed 1,5-disubstituted and 2,5-disubstituted tetrazolic derivatives. PD12 was identified as the most active inhibitor with an IC₅₀ value of 30 nM. In all these type of analogues, 2,5-substituted tetrazole compounds exerted higher activity of inhibition than 1,5-substituted tetrazole. The authors believed that these compounds could serve as a scaffold to design novel and additional QS modulators.

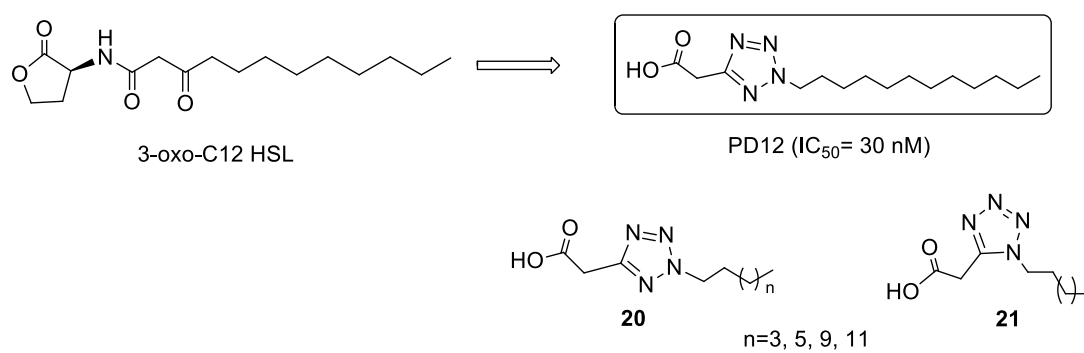


Figure 12. Tetrazole-containing QS inhibitor screened against LasR by Greenberg's group.

Inspired by the investigation of the tetrazole scaffold explored by Greenberg's group, our group [44] described the synthesis and the biological evaluation of a series of AHL analogues based on the triazole and tetrazole scaffolds. In this work, the novel LuxR-dependent QS modulators were structurally close to natural AHLs, the lactone part and the side chain being kept unmodified while only the amide function was replaced by a triazole or a tetrazole. Among the tetrazolic compounds, the lactone moiety is linked either to a carbon atom or a nitrogen atom of the tetrazole ring. It was found that the 1,5-disubstituted tetrazole compounds with a short chain were active. Interestingly, analogue **23** (antagonist) or analogue **25** (agonist) with the same chain length differ only by the connection between the lactone and the tetrazole, either a C-C or a C-N bond, demonstrating how small structural variations of AHLs analogues could induce different or even opposite biological activities. For 1,5-disubstitutions

of tetrazolic compounds **23** and **25**, the way of C-C connection between lactone moiety and tetrazole ring could serve as reverse amide mimic whereas C-N linkage could mimic amide function. In contrast, substitution at the 2,5-positions of tetrazole was completely inactive.

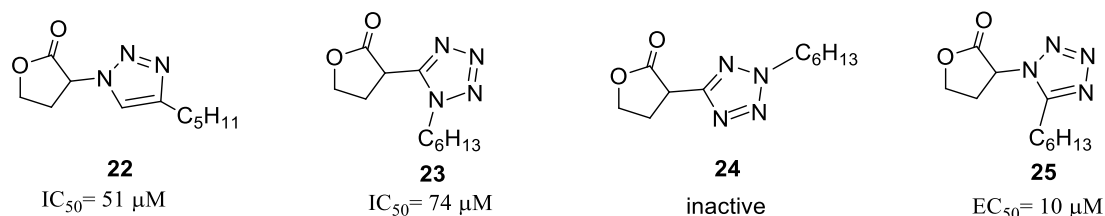


Figure 13. Triazole or tetrazole-containing QS modulator tested by our group.

At almost the same time, Brackman's group [43] synthesized a set of AHL analogues in which the central amide is substituted with a triazole ring. These compounds were evaluated for their biological activity on QS in *E. coli*, *P. aeruginosa* and *B. cenocepacia*. They found that this family of triazole analogues exerted antagonistic activity (LuxR QS system) depending on their concentration in *E. coli*. Only compounds bearing a long chain (C10 or C12) or phenyl group acted as antagonists (LasR) against the *P. aeruginosa* QSIS2 biosensor. Besides, the most active inhibitor of this study (compound **26**, n=11) at the concentration of 1 mM resulted in a significant decrease in biofilm formation of the *P. aeruginosa* and *B. cenocepacia* strains.

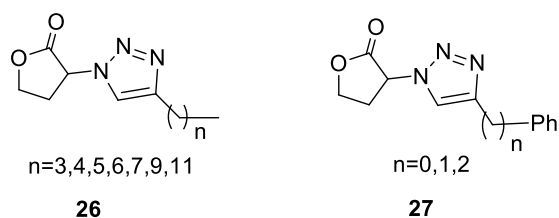


Figure 14. Triazole-containing QS modulator tested by Brackman's group.

More recently, our group focused on the synthesis and the QS modulation activity of a series of oxadiazoles, including 2,5-disubstituted 1,3,4-oxadiazole (**28**) and

3,5-disubstituted 1,2,4-oxadiazole (**29**, **30**). In this study, the lactone moiety was linked with the heterocyclic ring by the C-C bond. Finally, the evaluation of these compounds proved to be inactive towards the LuxR-type protein (unpublished data).

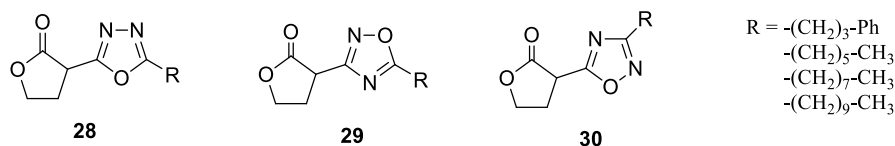


Figure 15. Oxadiazole-containing QS inhibitor tested by our group.

1.3.2 Heterocycles replacing the lactone moiety of AHLs

1.3.2.1 Non-aromatic heterocycles

In fact, the lactone ring plays a crucial role in providing a binding site in the LuxR protein. Thiolactones or lactams are structurally very close to the natural AHL signals. Many studies have reported such analogs, among which several were identified as potent inhibitors of QS by interacting with LuxR-type proteins. In 1993, Bycroft and colleagues [32] reported that thiolactones and lactams derived from native AHLs signals were able to restore the phenotype which is involved in carbapenem biosynthesis in *E. carotovora* at very low concentration.

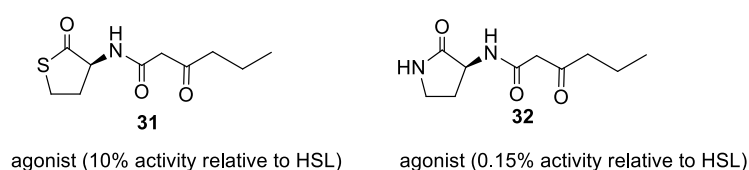


Figure 16. Thiolactone or lactam QS modulator in *E. carotovora* identified by Bycroft's group.

The general synthetic route to access AHLs either as a lactone or as thiolactone or lactam analogs is shown in Figure 17. Natural AHLs and its analogs with or without the 3-oxo group were prepared by the coupling of lactone, thiolactone or lactam with a corresponding carboxylic acid in the presence of EDC. Subsequently, 3-oxo derivatives were reduced by sodium cyanoborohydride to afford corresponding the 3-OH AHL analogs.

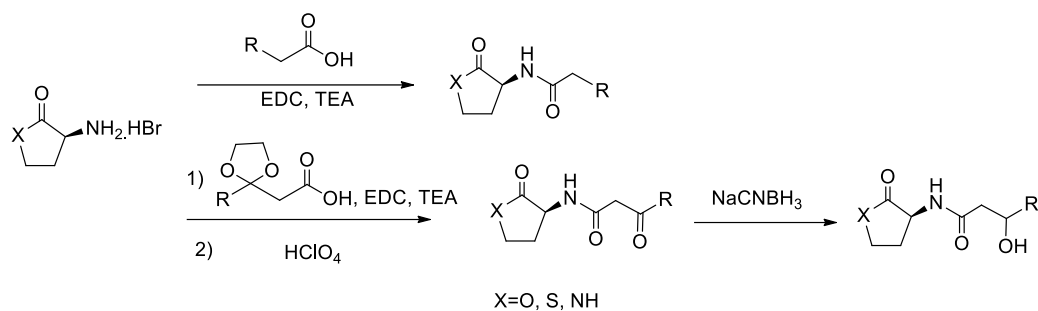


Figure 17. General synthetic approach to access native AHLs and its thiolactone or lactam analogs.

In 2011, Blackwell and her colleagues [33] identified thiolactone analogues of AHLs with enhanced hydrolysis stability and examined their activity as activators or inhibitors of LuxR-type receptors (LuxR, LasR, TraR) in *V. fischeri*, *E. coli*, *P. aeruginosa*, *A. tumefaciens*. Different structures with acyl chain bearing 3-oxo moiety or phenyl groups were designed and evaluated with respect to their QS activities. They discovered several highly potent QS agonists and antagonists, among which many are active against different receptors. Compounds **33-35**, **37-39**, **42-44** exerted strong inhibition activity of LuxR-type receptor with IC₅₀ value up to nanomolar. It was worthy to note that thiolactone **44** bearing a *p*-nitrophenyl group and compound **45** bearing an indole motif in the side chain proved to be significant agonists whereas their corresponding AHL analogues were identified as antagonists against *E. coli* LasR. Thus, the modification of the lactone part into thiolactone affects AHL analogues activity in some cases. This fine-tuning, which resulted in highly similar structures to the native AHLs, seemed to maintain a high level of biological activity.

The synthesis relies first on the reaction of an acyl chloride with Meldrum's acid led to the formation of acylated Meldrum's acid derivatives, followed by coupling with homocysteine thiolactones to afford the final thiolactone analogues.

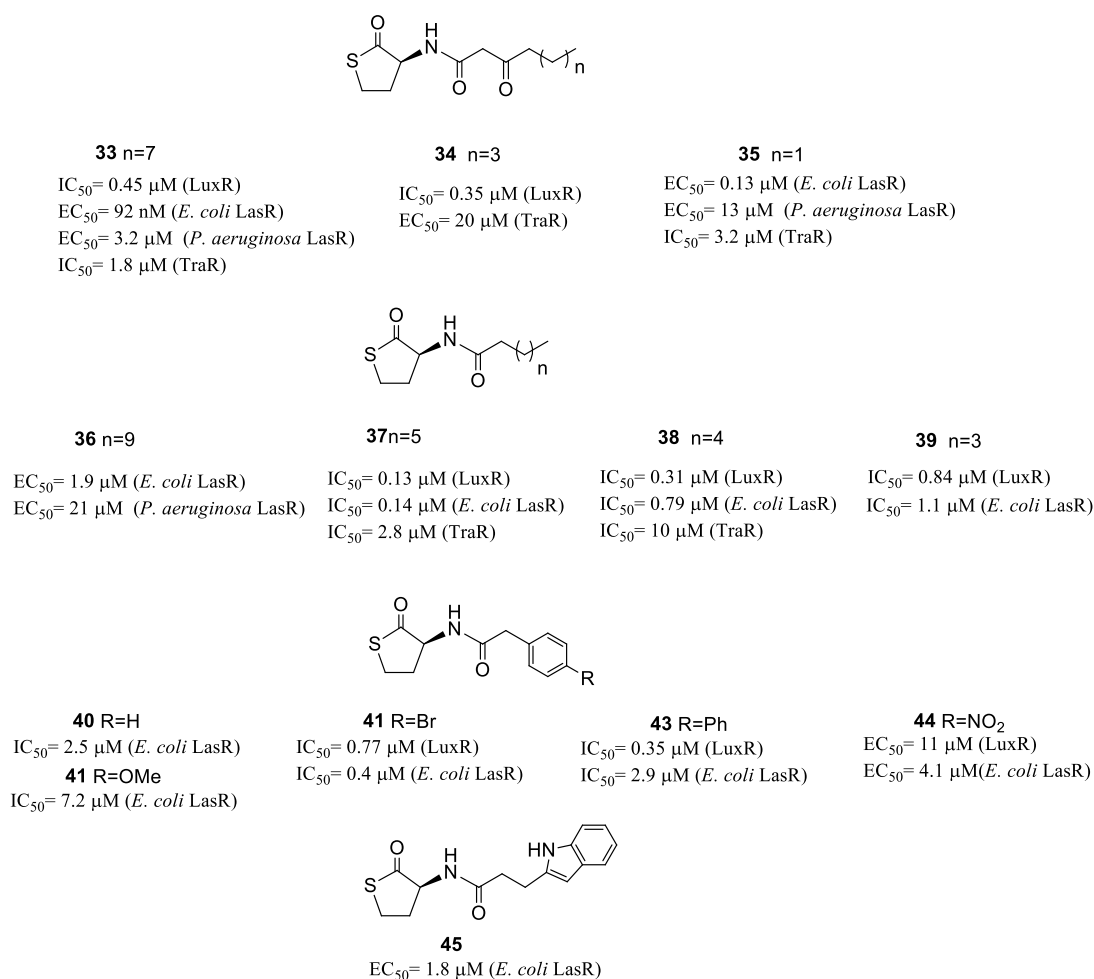


Figure 18. Thiolactone as QS modulator of LuxR-type receptor identified by Blackwell's group.

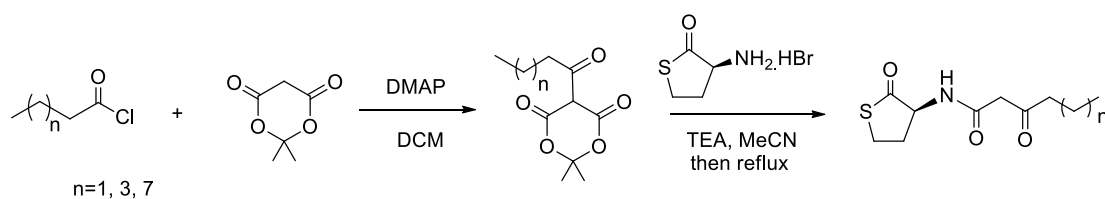


Figure 19. Synthetic approach to access acyl homocysteine thiolactones.

In *P. aeruginosa*, the protein RhlR receptor has become a promising target for the design of chemical signals able to interfere with the QS pathway. Both agonism and antagonism of QS RhlR receptor could regulate the gene expressions including virulence phenotypes. Previous studies of the synthetic ligands for QS RhlR focused on lactones [46]. A recent discovery was made by Bassler and coworkers [49], who analyzed and identified meta-bromo-phenoxy thiolactones as potent inhibitors to

block virulence factor and biofilm formation in *P. aeruginosa* quorum sensing receptor, LasR and RhlR. Further investigation determined that RhlR, not LasR, was a relevant target though both of them were partially inhibited. In their research, thiolactones (**46,47**) were found more active than the others and the configuration (*S/R*) of the ligands did not play a key role in the biological activity. More importantly, the authors uncovered that the most active molecule in their study, meta-bromo-phenoxy thiolactones also protected *Caenorhabditis elegans* and human lung epithelial cells from toxin by QS in *P. aeruginosa*.

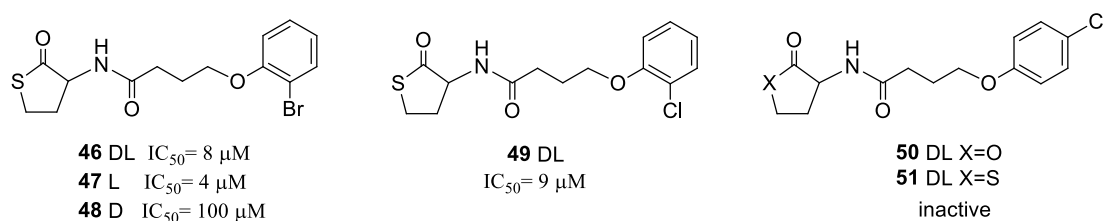


Figure 20. Thiolactonic QS modulators of LuxR-type receptor identified by the Bassler's group.

In 2019, Blackwell and her colleagues [34] reinvestigated acyl L-homocysteine thiolactones as non-native QS signals to modulate the activity of the RhlR receptor in *P. aeruginosa*. These compounds were among the most effective QS modulators (RhlR), as well as more stable than lactones. Besides, the activities of these compounds were evaluated in the *E. coli* RhlR system. Strong activities of these compounds were observed for two different bacterial strains. Compound **53** displayed agonistic activity in *P. aeruginosa* and *E. coli*, but at 5-times lower concentration in *P. aeruginosa* compared to *E. coli*. These compounds possessed higher selectivity to interact with the RhlR receptor relative to QS LasR receptor in *P. aeruginosa*. These studies indicated that thiolactone derivatives had the potential to be utilized as QS modulators in LuxR-type receptors.

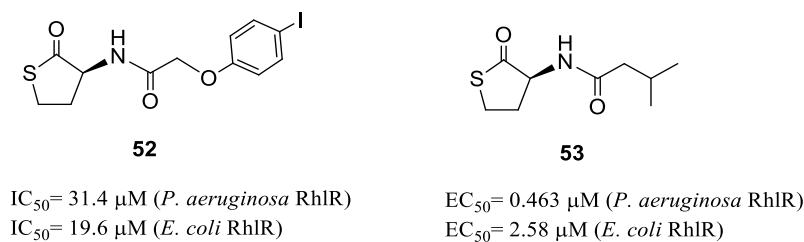


Figure 21. Thiolactone to modulate QS RhlR receptors identified by Blackwell's group.

Considering the low chemical stability of the lactone motif, modifications of the lactone head group drew more attention. Sintim and coworkers [50] revealed that oxazolidinone-based AHL analogue **54** was a very potent agonist which induced bioluminescence with remarkably similar intensities to the native ligand (3-oxo-C12 HSL) in *E. coli* (pSB1075). In another biological evaluation, the authors found that the compounds **54** and **55** responded to the CviR QS system, as their QS-regulated phenotype is the violacein production in *Chromobacterium violaceum* CV026. Compound **55** was able to activate the violacein production to act as an agonist whereas compound **54** could inhibit this phenotype in high concentration.

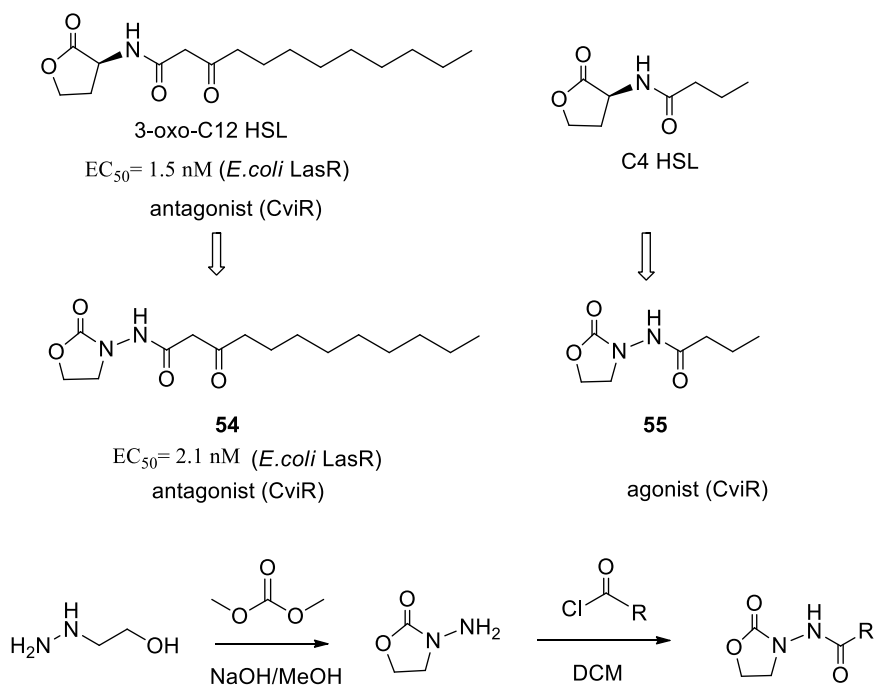


Figure 22. 3-Aminooxazolidinone AHLs analogues and its synthetic route.

1.3.2.2. Aromatic rings replacing lactone moiety of AHLs

Early researches demonstrated that the lactone moiety of synthetic AHL analogues is essential for signals recognition [32]. As mentioned before, the lactone or thiolactone part of QS modulators is at risk of being enzymatically degraded by lactonases. To avoid this problem, some groups have considered the use of aromatic rings to replace the lactone head group for designing novel QS modulators.

In 2015, Kumar and coworkers [51] managed to replace the lactone motif with an indole one as a head group of AHLs mimics and their QS inhibition assays of GFP fluorescence in *P. aeruginosa* were performed. Compounds **56-58** displayed 44% to 65% reduction of GFP fluorescence at 250 μ M, among which **58** was the most active.

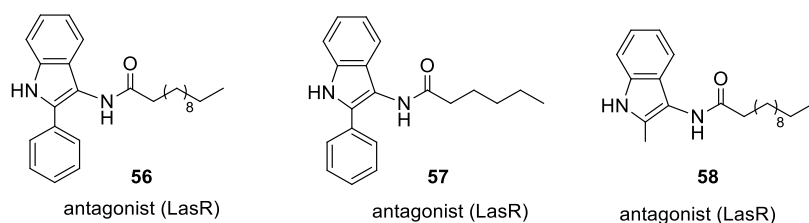


Figure 23. Aromatic ring replacing lactone of AHLs to act as QS modulator identified by Kumar's group.

In 2015, Helman and coworkers [52] reported that 1-(2-aminophenyl)ethanone diffused by *P. aeruginosa* specifically activated the QS response of LuxR in *V. fischeri*. Inspired by this finding, our group [53] designed and synthesized a set of LuxR QS inhibitors based on 2-substituted anilines as scaffolds. 2-Nitro aniline with the chain length of C4 was assessed to be most active.

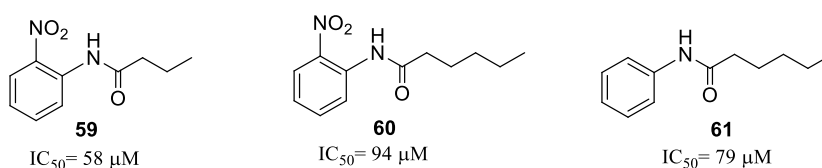


Figure 24. Aromatic ring replacing lactone of AHLs to act as QS modulator identified by our group.

More recently, Blackwell and her colleagues [54] reported a series of AHL analogues in which the lactone is replaced by an aromatic moiety, with very potent antagonistic activity against LasR reporter systems. Initially, compound **62** was discovered by a high-throughput screen of small chemical molecule libraries, which were among the most potent antagonist of LasR. Then compound **62** was served as a scaffold to design their derivatives with improved potencies. Derivatives building on heterocycles, furan **66-68** and thiophene **69-71** displayed similar antagonistic activities to compound **62**. The importance of tail length was noted. The result suggested firstly that analogues with side chains of 10 to 12 carbons were similarly as active as compound **62**, and secondly that analogues with shorter chain length (C5-C8) led to lower antagonistic activity. Analogues with shorter side chains may lack hydrophobic contacts during the binding interaction of receptors so they displayed less activities. On the other side, stronger potency in LasR of heterocycles analogues (**66,67,69,70**) than compound **62** was noticed. To clarify the antagonism of the LasR receptor by signals, the binding interactions between ligands and LasR receptor were characterized.

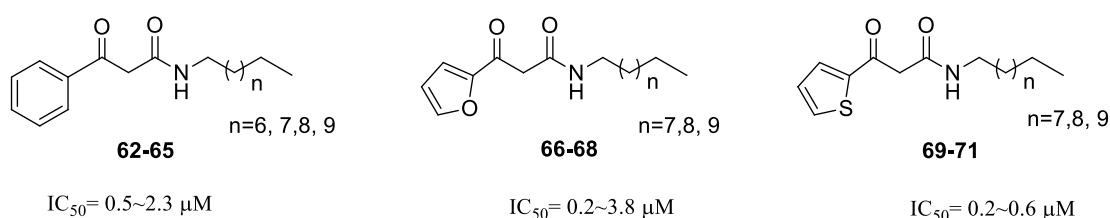


Figure 25. Novel LasR QS antagonists.

Building on their previous investigations on QS modulators, Suga's group [38] described the design, synthesis and biological evaluation of non-lactone AHL analogues. This set of phenyl systems or pyridyl bears meta- or ortho-substituents such as hydroxyl or carboxamide group that provides H-bonding abilities for interacting in the binding site. Compounds **72-76** which derived from aniline were evaluated as LasR antagonists in their assays. Compounds **78** and **79** which were

structurally similar to **73** and **76**, respectively, displayed no activity. These results indicated that the position of substituents played a key role in their activities. The authors concluded that a common characteristic of antagonistic activity was an aniline ring with a proper H-bonding site at meta- or ortho- position. The most active inhibitor was compound **73** which inhibited elastase production, one of the virulence factors controlled by QS in *P. aeruginosa*.

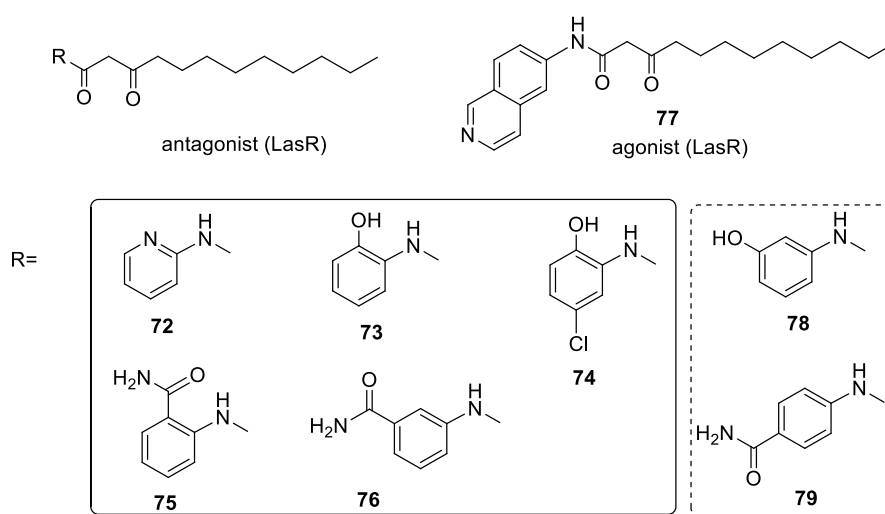


Figure 26. Aromatic ring replacing lactone of AHLs to act as QS modulator identified by Suga's group.

Other aromatic systems, not heterocyclic but close to those just shown above, such as polyaromatic systems identified by Greenberg and coworkers [55] using an ultrahigh-throughput screen of small molecule libraries have also been reported. Among these agonists, the triphenyl compound **TP-1** appeared to mimic the autoinducer 3-oxo-C12 HSL in the LasR receptor system, **TP-1** being even more potent. The EC_{50} value reached nanomolar (14 nM) and the level of activation relative to the native signal was 106%.

As the above results were obtained from high throughput experiments, further research was performed to gain better insight into the structure properties relationships related to these novel triphenyl compounds and their recognition by a

specific receptor LasR. The first structural characterization of the signaling receptor LasR-LBD interacted with ligands **TP-1** was determined by Zou and Nair [56].

Based on these findings, Blackwell and her colleagues [56,57] developed a series of novel QS antagonists of LasR in *P. aeruginosa*. In their study, they combined the 2-nitrobenzamide motif of **TP-1** with 1-bromo-ethylbenzene side chain part which was generated from the reported potent antagonist to design new QS modulators. The resulting activities revealed that compound **80** was found as the most potent antagonist with the IC₅₀ of 4.8 μM. Moreover, many antagonists exerted non-monotonic dose responses in the biological evaluation.

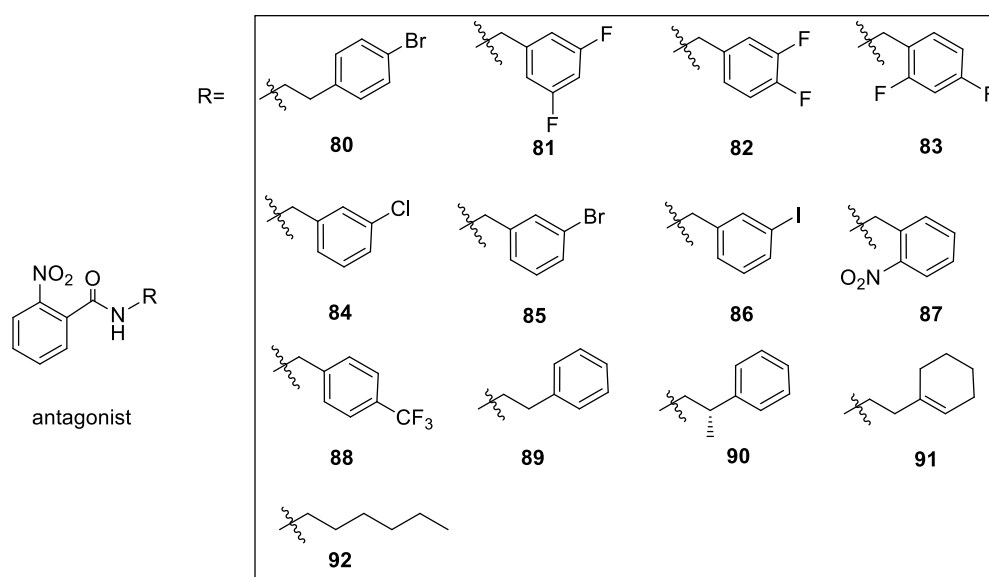


Figure 27. Novel LasR QS antagonists derived from **TP-1**.

1.3.3 Heterocycles contained in the side chain of AHLs

As the heterocyclic ring attracted considerable attention, some researchers looked into the modification of the AHL acyl chain with 1,2,3-triazole moiety targeting the QS pathway. Blackwell's group collaborated with Nielsen's group [58] reported the design and biological screening of a large number of novel triazole derivatives in the QS system based on the LasR protein in *P. aeruginosa*. Several triazole derivatives were able to potently inhibit the LasR receptor. In this series of triazole derivatives

(**93-106**), the nitrogen atom of the triazole ring provided a binding site with the LasR protein which mimicked the 3-oxo moiety of the natural ligand. For compounds **93-96**, the issue of alkyl chain length was discussed. Analogues with short chain ($n=3, 4$) were strong antagonists with an IC_{50} value up to $3.3 \mu M$ whereas analogues with long chain ($n=5$) displayed weak agonistic activity. For compounds **97-99**, analogues with larger rings ($n=3,4$) displayed higher antagonistic activity than smaller rings. Among all antagonists in their study, compound **107** was among the most active antagonists with an IC_{50} value of $2.6 \mu M$. Indeed, the biological results indicated that these types of triazole derivatives as QS modulators displayed higher activity than the previously described AHLs analogues whose amide function was replaced by triazole ring.

As for *E. coli* QS assay, it was observed that the affinity between LuxR and compound **101** was high, so that compound **101** was very active with an IC_{50} value of $5 \mu M$ [59]. Except for compound **101**, compounds **93, 97, 98, 106** displayed antagonistic activity against the QS LuxR with the IC_{50} value below $100 \mu M$. For the agonists, compounds **94-96, 98-102, 105** activated QS LasR system in *E. coli* with an EC_{50} value ranging from $1 \mu M$ to $71 \mu M$. It is interesting to note that some compounds display both antagonistic and agonistic activity in different strains.

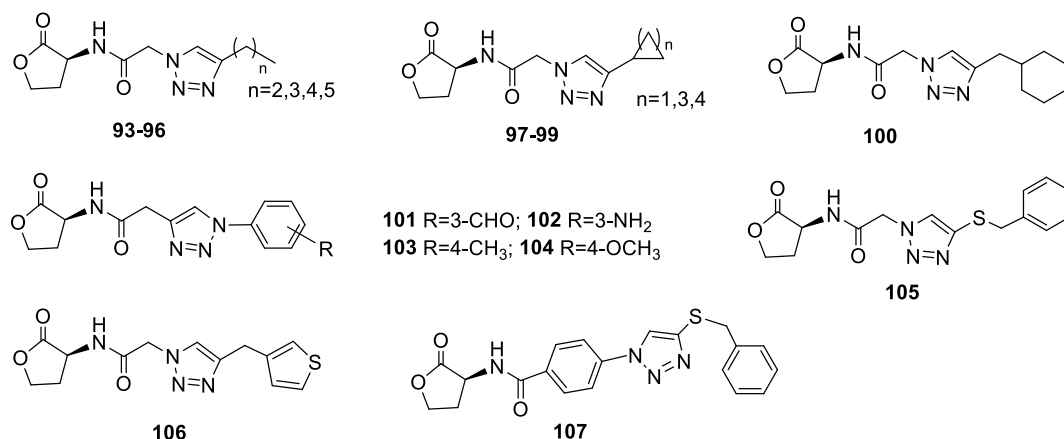


Figure 28. Triazole-containing QS modulator.

1.3.4 Project

The part of my project related to the synthesis, biological evaluation and docking study of novel AHL analogues concerns two sets of compounds. Firstly, in the context of our previous studies on QS modulations, we investigated novel modulations of the AHL amide function including carbamates, thiocarbamates, hydrazides, imidazole and triazole AHL analogues. Secondly, we investigated the modulation of the AHL side chain by including a 2-OH group close to the amide bond. Additionally, a methodological investigation was performed on the synthesis of AHLs derivatives through a late lactone formation strategy.

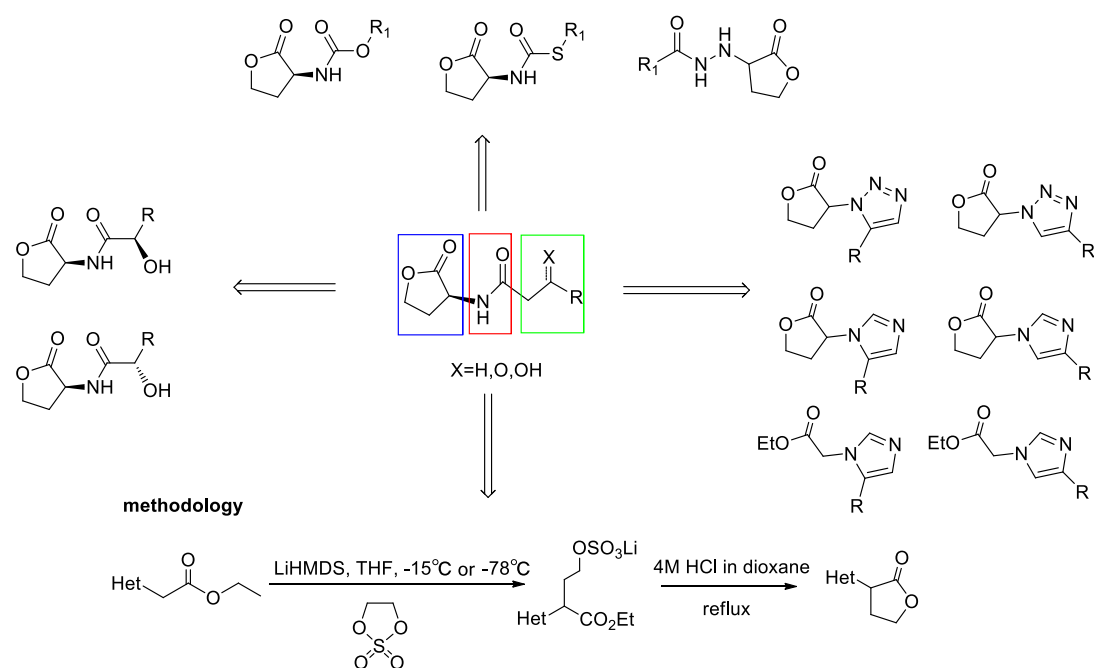


Figure 29. My project on AHLs synthesis and evaluation.

Chapter 2. Result and discussion

2.1 Studies of novel carbamate, thiocarbamate and hydrazide analogues of AHLs as *Vibrio fischeri* quorum sensing modulators

(The work reported in this section has been published in *Biomolecules*. Zhang, Q.; Queneau, Y.; Soulère, L. Biological Evaluation and Docking Studies of New Carbamate, Thiocarbamate, and Hydrazide Analogues of Acyl Homoserine Lactones as *Vibrio fischeri*-Quorum Sensing Modulators. *Biomolecules* 2020, 10, 455.)

2.1.1 Introduction

The previous bibliographic chapter has depicted in detail the bacterial quorum sensing (QS) as an important communication system that regulates various phenotypes such as bioluminescence, virulence, reproduction, and biofilm formation. Being a promising alternative to antibiotics, QS inhibition brings to bear less selective pressure that can forbid the development of bacterial resistance. In Gram-negative bacteria, the quorum sensing signal molecules are typically based on acyl homoserine lactone (AHL) skeleton, synthesized by LuxI-type synthases and detected by LuxR-type transcriptional regulators.

Our group described several AHLs analogues based on the modification on the amide function with bioisosteres such as urea [40], sulfonamide [39], reverse amide [42] and heterocycles [43,44]. As reported by Ghosh and Brindisi, compounds containing carbamate/thiocarbamate moiety are widely used as bioactive compounds with amide bioisosteres [60]. To our knowledge, a systematic study of this set of compounds is missing in the literature involving quorum sensing regulated via AHLs. Only one example, *O*-hexyl-*N*-HSL carbamate, occurred as the TraR QS modulator [61]. Following our research on urea analogues of AHLs as LuxR quorum sensing modulators [40], we report our studies towards the biological evaluation and molecular docking of synthetic carbamate and thiocarbamate analogues of AHLs. In these compounds, the additional NH group of urea AHL analogues is replaced by oxygen or a sulfur atom as shown in Figure 30. We also depicted hydrazide AHLs analogues for which the urea functional group has been reversed. The inhibition or activation activity was assessed in the *Vibrio fischeri* LuxR system for which a simple and convenient bioluminescence assay is available.

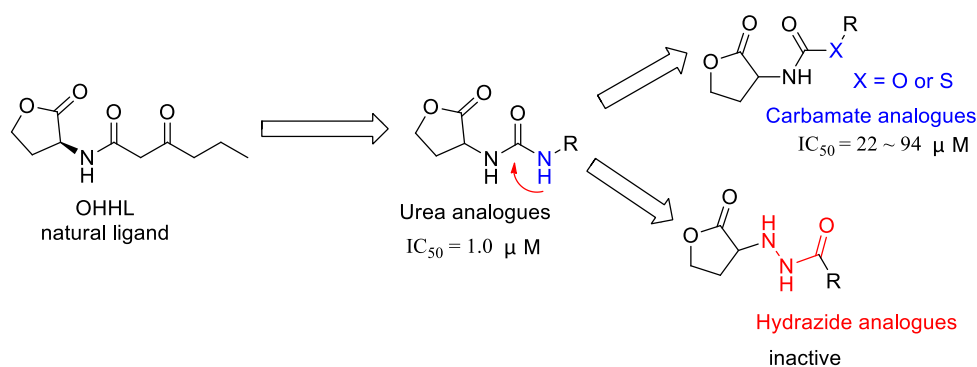
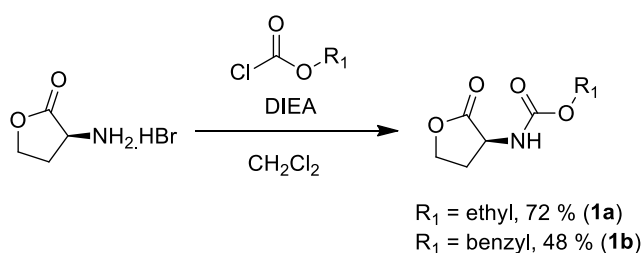


Figure 30. Design of analogues of OHHL modified on the amide group.

2.1.2 Synthesis of carbamate, thiocarbamate and hydrazide analogues of AHLs

Homoserine lactone hydrobromide in their pure enantiomeric form were prepared from L- or D-methionine as previously reported [62]. Three series of new AHL analogues were synthesized, including carbamate, thiocarbamate and hydrazide.

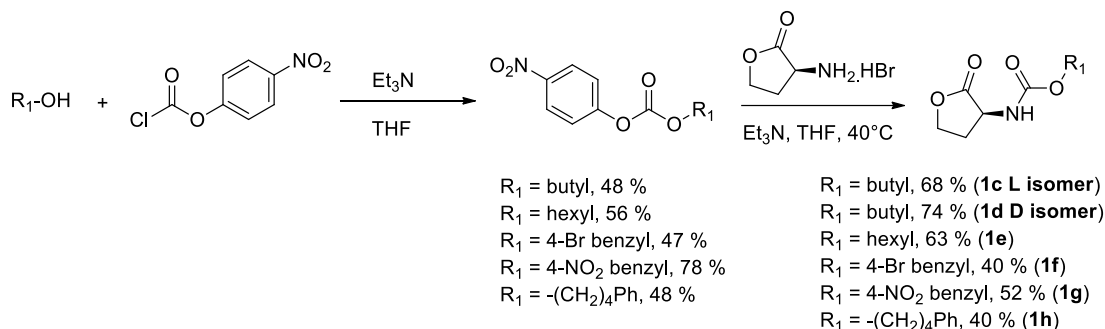
Starting from the corresponding commercially available ethyl or benzyl chloroformate, the preparation of ethyl (**1a**) and benzyl (**1b**) carbamate analogues was accomplished in 72% and 48% yield respectively (Scheme 1).



Scheme 1. Synthesis of carbamate analogues of acylhomoserine lactone.

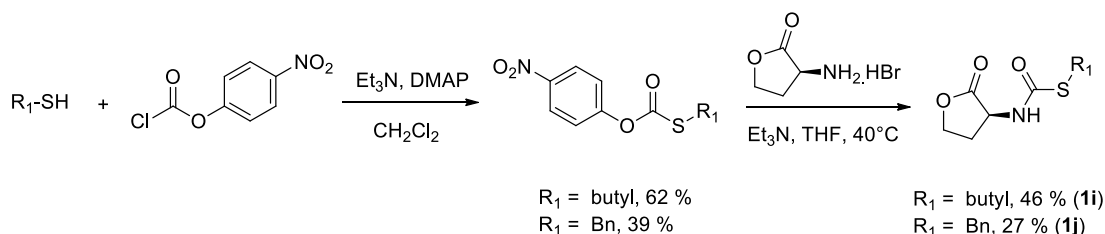
In other cases, the novel carbamate analogues were obtained in two steps. In the first step, the reaction of *para*-nitrophenyl chloroformate with various alcohols in the presence of triethylamine afforded the corresponding *para*-nitrophenyl carbonates in about 50% yields. In the second step, activated *para*-nitrophenyl carbonates were further involved in the reaction with L-homoserine lactone (Scheme 2). Meanwhile,

the D-enantiomer **1d** was prepared from D-homoserine lactone for comparing its biological activity with the L-enantiomer **1c**. Careful purification was achieved and purity was assessed using NMR spectroscopy. Thus, compounds **1c-1h** were synthesized in high purity with yields ranging from 40% to 74%.



Scheme 2. Synthesis of carbamate analogues of acylhomoserine lactone.

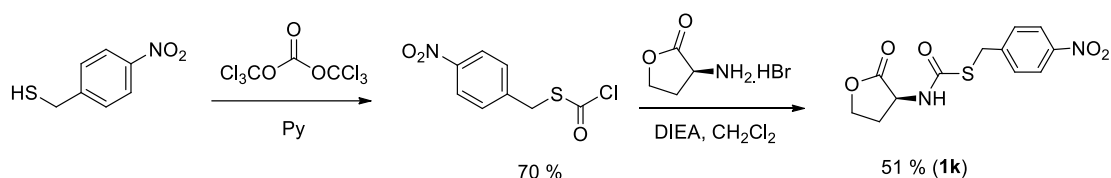
In a similar approach, the new thiocarbamate analogues were also obtained in two steps. The reaction of several thiols with *para*-nitrophenyl chloroformate was first conducted to generate activated *para*-nitrophenyl thiocarbonates which were further reacted with L-homoserine lactone. The desired product **1i** was obtained in an acceptable yield (Scheme 3). In the preparation of the compound **1j**, the starting material *para*-nitrophenyl thiocarbonate was never fully consumed in the coupling reaction, and remained not totally converted even at 60 °C overnight. Thus, the final product **1i** was obtained in low yield.



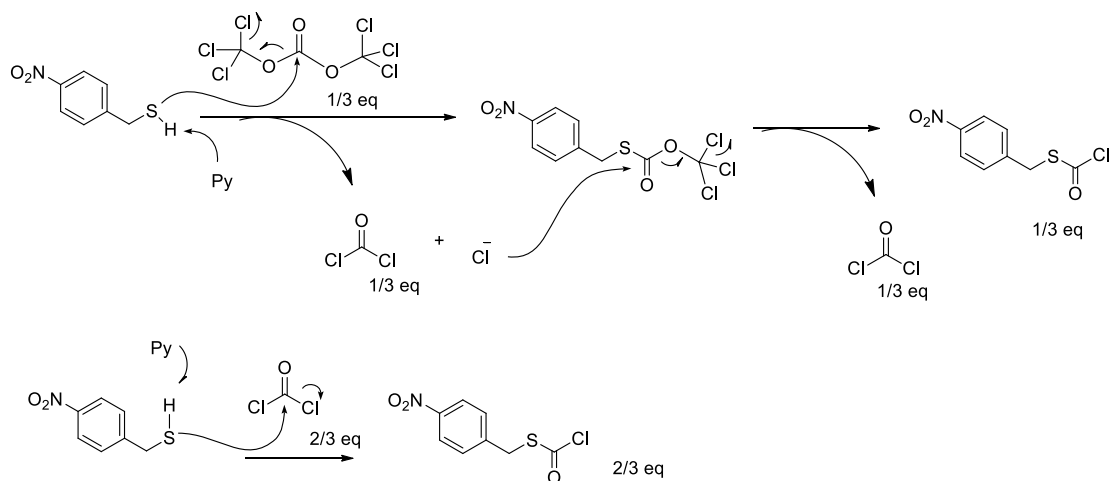
Scheme 3. Synthesis of thiocarbamate analogues of acylhomoserine lactone.

We failed to get the product **1k** using the above synthetic route owing to the problematic purification of the corresponding intermediate *para*-nitrophenyl

thiocarbonate. Then we turned our attention to an alternative approach. The preparation of **1k** was achieved by coupling *S*-4-nitrobenzyl chlorothioformate and L-homoserine lactone in the presence of DIEA (Scheme 4). For this purpose, *S*-4-nitrobenzyl chlorothioformate was first synthesized by the reaction of 4-nitrobenzylmercaptan with triphosgene (triphosgene is a toxic white solid, due to decomposition at high temperature or under wet conditions even trace of water. The reagent must be carefully handled) [63]. In this process, only 1/3 equivalent triphosgene was needed to provide 1.0 equivalent phosgene. The possible mechanism of chlorothioformate formation in the reaction of triphosgene was shown in Scheme 5.



Scheme 4. Synthesis of thiocarbamate and hydrazide analogues of acylhomoserine lactone.

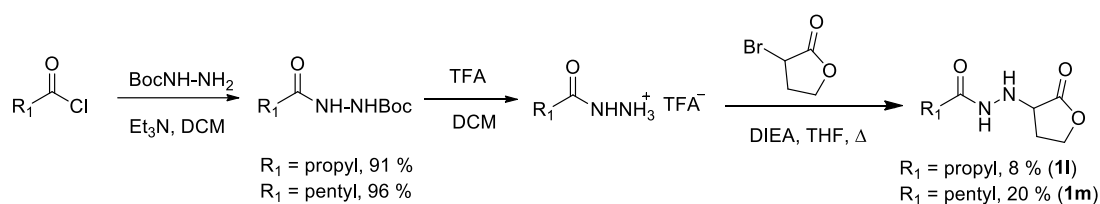


Scheme 5. Possible mechanism of chlorothioformate formation in the reaction with triphosgene.

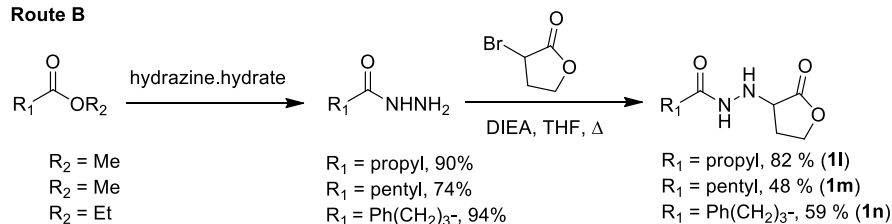
For hydrazide analogues, we envisaged two different routes (Scheme 6). In route A, the tert-butyloxycarbonyl (Boc) group protected hydrazine reacted with two different acyl chlorides leading to the formation of Boc protected hydrazides. Subsequent deprotection by TFA gave hydrazides which were further alkylated with

α -bromo- γ -butyrolactone. Unfortunately, the alkylation step gave a very low yield even the excess amount of DIEA was used. In the route B, the reaction of hydrazine with various esters gave the corresponding hydrazides which were further subjected to the alkylation step with α -bromo- γ -butyrolactone. The final hydrazides AHLs analogues **1l-1n** were obtained in good yield over 2 steps. Also, it was worthy to note that the reaction of hydrazine with ethyl acetoacetate gave cyclic product pyrazolone derivative instead of 3-oxobutan hydrazide.

Route A



Route B



Scheme 6. Synthesis of hydrazide analogues of acylhomoserine lactone.

2.1.2.1 Characterization of carbamate, thiocarbamate and hydrazide analogues of AHLs

All new synthetic compounds were characterized by ^1H NMR, ^{13}C NMR, 2D-NMR, high resolution mass spectrometry and IR spectrum. Full assignment of the signals has been accomplished by NMR techniques. For these types of AHLs analogues, we take compound **1c** as an example to show the identification of its structure. It was clear to find NH at 5.39 ppm coupling with CH at 4.39 ppm, which was overlapped with one proton of the OCH_2 of lactone. Another proton of OCH_2 of lactone was found at 4.24 ppm. The two protons of CH_2 of lactone were also observed at different chemical shifts, 2.73 and 2.21 ppm, respectively. The OCH_2 of side chain as triplets at 4.07 ppm and the other protons of side chain at 1.5~0.7 ppm were identified (Figure 31).

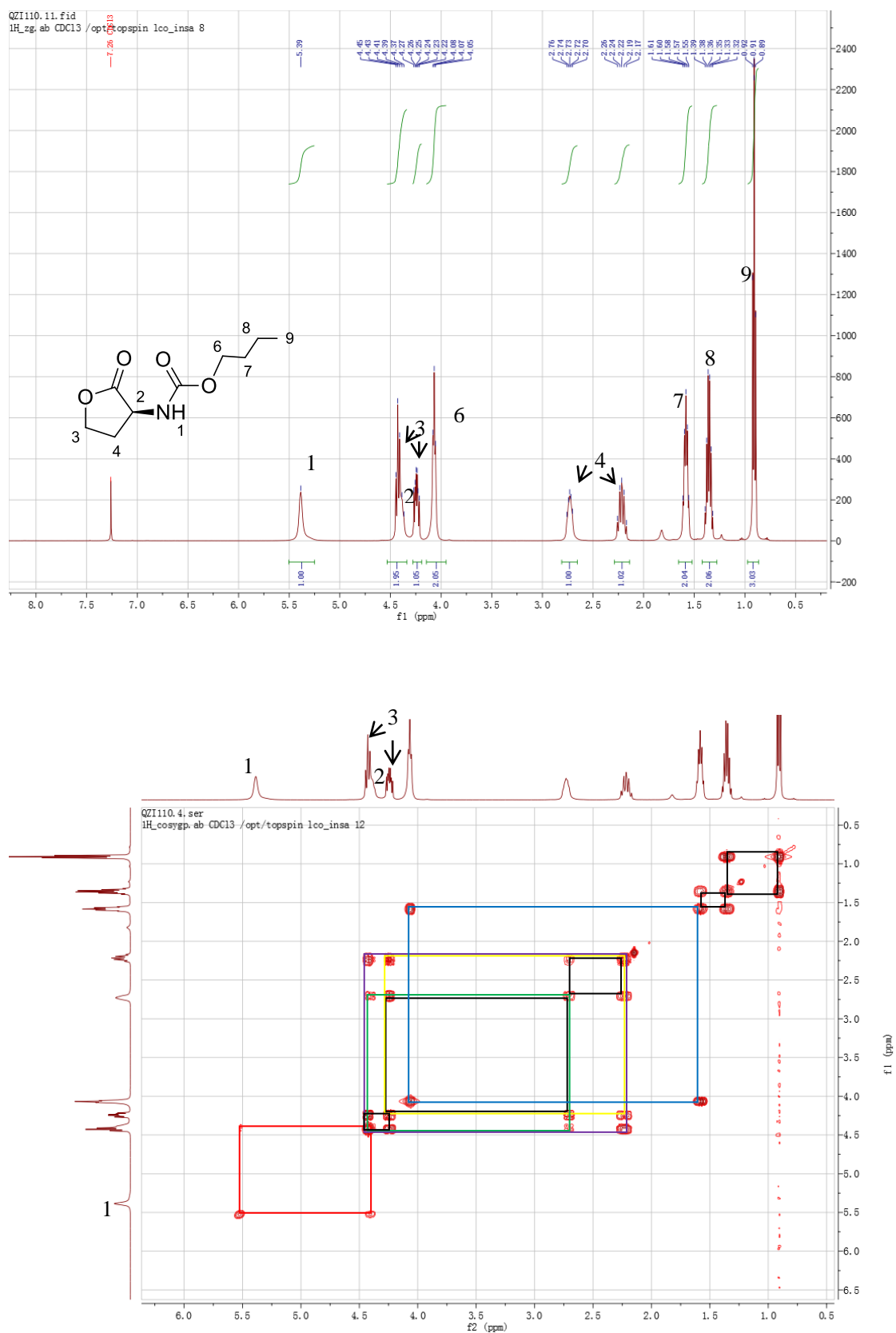


Figure 31. ^1H NMR and ^1H - ^1H cosy of **1c**. Identifications of each proton and each H-H correlation are shown, leading to unambiguous identification of compound **1c**.

For the ^{13}C NMR signals analysis of **1c**, it is easy to identify with the help of the HSQC 2D experiment. Two carbonyl carbon signals appeared at 175.2 and 156.5 ppm, which were also detected by IR spectra. The carbon signal of the OCH_2 group in the lactone was always found around 65.8 ppm, the signal of CH_2 in lactone around 30.3 ppm, the signal of CH in lactone around 50.4 ppm (Figure 32).

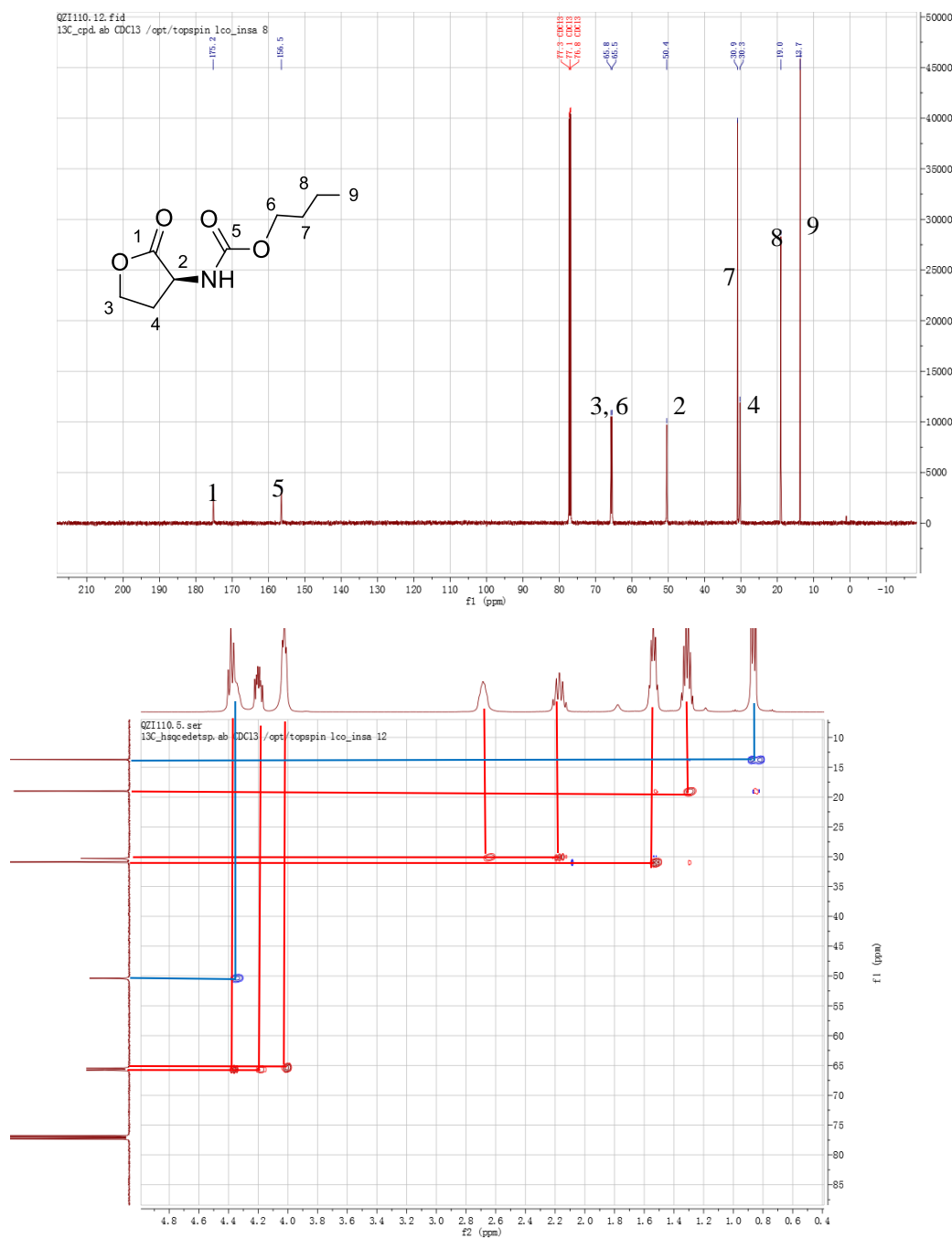


Figure 32. ^{13}C NMR and HSQC of **1c**. Identifications of each proton and each C-H correlation are shown, leading to unambiguous identification of compound **1c**.

It is known that *O*-thiocarbamates can isomerize to *S*-thiocarbamate at high temperature. To make sure that our compounds possess the right *O*-thiocarbamate functional group, we investigated carefully the NMR assignment and IR spectra of all thiocarbamate analogues. IR spectra showed that two carbonyl group signals appeared around 1775cm^{-1} and 1650cm^{-1} as it is anticipated for *O*-thiocarbamate systems.

2.1.3 Biological evaluation

All final compounds synthesized above were subjected to biological evaluation. The goal was to assess their ability to induce bioluminescence (agonistic activity) or to decrease bioluminescence (antagonistic activity) in the presence of 200 nM 3-oxo-hexanoyl-L-homoserine lactone (OHHL) [64]. For this purpose, our test is based on a recombinant *Escherichia coli* strain NM522 having the sensor plasmid pSB401 which are equipped with specific genes from *Vibrio fischeri* responsible for the QS-regulated bioluminescence measured by a luminometer. Bacteria were grown at 30 °C for 18h. Then this bacterial culture was diluted 10 times with culture media in the assay using 96 wells plates (100 μL per well). For agonistic activity, serially diluted compounds were tested in DMSO (max 2% in a total volume of 200 μL of LB). For antagonistic activity, serially diluted compounds were tested in competition with OHHL (200 nM) in DMSO (max 2% in a total volume of 200 μL).

Examination of the three series of AHL analogues revealed that some compounds exhibited activity as quorum sensing modulators. While the three hydrazide AHL analogues **1l-1n** with different acyl chains were deprived of any activity, the ethyl carbamate derivative (**1a**) was found to be a very weak agonist by inducing at 200 μM 18% of the bioluminescence obtained with the natural ligand OHHL at a concentration of 200 nM. The better antagonistic activity was found in the group of carbamate or thiocarbamate analogues. Indeed, a considerable decrease of the bioluminescence produced by 200 nM OHHL was observed for compounds **1b-1c**, **1e-1g** and **1i-1k** at 100 μM (Figure 33). In order to present the influence of configuration on biological activity, the butyl carbamate derivative **1c** and its

D-isomer **1d** were compared. The results show that residual bioluminescence of 42% was measured for **1c** versus 89% for **1d**. The hexyl carbamate analog **1e** was the most active alkyl carbamate analogs with 22% remaining luminescence observed. Around 10% residual bioluminescence was observed for the aromatic substituted carbamate or thiocarbamate analogs **1g**, **1k** which were the most active aromatic analogs. Interestingly, the thiocarbamates analogs **1i** and **1j** were found more active than the corresponding carbamate analogs counterparts **1c** and **1b**.

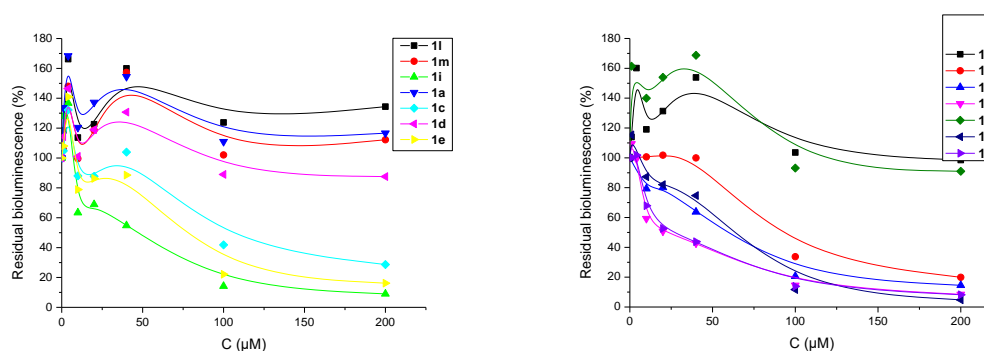


Figure 33. Antagonistic activity of carbamate, thiocarbamate and hydrazide analogs **1a-1n**: Residual bioluminescence observed for all compounds.

We determined IC_{50} values for compounds **1b**, **1c**, **1e-1g**, **1i-1k** (antagonist activity) with an increasing concentration of each compound in competition with 200 nM of OHHL (Table 2). IC_{50} values ranging from 22 μ M to 94 μ M were measured. Given predicted logP, we speculated that the hydrophobic properties would be important for the antagonistic activity, thus we considered butyl (**1c**) versus hexyl (**1e**) substituents and benzyl (**1b**) versus 4-bromobenzyl (**1f**) substituents. Comparing **1c** with **1i**, and **1b** with **1j**, the results showed that thiocarbamates were more active than their oxygenated counterparts, which could be related to the higher value of predicted logP. Our most active antagonists (4-nitrobenzyl derivatives **1g** and **1k**) exhibited an IC_{50} value of 22-23 μ M. Although logP of **1g** was lower than **1k**, no similar influence of the presence of the sulfur was found. Therefore, these different observations suggested that the presence of 4-nitro substituent seems to be the most important factor leading to the same antagonistic activity.

Compounds	Predicted logP	IC ₅₀ (μM)
Bn (1b)	1.14	86 (± 3)
Butyl (1c)	0.65	94 (± 1)
Hexyl (1e)	1.19	73 (± 3)
4-BrBn (1f)	1.97	64 (± 4)
4-NO₂Bn (1g)	0.51	22 (± 3)
ButylS (1i)	1.22	45 (± 7)
BnS (1j)	1.71	64 (± 3)
4-NO₂BnS (1k)	1.17	23 (± 4)

Table 2. Predicted logP and IC₅₀ values for compounds **1b**, **1c**, **1e-1g** and **1i-1k**. IC₅₀ values were assessed with an increasing concentration of each compound against 200 nM OHHL.

2.1.4 Docking study

To understand the structure-activity relationships in this series, we studied the binding modes of these compounds based on the LuxR model. 3D structures of the compounds were drawn with Vega ZZ. This previously reported LuxR model was used in docking experiment which was realized by using Arguslab [65].

The results of binding modes for active compounds as flexible ligands are shown in Table 3. The docking results showed that all the compounds induced the hydrogen bonds with Trp66 and Asp79 like the natural ligand OHHL does. As reported above, compound **1a** bearing a small ethyl substituent is an agonist. Consistently, the observed binding mode for **1a** was similar compared with the natural ligand. They displayed the same hydrogen bond network, only with some differences in terms of distances.

Compounds **1c**, **1e**, **1i** are more hydrophobic due to their longer alkyl chain. Interestingly, they led to slightly different docking results as compared with the natural ligand and shorter chain analogs. The additional oxygen atom of the carbamate function and the alkyl chain jointly orientate the carbamate part of the molecules towards Tyr70 leading to hydrophobic interactions. A supplementary

hydrogen bond with Tyr70 (a conserved residue in the LuxR proteins family) was also found. Because of a distance superior to 3.5 Å between the C=O of the carbamate and Tyr62, this particular orientation makes the usual hydrogen bond with Tyr62 absent in this case. The binding mode for compounds bearing an aromatic substituent is generally due to attractive interactions (hydrophobic interaction, π - π stacking interaction) and a hydrogen bond with Tyr70.

Compounds	Trp66	Asp79	Tyr62	Tyr70	Lys178
OHHL	+2.34 (C=O lactone)	+3.01 (NH)	+3.01 (C=O amide)	-	-
Ethyl (1a)	+2.44 (C=O lactone)	+3.0 (NH)	+2.91 (C=O carbamate)	-	-
Bn (1b)	+2.89 (C=O lactone)	+2.98 (NH)	-	+3.01 (O carbamate)	-
Butyl (1c)	+2.20 (C=O lactone)	+2.92 (NH)	-	+2.97 (O carbamate)	-
Hexyl (1e)	+2.22 (C=O lactone)	+2.98 (NH)	-	+2.61 (O carbamate)	-
4-BrBn (1f)	+2.35 (C=O lactone)	+2.95 (NH)	+3.01 (C=O carbamate)	+3.32 (O carbamate)	-
4-NO ₂ Bn (1g)	+2.07 (C=O lactone)	+2.99 (NH)	-	+3.04 (O carbamate)	++ 2.22 and 3.05 (NO ₂)
ButylS (1i)	+2.63 (C=O lactone)	+3.00 (NH)	+3.09 (C=O carbamate)	+3.19 (S carbamate)	-
BnS (1j)	+2.89 (C=O lactone)	+2.98 (NH)	+3.13 (C=O carbamate)	+3.08 (S carbamate)	-
4-NO ₂ BnS (1k)	+2.12 (C=O lactone)	+3.14 (NH)	-	+ 3.25 (S carbamate)	++ 1.96 and 3.85 (NO ₂)
Hydrazide (1l)	+2.45 (C=O lactone)	+2.94 (NH)	-	+ 2.21 (C=O hydrazide)	-

Table 3. Occurrence and distances for hydrogen bonds between Trp66, Asp79, Tyr 62, Tyr70 and the main chemical functions of studied compounds with distances (Å). + indicates a possible H-bond; the function implicated is indicated in brackets.

Thiocarbamate derivatives **1i**, **1j** give docking results different from their oxygenated carbamate derivatives **1c**, **1b**. Apart from the observation of an additional hydrogen bond with Tyr70 [66], a hydrogen bond between the C=O of the thiocarbamate group and Tyr62 was observed. But this interaction was not observed in the carbamate derivatives **1c**, **1b**. This different interaction may explain the stronger activity of the thiocarbamate derivatives than their corresponding carbamate derivatives for the

non-nitrated compounds. Overall, an additional hydrogen bond with the residue Tyr70 seems to be encountered with carbamates and thiocarbamates. This residue was found to be particularly important for interactions with AHLs analogues in LasR (Tyr70 is equivalent to Tyr64 in LasR) [67].

The proposed binding mode of compound **1c** taken as an example is depicted in Figure 34 as well as the binding mode of the most active compound **1g**. This latter compound seems to be a robust binder of LuxR due to an overall binding mode already described above as well as additional hydrogen bonds involving the nitro group with Lys178 which probably favored the binding of this antagonist. The same explanation may be also formulated for the thiocarbamate **1k** bearing a nitro substituent, this latter group which seems to be predominant as these two compounds exert the same activity.

For hydrazide analogues, docking study of compound **1l** revealed that the carbonyl of the hydrazide group is involved in a hydrogen bond with Tyr70 and is not located at the place as it is usually for natural ligands or other type of analogues such as the butyl urea [40] or carbamates analogues (Figure 34C). This opposite orientation may be correlated to the lack of activity of these compounds.

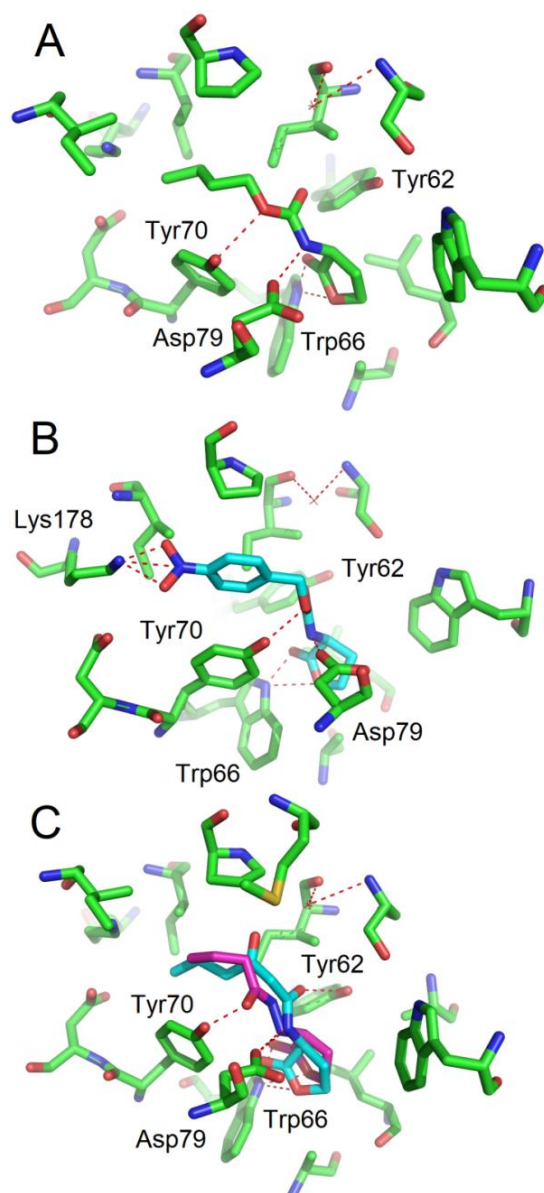


Figure 34. Proposed binding modes of compounds **1c** (A) and **1g** (B) and **1l** (magenta) and OHHL (cyan) (C) within the binding site of the LuxR model obtained by docking experiments. Hydrogen bonds are indicated in red dashes.

2.1.5 Conclusions

Novel types of AHL analogs having the amide replaced by bioisosteric hydrazides, carbamates and thiocarbamates have been synthesized and evaluated concerning their quorum sensing activity in the *Vibrio fischeri* system. This series based on the carbamate/thiocarbamate functional group led to both agonistic and antagonistic activities and the activity could be discussed in terms of hydrogen bond network and

key interactions within the receptor binding site thanks to docking experiments. The supplementary oxygen or sulfur atom is proposed to be involved in a new hydrogen bond with Tyr70, an important conserved residue in the LuxR family. This study showed the potentialities of this group to mimic the amide group for fine-tuning QS modulation.

2.2 2-Hydroxy AHL analogs: synthesis and biological evaluation in *Vibrio fischeri* quorum sensing

(The work reported in this section has been published in *Bioorganic Chemistry*. Qiang Zhang, Erwann Jeanneau, Yves Queneau, Laurent Soullère, (2*R*)- and (2*S*)- 2-hydroxy- hexanoyl and octanoyl-L-homoserine lactones: New highly potent Quorum Sensing modulators with opposite activities, *Bioorganic Chemistry*, 2020, 104, 104307.)

2.2.1 Introduction

Acyl homoserine lactones (AHLs) are structurally different according to the bacteria and is shown in Figure 35. One important structural feature is the possible presence on the acyl chain of a 3-oxo, like in the case of *Vibrio fischeri* or *Pseudomonas aeruginosa*, or of a (3*R*)-hydroxyl functional group, like in the case of *Vibrio harveyi* [68].

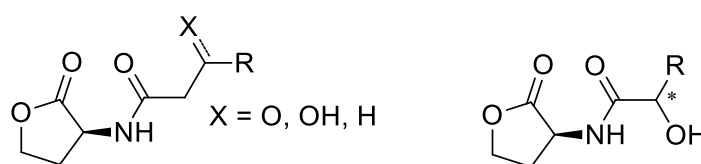


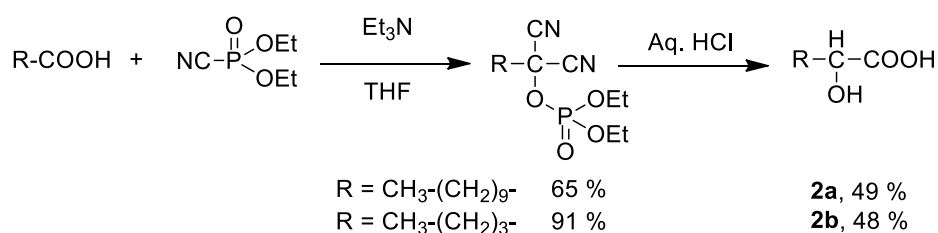
Figure 35. Structure of AHLs as autoinducers in Gram negative bacteria and of a new series of analogs with a hydroxyl group in position 2.

It is known that the 3-oxo group can bind one water molecule bridging with residues in the LuxR receptor of some bacterial strains [69]. Very little has been reported on variations in the position of the oxo or OH groups. For 2-oxo analogs, only two publications mention them, as inactive compounds [70,71]. For the 3-OH compounds, the influence of the configuration has been investigated with respect to the activity in the pathogen *Acinetobacter baumannii*. Both (3*R*) and (3*S*) hydroxyl C12 homoserine-L-lactone diastereoisomers exerted agonistic activities, the (3*R*) isomer being the more active and likely the natural autoinducer [45]. However, 2-hydroxy AHL analogs have not been investigated systematically. Only one paper mentions 2-hydroxybutanoyl homoserine lactones, but as a mixture of the four possible isomers (2*R* or *S* and homoserine D or L) and reported as inactive on *Vibrio harveyi* QS [72].

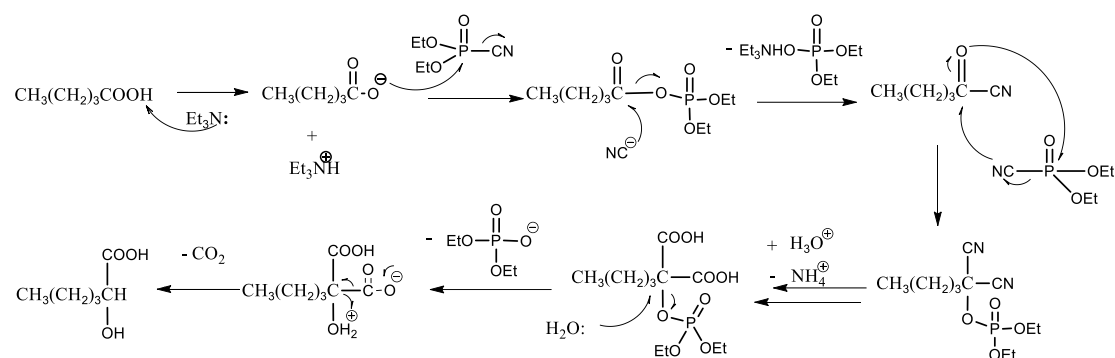
The work described below aims at giving a complete and systematic view of the 2-OH modification on the acyl chain of AHLs, with their synthesis in enantiomerically pure form, their biological evaluation and docking studies.

2.2.2 Synthesis of 2-hydroxy AHL analogs

To synthesize 2-hydroxy AHLs, the starting 2-hydroxy carboxylic acids is first required. 2-Hydroxy carboxylic acids are very important both as synthetic intermediates and in themselves. Some hydroxy acids required for our study were not commercially available, even as racemic mixtures, so we had to prepare them. Many methods have been explored for their preparation, including regioselective 2-hydroxylation of fatty acids by biocatalysts [73]. Another previously explored reaction [74] used to prepare 2-hydroxy carboxylic acid involves first the treatment of the carboxylic acid with diethyl phosphorocyanidate (DEPC) in presence of trimethylamine, affording a dicyanophosphate (Scheme 7). In a second step, the intermediate dicyanophosphate is hydrolyzed in acidic condition. Overall, this route provides 2-hydroxy carboxylic acid with one carbon extension, starting from a carboxylic acid. The possible mechanism of this synthetic route is suggested in Scheme 8. The reaction starts with the initial formation of the acyl cyanide, followed by an addition to carbonyl group with a second equivalent DEPC to afford the dicyanophosphate. Subsequent hydrolysis of the two cyano group and the phosphate group affords the target product along with phosphate ammonium salt and carbon dioxide. Using this method, we prepared racemic 2-hydroxy hexanoic or dodecanoic acid.

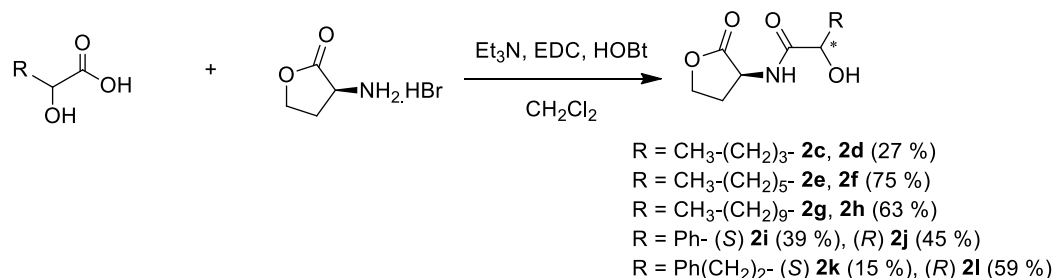


Scheme 7. Synthesis of 2-hydroxy carboxylic acids.



Scheme 8. Possible mechanism of 2-hydroxy carboxylic acid formation.

The 2-hydroxy acids were then coupled with L-homoserine lactone in the presence of 1-hydroxybenzotriazole (HOBt) and using 1-(3-dimethylaminopropyl)-3-ethyl carbodiimide (EDC) as a coupling agent (Scheme 9). For the reaction starting from the racemic 2-hydroxy hexanoic, octanoic or dodecanoic acids, two diastereoisomers were produced, which were separated by column chromatography. For the coupling reaction starting from commercially available (*R* or *S*)-mandelic acid, (*R* or *S*)-2-hydroxy-4-phenylbutyric acid, the final desired products were achieved.



Scheme 9. Synthesis of 2-hydroxy acylhomoserine lactones

2.2.2.1 Characterization of 2-hydroxy AHL analogues

All the compounds were confirmed by ^1H NMR, ^{13}C NMR, 2D-NMR and high resolution mass spectrometry. To determine the configuration of the two diastereoisomers, X-ray diffraction experiment of the single crystal was conducted for compound **2e**. The data gave clear evidence that compound **2e** exhibited a 2-*S* configuration for the carbon atom with the hydroxyl functional group (Figure 36).

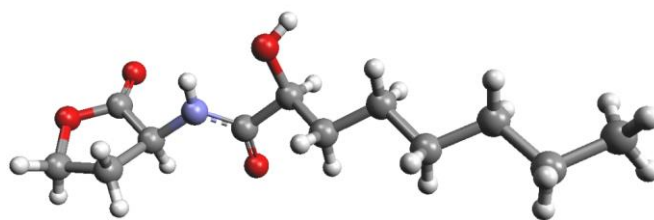


Figure 36. Tridimensional structure of diastereoisomer **2e** from XRD

A careful comparison of all NMR data (Table 4) led to the observation that compounds **2c** and **2g** shared very similar chemical shifts and coupling constants of some key protons with compound **2e**. And their isomers compounds **2d** and **2h** exhibited very similar chemical shifts and coupling constants of some key protons as compound **2f**. So compounds **2c** and **2g** were speculated as *S* configuration, their isomers as *R* configuration.

Compounds/ Proton	CH-NH (δ , J)	OCHH-lactone (δ , J)	OCHH-lactone (δ , J)	CH-OH (δ , J)
2-OH-HHL 2c (Chloroform- <i>d</i>)	4.77 (dt, J = 11.7, 8.4 Hz)	4.46 (td, J = 9.1, 1.3 Hz)	4.29 (ddd, J = 11.2, 9.2, 6.0 Hz)	4.17 (dt, J = 8.3, 4.1 Hz)
2-OH-HHL 2d (Chloroform- <i>d</i>)	4.55 (ddd, J = 11.1, 8.7, 6.9 Hz)	4.49 (td, J = 9.0, 1.5 Hz)	4.29 (ddd, J = 10.9, 9.2, 6.2 Hz)	4.14 (dt, J = 8.1, 4.1 Hz)
(<i>S</i>)-2-OH-OHL 2e (Chloroform- <i>d</i>)	4.74 (ddd, J = 11.8, 8.7, 7.5 Hz)	4.47 (td, J = 9.0, 1.2 Hz)	4.30 (ddd, J = 11.2, 9.3, 6.0 Hz)	4.18 (ddd, J = 8.5, 5.0, 3.7 Hz)
(<i>R</i>)-2-OH-OHL 2f (Chloroform- <i>d</i>)	4.55 (ddd, J = 11.3, 8.8, 6.9 Hz)	4.49 (td, J = 9.1, 1.4 Hz)	4.29 (ddd, J = 10.6, 9.2, 6.1 Hz)	4.14 (ddd, J = 8.7, 5.3, 3.8 Hz)
2-OH-dDHL 2g (Chloroform- <i>d</i>)	4.75 (dt, J = 11.7, 8.2 Hz)	4.47 (td, J = 9.0, 1.2 Hz)	4.29 (ddd, J = 11.2, 9.2, 5.9 Hz)	4.17 (dd, J = 8.2, 3.7 Hz)
2-OH-dDHL 2h (Chloroform- <i>d</i>)	4.55 (ddd, J = 11.4, 8.8, 6.9 Hz)	4.49 (td, J = 9.1, 1.5 Hz)	4.29 (ddd, J = 11.0, 9.3, 6.2 Hz)	4.14 (dd, J = 8.2, 3.8 Hz)

Table 4. Comparison of ^1H NMR chemical shifts and coupling constants in the series.

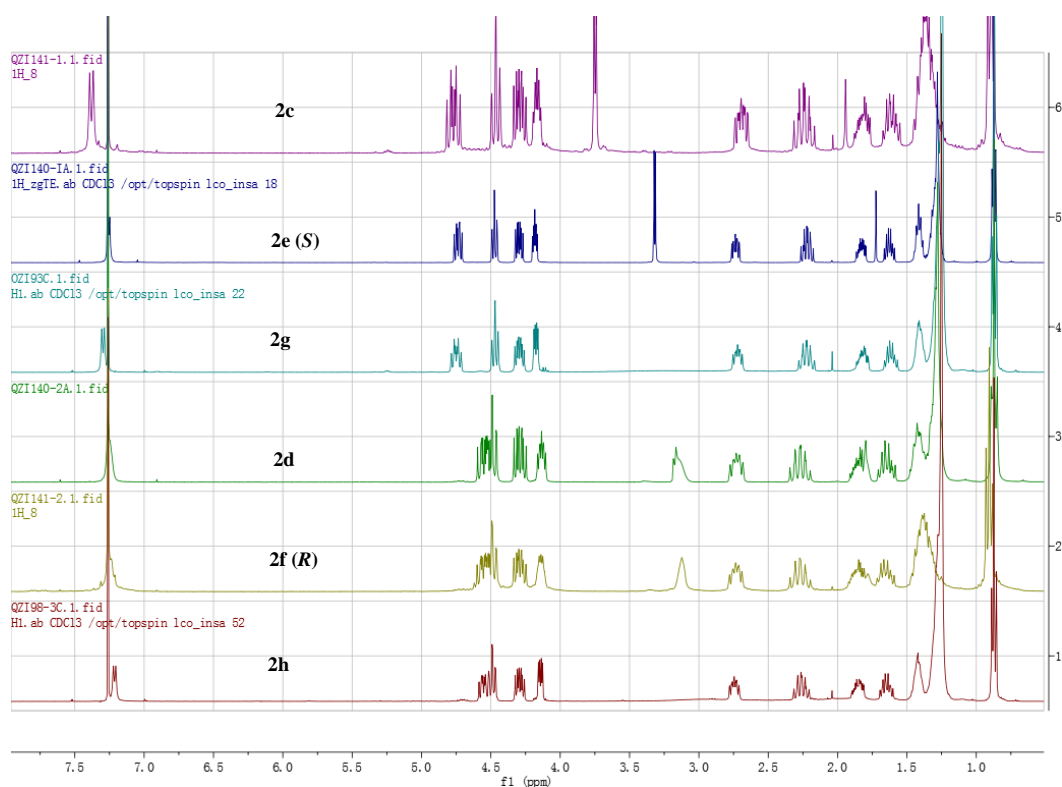


Figure 37. Comparison of ^1H NMR chemical shifts in the series.

After the comparison of proton chemical shift, the rotation value of these compounds were examined and compared. The results as shown in Table 5 also supported this conclusion to some degree. For comparison of ^{13}C NMR chemical shifts, it is logical that these compounds share similar ^{13}C NMR chemical shifts (Table 6).

configuration/ compound	<i>S</i>	<i>R</i>
2-OH-HHL	$[\alpha]^{24}_D = -60$ (c=0.5, acetone).	$[\alpha]^{24}_D = +9.6$ (c=0.4, acetone)
2-OH-OHL (2c)	$[\alpha]^{24}_D = -47.3$ (c=0.5, acetone)	
2-OH-OHL (2d)	$[\alpha]^{24}_D = +6.2$ (c=0.3, acetone)	
OH-dDHL (2g)	$[\alpha]^{24}_D = -36$ (c=0.4, acetone).	
OH-dDHL (2h)	$[\alpha]^{24}_D = 0$ (c=0.6, acetone).	
2-OH-PAHL	$[\alpha]^{24}_D = +14$ (c=0.4, acetone)	$[\alpha]^{24}_D = -59$ (c=0.6, acetone)
2-OH-PBHL	$[\alpha]^{24}_D = -35$ (c=0.5, acetone)	$[\alpha]^{24}_D = -8.3$ (c=0.5, acetone)

Table 5. Comparison of rotation values in the series.

Compounds	CH-OH (δ)	OCH ₂ -lactone (δ)	CH-NH (δ)	CH ₂ -lactone (δ)
Chloroform- <i>d</i>				
2-OH-HHL 2c	72.2	66.0	48.2	29.7
2-OH-HHL 2d	72.2	66.1	48.8	29.6
(<i>S</i>)-2-OH-OHL 2e	72.3	66.0	48.3	29.9
(<i>R</i>)-2-OH-OHL 2f	72.2	66.1	48.8	29.6
2-OH-dDHL 2g	72.3	66.6	48.3	29.6
2-OH-dDHL 2h	72.3	66.1	48.8	29.6
(<i>S</i>)- 2-OH-PBHL 2k	71.5	66.0	48.3	29.7
Acetone- <i>d</i> ₆				
(<i>S</i>)-2-OH-PAHL 2i	73.9	65.2	48.0	28.7
(<i>R</i>)-2-OH-PAHL 2j	74	65.2	48.1	28.5
(<i>R</i>)-2-OH-PBHL 2l	70.8	65.2	47.9	28.6

Table 6. Comparison of ¹³C NMR chemical shifts in the series.

2.2.3 Biological evaluation

Having in hands the collection of novel and enantiomerically pure 2-OH AHL analogues, we could undertake the evaluation of their biological properties. Using the same *Vibrio fischeri* assay as the one used in the previous section, all synthetic compounds were evaluated for their capacity to induce the bioluminescence or inhibit the bioluminescence in the presence of the natural ligand. Thus, variations in chain length, presence of an aromatic moiety and the effect of the (*S/R*) configuration of the carbon atom with hydroxyl functional group on agonistic or antagonistic activities could be investigated.

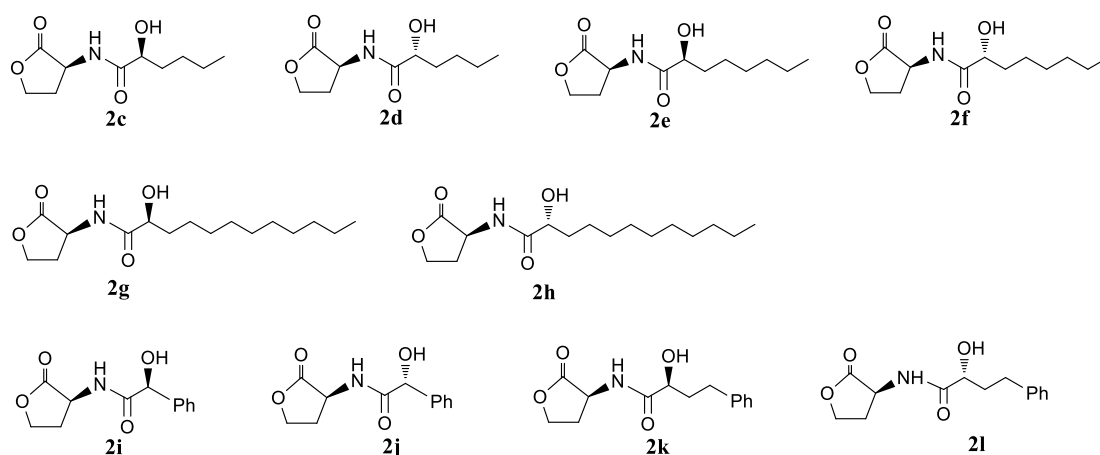


Figure 38. All structures of 2-OH AHL analogues in this study.

After EC_{50} and IC_{50} values were determined, we could observe striking differences between the short chain compounds **2c-2f** as compared to longer chain analogues. Indeed, short chain compounds **2c** and **2e**, both being *2S* isomers, were found agonists with EC_{50} values of 15-16 μ M whereas the other diastereoisomers (*2R*) **2d** and **2f** were found to be potent antagonists with IC_{50} values of 11 and 4 μ M, respectively. For the other compounds equipped with longer chains or phenyl group, both *2S* and *2R* compounds exhibited similar biological activities, all being antagonists with IC_{50} values ranging from 15 to 84 μ M. Thereby, the analogues in the series which are structurally far away from the natural ligand OHHL exert an antagonistic activity whatever their configuration at C-2.

Though both strong antagonists at low concentrations, compounds **2d** and **2f** displayed also a weak agonistic activity at high concentrations. Similarly, diastereoisomers **2k** and **2l**, both antagonists at low concentrations, exerted a weak agonistic activity at high concentrations in particular for the (*S*) 2-hydroxy isomer **2k**.

Overall, the main observation of this biological evaluation showed the high potency of 2-hydroxy hexanoyl HSL and 2-hydroxy octanoyl HSL, with opposite activity depending on the *R/S* configuration of the carbon atom bearing the hydroxyl group.

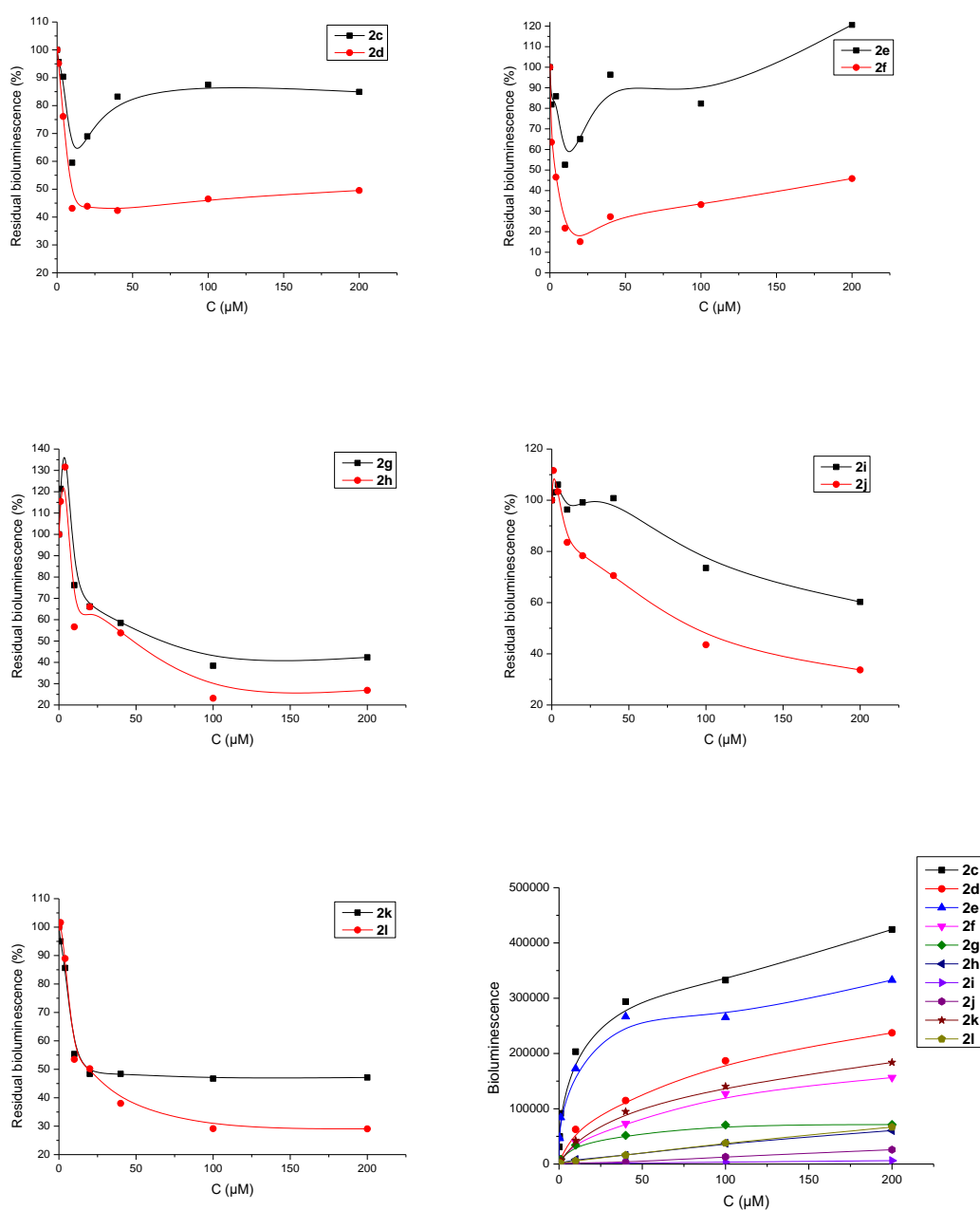


Figure 39. Curves for antagonistic activities and agonistic activities of all compounds.

2.2.4 Docking study

Molecular modeling using the LuxR model was used for docking experiments to get insight into the structure-activity relationship in this series also. Below, the docking results for the isomers (*S*)-2-OH hexanoyl HSL, (*R*)-2-OH hexanoyl HSL are presented. Interestingly, the (*S*)-isomer adopts a binding mode very close to the

natural ligand, with the same hydrogen bonds network, and importantly, with the hydroxyl group involved in a hydrogen bond with the water molecule just like the 3-oxo function does. In contrast, the (*R*)-isomer gave a different result regarding the hydroxyl group involved in hydrogen bonds with Tyr70 and Asp79, two important residues strictly conserved in the LuxR family [75]. This molecular modeling study, together with the biological evaluation suggests strongly that (*S*)-isomer is leading to the agonistic activity and the (*R*)-isomer is leading to antagonistic activity.

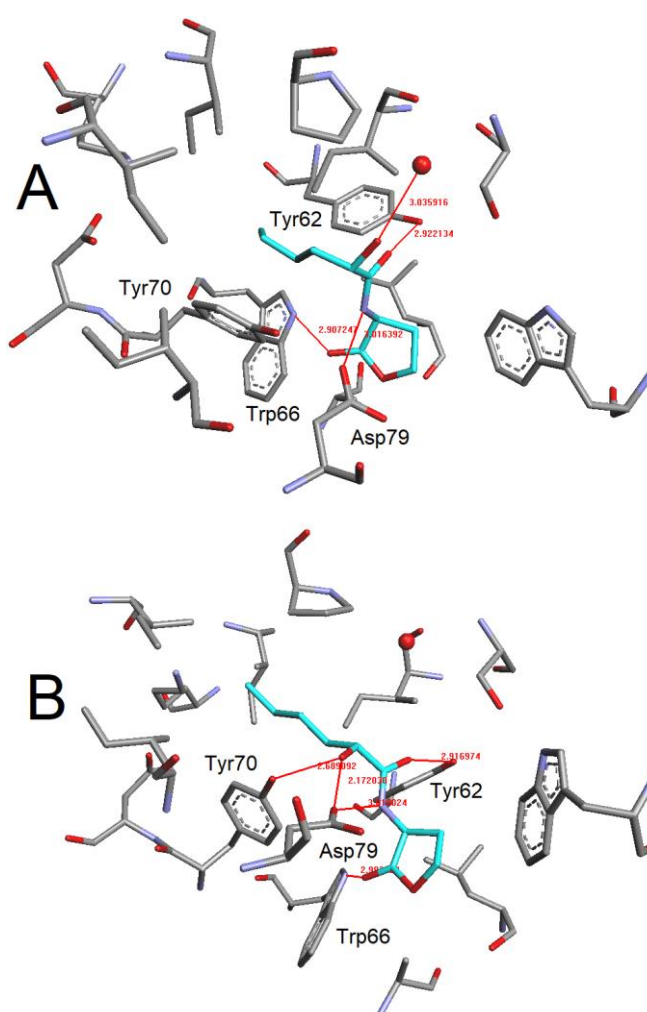


Figure 40. Docking results of the diastereoisomers (*S*)-2-OH hexanoyl HSL (**A**), (*R*)-2-OH hexanoyl HSL (**B**) within the binding site of the LuxR model.

2.2.5 Conclusions

In summary, our work on 2-hydroxy AHL analogs as *Vibrio fischeri*-quorum sensing modulators has resulted in the identification of novel potent QS modulators and shown that the configuration at C-2 was essential for directing the activity towards either agonistic or antagonistic for short chain compounds. The docking experiments could confirm the importance of specific H-bonds within the binding site, consistent with the results obtained from the biological assays. The two diastereoisomers of 2-hydroxy hexanoyl HSL and 2-hydroxy octanoyl HSL are among the most potent compounds we have ever studied.

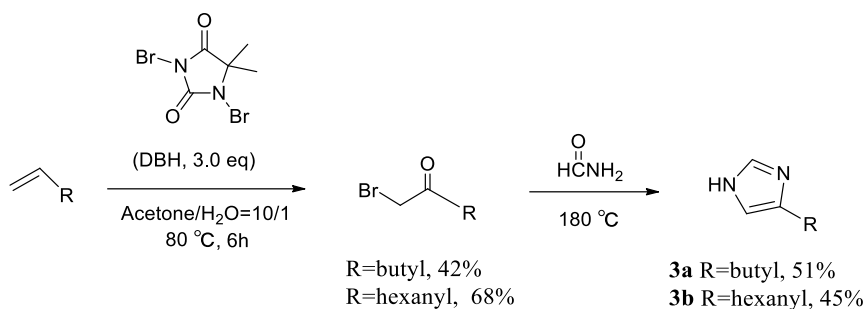
2.3 Studies of new AHL analogs based on imidazole or triazole scaffolds

2.3.1 Introduction

Imidazole and triazole are important motifs frequently considered as scaffolds to design bioactive compounds or pharmaceutical agents. In this part of the thesis, we investigated new QS modulators designed by replacing the amide function of AHLs with heterocyclic rings which are proper bioisosteres of the amide group. We prepared 1,4-disubstituted and 1,5-disubstituted imidazoles or triazoles AHL analogues. Up to date, only a few AHL analogues containing imidazolium, triazole or tetrazolic compounds have been described [43,44,48,59]. Moreover, no AHL modulators built by replacing the amide function of AHLs with an imidazole ring have been ever reported.

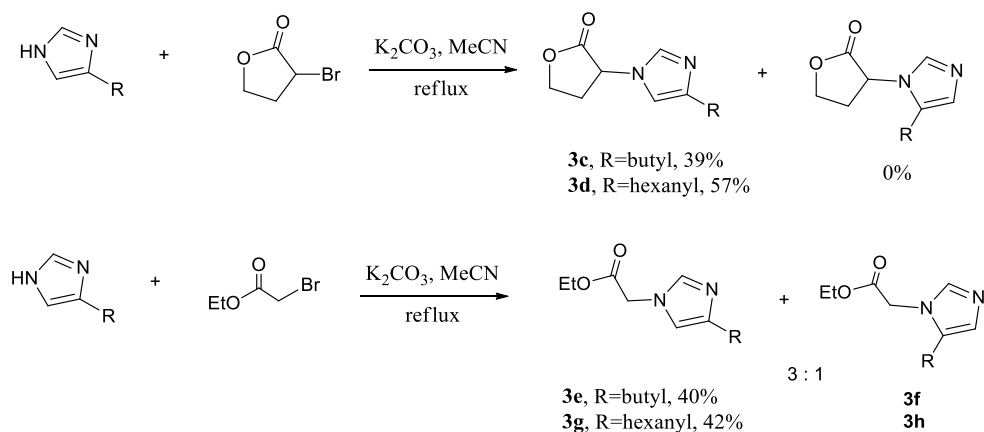
2.3.2 Synthesis of AHL analogs based on imidazole or triazole scaffolds

In the present study, a general method was used for the conversion of bromo-ketones into 4(5)-substituted imidazoles which are key precursors for the preparation of the targeted 1,4-disubstituted or 1,5-disubstituted imidazoles (Scheme 10). Olefins were converted through a two-step synthetic pathway into the corresponding 4(5)-substituted imidazoles. In this process, it is worthy to note that formamide should be preheated before adding the starting material bromo-ketone [76]. The reason for this operation is probably to produce additional ammonia which is required for the construction of the imidazole ring. Finally, 4(5)-butylimidazole and 4(5)-hexanylimidazole rings were prepared in moderate yield through the reaction of bromo-ketones with formamide [77].



Scheme 10. Synthesis of 4(5)-substituted imidazole.

To obtain these compounds, we initially hypothesized that the two isomers of desired alkylated products could be prepared by the reaction of 4(5)-substituted imidazole with bromo-lactone in presence of potassium carbonate. Surprisingly, we only observed the production of 1,4-disubstituted imidazoles as a single regioisomer without any formation of 1,5-disubstituted imidazoles (Scheme 11). This result could be explained by the steric hindrance of bromo lactone. When we used bromo ethyl acetate as an alkylation reagent, 1,4-disubstituted and 1,5-disubstituted imidazoles were obtained as a mixture of two isomers in a 3:1 ratio.



Scheme 11. Synthesis of 1,4-disubstituted imidazoles.

Each compound was fully characterized by ^1H NMR, ^{13}C NMR, 2D-NMR and high resolution mass spectrometry. Here, we take compound **3c** as an example to explain the determination of structure. Two peaks at 7.43 ppm and 6.63 ppm belong to protons

in the imidazole ring. And the other protons were analyzed in the ^1H -NMR spectra (Figure 41). ^{13}C NMR spectra of compound **3c** shows that C-1, C-2 and C-6 locate in 136.0, 113.2, and 144.3 ppm, respectively (Figure 42). To make sure that the alkylation position of lactone moiety is the N-1 imidazole position, we analyzed the HMBC experiment to identify their distant protons-carbons correlations. In the 2D-NMR spectra, a three-bond correlation between C-2 and proton 3 is observed (circled in blue), as well as the correlation between C-1 and proton 3 (circled in blue). Being four bonds apart, there is no correlation between C-6 and proton 3. So we confirmed this structure is the 1,4-disubstituted imidazole and not the 1,5-one. Moreover, the one-bond C-H correlations (HSQC artifacts) were observed as a pair of responses (circled in red) in HMBC 2D spectra (Figure 43).

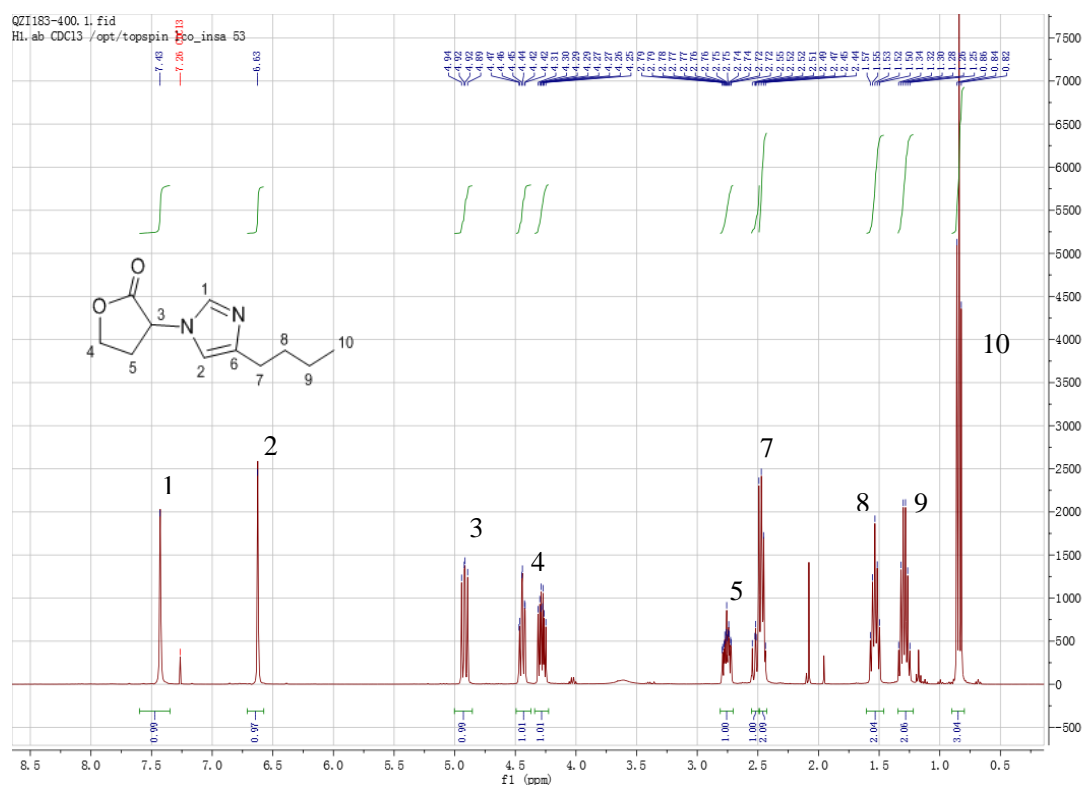


Figure 41. ^1H -NMR of compound **3c**. Identifications of each proton are shown, leading to unambiguous identification of compound **3c**.

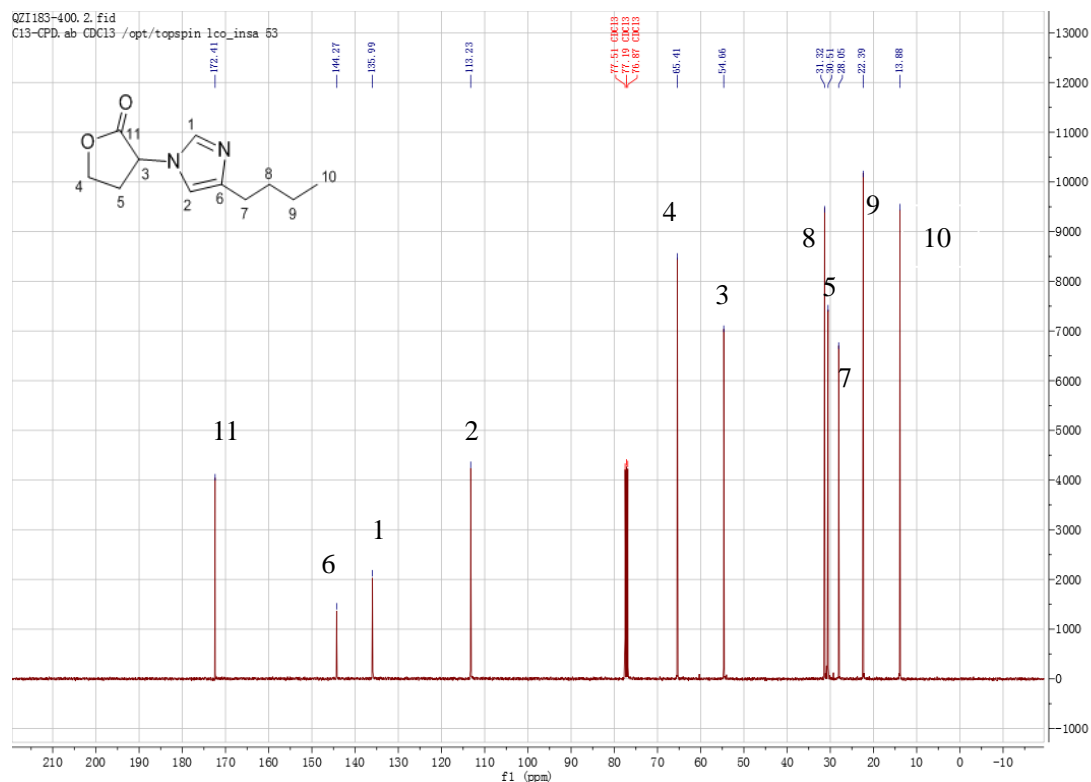


Figure 42. ^{13}C -NMR of compound **3c**. Identifications of each carbon of compound **3c** are shown.

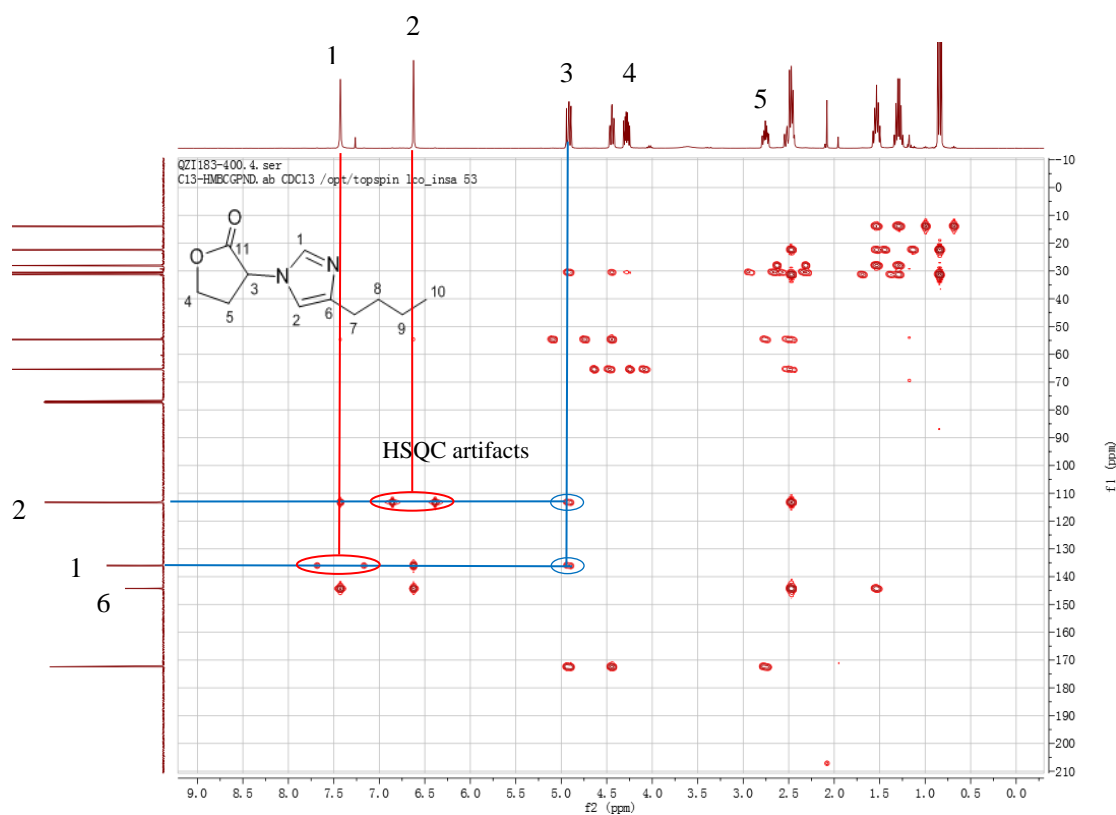
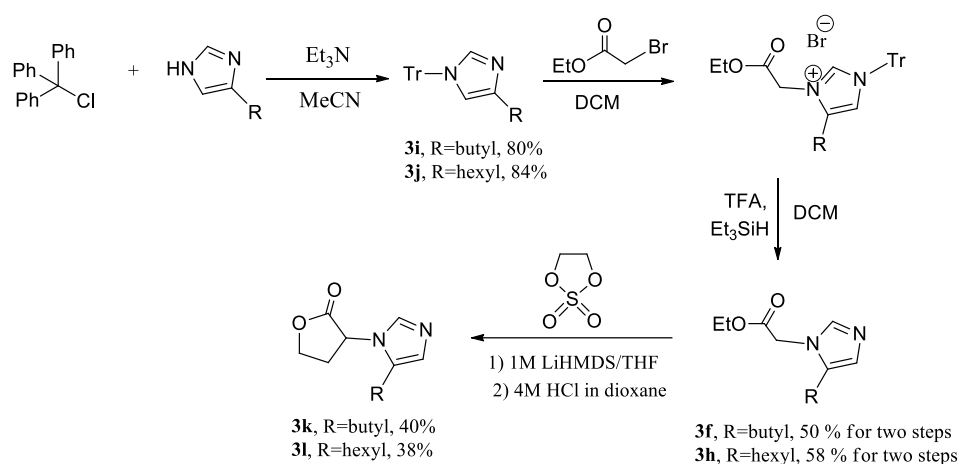


Figure 43. HMBC of compound **3c**. Identifications of each distant C-H correlations are shown.

Then we looked for other accesses to 1,5-disubstituted imidazoles (Scheme 12). The synthetic route involved the protection of the NH group using trityl chloride [78]. 4(5)-Butylimidazole and 4(5)-hexanylimidazole [77] were readily transformed into the corresponding 1-trityl-imidazole derivatives. Alkylation of **3i/3j** with bromo ethyl acetate was achieved to generate a quaternary salt, which was deprotected with TFA [78] to give the targeted 1,5-disubstituted imidazoles **3f/3h**. Finally, the ethyl ester **3f** was subjected to a late lactone formation (see next section). Alkylation of α -H in acetate with cyclic sulfate and subsequent cyclization with 4M HCl led to the generation of final lactone.



Scheme 12. Synthesis of 1,5-disubstituted imidazole.

1,5-Disubstituted imidazoles were fully characterized. Here we take the 1,5-disubstituted imidazole **3l** as an example to explain how their structure was determined. The typical signals belonging to the protons of the imidazole ring appear as expected at 7.49 ppm and 6.62 ppm (Figure 44). ^{13}C NMR spectra of compound **3l** shows that C-1, C-2 and C-6 locate as expected at 135.3, 125.7 and 132.3 ppm, respectively (Figure 45). The HMBC experiment allowed us to identify their distant protons-carbons correlations. In the 2D-NMR spectra, the three bond correlation between C-1 and proton 3 is observed, as well as the correlation between C-6 and proton 3 (Figure 46). So we confirmed this structure as the 1,5-disubstituted imidazole.

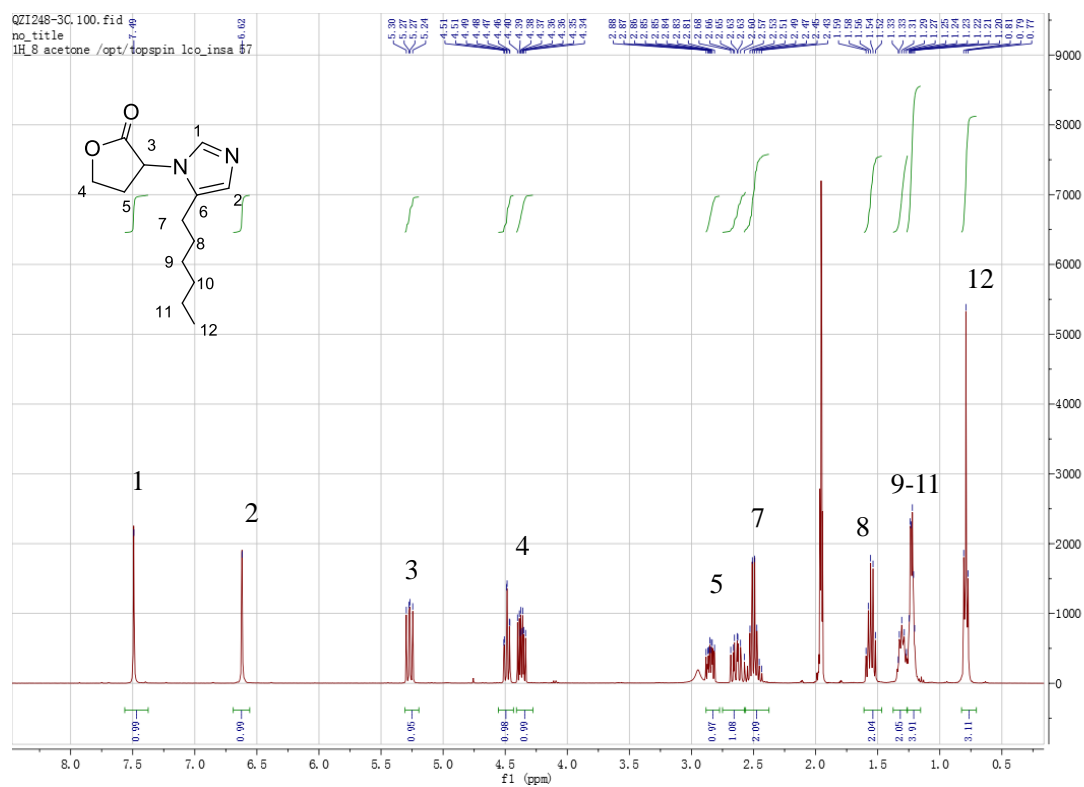


Figure 44. ^1H -NMR of compound 31. Identifications of each proton of compound 31 are shown.

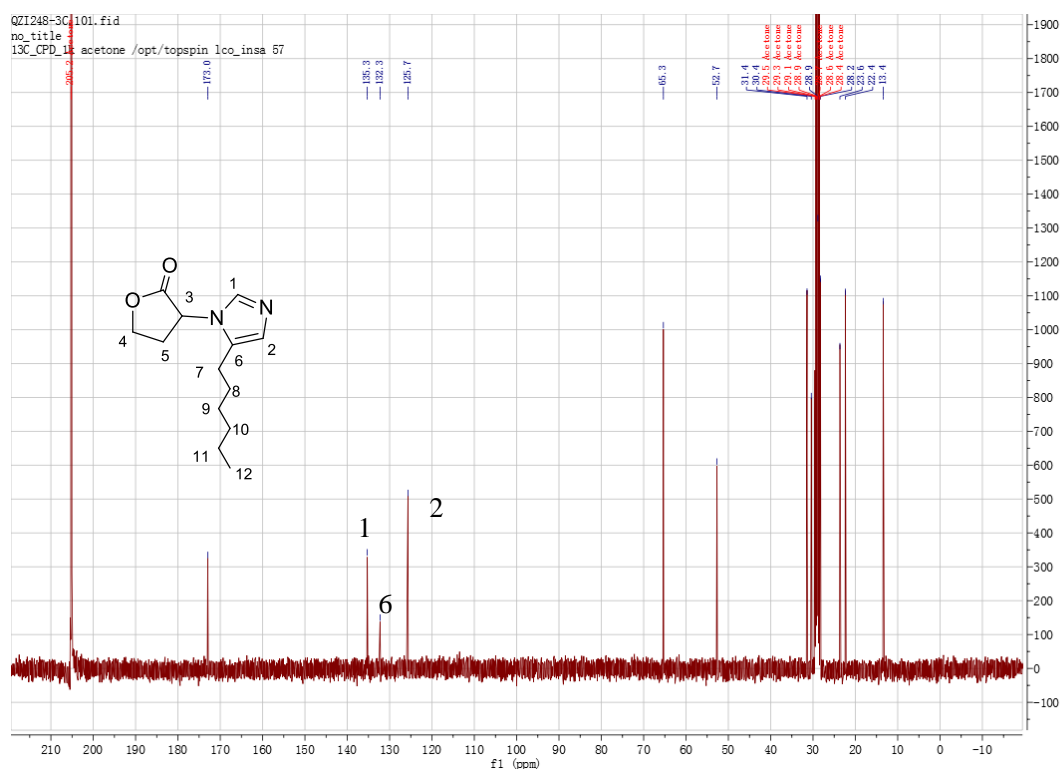


Figure 45. ^{13}C -NMR of compound 31.

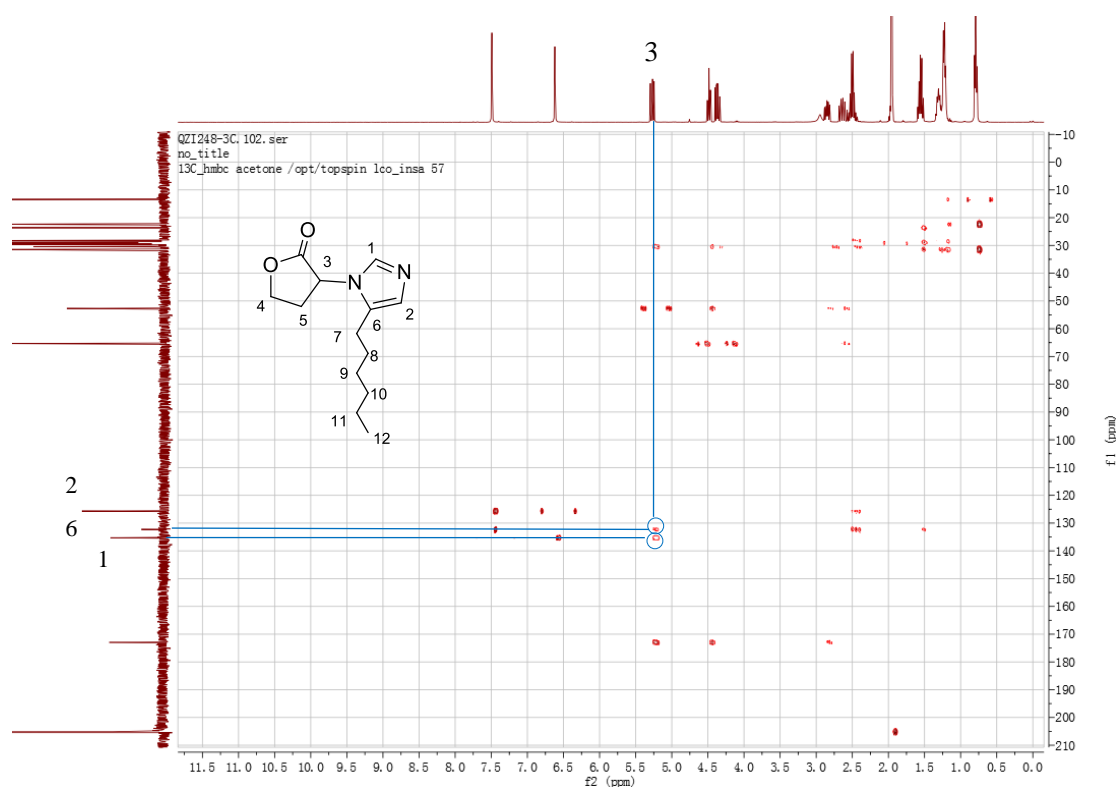
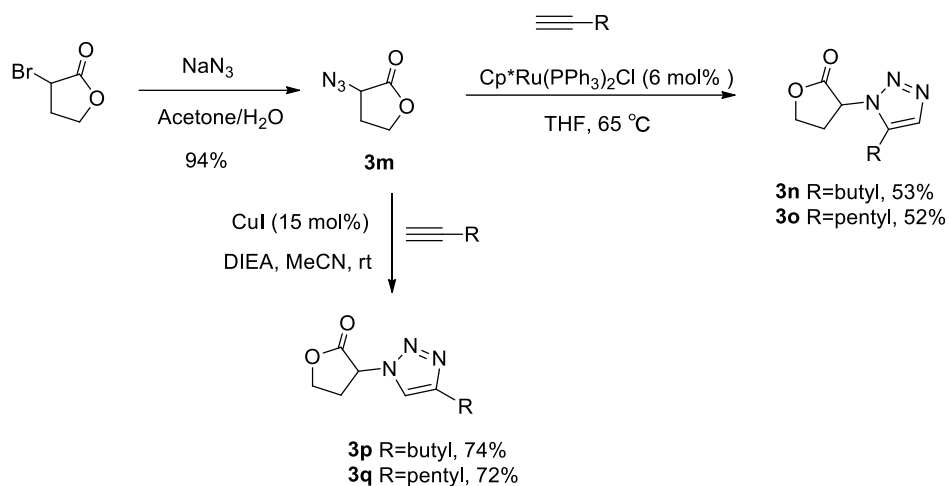


Figure 46. HMBC of compound **3l**. Identifications of distant C-H correlation of compound **3l** are shown.

After the imidazole series, we then turned our attention to the synthesis of AHL analogues involving the replacement of the amide function with a 1,2,3-triazole moiety, including 1,4-disubstituted triazoles and 1,5-disubstituted triazoles (Scheme 13). A general procedure was followed to prepare the intermediate azide. Sodium azide was used as azidation reagent to form azidolactone **3m** in high yield [79]. In the presence of CuI as a catalyst [80], the CuAAC reaction of **3m** with different alkynes provided the 1,4-disubstituted triazoles in good yields. In the presence of a ruthenium catalyst, the cycloaddition reaction of **3m** with different alkynes gave the 1,5-disubstituted triazoles [81] in moderate yields. All the triazole derivatives were fully characterized. The two regioisomers 1,4- and 1,5-disubstituted triazoles give very similar proton spectra with the only slight difference of the chemical shift in proton 2 (Figure 47). Compound **3o** was identified as the 1,5-disubstituted triazole by HMBC experiment (Figure 48).



Scheme 13. Synthesis of 1,4- or 1,5-disubstituted triazole.

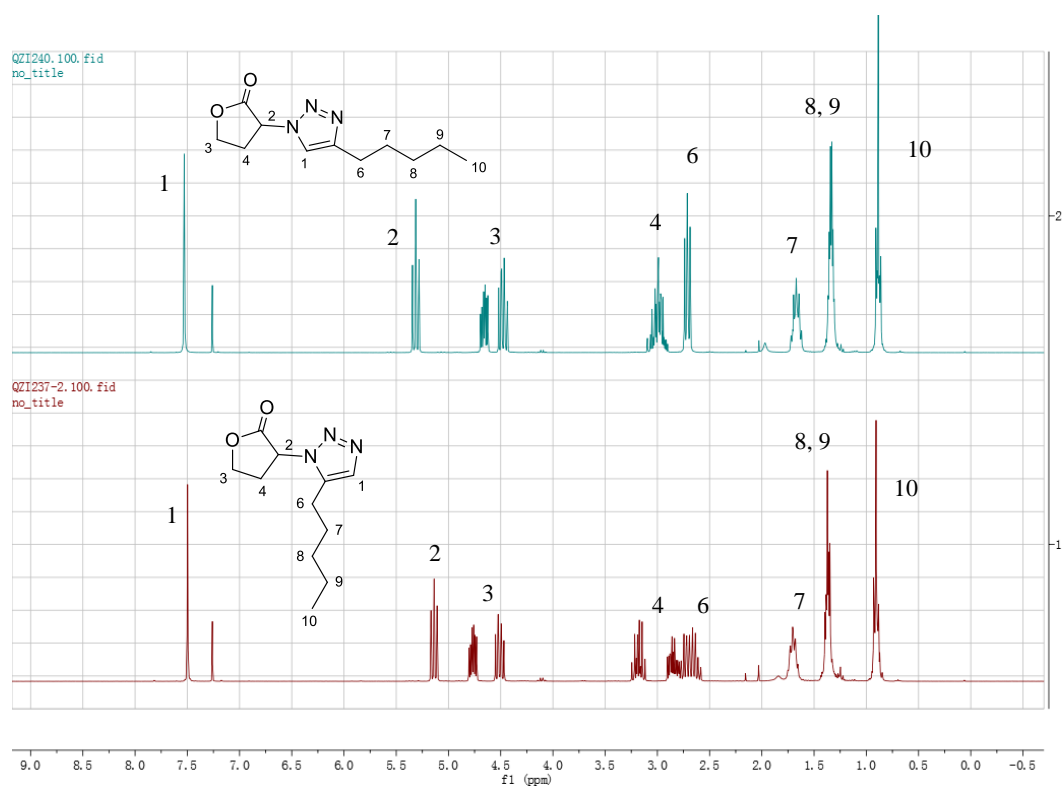


Figure 47. ^1H -NMR of compound **3o** and **3q**. Identifications of each proton of compound **3o** and **3q** are shown.

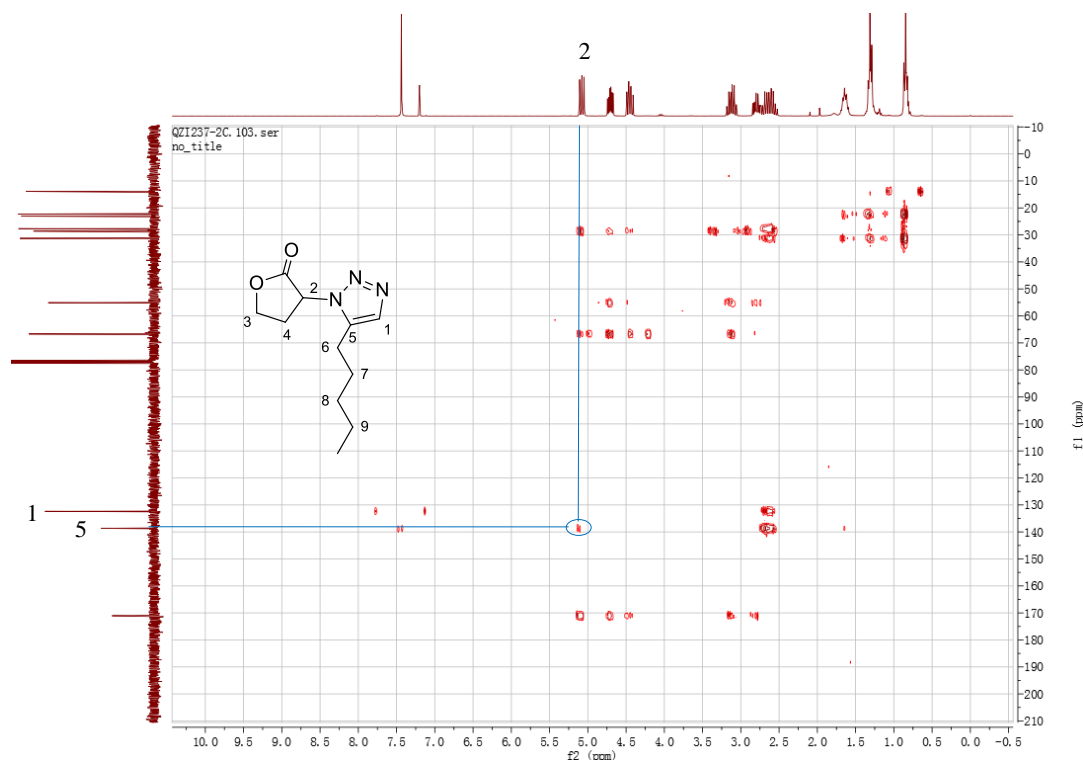


Figure 48. HMBC of compound **3o**. Identifications of distant C-H correlation of compound **3o** are shown.

2.3.3 Biological evaluation

Having the series of synthetic imidazole and triazole derivatives in hands, we evaluated their quorum sensing activity through the QS assay. For the agonistic activity, compounds were assessed for their ability to activate the bioluminescence in NM522 *E. coli* strain. For the antagonistic activity, compounds were evaluated for their ability to decrease the bioluminescence induced by 200 nM 3-oxo-hexanoyl-L-homoserine lactone (OHHL).

The results showed that 1,5-disubstituted triazole derivatives (**3n**, **3o**) and 1,5-disubstituted imidazole derivatives containing lactone (**3k**, **3l**) were antagonists with IC₅₀ value ranging from 87 to 190 μ M. Concerning 1,4-disubstituted triazole or imidazole derivatives containing lactone, the only compound **3q** displayed antagonistic activity. Surprisingly, ethyl ester **3g** was the most active antagonist in this study which is structurally less related to the natural ligand. The results of the inhibitory and activation activity are shown in table 7.

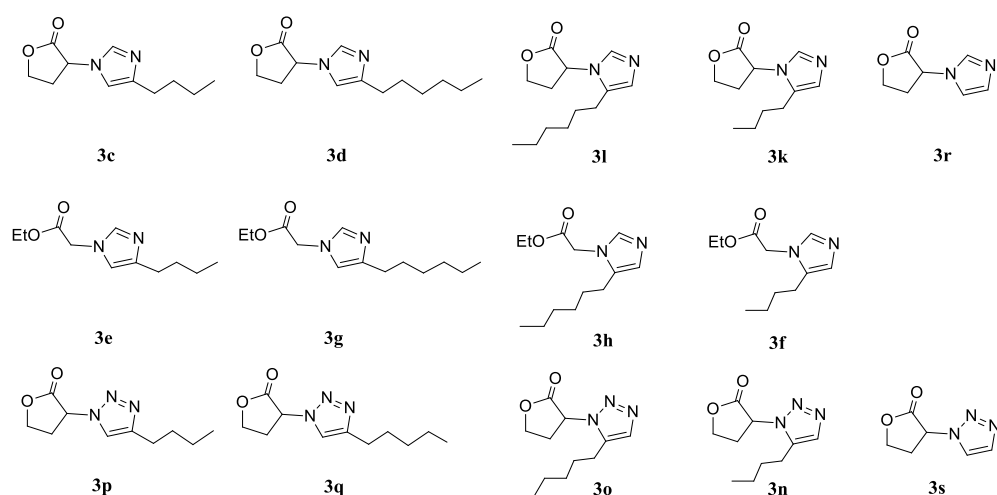


Figure 49. Structures of AHLs analogues containing imidazole or triazole moiety in this study.

Compounds	IC ₅₀ (μM)
1,5-triazole-C4-lactone (3n)	94 ± 3
1,5-triazole-C5-lactone (3o)	87 ± 4
1,4-triazole-C4-lactone (3p)	>200 ^a
1,4-triazole-C5-lactone (3q)	97 ± 4
1,4-imidazole-C6-acetate (3g)	87 ± 7
1,4-imidazole-C4-acetate (3e)	>200 ^a
1,5-imidazole-C6-acetate (3h)	>200 ^a
1,5-imidazole-C4-acetate (3f)	>200 ^a
1,5-imidazole-C4-lactone (3k)	190 ± 9
1,5-imidazole-C6-lactone (3l)	110 ± 20

a. compounds **3p**, **3e**, **3h**, **3f** showed 40%, 27%, 36%, 22% inhibition at 200 μM.

Table 7. IC₅₀ and EC₅₀ values for compounds **3e-3q**.

Overall, 1,4- and 1,5-disubstituted imidazole derivatives exhibit quite different response in QS modulation. And 1,5-disubstituted triazole or imidazole derivatives tend to be more active than 1,4-disubstituted triazole or imidazole derivatives.

2.3.4 Docking study

The docking modeling of this series of AHL analogs was then performed using the LuxR model [75]. First, for all heterocyclic compounds of this study, a hydrogen bond network comparable to the one described for compound **3q** is obtained [44] as depicted in figure 50. The lactone ring is involved in hydrogen bonds with Trp66 and the heterocyclic triazole ring is involved in hydrogen bonds with Tyr62 and Ser137. For imidazole derivatives, the heterocyclic ring is also involved in hydrogen bonds with Tyr62 and Ser137 via the same nitrogen atom.

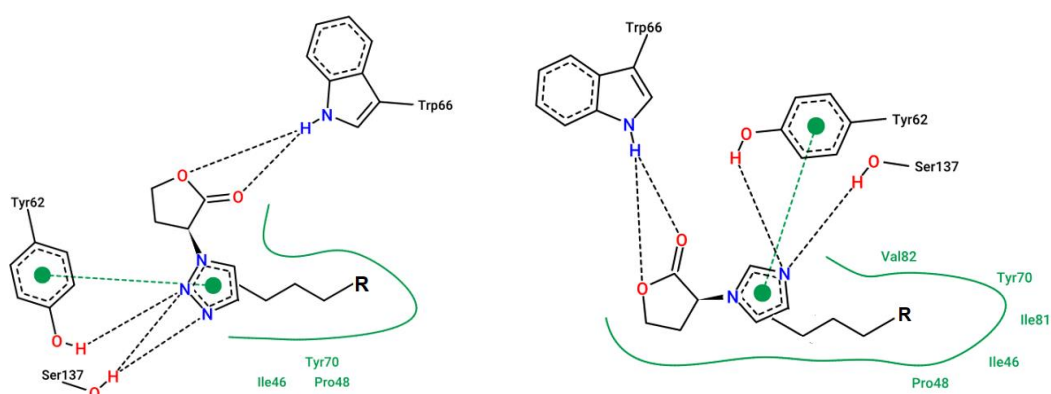


Figure 50. Hydrogen bond network obtained for compound triazole and imidazole derivatives within the binding of the LuxR model.

For compounds with a lactone bearing 1,4 or 1,5 imidazole, an unfavorable acyl chain orientation is observed for the 1,4 substitution. For compounds with an ethyl acetate group bearing 1,4 or 1,5 imidazole, the location of the heterocyclic ring is slightly different, this might explain the different activities. For the triazole derivatives, the orientation of the alkyl chain is significantly different to explain the effect of the agonistic or antagonistic activity (Figure 51).

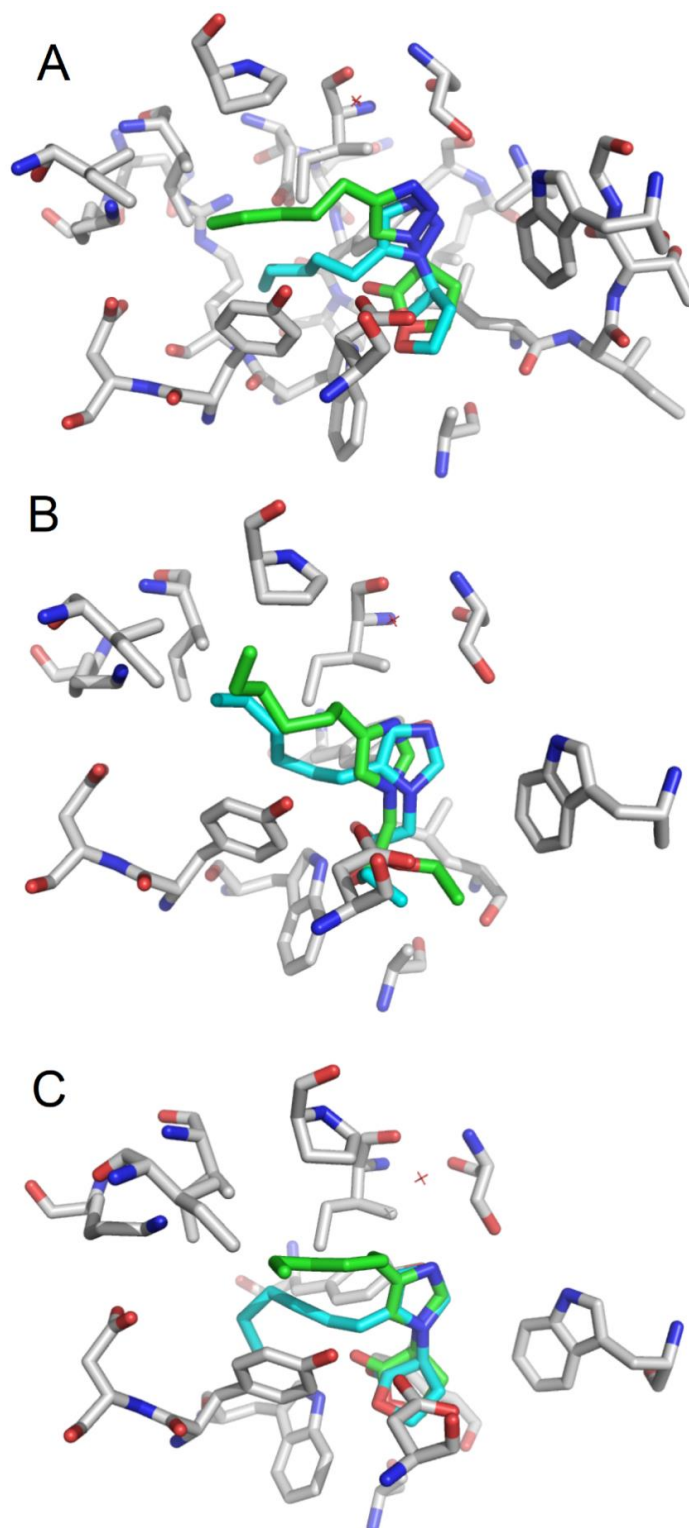


Figure 51. Docking results of compounds **3o** and **3q** (A), **3g** and **3h** (B), **3d** and **3l** (C) within the binding site of the LuxR model.

2.3.5 Conclusions

We synthesized a range of AHLs analogues involving the replacement of amide function with a triazole or imidazole moiety. The biological evaluation showed that 1,5-disubstituted triazole or imidazole derivatives containing lactone functioned as antagonists whereas 1,4-disubstituted imidazole derivatives containing lactone were inactive. The imidazole analogs **3g** with an ethyl acetate replacing the lactone group structurally less related to natural AHL was identified as the most potent antagonist in this study whereas the corresponding analog with a lactone **3d** was inactive.

.

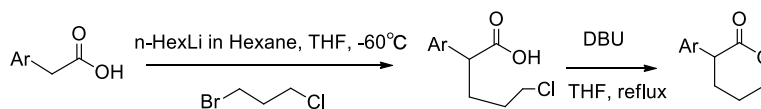
2.4 Alternative route towards AHL analogues by late lactone formation

2.4.1 Introduction

Lactones are very frequent structures in many natural compounds and are also important motifs for the design of bioactive molecules. Normally, homoserine lactone itself is used as a starting building block in the synthetic strategies towards close AHL analogues. However, in some cases, an alternative strategy is preferable, based on a late lactone formation.

Recently, several approaches for late lactone formation were reported, such as oxidative lactonization of diols [82,83], oxidative lactonization of carboxylic acids [84,85], selective reduction of L-aspartic acid [86-88] and solid-phase synthetic route to deliver chiral AHLs [89]. Apart from these methods, there is a limited number of reported approaches based on C-alkylation of the acetic ester derivatives followed intramolecular ring-closure [90-92].

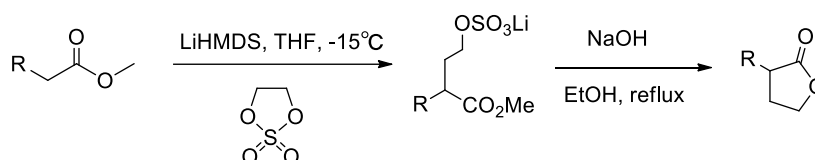
In 2003, James [90] prepared various 3-aryl- δ -lactones from corresponding arylacetic acids using 1-bromo-3-chloropropane as an alkylation reagent and DBU for cyclization (Scheme 14). The authors found that the alkylated intermediate was cleanly formed and surprisingly stable in this process. Considering the intermediate as the lithium carboxylate, they tried to conduct the cyclization step under simple heating but they did not observe any lactone formation. Then they turned to the mild base DBU known for enhancing the nucleophilicity of carboxylates. Under these optimized conditions, 3-aryl lactones were obtained in good yields over two steps.



Scheme 14. Synthesis of 3-aryl- δ -lactones.

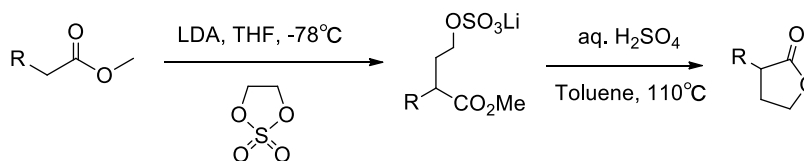
In 2015, Bernhard [91] employed a cyclic sulfate as an alkylation reagent (Scheme 15). In the first step, the carboxylic esters were deprotonated with LiHMDS followed

by alkylation with ethylene sulfate to form the sulfuric acid monoester. The alkylated intermediate was subjected to the next cyclization step without further purification. They chose a basic condition to hydrolyze the intermediate to afford the lactones in moderate yield.



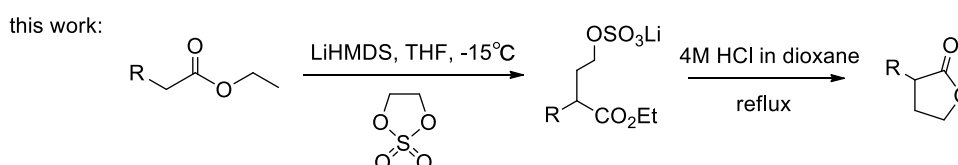
Scheme 15. Synthesis of δ -lactones.

Later, a modified synthetic scheme was proposed starting from the carboxylic esters [92]. LDA was chosen as an alkylation base to afford the sulfuric acid monoesters, then aqueous sulfuric acid was used for the cyclization to afford the desired lactone in good yields (Scheme 16).



Scheme 16. Synthesis of δ -lactones.

However, the generality of these methods is not complete and rather harsh conditions are required. For AHL analog design, considering the wide availability of acetic ester derivatives, it would be nice to establish an alternative late lactone formation strategy. We have briefly addressed this issue by employing the mild base LiHMDS for deprotonation followed by 4M HCl in dioxane applied to AHL type targets (Scheme 17). Below we describe the details of this investigation.



Scheme 17. Synthesis of δ -lactones developed by our group.

2.4.2 Alkylation and cyclization to synthesize lactone

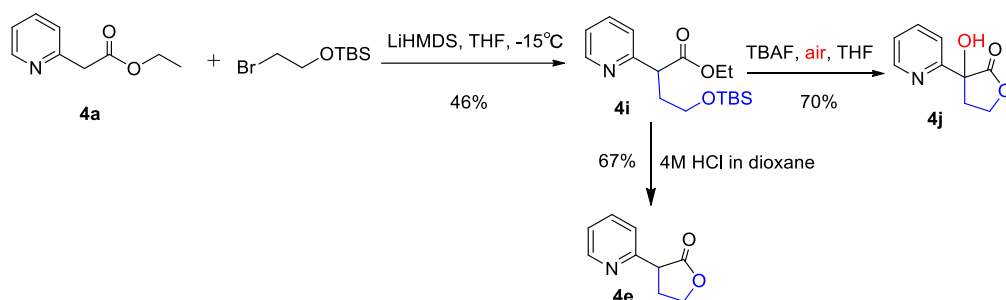
To expand the scope of this reaction, we targeted some heterocyclic compounds, such as imidazole and pyrazole derivatives (Table 8). The reaction of ethyl pyridine acetate or ethyl pyrazole acetate as substrate led to the formation of the corresponding lactone products with acceptable yield when the reaction was conducted at -15°C . Treatment with ethyl benzimidazole acetate or ethyl imidazole acetate in the same condition gave very poor yields. Considering the presence of a reactive proton in the imidazole, we decreased the temperature to -78°C to inhibit the side reaction and allowing the formation of the desired products with moderate yields, 44% and 34%, respectively.

Table 8. Synthesis of δ -lactones based on a late lactone formation.

Entry	Substrates	Products	Yields
1 ^a	 4a	 4e	62%
2 ^a	 4b	 4f	49%
3 ^b	 4c	 4g	34%
4 ^b	 4d	 4h	44%

Condition a: alkylation at -15°C , 6h; Condition b: alkylation at -78°C -rt, overnight

Considering the presence of a chiral center in the final lactone product, the use of esters having a chiral moiety as starting materials could be a way to form diastereoisomers. It would thus be necessary to separate easily the alkylated intermediate. So we looked if such isolation of the intermediate was possible when using (2-bromoethoxy)(tert-butyl)dimethylsilane as an alkylation reagent to replace the previous reagent, cyclic sulfate. Initially, ethyl pyridine acetate was chosen as a substrate to form the lactone without consideration of the chirality. The result of cyclization indicated treatment of alkylated product with 4M HCl in dioxane gave the desired product, with TBAF gave the hydroxylated lactone (Scheme 18). The hydroxylated lactone **4j** were fully characterized by NMR spectra (Figure 52-54).



Scheme 18: The proposed cyclization approach using (2-bromoethoxy)(tert-butyl)dimethylsilane.

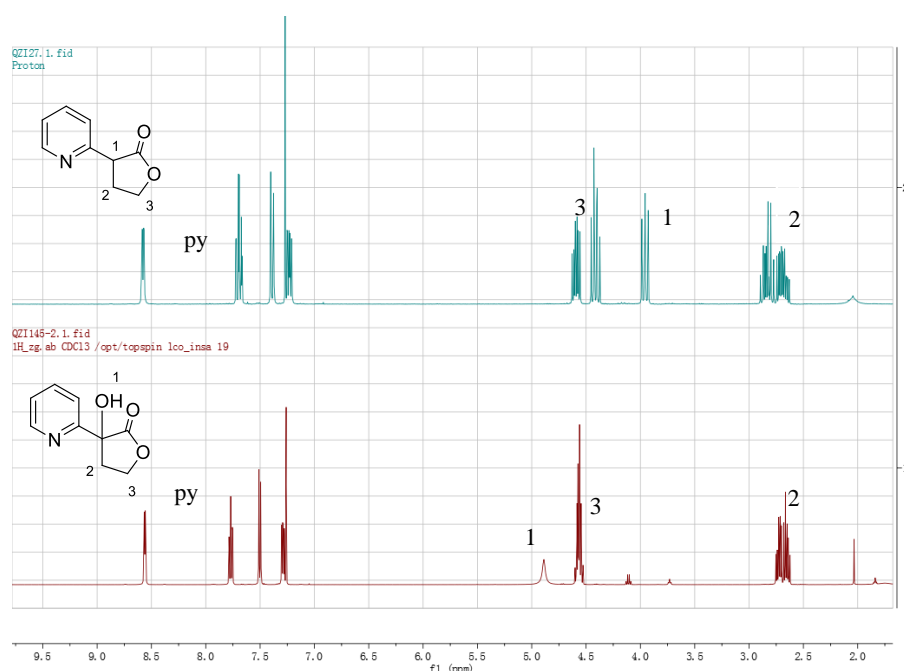


Figure 52. Identifications of each proton of compound **4e** and **4j** in their ¹H-NMR spectra.

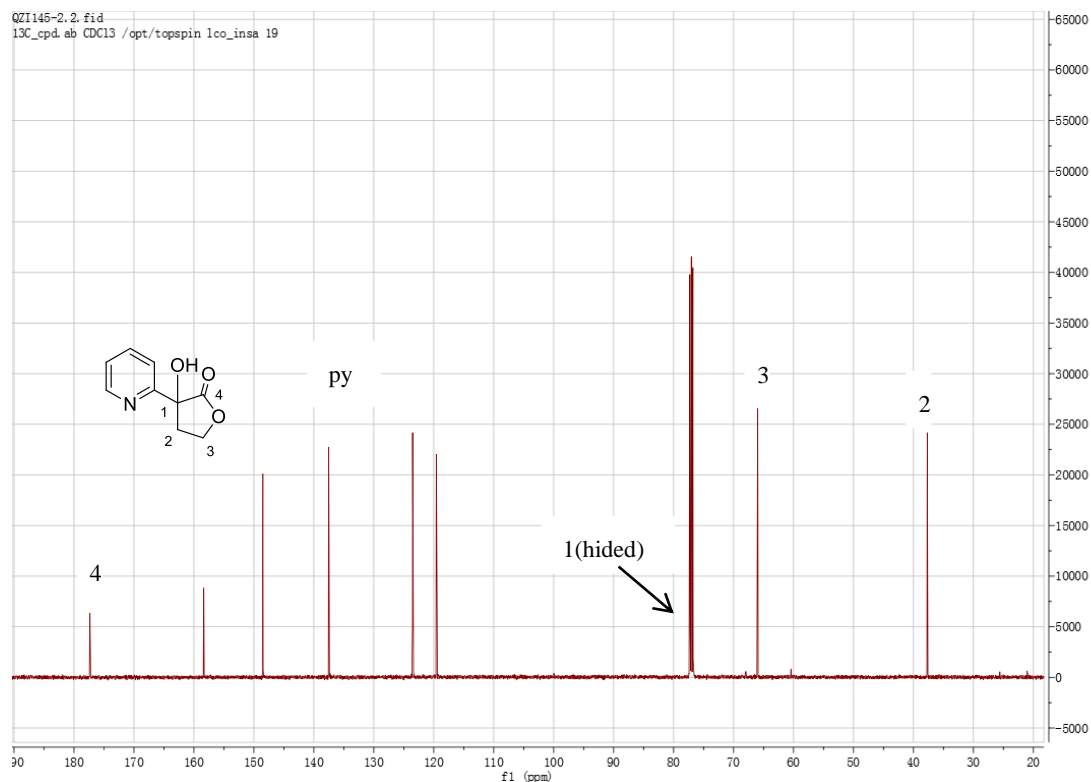


Figure 53. Identifications of each carbon of compound **4j** in ¹³C-NMR spectra.

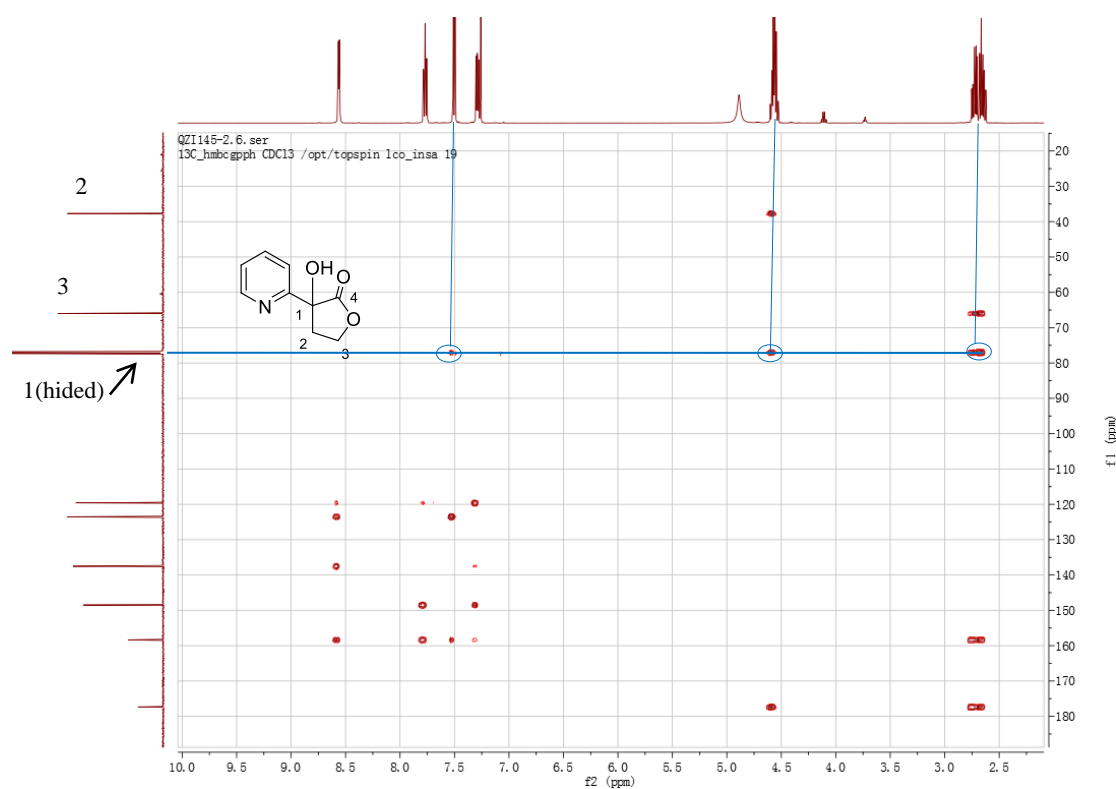
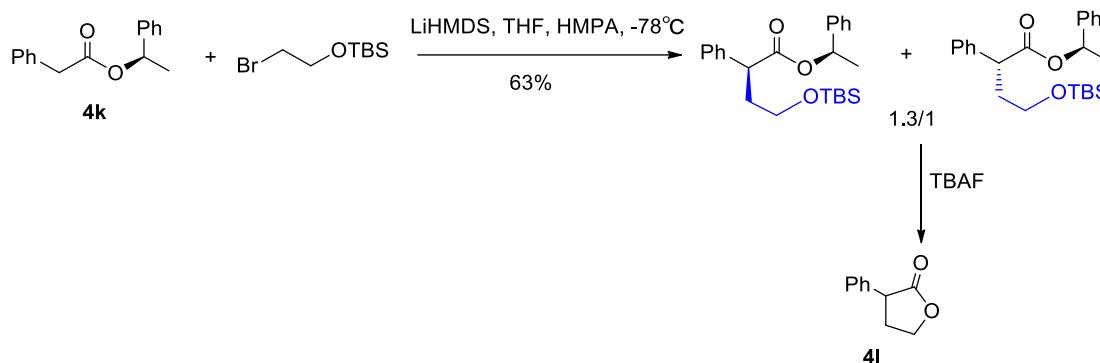


Figure 54. Identifications of distant C-H correlations of compound **4j** in HMBC spectra.

Starting from compound **4k** equipped with one chiral group, we conducted the alkylation reaction in a similar condition which yields two diastereoisomers in a 1:1.3 ratio determined by ^1H NMR spectra (Scheme 19). Unfortunately, two isomers are difficult to separate from each other. The cyclization of the mixture intermediates with TBAF gave the final lactone **4l**.



Scheme 19: Cyclization approach starting from chiral substrate.

2.4.3 Conclusions

We developed a synthetic method of the late lactone formation which provides non-native AHLs analogues. It was proved to be an alternative synthetic route to access AHLs analogues containing heterocycles. A short scope and chiral issue of this method was investigated. Other chiral auxiliaries should be further explored in the future to improve the separability of the diastereoisomers and thus propose access towards chiral targets.

References

1. K. Papenfort and B. L. Bassler, *Nat. Rev. Microbiol.*, 2016, 14, 576-588.
2. S. T. Rutherford and B. L. Bassler, *Cold Spring Harbor Perspect. Med.*, 2012, 2, 1-25.
3. W. C. Fuqua, S. C. Winans and E. P. Greenberg, *J. Bacteriol.*, 1994, 176, 269-275.
4. M. Schuster, D. Joseph Sexton, S. P. Diggle and E. Peter Greenberg, *Annu. Rev. Microbiol.*, 2013, 67, 43-63.
5. K. Papenfort and J. Vogel, *Cell Host Microbe*, 2010, 8, 116-127.
6. X. Chen, S. Schauder, N. Potier, A. Van Dorsselaer, I. Pelczar, B. L. Bassler and F. M. Hughson, *Nature*, 2002, 415, 545-549.
7. Z. Erez, I. Steinberger-Levy, M. Shamir, S. Doron, A. Stokar-Avihail, Y. Peleg, S. Melamed, A. Leavitt, A. Savidor and S. Albeck, *Nature*, 2017, 541, 488-493.
8. J. E. Silpe and B. L. Bassler, *Cell*, 2019, 176, 268-280.
9. T. A. Gould, W. T. Watson, K.-H. Choi, H. P. Schweizer and M. E. Churchill, *Acta Crystallogr. D Biol. Crystallogr.*, 2004, 60, 518-520.
10. D. Shin, C. Gorgulla, M. E. Boursier, N. Rexrode, E. C. Brown, H. Arthanari, H. E. Blackwell and R. Nagarajan, *ACS Chem. Biol.*, 2019, 14, 2305-2314.
11. Y.-H. Dong, L.-H. Wang, J.-L. Xu, H.-B. Zhang, X.-F. Zhang and L.-H. Zhang, *Nature*, 2001, 411, 813-817.
12. Y. H. Lin, J. L. Xu, J. Hu, L. H. Wang, S. L. Ong, J. R. Leadbetter and L. H. Zhang, *Mol. Microbiol.*, 2003, 47, 849-860.
13. S. D. L. Marin, Y. Xu, M. M. Meijler and K. D. Janda, *Bioorg. Med. Chem. Lett.*, 2007, 17, 1549-1552.
14. G. F. Kaufmann, R. Sartorio, S.-H. Lee, C. J. Rogers, M. M. Meijler, J. A. Moss, B. Clapham, A. P. Brogan, T. J. Dickerson and K. D. Janda, *Proc. Natl. Acad. Sci. U.S.A.*, 2005, 102, 309-314.
15. E. V. Piletska, G. Stavroulakis, L. D. Larcombe, M. J. Whitcombe, A. Sharma, S. Primrose, G. K. Robinson and S. A. Piletsky, *Biomacromolecules*, 2011, 12, 1067-1071.
16. E. P. Magennis, F. Fernandez-Trillo, C. Sui, S. G. Spain, D. J. Bradshaw, D. Churchley, G. Mantovani and K. Winzer, *Nat. Mater.*, 2014, 13, 748-755.
17. A. Motib, A. Guerreiro, F. Al-Bayati, E. Piletska, I. Manzoor, S. Shafeeq, A. Kadam, O. Kuipers, L. Hiller, T. Cowen, S. Piletsky, P. W. Andrew and H. Yesilkaya, *Angew. Chem. Int. Ed.*, 2017, 56, 16555-16558.
18. M. J. Bottomley, E. Muraglia, R. Bazzo and A. Carfi, *J. Biol. Chem.*, 2007, 282, 13592-13600.
19. J. Engebrecht, K. Nealson and M. Silverman, *Cell*, 1983, 32, 773-781.
20. J. Engebrecht and M. Silverman, *Proc. Natl. Acad. Sci. U.S.A.*, 1984, 81, 4154-4158.
21. A. Eberhard, A. L. Burlingame, C. Eberhard, G. L. Kenyon, K. H. Nealson and N. J. Oppenheimer, *Biochemistry*, 1981, 20, 2444-2449.
22. P. Williams, *Microbiology*, 2007, 153, 3923-3938.
23. M.-L. Lee and G. Schneider, *J. Comb. Chem.*, 2001, 3, 284-289.
24. L. Du, A. J. Robles, J. B. King, D. R. Powell, A. N. Miller, S. L. Mooberry and R. H. Cichewicz, *Angew. Chem. Int. Ed.*, 2014, 53, 804-809.

25. A. Bauer and M. Brönstrup, *Nat. Prod. Rep.*, 2014, 31, 35-60.
26. M. Scheepstra, L. Nieto, A. K. Hirsch, S. Fuchs, S. Leysen, C. V. Lam, L. In Het Panhuis, C. A. Van Boeckel, H. Wienk and R. Boelens, *Angew. Chem. Int. Ed.*, 2014, 53, 6443-6448.
27. D. G. Brown, T. Lister and T. L. May-Dracka, *Bioorg. Med. Chem. Lett.*, 2014, 24, 413-418.
28. T. Rodrigues, D. Reker, P. Schneider and G. Schneider, *Nat. Chem.*, 2016, 8, 531.
29. H. V. Hattum and H. Waldmann, *J. Am. Chem. Soc.*, 2014, 136, 11853-11859.
30. W. R. Galloway, J. T. Hodgkinson, S. D. Bowden, M. Welch and D. R. Spring, *Chem. Rev.*, 2011, 111, 28-67.
31. M. Welch, J. M. Dutton, F. G. Glansdorp, G. L. Thomas, D. S. Smith, S. J. Coulthurst, A. M. Barnard, G. P. Salmond and D. R. Spring, *Bioorg. Med. Chem. Lett.*, 2005, 15, 4235-4238.
32. S. R. Chhabra, P. Stead, N. J. Bainton, G. P. Salmond, G. S. STEWART, P. Williams and B. W. Bycroft, *J. Antibiot.*, 1993, 46, 441-454.
33. C. E. McInnis and H. E. Blackwell, *Bioorg. Med. Chem.*, 2011, 19, 4820-4828.
34. M. E. Boursier, J. B. Combs and H. E. Blackwell, *ACS Chem. Biol.*, 2019, 14, 186-191.
35. M. Givskov, R. de Nys, M. Manefield, L. Gram, R. Maximilien, L. Eberl, S. Molin, P. D. Steinberg and S. Kjelleberg, *J. Bacteriol.*, 1996, 178, 6618-6622.
36. M. Manefield, R. de Nys, K. Naresh, R. Roger, M. Givskov, S. Peter and S. Kjelleberg, *Microbiology*, 1999, 145, 283-291.
37. J. C. Janssens, K. Metzger, R. Daniels, D. Ptacek, T. Verhoeven, L. W. Habel, J. Vanderleyden, D. E. De Vos and S. C. De Keersmaecker, *Appl. Environ Microbiol.*, 2007, 73, 535-544.
38. K. M. Smith, Y. Bu and H. Suga, *Chem. Biol.*, 2003, 10, 563-571.
39. S. Castang, B. Chantegrel, C. Deshayes, R. Dolmazon, P. Gouet, R. Haser, S. Reverchon, W. Nasser, N. Hugouvieux-Cotte-Pattat and A. Doutheau, *Bioorg. Med. Chem. Lett.*, 2004, 14, 5145-5149.
40. M. Frezza, S. Castang, J. Estephane, L. Soulere, C. Deshayes, B. Chantegrel, W. Nasser, Y. Queneau, S. Reverchon and A. Doutheau, *Bioorg. Med. Chem.*, 2006, 14, 4781-4791.
41. M. Frezza, L. Soulere, S. Reverchon, N. Guiliani, C. Jerez, Y. Queneau and A. Doutheau, *Bioorg. Med. Chem.*, 2008, 16, 3550-3556.
42. M. Boukraa, M. Sabbah, L. Soulere, M. L. El Efrat, Y. Queneau and A. Doutheau, *Bioorg. Med. Chem. Lett.*, 2011, 21, 6876-6879.
43. G. Brackman, M. Risseuw, S. Celen, P. Cos, L. Maes, H. J. Nelis, S. Van Calenbergh and T. Coenye, *Bioorg. Med. Chem.*, 2012, 20, 4737-4743.
44. M. Sabbah, F. Fontaine, L. Grand, M. Boukraa, M. L. Efrat, A. Doutheau, L. Soulere and Y. Queneau, *Bioorg. Med. Chem.*, 2012, 20, 4727-4736.
45. D. M. Stacy, M. A. Welsh, P. N. Rather and H. E. Blackwell, *ACS Chem. Biol.*, 2012, 7, 1719-1728.
46. G. D. Geske, J. C. O'Neill and H. E. Blackwell, *Chem. Soc. Rev.*, 2008, 37, 1432-1447.
47. A. M. Stevens, Y. Queneau, L. Soulere, S. V. Bodman and A. Doutheau, *Chem. Rev.*, 2011, 111, 4-27.
48. U. Müh, M. Schuster, R. Heim, A. Singh, E. R. Olson and E. P. Greenberg, *Antimicrob. Agents Chemother.*, 2006, 50, 3674-3679.

49. C. T. O'Loughlin, L. C. Miller, A. Siryaporn, K. Drescher, M. F. Semmelhack and B. L. Bassler, *Proc. Natl. Acad. Sci. U.S.A.*, 2013, 110, 17981-17986.
50. M. Guo, Y. Zheng, R. Starks, C. Opoku-Temeng, X. Ma and H. O. Sintim, *MedChemComm*, 2015, 6, 1086-1092.
51. N. N. Biswas, S. K. Kutty, N. Barraud, G. M. Iskander, R. Griffith, S. A. Rice, M. Willcox, D. S. Black and N. Kumar, *Org. Biomol. Chem.*, 2015, 13, 925-937.
52. I. Kviatkovski, L. Chernin, T. Yarnitzky, I. Frumin, N. Sobel and Y. Helman, *Chem. Commun.*, 2015, 51, 3258-3261.
53. S.-Z. Li, J. Wawrzyniak, Y. Queneau and L. Soullère, *Molecules*, 2017, 22, 2090.
54. D. E. Manson, M. C. O'Reilly, K. E. Nyffeler and H. E. Blackwell, *ACS Infect. Dis.*, 2020, 6, 649-661.
55. U. Müh, B. J. Hare, B. A. Duerkop, M. Schuster, B. L. Hanzelka, R. Heim, E. R. Olson and E. P. Greenberg, *Proc. Natl. Acad. Sci. U.S.A.*, 2006, 103, 16948-16952.
56. Y. Zou and S. K. Nair, *Chem. Biol.*, 2009, 16, 961-970.
57. M. C. O'Reilly and H. E. Blackwell, *ACS Infect. Dis.*, 2016, 2, 32-38.
58. D. M. Stacy, S. T. Le Quement, C. L. Hansen, J. W. Clausen, T. Tolker-Nielsen, J. W. Brummond, M. Givskov, T. E. Nielsen and H. E. Blackwell, *Org. Biomol. Chem.*, 2013, 11, 938-954.
59. M. R. Hansen, T. H. Jakobsen, C. G. Bang, A. E. Cohrt, C. L. Hansen, J. W. Clausen, S. T. Le Quement, T. Tolker-Nielsen, M. Givskov and T. E. Nielsen, *Bioorg. Med. Chem.*, 2015, 23, 1638-1650.
60. A. K. Ghosh and M. Brindisi, *J. Med. Chem.*, 2015, 58, 2895-2940.
61. J. Zhu, J. W. Beaber, M. I. Moré, C. Fuqua, A. Eberhard and S. C. Winans, *J. Bacteriol.*, 1998, 180, 5398-5405.
62. T. Persson, T. H. Hansen, T. B. Rasmussen, M. E. Skindersø, M. Givskov and J. Nielsen, *Org. Biomol. Chem.*, 2005, 3, 253-262.
63. Y.-H. Ahn, Y. Hwang, H. Liu, X. J. Wang, Y. Zhang, K. K. Stephenson, T. N. Boronina, R. N. Cole, A. T. Dinkova-Kostova and P. Talalay, *Proc. Natl. Acad. Sci. U.S.A.*, 2010, 107, 9590-9595.
64. S. Reverchon, B. Chantegrel, C. Deshayes, A. Doutheau and N. Cotte-Pattat, *Bioorg. Med. Chem. Lett.*, 2002, 12, 1153-1157.
65. M. A. Thompson, ArgusLab 4.0.1, Seattle, WA planetaria Software LLC (2004).
66. S.-Z. Li, R. Xu, M. Ahmar, C. Goux-Henry, Y. Queneau and L. Soullère, *Bioorg. Chem.*, 2018, 77, 215-222.
67. M. Ahumado, J. C. Drosos and R. Vivas-Reyes, *Mol. Biosyst.*, 2014, 10, 1162-1171.
68. X. Ke, L. C. Miller, B. L. Bassler, *Mol. Microbiol.*, 2015, 95, 127-42.
69. R. G. Zhang, K. M. Pappas, J. L. Brace, P. C. Miller, T. Oulmassov, J. M. Molyneaux, J. C. Anderson, J. K. Bashkin, S. C. Winans, A. Joachimiak, *Nature*, 2002, 417, 971-974.
70. A. Eberhard, C. A. Widrig, P. McBath, J. B. Schineller, *Arch. Microbiol.*, 1986, 146, 35-40.
71. A. L. Schaefer, B. L. Hanzelka, A. Eberhard and E. Greenberg, *J. Bacteriol.*, 1996, 178, 2897-2901.
72. J. G. Cao, Z. Y. Wei, E. A. Meighen, *Biochem. J.*, 1995, 312, 439-444.
73. S. Gandomkar, A. Dennig, A. Dordic, L. Hammerer, M. Pickl, T. Haas, M. Hall and K. Faber, *Angew. Chem. Int. Ed.*, 2018, 57, 427-430.

74. M. Mizuno and T. Shioiri, *Tetrahedron lett.*, 1998, 39, 9209-9210.
75. L. Soulère, M. Frezza, Y. Queneau and A. Doutheau, *J. Mol. Graph. Model.*, 2007, 26, 581-590.
76. S. Xu, P. Wu and W. Zhang, *Org. Biomol. Chem.*, 2016, 14, 11389-11395.
77. K. Li, Y. Wang, G. Yang, S. Byun, G. Rao, C. Shoen, H. Yang, A. Gulati, D. C. Crick and M. Cynamon, *ACS Infect. Dis.*, 2015, 1, 215-221.
78. G. Agelis, A. Resvani, C. Koukoulitsa, T. Tûmová, J. Slaninová, D. Kalavrizioti, K. Spyridaki, A. Afantitis, G. Melagraki and A. Siafaka, *Eur. J. Med. Chem.*, 2013, 62, 352-370.
79. E. L. Myers and R. T. Raines, *Angew. Chem. Int. Ed.*, 2009, 48, 2359-2363.
80. T. Jin, S. Kamijo and Y. Yamamoto, *Eur. J. Org. Chem.*, 2004, 3789-3791.
81. L. Zhang, X. Chen, P. Xue, H. H. Sun, I. D. Williams, K. B. Sharpless, V. V. Fokin and G. Jia, *J. Am. Chem. Soc.*, 2005, 127, 15998-15999.
82. X. Xie and S. S. Stahl, *J. Am. Chem. Soc.*, 2015, 137, 3767-3770.
83. A. Bhatia, M. Kannan and S. Muthaiah, *Synlett*, 2019, 30, 721-725.
84. T. Duhamel and K. Muñiz, *Chem. Commun.*, 2019, 55, 933-936.
85. S. Sathyamoorthi and J. Du Bois, *Org. Lett.*, 2016, 18, 6308-6311.
86. M. Seki, T. Shimizu and K. Matsumoto, *J. Org. Chem.*, 2000, 65, 1298-1304.
87. S. P. Singh, A. Michaelides, A. R. Merrill and A. L. Schwan, *J. Org. Chem.*, 2011, 76, 6825-6831.
88. M. S. Lall, Y. K. Ramtohul, M. N. James and J. C. Vederas, *J. Org. Chem.*, 2002, 67, 1536-1547.
89. G. D. Geske, R. J. Wezeman, A. P. Siegel and H. E. Blackwell, *J. Am. Chem. Soc.*, 2005, 127, 12762-12763.
90. J. D. Rosen, T. D. Nelson, M. A. Huffman and J. M. McNamara, *Tetrahedron lett.*, 2003, 44, 365-368.
91. A. K. Strunz, A. J. Zweemer, C. Weiss, D. Schepmann, A. Junker, L. H. Heitman, M. Koch and B. Wünsch, *Bioorg. Med. Chem.*, 2015, 23, 4034-4049.
92. D. Katayev, V. C. Matoušek, R. Koller and A. Togni, *Org. Lett.*, 2015, 17, 5898-5901.

**Part II. Synthesis of agrocinopine D and D-glucose-2-phosphodiester
involved in the regulation of quorum sensing in *Agrobacterium*
fabrum C58.**

Chapter 3. Quorum sensing in *Agrobacterium* and agrocinopines

3.1 Introduction

As a type of gram-negative bacteria, *Agrobacterium fabrum* C58 uses 3-oxo-octanoyl homoserine lactone (OOHL) as a signal for quorum sensing. In this cell-cell communication mechanism, the protein TraI is the synthase which catalyses the synthesis of QS signal molecules. Once a threshold concentration of the molecular signal is reached, it binds to the protein TraR, homologous to LuxR. The formed transcription factor then regulates the biological function in tumor-inducing (Ti) plasmids horizontal transfer. Ti-plasmids contains a virulence gene, which is essential for the bacteria to transfer the genetic material into the infected plant cells. The functional characterization of the protein TraR [1,2] in *Agrobacterium fabrum* C58 bound to 3-oxo-OHL is an outstanding model for the insight of the LuxI/LuxR QS system.

Agrobacterium is a well-known genus that can insert its transfer DNA (T-DNA) into plants. Therefore, it has become an important biology material for genetic engineering. Once the plants are infected by *Agrobacterium fabrum* C58, it can cause a crown tumor disease in plants, which is expressed by T-DNA. T-DNA is a segment of Ti plasmid, which is capable of modifying the host plant cell to synthesize opines. Opines found in plant tumors are small molecules, such as amino acids or carbohydrate phosphates. Then opines can be used by *Agrobacterium* as a source of nitrogen, carbon and signals to activate quorum sensing in *Agrobacterium*. Ti plasmids themselves are divided into different classes according to the types of opine, namely octopine, nopaline, mannopine, and agrocinopine families (Figure 55).

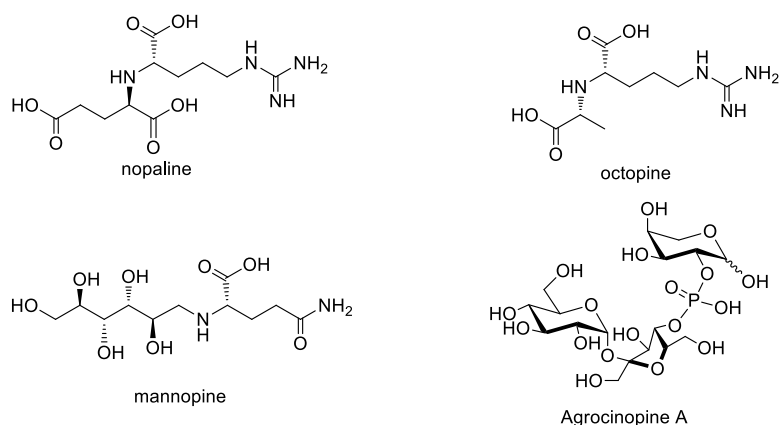


Figure 55. Chemical structures of four types of opines.

Among these four opines, the agrocinnopine family is less investigated. In the process of the interaction between *Agrobacterium fabrum* C58 and its hosts, agrocinnopines provide a source of carbon and function as a molecular signal for *Agrobacterium fabrum* C58. Bacterial population senses and responds to the produced signal, which activates the spread of virulence genes [3,4]. The carbohydrate feature of the agrocinnopines is critical for the recognition of protein-carbohydrate in the *acc* cascade. Firstly, it is responsible for the import of agrocinnopine back into the bacteria through specific recognition by the periplasmic binding proteins AccA. Then, once imported, it is recognized and hydrolyzed by the phosphodiesterase AccF (Figure 56). Finally, the resulting fragment binds with AccR responsible for virulence expression through activating the synthesis of quorum sensing signal [3].

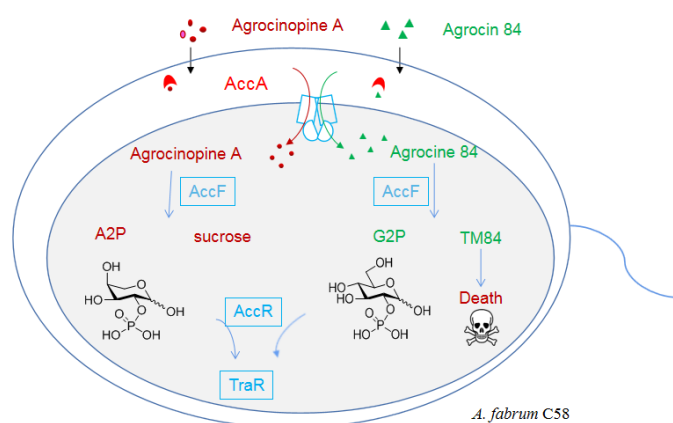


Figure 56. The roles of agrocinnopine A and agrocinn 84 in *A. fabrum* C58.

Agrocin 84 is a natural antibiotic that blocks the formation of plant crown gall [5], produced by a non-pathogenic *Agrobacterium radiobacter* K84. *Agrobacterium radiobacter* is considered to be the most successful bacterial biocontrol agent, thus it usually plays an important role in agricultural production. To enter into pathogenic *A. fabrum* cells, the carbohydrate phosphate moiety of agrocin 84 is indispensable [5]. After entering into the cells, agrocin 84 is cleaved into TM84 and D-glucose-2-phosphate (G2P) by enzyme AccF, which cleaves agrocinopine A into sucrose and L-arabinose-2-phosphate. As shown in figure 56, agrocin 84 imitates the specific transport pathway in *Agrobacterium fabrum* C58 of agrocinopine A thanks to the sugar-2-phosphate moiety. Agrocin 84 structure was originally proposed to be a glucofuranose 1-*O*-phosphate [6,7], but its structure was only recently fully identified as a glucose-2-phosphoryl derivative by X-ray crystal diffraction of its complex bound to AccA [8]. The ability of G2P esters to dupe the *acc* cascade of *Agrobacterium fabrum* C58 was also confirmed using the G2P lactic acid ester (G2LP) found to be the first non-natural G2P ester to mimic the role of natural agrocinopine A [9].

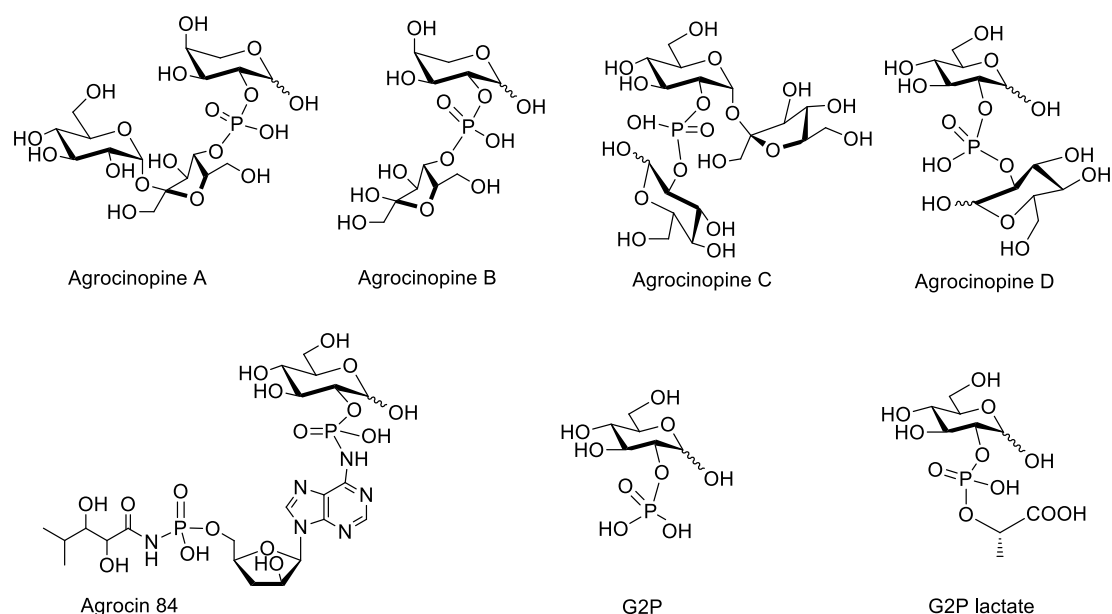


Figure 57. Structures of agrocinopines A, B, C and D, D-glucose-2-phosphate (G2P) and its esters G2P lactate, its amide agrocin 84.

Four agrocinopines (A, B, C and D) were firstly detected and identified in 1981, which were found to be specific to *A. fabrum* strain C58 and strain Bo542 [10]. Because they have consistent biological properties with known opines and agrocin 84, these four compounds are named agrocinopines. Agrocinopines were partly characterized as phosphorylated sugar derivatives [10]. Under mild acid conditions, agrocinopine B could be obtained from the hydrolysis of agrocinopine A, as well as agrocinopine D from agrocinopine C. In other words, there exists a similar structural relationship between agrocinopine A and agrocinopine B, and between agrocinopine C and agrocinopine D, respectively. Three years later, the detailed chemical structures of agrocinopine A and agrocinopine B were determined [11]. Agrocinopine A is constructed with an L-arabinose O-2 linked with a sucrose O-4 via a phosphodiester bond. Agrocinopine B is the 2-O-L-arabinose-4-O-D-fructose phosphodiester which originates from the cleavage of the glycosidic bond in the sucrose moiety of agrocinopine A. A few years later, the first reported structure of agrocinopine C was proposed a connection between sucrose at O-6 linked with glucose at O-2 via a phosphodiester bond, which showed similar biological activity compared with the natural agrocinopine C but very different degradative behaviors [12]. When reinvestigated, it was concluded that the phosphodiester actually linked at O-2 of the sucrose building block instead of O-6 [12]. This also meant that agrocinopine D had a symmetrical structure that combines two glucose at O-2 through a phosphodiester bond, which lacks the fructofuranosyl moiety of agrocinopine C (Figure 57).

In all these structures, the presence of an unfunctionalized anomeric carbon results in mixtures of anomers, and possibly also of furanose and pyranose forms, leading to rather difficult identification and characterization.

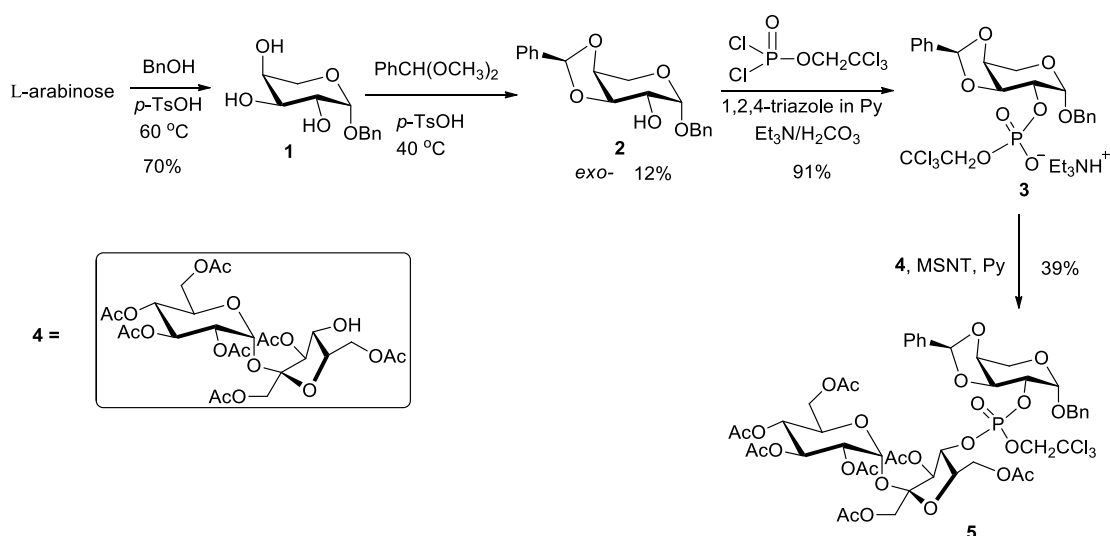
3.2 Background on the structural and synthetic chemistry of agrocinopines and their analogues

Carbohydrate phosphates and phosphodiester are of great importance in many biological processes. In the past few years, several groups have focused on the total

synthesis of this kind of natural molecules. The phosphorylation is a decisive step in the synthesis of carbohydrate phosphodiester. To realize selective phosphorylation in agrociniopines, the syntheses involve first appropriate regioselective protection of the carbohydrate building blocks. In this section, we summarized the different routes to synthesize natural agrociniopines and non-natural analogs.

3.2.1 Agrociniopine A

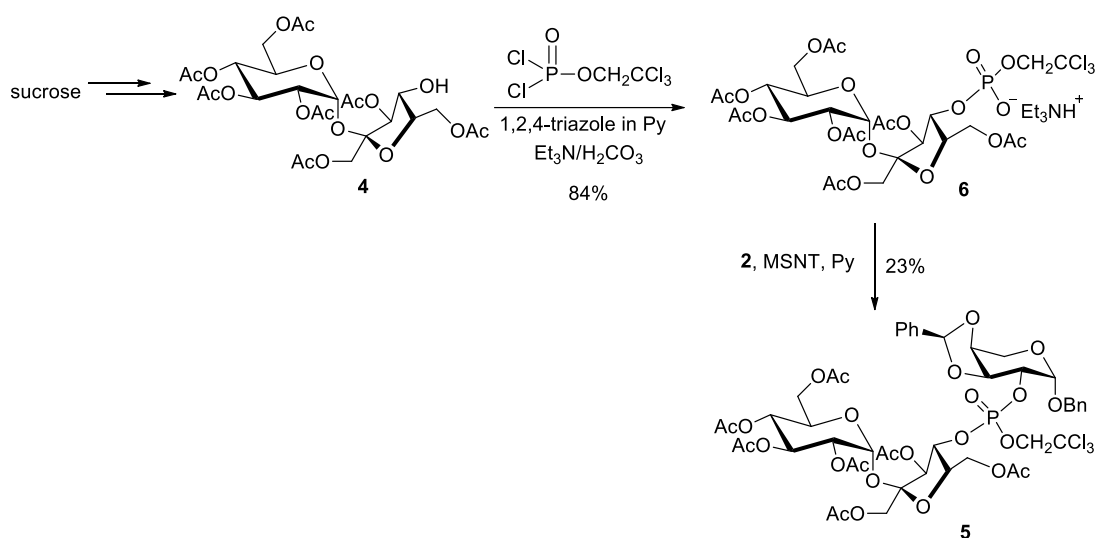
Agrociniopine A, firstly discovered and identified in 1981, is the structure of L-arabinose O-2 linked with a sucrose O-4 via a phosphodiester bond [11]. The oldest synthetic exploration on agrociniopine A was published in 1987 by Thiem's group [13] who realized the synthesis of the agrociniopine A precursor **5**. This initial work focused on an improved phosphorylation method to obtain this rare phosphodiester linkage. As shown in Scheme 20, *p*-TsOH-mediated glycosylation with benzyl alcohol afforded benzyl β-L-arabinose **1** in 70% yield. Subsequent protection of **1** with benzaldehyde dimethyl acetal led to two isomers, including the desired alcohol **2** in 12% yield. The regiospecifically protected L-arabinose building block **2** was phosphorylated with 2,2,2-trichloroethyl phosphorodichloridate in the presence of 1,2,4-triazole in pyridine, followed by hydrolysis with 1M buffer (Et₃N/H₂CO₃, 1:1), leading to the formation of phosphodiester triethylammonium salt **3**.



Scheme 20. Partial synthesis of agrociniopine A.

Sucrose 2,3,4,6,1',3',6'-hepta-acetate **4** [14] was obtained in 6% yield by partial de-esterification of sucrose octa-acetate in contact with the alumina for 44 hours in a column, which was speculated to arise from acetyl migration of 4'-position to primary 6'-position. Subsequent coupling of phosphodiester **3** with **4** gave protected agrocinopine A in 39% yield in the presence of pyridine and 1-(mesitylene-2-sulfonyl)-3-nitro-1*H*-1,2,4-triazole (MNST) as activating agent. In this case, it was expected to obtain the final product **5** as a 1:1 mixture of two diastereomers at the phosphorus atom chiral center.

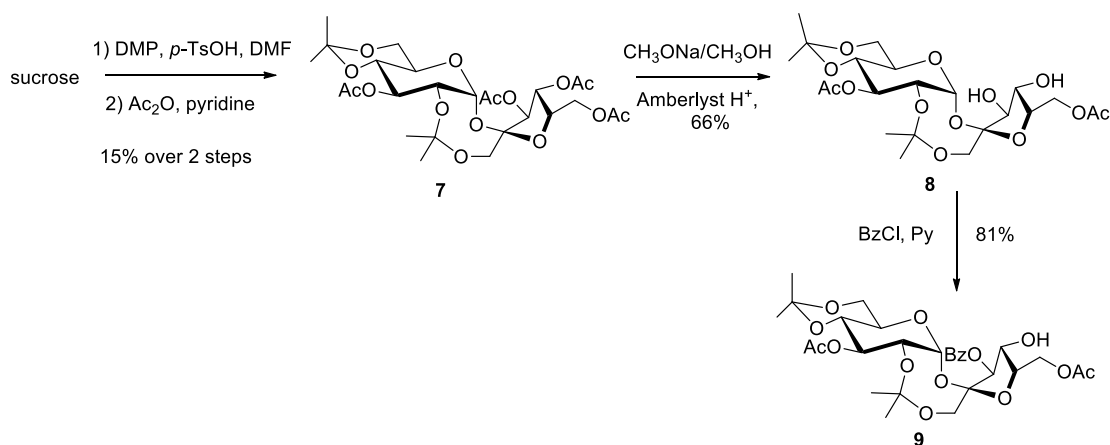
Alternatively, the target compound **5** could be obtained in 23% yield from the condensation of alcohol **2** with phosphodiester triethylammonium salt **6** by using the same conditions (Scheme 21). Interestingly, the diastereomerically pure product **5** was produced in this latter sequence.



Scheme 21. Partial synthesis of agrocinopine A.

In 1988, the first total synthesis of agrocinopine A was completed by Lindberg and Norberg [15]. Different methods were applied to access the sucrose and arabinose building blocks. In this case, the phosphorylation reagent was changed to phosphorus triimidazolide. The starting sucrose building block used in this synthesis is 3,3',4',6'-tetra-*O*-acetyl-2,1':4,6-di-*O*-isopropylidenesucrose **7**. This fully protected sucrose derivative was synthesized in two steps from the sucrose in an overall 15%

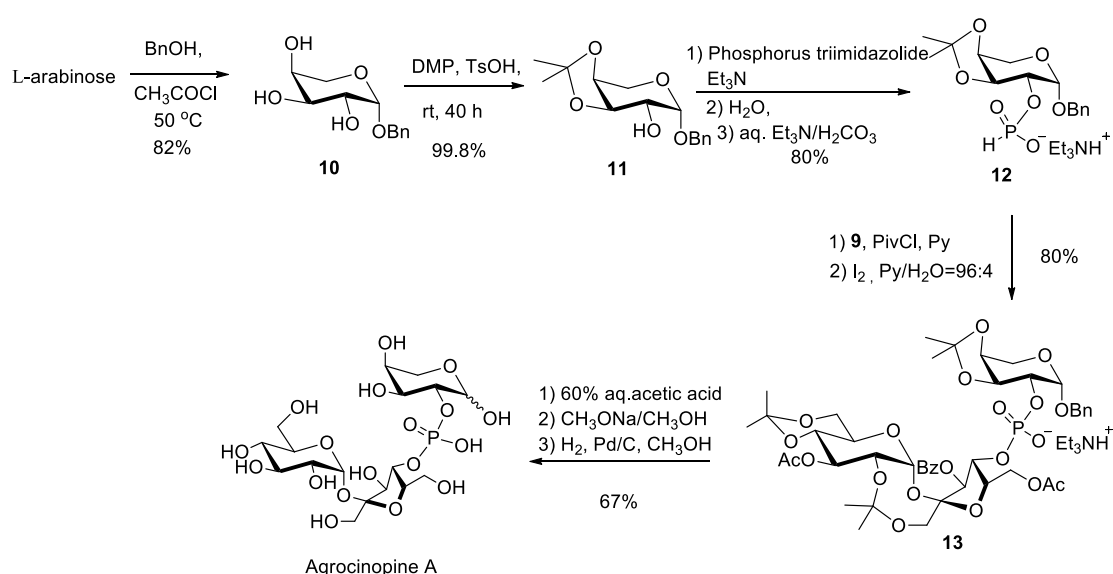
isolated yield following a method reported earlier by Khan and coworkers [16]. In 1985, Sheridan and coworkers [17] obtained the partially deacetylated product **8** from the fully protected sucrose **7** by treatment with a catalytic amount of sodium methoxide. The diol **8** was then monobenzoylelated using 1.1 eq benzoyl chloride in pyridine to form the 4'-OH unprotected sucrose derivative **9** in high yield (Scheme 22). This method was employed by Lindberg and coworkers [15] in their preparation of the sucrose building block. However, this synthetic sequence lacks efficiency due to the low overall yield for reaching the intermediate **7** from sucrose and the formation of by-products which are difficult to remove by column chromatography. The key step was the regioselective protection of sucrose by 2,2-dimethoxypropane (DMP) in the presence of *p*-TsOH to give the 2,1':4,6-di-*O*-isopropylidene sucrose intermediate. In 2000, Parrilli [18] developed a more efficient acetonation method catalyzed by ceric ammonium nitrate (CAN) instead of *p*-TsOH leading to obtaining 2,1':4,6-di-*O*-isopropylidene sucrose up to 71% yield.



Scheme 22. Synthesis of 3,6'-di-*O*-acetyl-3'-*O*-benzoyl-2,1':4,6-di-*O*-isopropylidene sucrose.

Among different arabinose building blocks bearing a free OH-2, Lindberg's team used the convenient benzyl 3,4-*O*-isopropylidene- β -L-arabinoside **11** in their preparation of agrocinopine A [15]. Alcohol **11** was generated from the protection as an acetal of OH-3 and OH-4 of the benzyl arabinoside **10** using 2,2-dimethoxypropane(DMP) in the presence of *p*-TsOH [19].

Hydrogen phosphonate **12** was obtained by the reaction of compound **11** with phosphorus triimidazolid followed by hydrolysis. The condensation of hydrogen phosphonate **12** with the sucrose derivative **9** in pyridine, using pivaloyl chloride as a coupling reagent, gave the hydrogen phosphodiester, which was further oxidized *in situ* with iodine in Py-water to give the protected phosphodiester **13**. Deprotection of **13** was accomplished by successive deacetalization followed by deacetylation and hydrogenolysis to give the final product in 67% yield (Scheme 23).



Scheme 23. First total synthesis of agrociniopine A by Lindberg and Norberg.

The suggested mechanism of the oxidation of hydrogen phosphodiester was that the reaction involved the formation of an iodophosphate intermediate (Figure 58). Firstly, the *H*-phosphonate tautomerized to three-coordinate hydroxy phosphite. Secondly, the resulting phosphonium salt lost a proton to form the iodophosphate intermediate. Finally, the displacement of iodine in the iodophosphate intermediate with water gave the phosphodiester. Moreover, this process proceeded non-stereospecifically [20].

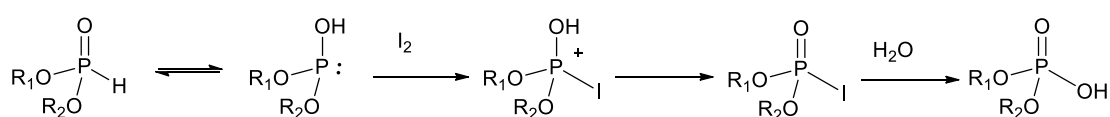
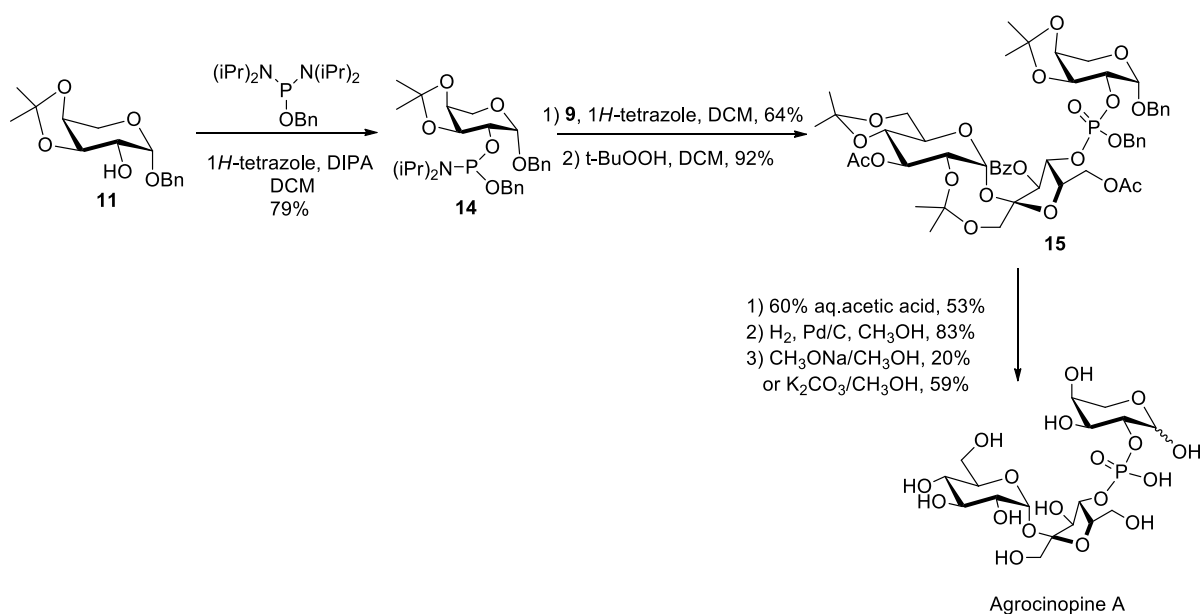


Figure 58. Mechanism of I₂-water promoted oxidation of *H*-phosphonate diesters.

Another wide general strategy of phosphodiester synthesis is the use of a phosphoramidite intermediate. Recently, in a study of the biological role of agrocinopine A in quorum sensing regulation in *Agrobacterium fabrum* C58, our lab [8] reported a modified access to agrocinopine A based on this convenient phosphorylation reagent (Scheme 24). In this synthesis, a phosphoramidite was used for reaching the intermediate **14**, which was further coupled with the sucrose building block **9** in the presence of 1*H*-tetrazole followed by oxidation with *t*-BuOOH. Product **15** was then subjected to a multiple deprotection procedure. Actually, the order of the deprotection steps is an important issue considering the stability of the intermediate products. Overall, the most efficient sequence was to perform the debenzoylation procedure before the deacetylation step.



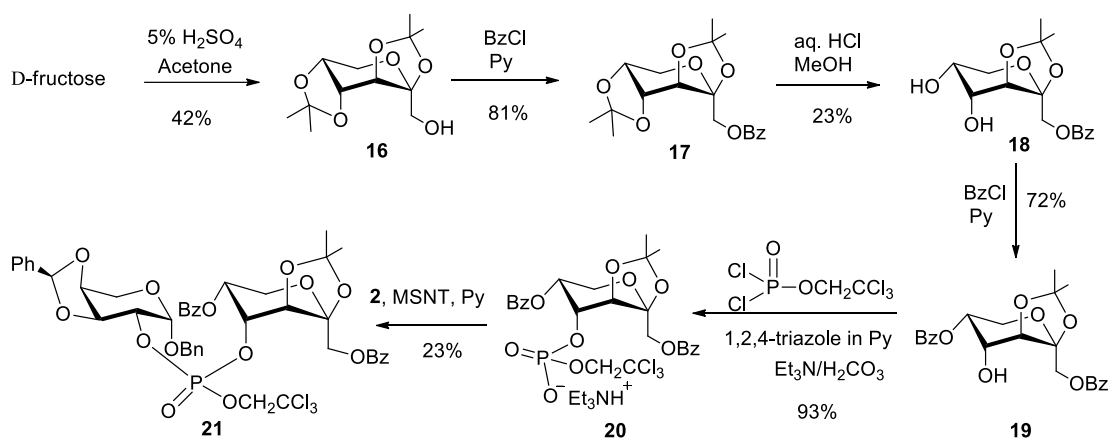
Scheme 24. Total synthesis of agrocinopine A.

3.2.2 Agrocinopine B

The reported syntheses of agrocinopine B are very few. Based on the same sequence used in their synthesis of a protected agrocinopine A, Thiem and coworkers [13] first reported the synthesis of protected agrocinopine B in 1987 (Scheme 25). The fructose with only OH-4 unprotected is a key substance in the synthesis of agrocinopine B.

Diol **18** was given through a three steps synthesis, acetal protection of D-fructose, benzylation with benzoyl chloride, and regioselective deacetalization [21]. The benzylation of the diol **18** with 1.0 equivalent of benzoyl chloride in the presence of pyridine, which was practically regio-specific, yielded the 5-*O*-benzoylated product **19** with small quantities of the 4-*O*-benzoylated product (ratio 96:4).

Subsequently, compound **19** was subjected to a condensation step by coupling with the phosphodiester triethylammonium salt **2** to afford protected agrocinopine B in 23% yield. Alternatively, the synthesis of the target phosphodiester **21** was achieved by coupling the phosphodiester **3** with the fructose **19** in 55% yield. In each approach, the target product **21** was obtained as a mixture of two diastereoisomers in a 1:2 ratio.



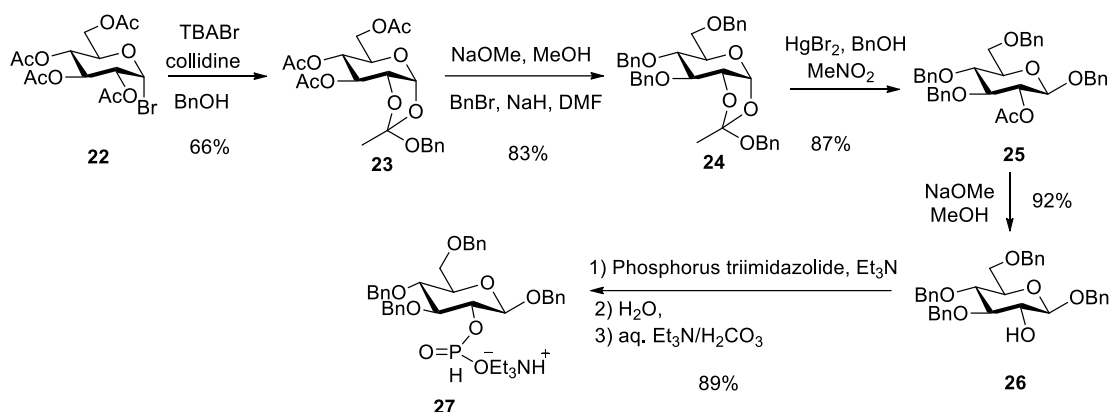
Scheme 25. Partial synthesis of agrocinopine B.

3.2.3 Agrocinopine C

Agrocinopine C was originally proposed to have the D-glucos-2-yl sucros-6-yl phosphate **34** structure. This compound was first synthesized by Oscason and coworkers [22] according to similar sequences and reagents as in their previous on agrocinopine A.

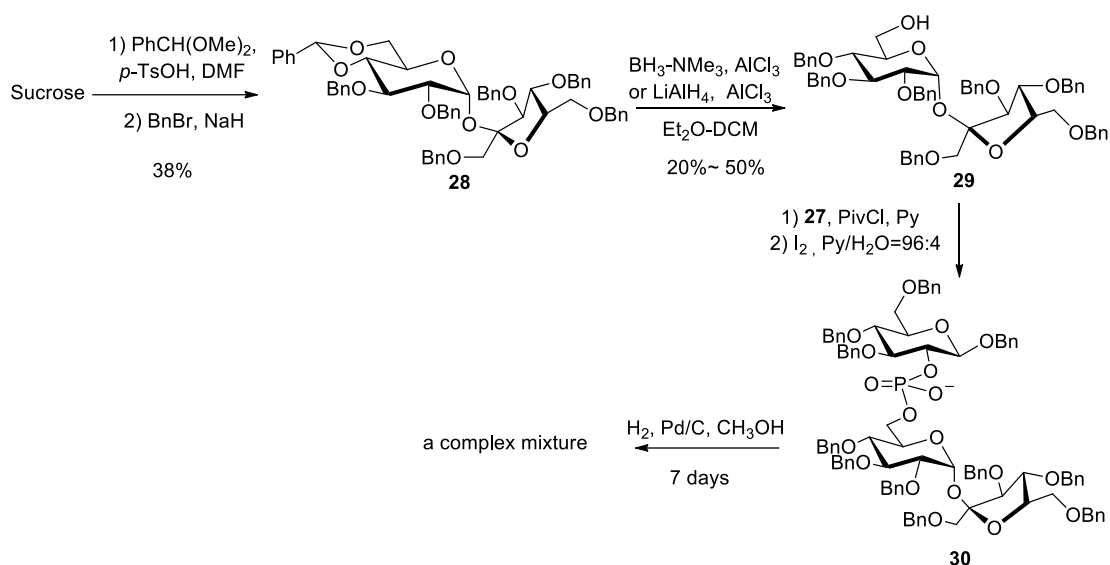
In this work, regarding the glucose moiety, Oscason and coworkers prepared **26** via 1,2-orthoester approach [23] starting from bromoacetoglucose **22** (Scheme 26). The reaction with benzyl alcohol in the presence of base and TBABr gave the

1,2-orthoester **23**. Consecutive deacetylation and benzylation gave the 3,4,6-tri-*O*-benzyl 1,2-orthoester **24**, that then underwent β stereoselective HgBr₂-mediated glycosylation of benzyl alcohol giving the β benzyl glucoside **25**. After deacetylation of **25** to glucoside **26**, the reaction of glucoside **26** with phosphorus triimidazolid followed by hydrolysis gave the hydrogen phosphonate **27**.



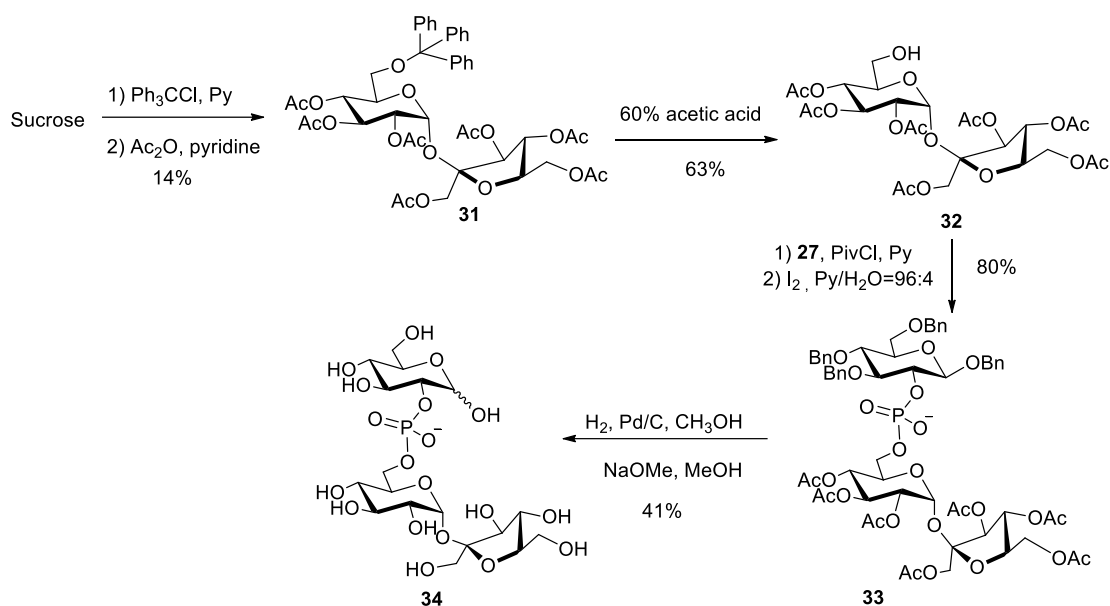
Scheme 26. Synthetic route for benzylated glucose with 2-OH free.

Regarding the sucrose moiety, they selected the sucrose building block **29** bearing OH-6 free as the acceptor for the construction of phosphodiester. Treatment of sucrose with benzaldehyde dimethyl acetal in the presence of *p*-TsOH in DMF gave 4,6-*O*-benzylidene sucrose as the main product and 2,1':4,6-di-*O*-benzylidene sucrose as the minor product [24]. The mixture was then benzylated by an excess benzyl bromide to give the fully protected sucrose **28** in 38% yield. Regioselective reductive ring opening of the 4,6-*O*-benzylidene acetal at *O*-6 position was promoted by LiAlH₄-AlCl₃ or BH₃·NMe₃-AlCl₃, giving the desired product **29** in yields ranging from 20% to 50% (Scheme 27).



Scheme 27. Synthesis of D-glucos-2-yl sucros-6-yl phosphate.

The condensation of the hydrogen phosphonate **27** with the sucrose **29** in pyridine, activated by pivaloyl chloride [25,26], gave the intermediate hydrogen phosphodiester, not isolated and immediately oxidized with iodine in pyridine-water to give the phosphate **30**. However, subsequent deprotection of **30** proved to be problematic. Only a small amount of fully deprotected product was observed and the final products were identified in a mixture of other partially debenzylated compounds and by-products of hydrolysed phosphodiester linkage. To avoid the problem at the step of debenzylation of compound **30**, an alternative route using partially acetylated sucrose **32** was proposed. The route to the sucrose building block **32** was starting from sucrose involving sequentially a tritylation, acetylation, and detritylation process [27]. The tritylation step, providing the target intermediate mixed with 6'-*O*-tritylsucrose, di-*O*-tritylsucrose, and tri-*O*-tritylsucrose, gave the sucrose derivative **31** in a poor yield. Then, the coupling of **32** with the previously used glucose building block **27** in the presence of the condensing agent, followed by oxidation, proceeded the phosphodiester **33** in 80% yield. Debenzylation and subsequent deacetylation were achieved in 41% yield to afford the expected product **34** (Scheme 28).



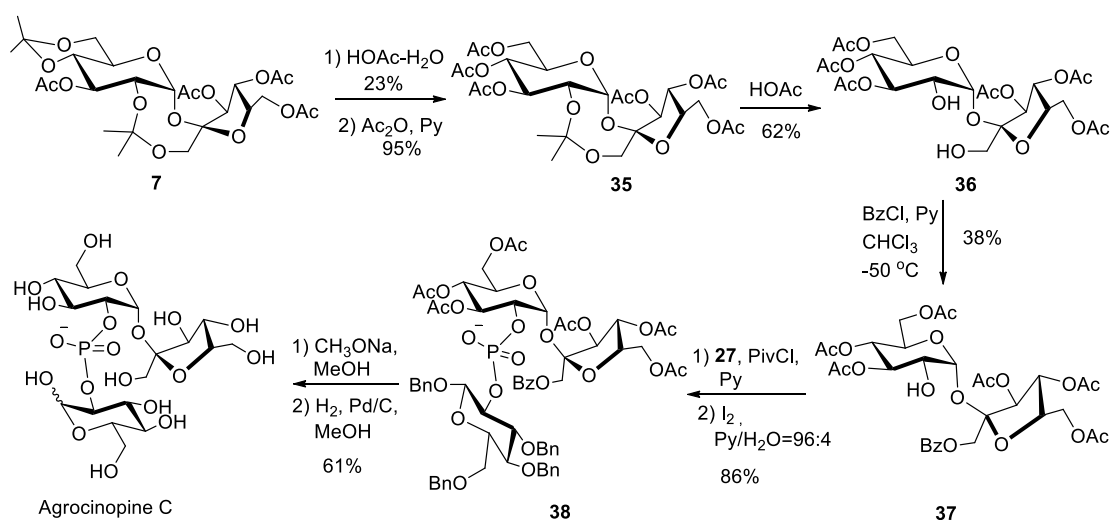
Scheme 28. Synthesis of D-glucos-2-yl sucros-6-yl phosphate.

Once synthesized, the authors found that the ^{13}C NMR spectrum of compound **34** was different from the one isolated in natural material, and the biological evaluation also showed inconsistent results as compared with natural agrocinopine C. This triggered a novel, more precise investigation of the structure of natural agrocinopine C which pointed out that the phosphodiester was linked with the O-2 position in sucrose moiety instead of position OH-6 [22]. Based on this new data, changing the sucrose intermediate to a regiospecifically protected sucrose building block bearing OH-2 free was undertaken.

The sequence was first based on the work by Lindseth and Khan [28,29] who firstly reported selective de-acetalization of **7** by aqueous acetic acid, giving the desired intermediate 3,3',4',6'-tetra-*O*-acetyl-1',2-di-*O*-isopropylidenesucrose in 23% yield together with other possible products, namely the 4,6-monoacetal and the fully deacetalized product 3,3',4',6'-tetra-*O*-acetyl-sucrose in 4.7% and 28%, respectively. Considering the yields in monoacetals, it was concluded that the monoacetal with the eight-membered (1',2) ring was significantly stable, more than the six-membered (4,6) ring of the cyclic acetal group. Conventional acetylation and de-acetalization of the 1',2 cyclic acetal group gave the diol **36** in good yield. The desired product sucrose

derivative **37** with only O-2 unprotected was obtained as the product (38%) by treatment of 3,4,6,3',4',6'-hexa-*O*-acetyl sucrose **36** with benzoyl chloride in a mixture of pyridine and chloroform.

Following the same final steps as in their previous work, Lindberg and Oscarson [12] could successfully achieve the first total synthesis of the revised agrociniopine C structure (Scheme 29). The coupling with glucose building block **27** followed by oxidation led to precursor **38** in high yield even though both sugar building blocks were secondary alcohols. The deprotected product was obtained in a reasonable 61% yield. The ^{13}C NMR spectrum recorded of this synthetic agrociniopine C was fully consistent with the natural one.

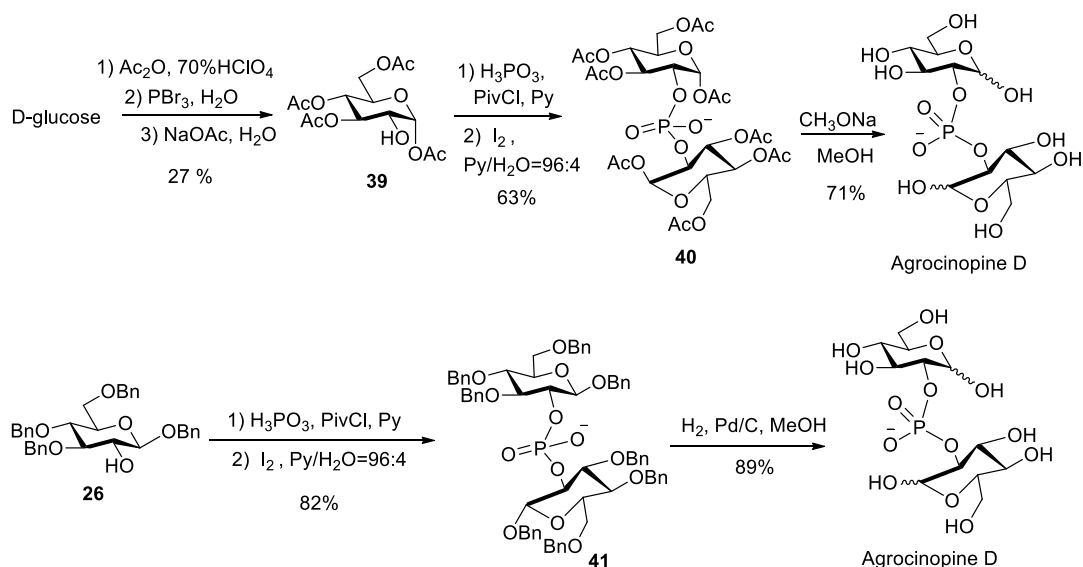


Scheme 29. First total synthesis of agrociniopine C by Lindberg and Oscarson.

3.2.4 Agrociniopine D

Agrociniopine D is a symmetrical compound connecting two glucose moieties at O-2 via a phosphodiester bond. Based on the same hydrogen-phosphate approach as they used before, Lindberg and Oscarson [12] proposed an easy synthetic route to hydrogenphosphate diesters via the reaction of phosphonic acid with excess (more than two equivalents) alcohols (Scheme 30). Two different kinds of regiospecifically protected glucose building blocks were employed, either acetylated or benzylated.

Many possibilities can provide selectively protected glucose building block bearing a free OH-2. Among approaches, bromoacetoglucose **22** is a key and common starting material. As already mentioned above, compound **26** can be prepared from bromoacetoglucose **22**. Alternatively, the direct hydrolysis of bromoacetoglucose [30] can provide α -1,3,4,6-tetraacetyl-glucose **39**.



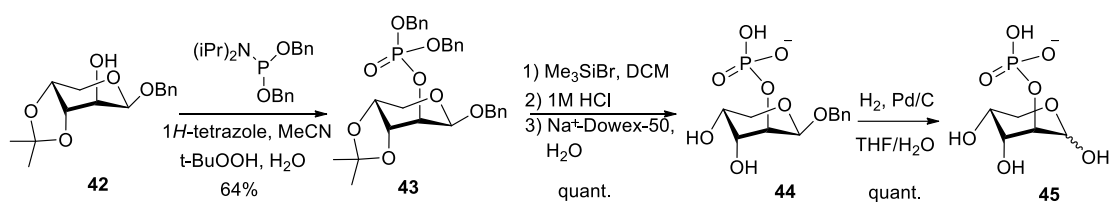
Scheme 30. First total synthesis of agrocinopine D.

The acetylated or the benzylated glucose derivatives (at least 2.5 equivalents) were used in the reaction with phosphonic acid in pyridine in the presence of pivaloyl chloride as an activating agent, followed by *in situ* oxidation in a mixture of pyridine-water (96:4) using iodine. This afforded the phosphodiesters **40** in 63% yield and **41** in 82% yield, respectively. Palladium-catalyzed hydrogenolysis of compound **41** gave agrocinopine D as an anomeric mixture in 89% yield. Deacetylation of compound **40** could also provide the target, but along with side products, probably arising from undesired cyclic glucose-1,2-phosphate formation.

3.2.5 Arabinose-2-phosphate (A2P) and their derivatives

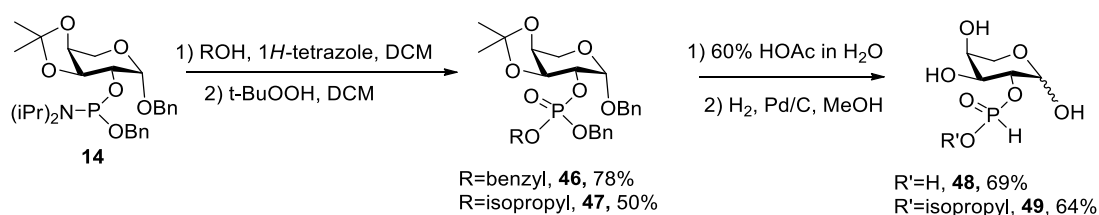
In 2008, D-arabinose-2-phosphate [31] was prepared by Sutherland's team via the phosphoramidite approach (Scheme 31). Synthesis of D-A2P **45** started from benzyl

3,4-*O*-isopropylidene- β -D-arabinoside **42** which was generated from the protection OH-3 and OH-4 of benzyl arabinose using 2,2-dimethoxypropane (DMP) in the presence of TsOH [19]. Phosphate triester **43** was afforded in good yield by coupling **42** with dibenzyl bis isopropylamino phosphoramidite followed by oxidation. Treatment of **43** with TMSBr and subsequent deacetal step could not afford the fully deprotected product **45** as the anomeric benzyl group remained in the product **44**. Further hydrogenolysis of **44** gave the final D-arabinose-2-phosphate in high yield.



Scheme 31. Synthesis of D-arabinose-2-phosphate.

Based on a similar sequence, our group [8] synthesized L-arabinose-2-phosphate **48** and its isopropyl phosphodiester **49** (Scheme 32). The reaction of phosphoramidite **14** with benzyl alcohol or isopropanol gave the phosphotriester **46** and **47**, respectively. After the deprotection, L-arabinose-2-phosphate or its isopropyl ester were obtained in fair yields.

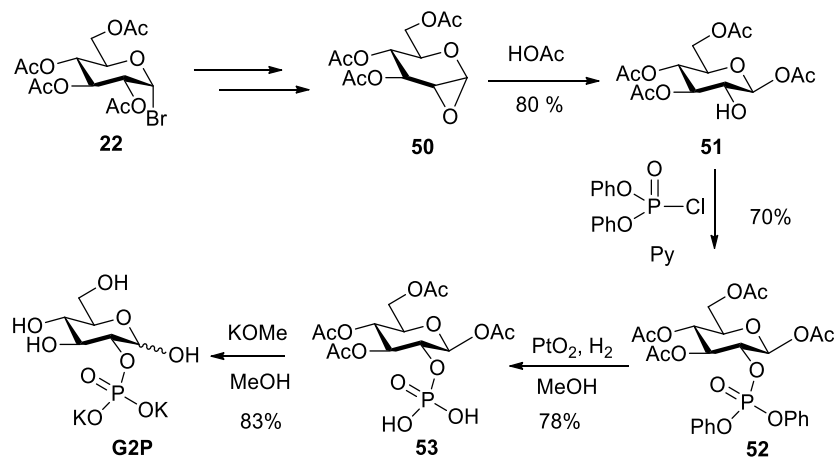


Scheme 32. Synthesis of L-arabinose-2-phosphate and its isopropyl ester.

3.2.6 D-Glucose-2-phosphate (G2P)

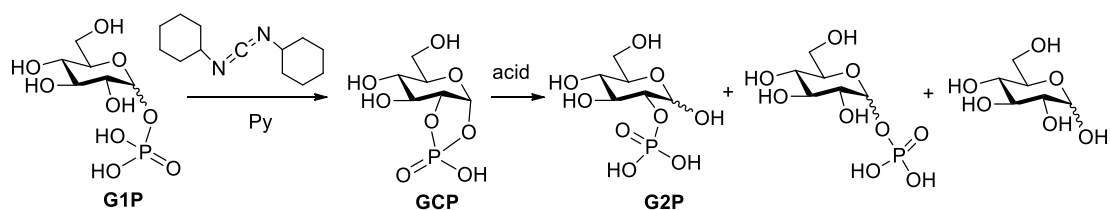
The D-glucose-2-phosphate (G2P) moiety is quite rare in natural molecules, only found in glycogen, agrocinopine D and agrocin 84. The earliest preparation of D-glucose-2-phosphate (G2P) was achieved in 1949 by Farrar [32] who

unambiguously synthesized G2P using diphenyl chlorophosphate as phosphorylation reagent (Scheme 33). The key substance **51** was prepared by reaction of 3,4,6-tri-*O*-acetyl-1,2-anhydro- α -D-glucopyranose with HOAc [33]. The easy purification by crystallization makes this sequence quite efficient. After two different deprotection procedures, G2P was given in good yield.



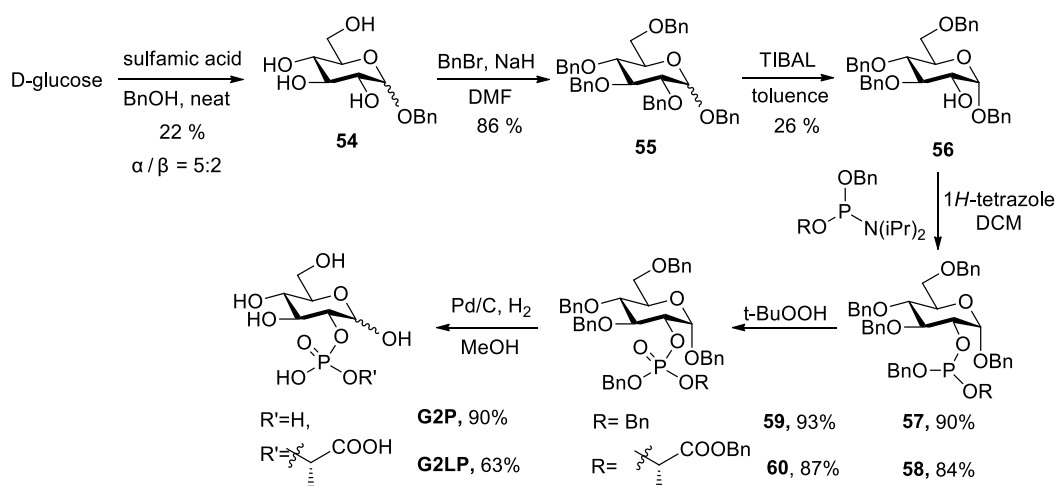
Scheme 33. First synthesis of G2P by an unequivocal method.

G2P can also originate from the hydrolysis of cyclic glucose-1,2-phosphate (GCP) prepared from the easily available glucose-1-phosphate in pyridine, activated by dicyclohexylcarbodiimide (DCC) (Scheme 34). In the course of the hydrolysis, G2P is more stable than G1P [32,34]. Many biologists collected the G2P in this way to study phosphate stability or hydrolysis rates [35,36] or for identification of the hydrolyzed monomeric forms of glycogen to understand the metabolism of the phosphate in glycogen [37,38].



Scheme 34. Synthesis of G2P by hydrolysis of the GCP.

Recently a collaborative work involving biologists in Gif and our group as chemists found that G2P activated the quorum sensing pathway of *Agrobacterium fabrum* C58 [8]. G2P was synthesized from benzyl 3,4,6-tri-*O*-benzyl- α -D-glucopyranoside **56** using a monoaminated phosphoramidite as a coupling reagent. The precursor **56** was prepared by selective reductive 2-*O*-debenzylation of perbenzylated glucose [8,9] with triisobutyl aluminum (TIBAL) [39]. Based on the same phosphorylation method as the synthesis of A2P, the non-natural glucose-2-*O*-(lactic acid phosphate) (G2LP) was obtained and found to enable the growth of *Agrobacterium fabrum* C58 [9].



Scheme 35. Synthesis of G2P and derivatives.

3.3 Conclusions

This bibliographic chapter outlines the structure and the biological role of natural agrocinosins and their derivatives with a focus on synthetic issues. We reviewed the coupling step creating the phosphate or the phosphodiester by different phosphorylation approaches. The availability of natural agrocinosins and synthetic analogues have helped to understand the role of these carbohydrate phosphodiesters in the infection process of plants by pathogenic *Agrobacterium fabrum* C58.

Building on these results, and aiming at diversifying the type of analogues, we have undertaken a methodological approach towards a family of novel G2P esters and G2P phosphodiester agrocinosin D.

Chapter 4. Result and discussion

4.1 Synthesis of agrocinopine D and D-glucose-2-phosphodiester

(The work reported in this section has been published in *Molecules*. Zhang, Q.; Li, S.-Z.; Ahmar, M.; Soulère, L.; Queneau, Y. Esters of Glucose-2-Phosphate: Occurrence and Chemistry. *Molecules* 2020, 25, 2829.)

4.1.1 Introduction

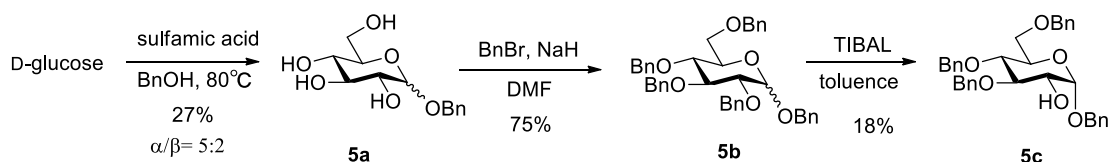
As mentioned in the previous section, the glucose-2-phosphate and its esters is a very rare structure, only found in a few natural molecules, such as agrocinopine D and agrocin 84. Apart from the family of agrocinopines and agrocin 84, the G2P moiety was also found in glycogen, together with G3P and the more common G6P. Glycogen-bound phosphate influences glycogen architecture with different branching and chain length. Even if glucose phosphates are structurally similar, G1P and G6P are involved in the glycogen degradation and synthesis processes, respectively. Oppositely, G2P or G3P residues cannot be confirmed by biochemical enzymatic assays as there is no known enzyme with specific activity towards these two phosphates [37,40,41]. Actually, glucose-2-phosphate itself was used for studying phosphate stability or hydrolysis rates [34,36], or for identification of the hydrolyzed monomeric forms of glycogen to understand the metabolism of the phosphate in this biopolymer [37,38]. The quite uncommon D-glucose-2-phosphate (G2P), which refers to a structure having the phosphate covalently bonded glucose hydroxyl at C-2 position, was firstly and unequivocally synthesized by Farrar [32] in 1949. The hydrolysis of the cyclic glucose-1,2-phosphate (GCP) can afford a mixture of G2P and G1P. During the hydrolysis, G2P esters exhibit higher stability versus G1P [32,34].

Considering the originality of the G2P motif, its interest in the chemistry and the biology of agrocinopines and analogues, and the lack of recent studies focusing on its chemistry as compared to the ubiquitous glucose-1-phosphates (G1P) or glucose-6-phosphates (G6P), we have investigated different sequences to access G2P and some of its phosphodiester.

4.1.2 Synthesis of the glucose building block bearing 2-OH

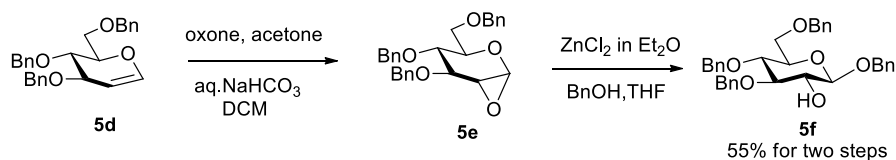
The regioselective protection of carbohydrates is an important issue in synthetic carbohydrate chemistry. The overall efficiency of total syntheses of agrocinopine D and its analogues counts on the availability of such a glucose building block bearing 2-OH as the only available one. To keep an easy and practical deprotection procedure in the final step, we chose benzyl ethers as protecting groups. Therefore, benzyl 3,4,6-tri-*O*-benzyl-D-glucosides appeared to be the ideal precursor.

The synthesis of benzyl 3,4,6-tri-*O*-benzyl- α -D-glucoside relies on a 3 steps route starting from D-glucose (Scheme 36). Firstly, the sulfamic acid catalyzed glycosylation of BnOH gave benzyl α -D-glucoside as the major product mixed with some amounts of β anomer (α : β 5:2). Subsequent perbenzylation of the anomeric mixture **5a** gave benzyl 2,3,4,6-tetra-*O*-benzyl-D-glucoside **5b**, which was then selectively 2-*O*-debenzylated by TIBAL. As the TIBAL-promoted debenzylation only proceeds on α -anomer of **5b**, the β anomer was untransformed. This last step, though simple and elegant, and able to provide the target compound, suffers from exhibiting a quite low yield.



Scheme 36. Synthesis of benzyl 3,4,6-tri-*O*-benzyl- α -D-glucoside.

Inspired by the reports on Lewis acid-catalyzed ring-opening reaction of the readily available 1,2-anhydro- α -D-hexopyranose [42,43], we found that this method provided the β target **5f** within only 2 steps from the commercially available benzylated glucal in good yield (Scheme 37). Obviously, the β -pathway to access glucose building block **5f** can be advantageous as compared to the α route.



Scheme 37. Synthesis of benzyl 3,4,6-tri-*O*-benzyl-β-D-glucoside.

The structure of the resulting **5f** was assessed by NMR data consistent with the literature, notably the chemical shift of the anomeric proton doublet at 4.24 ppm, with a 7.7 Hz coupling constant indicating the β configuration (Figure 59).

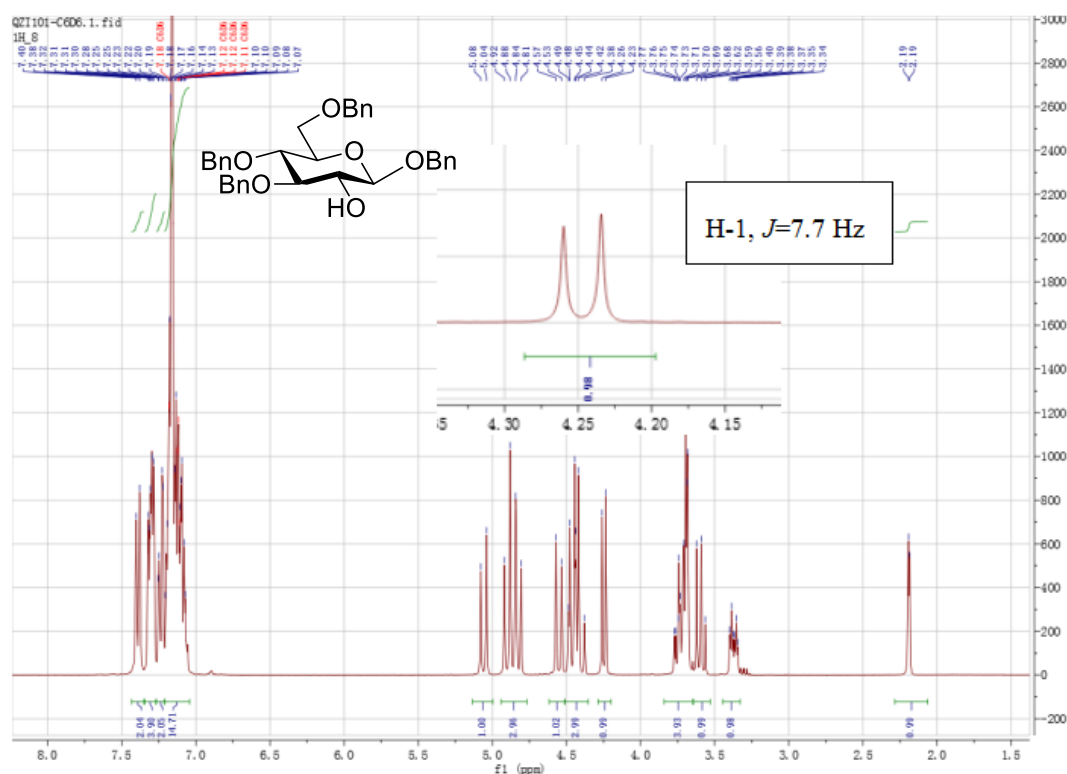


Figure 59. ^1H -NMR of compound **5f** confirming the β configuration .

4.1.3 Phosphorylation reagent

In cellular biology, phosphorylation and dephosphorylation are very important processes. Many protein phosphorylation patterns are involved in some critical cellular functions. In chemical biology, this has generated a strong interest in developing efficient phosphorylation strategies. Generally, such strategies involve P(V) or P(III) reagents as shown in figure 60.

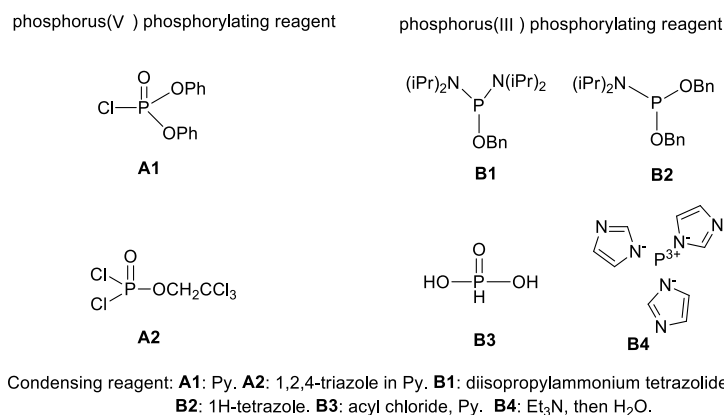
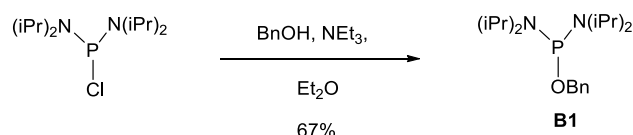


Figure 60. General phosphorylation reagents and their condensation reaction conditions.

Here, we targeted phosphoramidite **B1** as a phosphorylation reagent. The reaction of chloro-bis(diisopropylamino)phosphine with benzyl alcohol in presence of triethylamine gave the desired phosphoramidite in 67% yield (Scheme 38).



Scheme 38. Synthesis of phosphoramidite **B1**.

4.1.4 Synthesis of agrocino-pin D and D-glucose-2-phosphodiester

Having the glucose building block **5f** in hands, its coupling with benzyloxy bis(diisopropylamino)phosphine gave selectively the monoaminated phosphoramidite **5g** in 81% yield in the presence of diisopropylammonium tetrazolide as mild and hindered base preventing double diisopropylamino displacement [44]. Phosphoramidite **5g** was then coupled with alcohol **5f** again to afford the phosphite intermediate which was subjected to subsequent oxidation step using *tert*-BuOOH to give the precursor of agrocino-pin D. Then phosphoramidite **5g** was coupled with a short scope of primary or secondary alcohols including benzyl alcohol, cetearyl alcohol, cholesterol and dihydrocholesterol (Table 9). All reactions of **5g** gave fair to good yields, with primary alcohols gave phosphodiester **5h** in a higher yield, while secondary alcohols suffer from steric hindrance. The ³¹P NMR showed that **5i**, **5j** and **5k** were obtained as a mixture of the two diastereoisomers in nearly 1:1 ratio.

Table 9. Synthesis of D-glucose-2-phosphodiester and their derivatives.

Entry	ROH	Product	Yield
1	benzyl alcohol	 5h	88%
2	cetearyl alcohol	 5i	90% (1/1.1) ^a
3	cholesterol	 5j	70% (1/1.3) ^a
4	5α-cholestan-3β-ol	 5k	74% (1/1.4) ^a
5	benzyl 3,4,6-O-benzyl-β-D- glucopyranoside	 5l	53%

a. Diastereomeric ratio was measured by ³¹P-NMR.

The structures of all compounds were confirmed by ^1H NMR, ^{13}C NMR, ^{31}P NMR, 2D-NMR and high resolution mass spectrometry. Here, we take compound **5h** as an example to explain the identification of structures. The chemical shift of the anomeric proton of **5h** was 4.51 ppm, and the coupling constant was 10 Hz, indicating it's the β isomer (Figure 61). The chemical shift of H2 moved to the low field, suggesting that the *O*-2 position of **5h** bears an electron-withdrawing group, here the phosphate. Actually, we can also conclude it through the coupling constants between carbon and phosphorus atoms. Due to the coupling with the phosphorus atom, the carbon signals of C1, C2 and C3 recorded by ^{13}C NMR are split into doublets (Figure 62). Among the different coupling constants of found carbons observed, it is reasonable to find that the highest coupling constant is recorded in C2 since it's closest to the phosphorus atom (Figure 63).

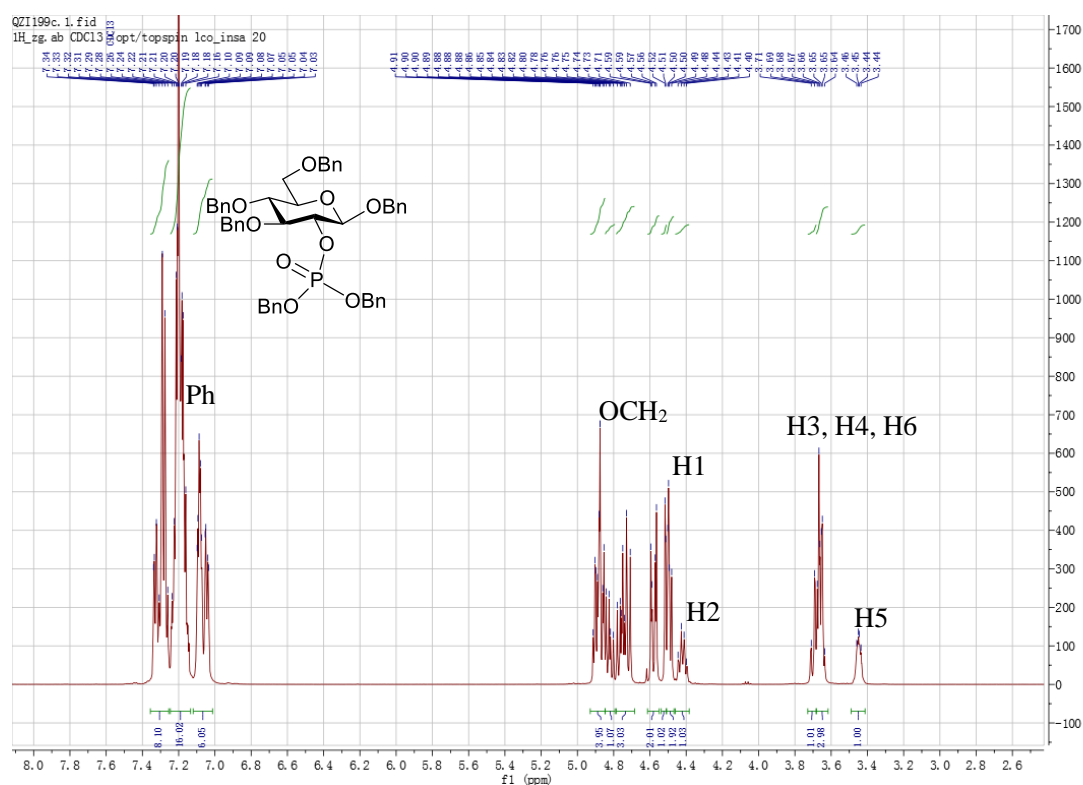


Figure 61. ^1H -NMR of compound **5h**. Identifications of each proton in compound **5h** are shown.

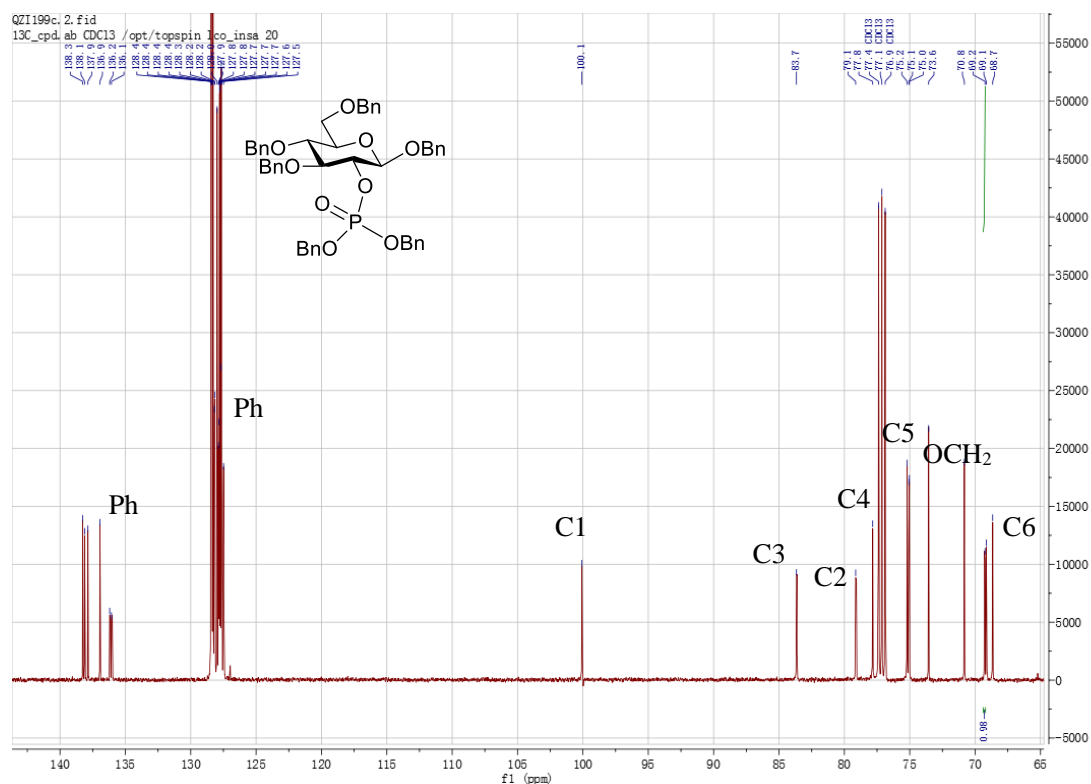


Figure 62. ¹³C-NMR of compound **5h**. Identifications of each carbon in compound **5h** are shown.

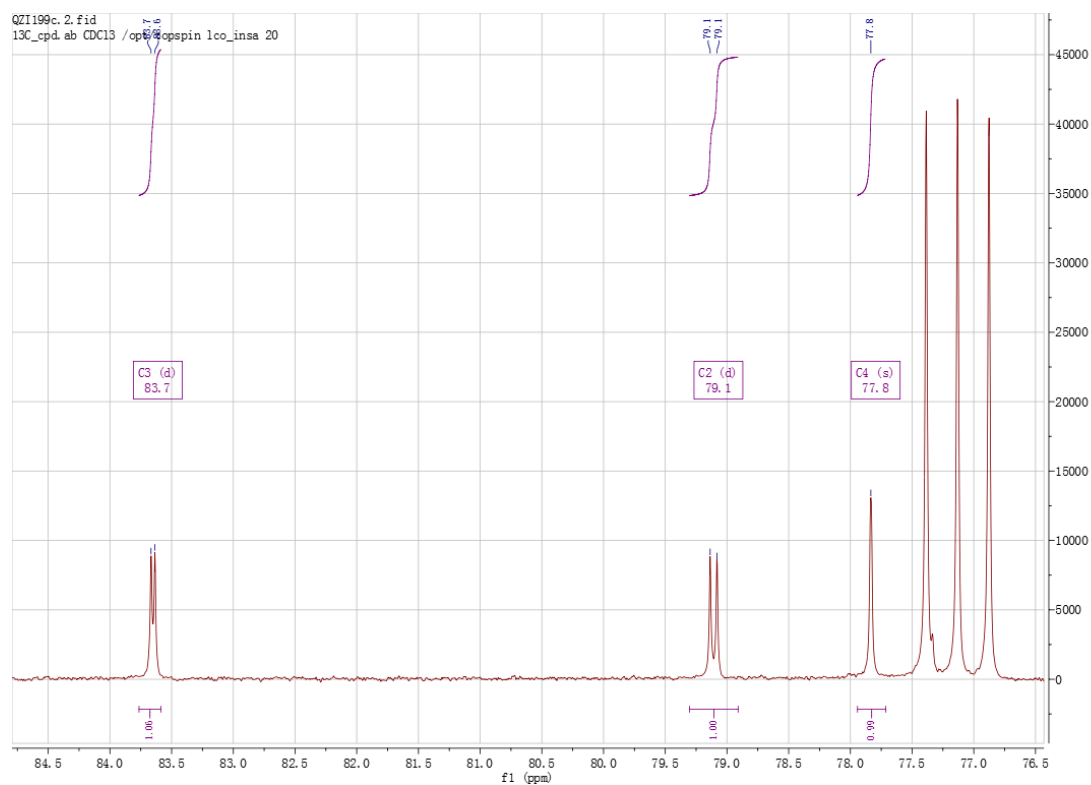
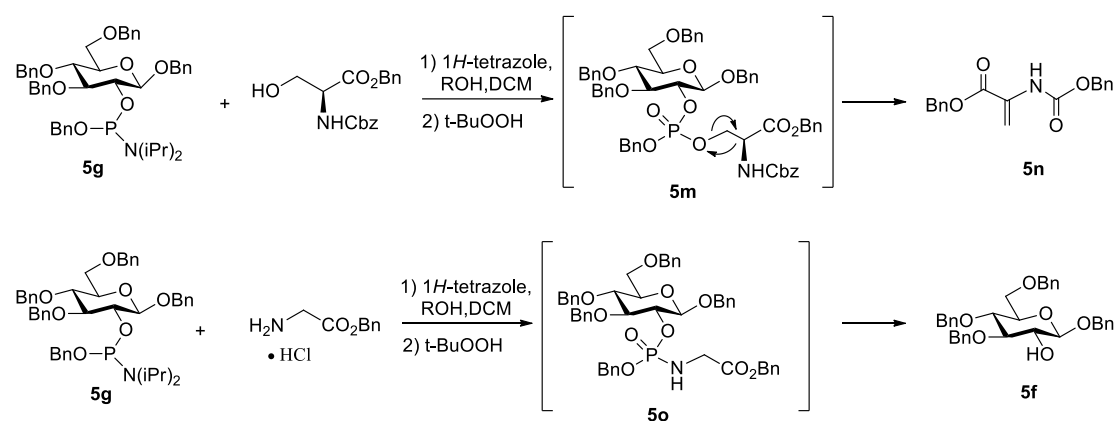


Figure 63. Partial ¹³C-NMR of compound **5h**. The carbon signals of C2, C3 in compound **5h** are split into doublets.

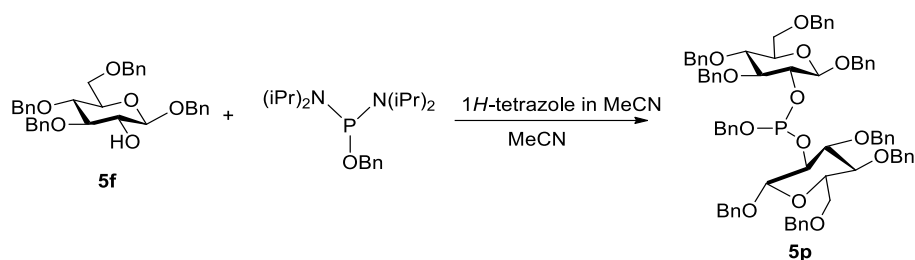
Additionally, attempts were made on the substances bearing other functional groups, including amino acids and amines. We examined the coupling of *N*-Cbz-L-serine benzyl ester and glycine benzyl ester hydrochloride (Scheme 39). Unfortunately, phosphate esters **5m** and **5o** were unstable. The intermediate compound **5m** decomposed to α,β -dehydroamino acid **5n** through α,β -elimination pathway under basic condition [45]. Due to the instability of the O-P-N bonds, *N*-phosphorylated derivatives are considered to be difficult to construct [46]. In the present case, the intermediate compound **5o** was unable to be purified by column chromatography and the glucose derivative **5f** was recovered.



Scheme 39. Phosphorylation of β -hydroamino acids or amines.

Considering the specific importance of agrocinosine D, and its symmetrical structure, we investigated a shorter route to the protected phosphodiester **5l** (perbenzylated agrocinosine D) in one-pot from the glucose building block **5f**. In this conversion, the key step is the formation of the intermediate bis-glucosyl phosphite starting from the glucose building block **5f**. This step was optimized with respect to the stoichiometry between substrate **5f**, the phosphoramidite and tetrazole (Table 10). When the reaction was carried out with only 1.0 equivalent of phosphoramidite, low conversion of substrate **5f** was observed. Increasing the amount of phosphoramidite to 2.0 equivalents led mainly to the formation of monoaminated phosphoramidite **5g**. The most favorable conditions were found to be 1.2 equivalents of phosphoramidite and 3 equivalents of 1*H*-tetrazole.

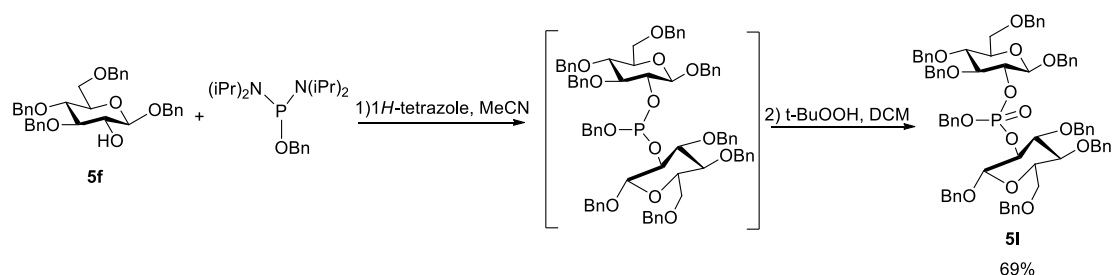
Table 10. Optimization of reaction conditions.



Entry	Compound 5f (eq)	Phosphoramidite (eq)	1 <i>H</i> -Tetrazole (eq)	Yield
1	2.0	1.0	2.5	34%
2	2.0	2.0	2.5	<5% ^a
3	2.0	1.5	2.5	28%
4	2.0	1.2	3.0	84% ^b

a. main product is compound **5g**; b. NMR yield.

Under the optimized reaction condition, the bis glucosyl phosphotriester **5l** was synthesized in one-pot from compound **5f** in a good yield (Scheme 40). Compared with the method developed by Lindberg and Oscarson, the purification of the final product **5l** only requires a simple silica gel chromatography instead of consecutive ion exchange columns.



Scheme 40. Synthesis of the precursor of agrocino-pin D by one-pot.

For compound **5l**, a slight difference between the H2 signals in the two glucose rings was observed by ¹H NMR (500 Hz). Although compound **5l** is regarded as a symmetrical structure, careful examination of its ¹H NMR and ¹³C NMR indicates

compound **5l** is not totally symmetrical, both glucose moieties being D-enantiomers, preventing any symmetry plan in the molecule. Slight differences of C1, C2, C3 in two glucose rings were also observed in ^{13}C NMR (Table 11).

Carbon in glucose ring 1	Carbon in glucose ring 1'
99.8 (d, $J_{\text{C-P}} = 4.2$ Hz, C1)	100.2 (d, $J_{\text{C-P}} = 2.9$ Hz, C1')
78.6 (d, $J_{\text{C-P}} = 6.8$ Hz, C2)	79.1 (d, $J_{\text{C-P}} = 7.4$ Hz, C2')
83.6 (d, $J_{\text{C-P}} = 4.8$ Hz, C3)	83.5 (d, $J_{\text{C-P}} = 3.6$ Hz, C3')

Table 11. Partial ^{13}C -NMR assignment of compound **5l**.

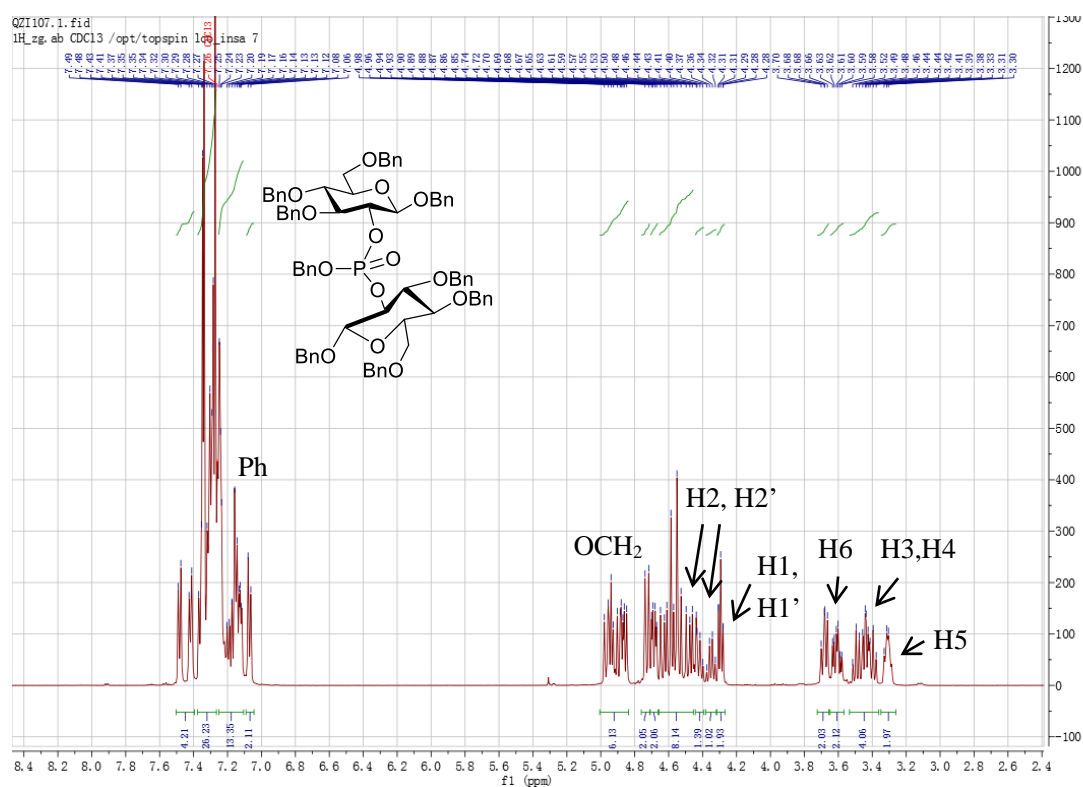


Figure 64. ^1H -NMR of compound **5l**. Identifications of each proton in compound **5l** are shown.

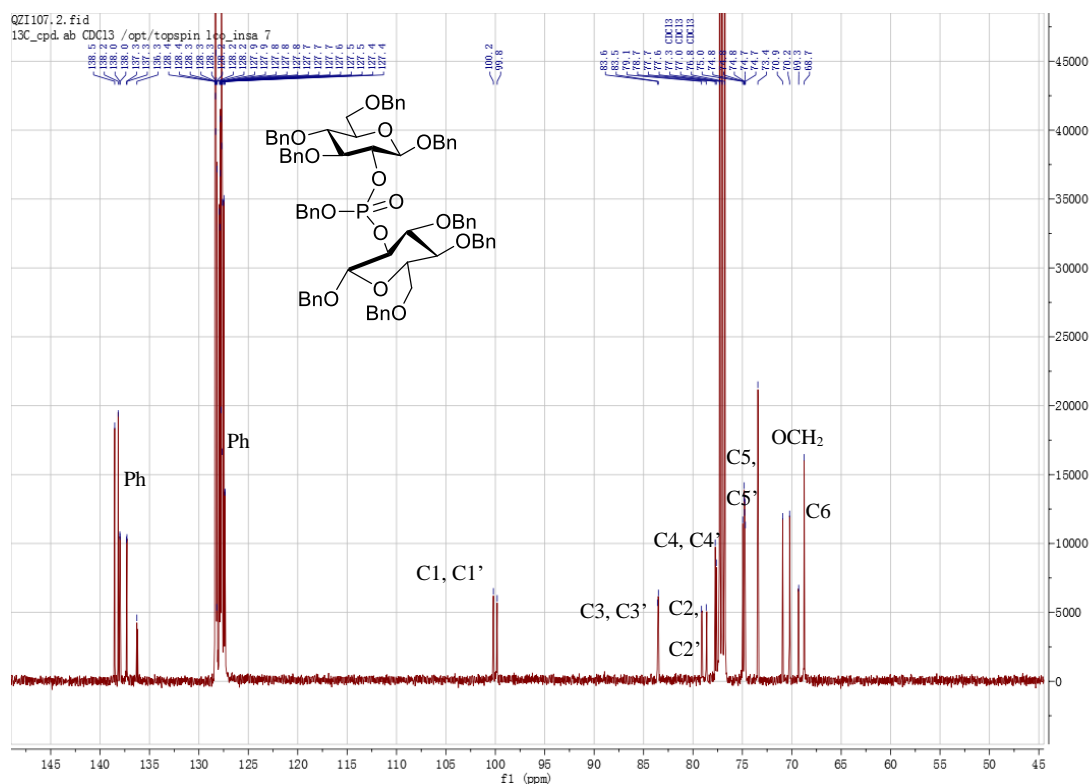


Figure 65. ^{13}C -NMR of compound **5I**. Identifications of each carbon in compound **5I** are shown.

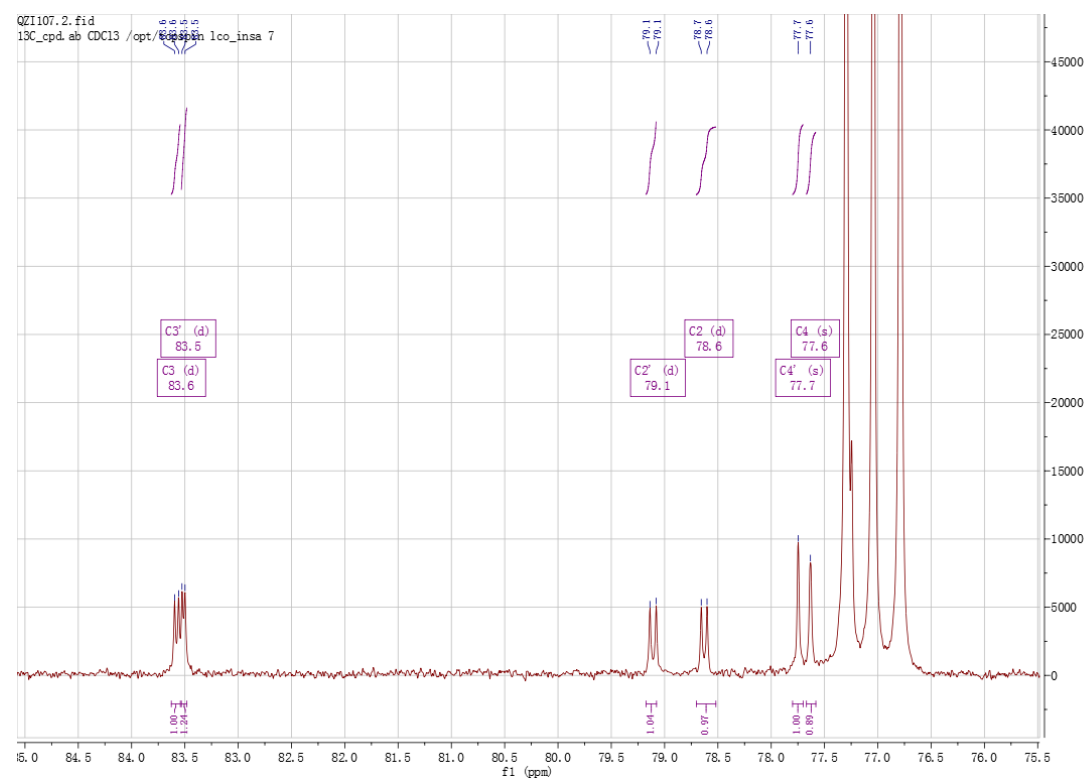


Figure 66. Partial ^{13}C -NMR of compound **5I**. The carbon signals of C2, C2', C3, C3' in compound **5I** are split into doublets.

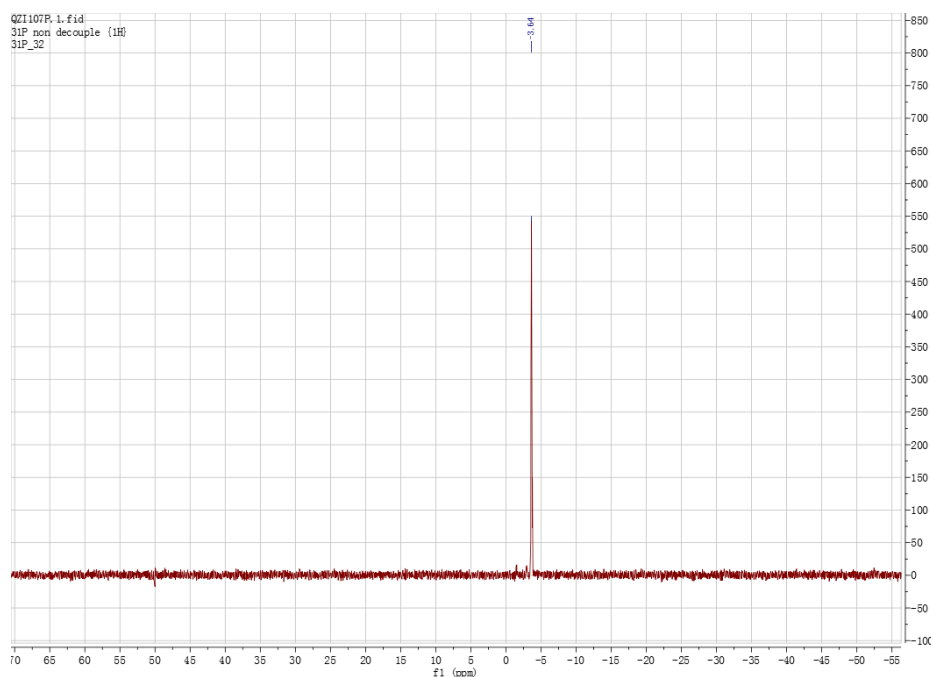
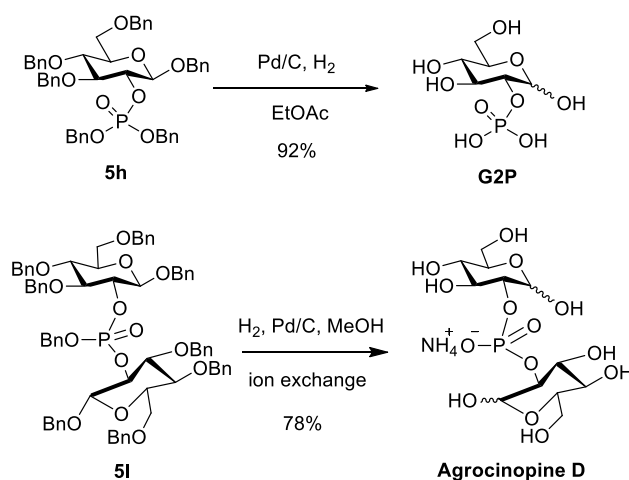


Figure 67. ^{31}P -NMR of compound **5l**.

In order to get the fully deprotected target G2P and agrociniopine D, palladium-catalyzed hydrogenolysis was performed using compounds **5h** and **5l**, using 1 atm H_2 and Pd/C in methanol or ethyl acetate. G2P was obtained in high yield and purity after debenzylation. Agrociniopine D was further purified by ion-exchange chromatography on a DEAE-Sephadex column to obtain pure agrociniopine D in its ammonium salt form in 78% yield free of any trace of glucose or G2P. Both compounds exhibited consistent NMR data as compared with the literature [9,12].



Scheme 41. Debenzylation of the precursor of G2P and agrociniopine D.

4.1.5 Biological studies using agrocinopine D

Our team is involved in a collaboration with Dr. Solange Morera and her coworkers at the I2BC laboratory in Gif-sur-Yvette. This collaboration aims at determining the level of specificity in the recognition of various agrocinopines and their analogues by different strains of *Agrobacterium fabrum*, notably C58 and Bo542. In particular, the binding mode of agrocinopine D with the periplasmic protein AccA of C58 or Bo542 strains will be determined and compared. This binding mode is yet unreported in the literature.

Thanks to the samples of agrocinopine D prepared by us and sent to them, they will perform experiments aiming at the crystallization of the AccA proteins in the presence of the ligands and hopefully obtain crystals of satisfactory quality for enabling their analysis by X-ray diffraction experiments. Based on these experiments, the precise binding mode of agrocinopine D with the periplasmic protein AccA of C58 or Bo542 will be fully assessed for the first time.

4.1.6 Conclusions

We developed a flexible synthetic method to access the rare glucose-2-phosphate and its esters including agrocinopine D. It relies on the coupling reaction of the phosphoramidite with benzyl 3,4,6-tri-*O*-benzyl- β -D-glucoside which is prepared from commercially available tri-*O*-benzyl-D-glucal. A short scope of the coupling strategy to reach G2P esters demonstrated its efficiency for the design of variously substituted analogs in the agrocinopine family.

References

1. L. Zhang, P. J. Murphy, A. Kerr and M. E. Tate, *Nature*, 1993, 362, 446-448.
2. K. R. Piper, S. Beck Von Bodman and S. K. Farrand, *Nature*, 1993, 362, 448-450.
3. S. Beck Von Bodman, G. T. Hayman and S. K. Farrand, *Proc. Natl. Acad. Sci. U.S.A.*, 1992, 89, 643-647.
4. J. G. Ellis, A. Kerr, A. Petit and J. Tempe, *Mol. Gen. Genet.*, 1982, 186, 269-274.
5. J. S. Reader, P. T. Ordoukhanian, J.-G. Kim, V. de Crécy-Lagard, I. Hwang, S. Farrand and P. Schimmel, *Science*, 2005, 309, 1533-1533.
6. W. P. Roberts, M. E. Tate and A. Kerr, *Nature*, 1977, 265, 379-381.
7. R. J. Thompson, R. H. Hamilton and C. F. Pootjes, *Antimicrob. Agents Chemother.*, 1979, 16, 293-296.
8. A. E. Sahili, S.-Z. Li, J. Lang, C. Virus, S. Planamente, M. Ahmar, B. G. Guimaraes, M. Aumont-Nicaise, A. Vigouroux, L. Soulère, J. Reader, Y. Queneau, D. Faure and S. Moréra, *PLoS Pathog*, 2015, 11, e1005071.
9. S.-Z. Li, A. Vigouroux, M. Ahmar, A. El Sahili, L. Soulère, L. Sago, D. Cornu, S. Moréra and Y. Queneau, *Org. Biomol. Chem.*, 2019, 17, 1090-1096.
10. J. Ellis and P. Murphy, *Mol. Gen. Genet.*, 1981, 181, 36-43.
11. M. H. Ryder, M. E. Tate and G. P. Jones, *J. Biol. Chem.*, 1984, 259, 9704-9710.
12. M. Lindberg and S. Oscarson, *J. Carbohydr. Chem.*, 1993, 12, 1139-1147.
13. M. Franzkowiak and J. Thiem, *Liebigs. Ann. Chem.*, 1987, 1065-1071.
14. J. M. Ballard, L. Hough and A. C. Richardson, *Carbohydr. Res.*, 1974, 34, 184-188.
15. M. Lindberg and T. Norberg, *J. Carbohydr. Chem.*, 1988, 7, 749-755.
16. R. Khan and K. S. Mufti, *Carbohydr. Res.*, 1975, 43, 247-253.
17. D. M. Clode, W. A. Laurie, D. McHale and J. B. Sheridan, *Carbohydr. Res.*, 1985, 139, 161-183.
18. E. Manzo, G. Barone and M. Parrilli, *Synlett*, 2000, 6, 887-889.
19. R. E. Ireland, L. Courtney and B. J. Fitzsimmons, *J. Org. Chem.*, 1983, 48, 5186-5198.
20. P. M. Cullis and M. Lee, *J. Chem. Soc., Chem. Commun.*, 1992, 1207-1208.
21. I. I. Cubero and M. T. Plaza López-Espinosa, *J. Carbohydr. Chem.*, 1986, 5, 299-311.
22. M. Lindberg, T. Norberg and S. Oscarson, *J. Carbohydr. Chem.*, 1992, 11, 243-253.
23. R. U. Lemieux and A. R. Morgan, *Can. J. Chem.*, 1965, 43, 2199.
24. R. Khan, K. S. Mufti and M. R. Jenner, *Carbohydr. Res.*, 1978, 65, 109-113.
25. B. C. Froehler and M. D. Matteucci, *Tetrahedron Lett.*, 1986, 27, 469-472.
26. J. Stawinski and M. Thelin, *J. Chem. Soc. Perkin Trans. 2*, 1990, 849-853.
27. T. Otake, *Bull. Chem. Soc. Jpn.*, 1970, 43, 3199.
28. R. Khan and H. Lindseth, *Carbohydr. Res.*, 1979, 71, 327-330.
29. R. Khan, M. R. Jenner and H. Lindseth, *Carbohydr. Res.*, 1980, 78, 173-183.
30. W. E. Dick Jr, *Carbohydr. Res.*, 1972, 21, 255-268.
31. C. Anastasi, F. F. Buchet, M. A. Crowe, M. Helliwell, J. Raftery and J. D. Sutherland, *Chem. Eur. J.*, 2008, 14, 2375-2388.
32. K. R. Farrar, *J. Chem. Soc.*, 1949, 3131-3135.
33. E. Hardegger and J. De Pascual, *J. Helv. Chim. Acta.*, 1948, 31, 281-286.

34. F. C. Kokesh, D. A. Cameron, Y. Kakuda and P. V. Kuras, *Carbohydr. Res.*, 1978, 62, 289-300.
35. S. Mikkola, *Curr. Org. Chem.*, 2013, 17, 1525-1544.
36. F. C. Kokesh, R. K. Stephenson and Y. Kakuda, *Biochim. et Biophys. Acta.*, 1977, 483, 258-262.
37. V. S. Tagliabracchi, C. Heiss, C. Karthik, C. J. Contreras, J. Glushka, M. Ishihara, P. Azadi, T. D. Hurley, A. A. DePaoli-Roach and P. J. Roach, *Cell Metab.*, 2011, 13, 274-282.
38. T. Whiteside, L. Carreira and S. Hilal, *QSAR Comb. Sci.*, 2007, 26, 587-595.
39. T. Lecourt, A. Herault, A. J. Pearce, M. Sollogoub and P. Sinaÿ, *Chem. Eur. J.*, 2004, 10, 2960-2971.
40. V. M. Chikwana, M. Khanna, S. Baskaran, V. S. Tagliabracchi, C. J. Contreras, A. DePaoli-Roach, P. J. Roach and T. D. Hurley, *Proc. Natl. Acad. Sci. U.S.A.*, 2013, 110, 20976-20981.
41. L. E. Young, C. O. Brizzee, J. K. Macedo, R. D. Murphy, C. J. Contreras, A. A. DePaoli-Roach, P. J. Roach, M. S. Gentry and R. C. Sun, *Carbohydr. Polym.*, 2020, 230, 115651.
42. D. M. Gordon and S. J. Danishefsky, *Carbohydr. Res.*, 1990, 206, 361-366.
43. D. Somasundaram, K. K. Balasubramanain and B. Shanmugasundaram, *Tetrahedron Lett.*, 2019, 60, 764-767.
42. F. C. Kokesh, D. A. Cameron, Y. Kakuda and P. V. Kuras, *Carbohydr. Res.*, 1978, 62, 289-300.
44. A. Barone, J.-Y. Tang, M. Caruthers, *Nucleic Acids Res.*, 1984, 12, 4051-4061.
45. F. Berti, C. Ebert and L. Gardossi, *Tetrahedron Lett.*, 1992, 33, 8145-8148.
46. M. Sekine, T. Moriguchi, T. Wada and K. Seio, *J. Synth. Org. Chem., Japan.*, 2001, 59, 1109-1120.

General conclusion

In summary, we have designed and synthesized a series of new AHLs analogues based on the modulation of the amide function or the side chain of AHLs which are *Vibrio fischeri*-quorum sensing modulators. AHLs analogues bearing a carbamate or a thiocarbamate were found to be antagonists whereas the hydrazide analogues were inactive. Concerning 2-OH AHLs, two diastereoisomerically pure isomers (*R/S*) with different chain lengths or phenyl groups were obtained and evaluated. The two diastereoisomers of 2-hydroxy hexanoyl HSL or 2-hydroxy octanoyl HSL were identified as highly potent modulators and they exerted opposite activity according to the configuration at C2. Docking studies performed with these two isomers showed that the *R*-isomer induced new hydrogen bonds with Tyr70 and Asp79 while the *S*-isomer gave a similar hydrogen binding network to the natural ligand. Based on imidazole and triazole scaffolds, we designed and synthesized 1,4- and 1,5-disubstituted triazoles or imidazole AHLs analogs. The biological evaluation revealed that both two kinds of triazole and some imidazole AHL analogues were antagonistic.

In the other aspect, flexible synthetic access to the rare glucose-2-phosphate structures, including the natural agrociniopine D, was developed. In this exploration, we employed an efficient one-pot method to synthesize the precursor of agrociniopine D. It relies on the coupling reaction of the phosphoramidite with benzyl 3,4,6-tri-*O*-benzyl- β -D-glucoside which is prepared from commercially available tri-*O*-benzyl-D-glucal. This method is very flexible to expand the synthesis of G2P analogues. Further biological investigation of agrociniopine D is ongoing.

To conclude, this thesis, which concerns two chemical aspects of bacterial quorum sensing, demonstrates how much chemistry can intervene in the design of new active molecules and the understanding of the QS pathway.

We have synthesized two natural compounds (agrociniopine D and G2P), several precursors and derivatives in the G2P series. Further biological investigations are still

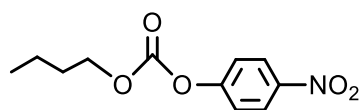
in progress. We have also prepared 46 AHL analogs among which several exhibit interesting activities. These new scaffolds might be a starting point for further pharmacomodulation. Further developments of the asymmetric late-lactone-formation strategy would enrich its applicability.

Experimental section

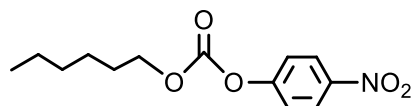
Supporting information (I)

General procedure A for the synthesis of *p*-nitrophenyl carbonate:

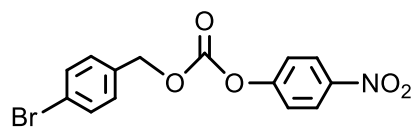
To a solution of alcohol (1.05 eq) in THF were added triethylamine (2.3 eq), *p*-nitrophenyl chloroformate (1 eq) at 0 °C. The reaction mixture was stirred overnight at rt. Then the mixture was diluted with 20 mL EtOAc and filtered. The solution was washed with brine (2×10 mL) and the organic phase was collected, dried over anhydrous Na₂SO₄, concentrated to give the desired carbonate.



Butyl 4-nitrophenyl carbonate: From butyl alcohol following general procedure A afforded butyl 4-nitrophenyl carbonate (48%) as a yellow liquid. ¹H NMR (300 MHz, Chloroform-*d*) δ 8.28 – 8.03 (m, 2H, Ph), 7.39 – 7.24 (m, 2H, Ph), 4.21 (t, *J* = 6.6 Hz, 2H, OCH₂), 1.80 – 1.56 (m, 2H, CH₂), 1.44 – 1.26 (m, 2H, CH₂), 0.89 (t, *J* = 7.4 Hz, 3H, CH₃) ppm.

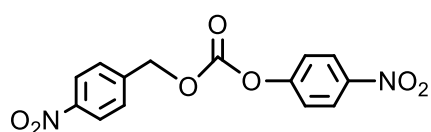


Hexyl 4-nitrophenyl carbonate: From hexyl alcohol following general procedure A afforded hexyl 4-nitrophenyl carbonate (56%) as a yellow liquid. ¹H NMR (300 MHz, Chloroform-*d*) δ 8.35 – 8.16 (m, 2H, Ph), 7.45 – 7.31 (m, 2H, Ph), 4.27 (t, *J* = 6.7 Hz, 2H, OCH₂), 1.83 – 1.61 (m, 2H, CH₂), 1.51 – 1.19 (m, 6H, 3×CH₂), 0.89 (t, *J* = 7.0, 3H, CH₃) ppm.

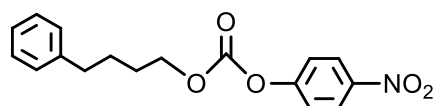


(4-Bromoophenyl)methyl 4-nitrophenyl carbonate: From 4-bromobenzyl alcohol

following general procedure A. Flash chromatography of the crude product (1:8 EtOAc-pentane) afforded (4-bromoophenyl)methyl 4-nitrophenyl carbonate (47%) as a white solid. ^1H NMR (300 MHz, Chloroform-*d*) δ 8.33 – 8.21 (m, 2H, Ph), 7.59 – 7.49 (m, 2H, Ph), 7.43 – 7.28 (m, 4H, Ph), 5.24 (s, 2H, OCH₂). ^{13}C NMR (76 MHz, Chloroform-*d*) δ 155.41 (CO), 152.38 (Ph), 145.45 (Ph), 133.18 (Ph), 132.01 (2C, Ph), 130.33 (2C, Ph), 125.34 (2C, Ph), 123.28 (Ph), 121.76 (2C, Ph), 70.10 (OCH₂) ppm. ESI-HRMS(M+Na)⁺: 373.9635; found: 373.9637.



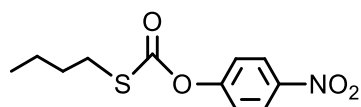
(4-Nitrophenyl)methyl 4-nitrophenyl carbonate: From 4-nitrobenzyl alcohol following general procedure A afforded (4-nitrophenyl)methyl 4-nitrophenyl carbonate (78%) as a yellow solid. ^1H NMR (300 MHz, Chloroform-*d*) δ 8.34 – 8.26 (m, 4H, Ph), 7.70 – 7.59 (m, 2H, Ph), 7.48 – 7.34 (m, 2H, Ph), 5.40 (s, 2H, CH₂) ppm.



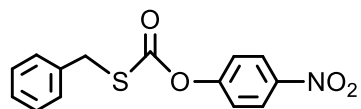
(4-Phenyl)butyl 4-nitrophenyl carbonate: From 4-phenyl butanol following general procedure A. Flash chromatography of the crude product (1:8 EtOAc-pentane) afforded (4-phenyl)butyl 4-nitrophenyl carbonate (48%) as a white solid. ^1H NMR (300 MHz, Chloroform-*d*) δ 8.34 – 8.18 (m, 2H, Ph), 7.46 – 7.32 (m, 2H, Ph), 7.32 – 7.11 (m, 5H, Ph), 4.36 – 4.22 (m, 2H, OCH₂), 2.67 (t, *J* = 6.9 Hz, 2H, CH₂), 1.94 – 1.68 (m, 4H, CH₂CH₂). ^{13}C NMR (76 MHz, Chloroform-*d*) δ 155.60 (CO), 152.56 (Ph), 145.35 (Ph), 141.73 (Ph), 128.46 (2C, Ph), 128.44 (2C, Ph), 126.02 (Ph), 125.32 (2C, Ph), 121.84 (2C, Ph), 69.43 (OCH₂), 35.37 (CH₂), 28.10 (CH₂), 27.47 (CH₂) ppm. ESI-HRMS(M+Na)⁺: 338.0999; found: 338.0999.

General procedure B for the synthesis of *p*-nitrophenyl thiocarbonate:

To a solution of different thiols (1 eq) in DCM were added respectively triethylamine (1.05 eq), 4-dimethylamino pyridine (DMAP) (1.05 eq), *p*-nitrophenyl chloroformate (1.05 eq) at 0 °C. The reaction mixture was stirred overnight at rt. The mixture was then diluted with 20 mL DCM and washed with water (2×10 mL), the organic phase was collected, dried over anhydrous Na₂SO₄, concentrated and purified by flash chromatography to get the desired product.



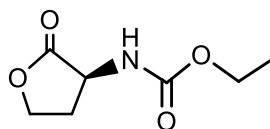
Butyl 4-nitrophenyl thiocarbonate: From butyl mercaptan following general procedure B. Flash chromatography of the crude product (1:10 EtOAc-pentane) afforded butyl 4-nitrophenyl thiocarbonate (62%) as a light yellow liquid. ¹H NMR (300 MHz, Chloroform-*d*) δ 8.39 – 8.06 (m, 2H, Ph), 7.42 – 7.30 (m, 2H, Ph), 2.96 (t, *J* = 7.3 Hz, 2H, SCH₂), 1.82 – 1.63 (m, 2H, CH₂), 1.53 – 1.33 (m, 2H, CH₂), 0.95 (t, *J* = 7.3 Hz, 3H, CH₃). ¹³C NMR (76 MHz, Chloroform-*d*) δ 169.77 (SCO), 155.65 (Ph), 145.33 (Ph), 125.29 (2C, Ph), 122.06 (2C, Ph), 31.46 (CH₂), 31.20 (CH₂), 21.81 (CH₂), 13.54 (CH₃) ppm. ESI-HRMS(M+Na)⁺: 278.0457; found: 278.0462.



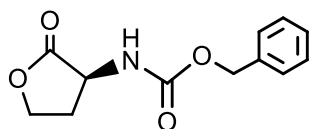
Benzyl 4-nitrophenyl thiocarbonate. From benzyl mercaptan following general procedure B. Flash chromatography of the crude product (1:11 EtOAc-pentane) afforded benzyl 4-nitrophenyl thiocarbonate (39%) as a white solid. ¹H NMR (300 MHz, Chloroform-*d*) δ 8.36 – 8.20 (m, 2H, Ph), 7.43 – 7.27 (m, 7H, Ph), 4.20 (s, 2H, SCH₂). ¹³C NMR (76 MHz, Chloroform-*d*) δ 169.24 (SCO), 155.57 (Ph), 145.43 (Ph), 136.15 (Ph), 128.97 (2C, Ph), 128.85 (2C, Ph), 127.90 (Ph), 125.32 (2C, Ph), 122.07 (2C, Ph), 35.84 (SCH₂Ph) ppm. ESI-HRMS(M+Na)⁺: 312.0301; found: 312.0302.

General procedure C for the synthesis of carbamate or thiocarbamate:

To a suspension of L- α -amino- γ -butyrolactone hydrobromide (100 mg, 0.55 mmol) in dry THF (2 mL) was added *N,N*-diisopropylethylamine (0.213 mL, 0.66 mmol) at 0 °C, the appropriate commercially available chloroformate or synthesized chlorothioformate (1.2 eq) was added dropwise. The mixture was stirred overnight at rt. The mixture was diluted with 10 mL EtOAc and washed with brine (10 mL), the organic phase was collected, dried over anhydrous Na₂SO₄, concentrated and purified by flash chromatography to give a white solid.

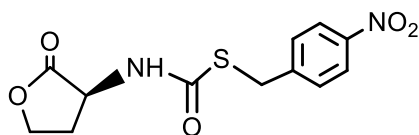


N-(ethoxycarbonyl)-L-homoserine lactone (**1a**). **1a** was obtained from commercially available ethyl chloroformate following general procedure C. Flash chromatography of the crude product (1:1 EtOAc-pentane) afforded **1a** (72%) as a white solid. IR (cm⁻¹): 3332 (N-H), 1785 (C=O, lactone), 1679 (C=O, carbamate), 1537 (-NHCO-). [α]_D²⁴ = -43.9 (c=0.34, acetone). ¹H NMR (300 MHz, Chloroform-*d*) δ 5.49 (d, *J* = 6.7 Hz, 1H, NH), 4.41 (m, 2H, OCHH-lactone, CH), 4.32 – 4.21 (m, 1H, OCHH-lactone), 4.12 (t, *J* = 7.1 Hz, 2H, OCH₂), 2.70 (m, 1H, CHH-lactone), 2.22 (m, 1H, CHH-lactone), 1.23 (t, *J* = 7.1 Hz, 3H, CH₃) ppm.



N-(benzyloxycarbonyl)-L-homoserine lactone (**1b**). **1b** was obtained from commercially available benzyl chloroformate following general procedure C. Flash chromatography of the crude product (1:3 EtOAc-pentane) afforded **1b** (48%) as a white solid. IR (cm⁻¹): 3324 (N-H), 1776 (C=O, lactone), 1686 (C=O, carbamate), 1539 (-NHCO-). [α]_D²⁴ = -27.9 (c=0.29, acetone). ¹H NMR (300 MHz, Chloroform-*d*)

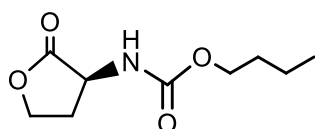
δ 7.34 (m, 5H, Ph), 5.61 (d, J = 6.3 Hz, 1H, NH), 5.11 (s, 2H, OCH₂Ph), 4.41 (m, 2H, OCHH-lactone, CH), 4.20 (m, 1H, OCHH-lactone), 2.68 (m, 1H, CHH-lactone), 2.23 (m, 1H, CHH-lactone) ppm.



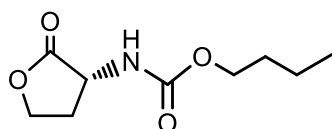
N-(4-nitrobenzylthiocarbonyl)-L-homoserine lactone (**1k**). To a solution of triphosgene (1 mmol) in DCM (2 mL) was added slowly 4-nitro benzylmercaptan (2.4 mmol) which was dissolved in DCM (2 mL) at 0°C, followed by addition of pyridine (0.2 mL, 2.48 mmol) dissolved in DCM (2 mL). After stirring for 2 h at 0°C, the reaction was quenched by addition of water (2 mL). The reaction mixture was diluted with DCM (16 mL) and washed with ice-cold water (8 mL). The organic layer was dried over anhydrous Na₂SO₄, concentrated to afford the *S*-4-nitrobenzyl chlorothioformate (390 mg, yield 70%) as a colorless oil, used immediately without further purification. ¹H NMR (300 MHz, Chloroform-*d*) δ 8.26 – 8.11 (m, 2H, Ph), 7.58 – 7.45 (m, 2H, Ph), 4.22 (s, 2H, CH₂). Following the general procedure C, flash chromatography of the crude product (1:1 EtOAc-pentane) afforded **1k** (51%) as a white solid. IR (cm⁻¹): 3307 (N-H), 1782 (C=O, lactone), 1640 (C=O, thiocarbamate), 1513 (-NHCO-), 1491 (Ar-NO₂), 1345 (Ar-NO₂). [α]_D²⁴ = -30.4 (c=0.09, acetone). ¹H NMR (300 MHz, Chloroform-*d*) δ 8.25 – 7.99 (m, 2H, Ph), 7.62 – 7.39 (m, 2H, Ph), 6.24 (d, J = 6.0 Hz, 1H, NH), 4.57 (ddd, J = 11.6, 8.6, 6.0 Hz, 1H, CH), 4.46 (td, J = 9.1, 1.2 Hz, 1H, OCHH-lactone), 4.27 (ddd, J = 11.3, 9.4, 5.8 Hz, 1H, OCHH-lactone), 4.19 (s, 2H, SCH₂), 2.79 (m, 1H, CHH-lactone), 2.22 (m, 1H, CHH-lactone). ¹³C NMR (75 MHz, Chloroform-*d*) δ 174.8 (CO-lactone), 167.1 (SCONH), 147.1 (Ph), 145.8 (Ph), 129.7 (2C, Ph), 123.8 (2C, Ph), 66.0 (OCH₂-lactone), 50.8 (CH-NH), 33.4 (SCH₂), 30.1 (CH₂-lactone). ESI-HRMS(M+Na)⁺: 319.0359 ; found: 319.0355.

General procedure D for the synthesis of carbamate or thiocarbamate:

To a suspension of L- α -amino- γ -butyrolactone hydrobromide (1 eq) in dry THF (2 mL) were added triethylamine (1 eq), various *p*-nitrophenyl carbonates (1.2 eq) dissolved in THF (1 mL) at room temperature. The reaction mixture was stirred overnight at 40 °C. The solution was filtered and the solvent was evaporated. The residue was purified by flash chromatography to give the corresponding carbamates as white solids.

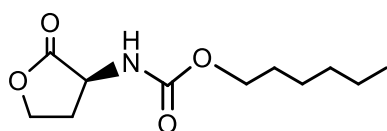


N-(butoxycarbonyl)-L-homoserine lactone (**1c**). According to the general procedure D, flash chromatography of the crude product (1:2 EtOAc-pentane) afforded **1c** (68%) as a white solid. IR (cm⁻¹): 3333 (N-H), 1775 (C=O, lactone), 1688 (C=O, carbamate), 1537 (-NHCO-). [α]_D²⁴ = -30 (c=0.44, acetone). ¹H NMR (500 MHz, Chloroform-*d*) δ 5.39 (s, 1H, NH), 4.56 – 4.33 (m, 2H, OCHH-lactone, CH), 4.24 (ddd, *J* = 11.4, 9.3, 5.9 Hz, 1H, OCHH-lactone), 4.07 (t, *J* = 6.7 Hz, 2H, OCH₂), 2.73 (m, 1H, CHH-lactone), 2.21 (m, 1H, CHH-lactone), 1.59 (m, 2H, CH₂), 1.36 (m, 2H, CH₂), 0.91 (t, *J* = 7.4 Hz, 3H, CH₃). ¹³C NMR (126 MHz, Chloroform-*d*) δ 175.2 (CO-lactone), 156.5 (OCONH), 65.8 (OCH₂-lactone), 65.5 (OCH₂), 50.4 (CH-NH), 30.9 (CH₂), 30.3 (CH₂-lactone), 19.0 (CH₂), 13.7 (CH₃). ESI-HRMS (M+Na)⁺: 224.0893; found: 224.0892.

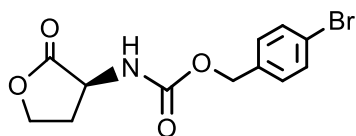


N-(butoxycarbonyl)-D-homoserine lactone (**1d**). Compound **1d** was obtained from the reaction of butyl 4-nitrophenyl carbonate with D- α -amino- γ -butyrolactone

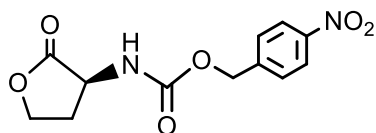
hydrobromide. Flash chromatography of the crude product (1:3 EtOAc-pentane) afforded **1d** (74%) as a white solid. IR (cm⁻¹): 3329 (N-H), 1775 (C=O, lactone), 1687 (C=O, carbamate), 1536 (-NHCO-). $[\alpha]^{24}_{\text{D}} = +35.3$ (c=0.4, acetone). ¹H NMR (500 MHz, Chloroform-*d*) δ 5.49 (d, *J* = 6.5 Hz, 1H, NH), 4.40 (m, 2H, OCHH-lactone, CH), 4.22 (ddd, *J* = 11.5, 9.1, 6.0 Hz, 1H, OCHH-lactone), 4.05 (t, *J* = 6.8 Hz, 2H, OCH₂), 2.69 (m, 1H, CHH-lactone), 2.21 (m, 1H, CHH-lactone), 1.57 (d, *J* = 7.3 Hz, 2H, CH₂), 1.40 – 1.24 (m, 2H, CH₂), 0.94 – 0.84 (t, *J* = 7.3 Hz, 3H, CH₃). ¹³C NMR (126 MHz, Chloroform-*d*) δ 175.4 (CO-lactone), 156.6 (OCONH), 65.8 (OCH₂-lactone), 65.5 (OCH₂), 50.4 (CH-NH), 31.0 (CH₂), 30.1 (CH₂-lactone), 19.1 (CH₂), 13.7 (CH₃). ESI-HRMS (M+Na)⁺: 224.0893; found: 224.0897.



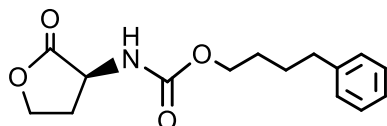
N-(hexyloxycarbonyl)-L-homoserine lactone (**1e**). According to the general procedure D, flash chromatography of the crude product (1:2 EtOAc-pentane) afforded **1e** (63%) as a white solid. IR (cm⁻¹): 3332 (N-H), 1775 (C=O, lactone), 1688 (C=O, carbamate), 1539 (-NHCO-). $[\alpha]^{24}_{\text{D}} = -26.9$ (c=0.35, acetone). ¹H NMR (500 MHz, Chloroform-*d*) δ 5.40 (s, 1H, NH), 4.41 (m, 2H, OCHH-lactone, CH), 4.24 (ddd, *J* = 11.4, 9.3, 5.9 Hz, 1H, OCHH-lactone), 4.05 (t, *J* = 6.7 Hz, 2H, OCH₂), 2.72 (m, 1H, CHH-lactone), 2.21 (m, 1H, CHH-lactone), 1.59 (m, 2H, CH₂), 1.43 – 1.19 (m, 6H, CH₂CH₂CH₂), 0.86 (t, *J* = 6.6 Hz, 3H, CH₃). ¹³C NMR (126 MHz, Chloroform-*d*) δ 175.2 (CO-lactone), 156.5 (OCONH), 65.8 (OCH₂-lactone), 65.8 (OCH₂), 50.4 (CH-NH), 31.4 (CH₂), 30.3 (CH₂-lactone), 28.8 (CH₂), 25.5 (CH₂), 22.5 (CH₂), 14.0 (CH₃). ESI-HRMS (M+Na)⁺: 252.1206; found: 252.1207.



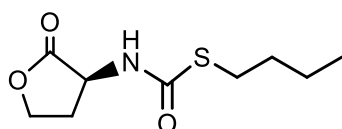
N-(4-bromobenzyloxycarbonyl)-L-homoserine lactone (**1f**). According to the general procedure D, flash chromatography of the crude product (1:3 EtOAc-pentane) afforded **1f** (40%) as a white solid. IR (cm⁻¹): 3306 (N-H), 1776 (C=O, lactone), 1695 (C=O, carbamate), 1538 (-NHCO-). [α]_D²⁴ = -23.5 (c=0.19, acetone). ¹H NMR (400 MHz, Chloroform-*d*) δ 7.55 – 7.41 (m, 2H, Ph), 7.25 – 7.15 (m, 2H, Ph), 5.39 (s, 1H, NH), 5.07 (s, 2H, OCH₂Ar), 4.42 (m, 2H, OCHH-lactone, CH), 4.25 (ddd, *J* = 11.2, 9.3, 5.7 Hz, 1H, OCHH-lactone), 2.88 – 2.66 (m, 1H, CHH-lactone), 2.21 (m, 1H, CHH-lactone). ¹³C NMR (101 MHz, Chloroform-*d*) δ 174.9 (CO-lactone), 156.0 (OCONH), 134.9 (Ph), 131.7 (2C, Ph), 129.8 (2C, Ph), 122.37 (Ph), 66.5 (OCH₂Ar), 65.8 (OCH₂-lactone), 50.5 (CH-NH), 30.4 (CH₂-lactone). ESI-HRMS (M+Na)⁺: 335.9842; found: 335.9843.



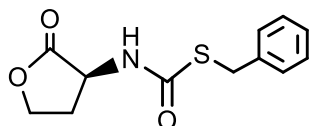
N-(4-nitrobenzyloxycarbonyl)-L-homoserine lactone (**1g**). According to the general procedure D, flash chromatography of the crude product (1:1 EtOAc-pentane) afforded **1g** (52%) as a white solid. IR (cm⁻¹): 3339 (N-H), 1783 (C=O, lactone), 1692 (C=O, carbamate), 1533 (-NHCO-), 1512 (Ar-NO₂), 1345 (Ar-NO₂). [α]_D²⁴ = -24.5 (c=0.45, acetone). ¹H NMR (300 MHz, Chloroform-*d*) δ 8.36 – 8.13 (m, 2H, Ph), 7.54 (d, *J* = 8.5 Hz, 2H, Ph), 5.42 (s, 1H, NH), 5.25 (s, 2H, OCH₂Ph), 4.57 – 4.39 (m, 2H, OCHH-lactone, CH-NH), 4.30 (m, 1H, OCHH-lactone), 2.83 (m, 1H, CHH-lactone), 2.26 (m, 1H, CHH-lactone).



N-(4-phenylbutoxycarbonyl)-L-homoserine lactone (**1h**). Following general procedure D, flash chromatography of the crude product (1:2 EtOAc-pentane) afforded **1h** (40%) as a white solid. IR (cm⁻¹): 3336 (N-H), 1776 (C=O, lactone), 1687 (C=O, carbamate), 1537 (-NHCO-). $[\alpha]^{24}_{\text{D}} = -17.4$ (c=0.13, acetone). ¹H NMR (500 MHz, Chloroform-*d*) δ 7.33 – 7.23 (m, 2H, Ph), 7.22 – 7.12 (m, 3H, Ph), 5.25 (d, *J* = 12.3 Hz, 1H, NH), 4.41 (m, OCHH-lactone, CH), 4.25 (ddd, *J* = 11.3, 9.3, 5.8 Hz, 1H, OCHH-lactone), 4.12 (t, *J* = 6.2 Hz, 2H, OCH₂), 2.77 (m, 1H, CHH-lactone), 2.64 (m, 2H, CH₂Ph), 2.20 (m, 1H, CHH-lactone), 1.69 (m, 4H, CH₂CH₂). ¹³C NMR (126 MHz, CDCl₃) δ 175.1 (CO-lactone), 156.4 (OCONH), 142.1 (Ph), 128.5 (2C, Ph), 128.4 (2C, Ph), 125.9 (Ph), 65.9 (OCH₂-lactone), 65.6 (OCH₂), 50.5 (CH-NH), 35.5 (CH₂), 30.6 (CH₂-lactone), 28.5 (CH₂), 27.7 (CH₂). ESI-HRMS (M+Na)⁺: 300.1206; found: 300.1210.



N-(butylthiocarbonyl)-L-homoserine lactone (**1i**). Following general procedure D, flash chromatography of the crude product (1:3 EtOAc-pentane) afforded **1i** (46%) as a white solid. IR (cm⁻¹): 3315 (N-H), 1775 (C=O, lactone), 1643 (C=O, thiocarbamate), 1522 (-NHCO-). $[\alpha]^{24}_{\text{D}} = -13.4$ (c=0.17, acetone). ¹H NMR (300 MHz, Chloroform-*d*) δ 6.12 (d, *J* = 5.9 Hz, 1H, NH), 4.56 (ddd, *J* = 11.6, 8.6, 5.8 Hz, 1H, CH), 4.50 – 4.37 (m, 1H, OCHH-lactone), 4.27 (ddd, *J* = 11.1, 9.3, 5.8 Hz, 1H, OCHH-lactone), 2.91 (t, *J* = 7.3 Hz, 2H, SCH₂), 2.80 (m, 1H, CHH-lactone), 2.22 (m, 1H, CHH-lactone), 1.61 (m, 2H, CH₂), 1.39 (m, 2H, CH₂), 0.91 (t, *J* = 7.3 Hz, 3H, CH₃). ¹³C NMR (76 MHz, Chloroform-*d*) δ 175.0 (CO-lactone), 168.9 (SCONH), 66.0 (OCH₂-lactone), 50.6 (CH-NH), 32.2 (CH₂), 30.4 (CH₂-lactone), 29.8 (SCH₂), 21.9 (CH₂), 13.6 (CH₃). ESI-HRMS (M+Na)⁺: 240.0664; found: 240.0653.

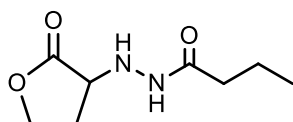


N-(benzylthiocarbonyl)-L-homoserine lactone (**1j**). Following general procedure D, flash chromatography of the crude product (1:3 EtOAc-pentane) afforded **1j** (27%) as a white solid. IR (cm⁻¹): 3321 (N-H), 1776 (C=O, lactone), 1661 (C=O, thiocarbamate), 1518 (-NHCO-). [α]_D²⁴ = -12.6 (c=0.11, acetone). ¹H NMR (500 MHz, Chloroform-*d*) δ 7.35 – 7.26 (m, 4H, Ph), 7.26 – 7.21 (m, 1H, Ph), 6.12 (d, *J* = 5.8 Hz, 1H, NH), 4.55 (m, 1H, CH), 4.44 (t, *J* = 9.0 Hz, 1H, OCHH-lactone), 4.25 (m, 1H, OCHH-lactone), 4.17 (s, 2H, SCH₂), 2.79 (m, 1H, CHH-lactone), 2.21 (m, 1H, CHH-lactone). ¹³C NMR (126 MHz, Chloroform-*d*) δ 174.8 (CO-lactone), 168.1 (SCONH), 137.6 (Ph), 128.8 (2C, Ph), 128.6 (2C, Ph), 127.4 (Ph), 66.0 (OCH₂-lactone), 50.7 (CH-NH), 34.3 (SCH₂Ph), 30.4 (CH₂-lactone). ESI-HRMS (M+Na)⁺: 274.0508; found: 274.0511.

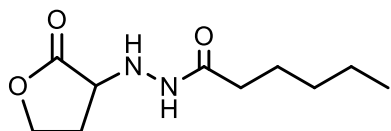
General procedure E for the synthesis of hydrazides:

(1) To a 25 ml flask were added 4 ml of hydrazine (80% in water) and carboxylic esters (1 g). The mixture was stirred at 70°C for 45 min and then cooled to room temperature. The reaction mixture was then extracted with EtOAc (30 mL) and washed with brine (30 mL). The organic phase was dried over anhydrous Na₂SO₄, concentrated and the residue was purified by flash chromatography to give corresponding hydrazide compounds.

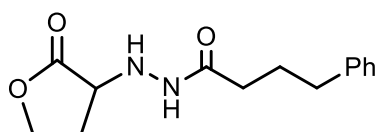
(2) To a solution of different hydrazides (1.0 eq) in dry DCM was added respectively DIEA (2.0 eq), α -bromo- γ -butyrolactone (2.0 eq) and TBABr (0.3 eq). The reaction mixture was stirred overnight at 40°C. The solvent was evaporated. The residue was purified by flash chromatography to give the corresponding hydrazide AHL analogues.



N'-(2-oxotetrahydrofuran-3-yl)butyrohrazide (**1l**). From methyl butanoic ester, butyrohrazide was obtained by flash chromatography of the crude product (95:5 EtOAc-MeOH) in 90% yield. According to the general procedure E, flash chromatography of the crude product (EtOAc) afforded **1l** (82%). ¹H NMR (300 MHz, Chloroform-*d*) δ 7.60 (s, 1H, NH), 4.40 (m, 1H, OCHH-lactone), 4.21 (m, 1H, OCHH-lactone), 3.91 (dd, *J* = 10.2, 8.4 Hz, 1H, CH), 2.48 (m, 1H, CHH-lactone), 2.29 – 2.08 (m, 3H, CHH-lactone, CH₂CO), 1.68 (m, 2H, CH₂), 0.94 (t, *J* = 7.4 Hz, 3H, CH₃). ¹³C NMR (101 MHz, Chloroform-*d*) δ 176.0 (CO), 173.2 (CO), 65.8 (OCH₂-lactone), 57.9 (CH-NH), 36.3 (CH₂CO), 27.5 (CH₂-lactone), 18.9 (CH₂), 13.7 (CH₃). ESI-HRMS (M+Na)⁺: 209.0897; found: 209.0900.



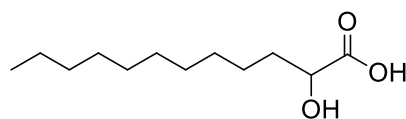
N'-(2-oxotetrahydrofuran-3-yl)hexanehydrazide (**1m**). From methyl hexanoic ester, hexanehydrazide was obtained by flash chromatography of the crude product (95:5 EtOAc-MeOH) in 74% yield. According to the general procedure E, flash chromatography of the crude product (4:1 EtOAc-pentane) afforded **1m** (48%). ¹H NMR (300 MHz, Chloroform-*d*) δ 7.56 (s, 1H, NH), 4.41 (m, 1H, OCHH-lactone), 4.22 (m, 1H, OCHH-lactone), 3.93 (m, 1H, CH), 3.93 (s, 1H, NH), 2.49 (m, 1H, CHH-lactone), 2.33 – 2.09 (m, 3H, CHH-lactone, CH₂CO), 1.62 (m, 2H, CH₂), 1.41 – 1.18 (m, 4H, CH₂CH₂), 0.97 – 0.78 (t, *J* = 6.6 Hz, 3H, CH₃). ¹³C NMR (101 MHz, Chloroform-*d*) δ 175.9 (CO), 173.3 (CO), 65.8 (OCH₂-lactone), 57.9 (CH), 34.5 (CH₂CO), 31.4 (CH₂), 27.5 (CH₂-lactone), 25.1 (CH₂), 22.3 (CH₂), 13.9 (CH₃). ESI-HRMS (M+H)⁺: 215.1390; found: 215.1394.



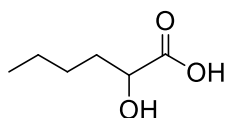
N'-(2-oxotetrahydrofuran-3-yl)-4-phenylbutanehydrazide (**1n**). From ethyl 4-phenylbutanoic ester, 4-phenylbutanehydrazide was obtained as a white solid (96%). According to the general procedure E, flash chromatography of the crude product (EtOAc) afforded **1n** (63%). ¹H NMR (400 MHz, Chloroform-*d*) δ 7.57 (s, 1H, NH), 7.32 – 7.26 (m, 2H, Ph), 7.22 – 7.12 (m, 3H, Ph), 4.39 (m, 1H, OCHH- lactone), 4.20 (m, 1H, OCHH-lactone), 3.89 (t, *J* = 8.3 Hz, 1H, CH), 3.78 (s, 1H, NH), 2.65 (t, *J* = 7.5 Hz, 2H, CH₂CO), 2.47 (m, 1H, CHH-lactone), 2.27 – 2.13 (m, 3H, CHH-lactone, CH₂Ph), 2.06 – 1.88 (m, 2H, CH₂). ¹³C NMR (101 MHz, Chloroform-*d*) δ 175.8 (CO), 172.8 (CO), 141.1 (Ph), 128.5 (2C, Ph), 128.5 (2C, Ph), 126.1 (Ph), 65.8 (OCH₂-lactone), 57.9 (CH-NH), 35.1 (CH₂CO), 33.7 (CH₂), 27.5 (CH₂-lactone), 26.8 (CH₂). ESI-HRMS (M+Na)⁺: 285.1210; found: 285.1203.

General procedure F for the synthesis of 2-hydroxy acid:

To a solution of undecanoic acid or pentanoic acid (2.0 mmol) and diethyl cyanophosphonate (DEPC) (90%, 4.2 mmol) in THF (4 mL) was added triethylamine (2.1 mmol) at -20°C. The reaction mixture was stirred at -20°C for 3 h. The mixture was diluted with ether or EtOAc (30 mL) and washed with water (2 x 20 mL), the organic phase was collected, dried over anhydrous Na₂SO₄, concentrated and purified by flash chromatography to get the intermediate product dicyanophosphate. A mixture of dicyanophosphate (0.7 mmol) and HCl (37%, 2.9 mL) was heated at reflux for 12 h. The reaction mixture was cooled, then extracted with ether (3 x 20 mL), and the organic phase was dried over anhydrous Na₂SO₄, concentrated and purified by flash chromatography to get the desired product 2-hydroxy acid.



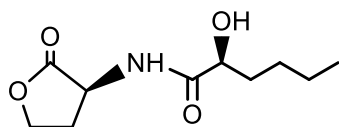
2-Hydroxydodecanoic acid (**2a**). From undecanoic acid following general procedure F, flash chromatography of the crude product (1:1 EtOAc-pentane) afforded 2-hydroxydodecanoic acid (32% for two steps) as a white solid. ^1H NMR (300 MHz, Chloroform-*d*) δ 4.53 – 4.18 (dd, $J = 7.5, 4.2$ Hz, 1H, *CHOH*), 1.98 – 1.58 (m, 2H, CH_2), 1.56 – 1.12 (m, 18H, $9\times\text{CH}_2$), 0.87 (t, $J = 6.5$ Hz, 3H, CH_3).



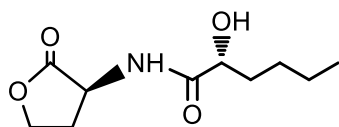
2-Hydroxyhexanoic acid (**2b**). From pentanoic acid following general procedure F, flash chromatography of the crude product (2:1 EtOAc-pentane) afforded 2-hydroxyhexanoic acid (44% for two steps) as a white solid. ^1H NMR (300 MHz, Chloroform-*d*) δ 4.29 (dd, $J = 7.4, 4.2$ Hz, 1H, *CHOH*), 1.86 (m, 2H, CH_2), 1.56 – 1.12 (m, 18H, $9\times\text{CH}_2$), 0.87 (t, $J = 6.5$ Hz, 3H, CH_3).

General procedure G for the synthesis of 2-OH AHLs:

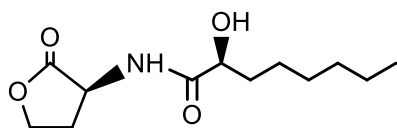
To a mixture of 2-hydroxy acid (0.5 mmol) and L- α -amino- γ -butyrolactone hydrobromide (0.6 mmol) in CH_2Cl_2 (4 mL) were added triethylamine (1.1 mmol) and 1-(3-dimethylaminopropyl)-3-ethyl carbodiimide hydrochloride (EDC) (0.55 mmol) and 1-hydroxybenzotriazole (HOBt) (0.5 mmol) at 0°C . The reaction mixture was stirred for 1 h at 0°C and overnight at room temperature. The solvent was evaporated and EtOAc (20 mL) was added. The mixture was washed respectively with brine, 1% HCl, 5% NaHCO_3 , and brine, dried over anhydrous Na_2SO_4 , concentrated and purified by flash chromatography to get the desired product.



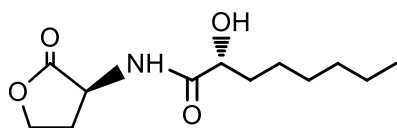
(*S*)-2-hydroxy-*N*-((*S*)-2-oxotetrahydrofuran-3-yl)hexanamide (**2c**). According to the general procedure G, flash chromatography of the crude product (3:1 EtOAc-pentane) afforded **2c** and **2d** (27%) as a white solid. ^1H NMR (300 MHz, Chloroform-*d*) δ 7.38 (d, $J = 7.9$ Hz, 1H, NH), 4.77 (dt, $J = 11.4, 8.4$ Hz, 1H, CH-NH), 4.46 (td, $J = 9.1, 1.3$ Hz, 1H, OCHH-lactone), 4.29 (ddd, $J = 11.2, 9.2, 6.0$ Hz, 1H, OCHH-lactone), 4.17 (dt, $J = 8.3, 4.1$ Hz, 1H, CH-OH), 3.75 (d, $J = 4.8$ Hz, 1H, OH), 2.69 (m, 1H, CHH-lactone), 2.34 – 2.14 (m, 1H, CHH-lactone), 1.81 (m, 1H, CHH), 1.60 (m, 1H, CHH), 1.45 – 1.26 (m, 4H, 2 \times CH₂), 0.84 (t, $J = 7.1$ Hz, 3H, CH₃). ^{13}C NMR (75 MHz, Chloroform-*d*) δ 175.9 (CO), 175.5 (CO), 72.2 (CHOH), 66.0 (OCH₂-lactone), 48.2 (CH-NH), 34.1 (CHCH₂), 29.7 (CH₂-lactone), 27.2 (CH₂), 22.4 (CH₂), 14.0 (CH₃). ESI-HRMS(M+Na)⁺: 238.1050; found: 238.1052. $[\alpha]^{24}_{\text{D}} = -60$ (c=0.5, acetone).



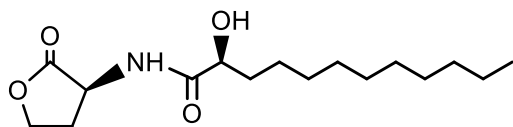
(*R*)-2-hydroxy-*N*-((*S*)-2-oxotetrahydrofuran-3-yl)hexanamide (**2d**). ^1H NMR (300 MHz, Chloroform-*d*) δ 7.24 (d, $J = 7.5$ Hz, 1H, NH), 4.55 (ddd, $J = 11.1, 8.7, 6.9$ Hz, 1H, CH-NH), 4.49 (td, $J = 9.0, 1.5$ Hz, 1H, OCHH-lactone), 4.29 (ddd, $J = 10.9, 9.2, 6.2$ Hz, 1H, OCHH-lactone), 4.14 (dt, $J = 8.1, 4.1$ Hz, 1H, CH-OH), 3.12 (s, 1H, OH), 2.84 – 2.63 (m, 1H, CHH-lactone), 2.27 (m, 1H, CHH-lactone), 1.84 (m, 1H, CHH), 1.65 (m, 1H, CHH), 1.48 – 1.23 (m, 4H, 2 \times CH₂), 0.91 (t, $J = 7.1$ Hz, 3H, CH₃). ^{13}C NMR (75 MHz, Chloroform-*d*) δ 175.4 (CO), 174.9 (CO), 72.2 (CHOH), 66.1 (OCH₂-lactone), 48.8 (CH-NH), 34.2 (CHCH₂), 29.6 (CH₂-lactone), 27.1 (CH₂), 22.4 (CH₂), 13.9 (CH₃). ESI-HRMS(M+Na)⁺: 238.1050; found: 238.1052. $[\alpha]^{24}_{\text{D}} = +9.6$ (c=0.415, acetone).



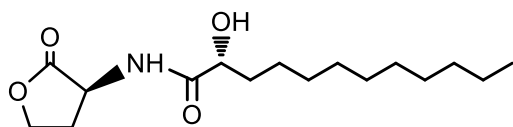
(*S*)-2-hydroxy-*N*-((*S*)-2-oxotetrahydrofuran-3-yl)octanamide (**2e**). From commercial available 2-hydroxyoctanoic acid following general procedure G, flash chromatography of the crude product (3:1 EtOAc-pentane) afforded **2e** and **2f** (75%) as a white solid. ^1H NMR (500 MHz, Chloroform-*d*) δ 7.25 (d, J = 6.0 Hz, 1H, NH), 4.74 (dt, J = 12.5, 8.5 Hz, 1H, CH-NH), 4.47 (td, J = 9.0, 1.2 Hz, 1H, OCHH-lactone), 4.30 (ddd, J = 11.2, 9.3, 6.0 Hz, 1H, OCHH-lactone), 4.18 (ddd, J = 8.5, 5.0, 3.7 Hz, 1H, CH-OH), 3.32 (d, J = 5.0 Hz, 1H, OH), 2.74 (m, 1H, CHH-lactone), 2.22 (m, 1H, CHH-lactone), 1.83 (m, 1H, CH-CHH), 1.62 (m, 1H, CH-CHH), 1.41 (p, J = 7.1, 6.6 Hz, 2H, CH₂), 1.36 – 1.20 (m, 6H, 3 \times CH₂), 0.87 (t, J = 7.0 Hz, 3H, CH₃). ^{13}C NMR (126 MHz, Chloroform-*d*) δ 175.6 (CO), 175.2 (CO), 72.3 (CHOH), 66.0 (OCH₂-lactone), 48.3 (CH-NH), 34.5 (CHCH₂), 31.7 (CH₂), 29.9 (CH₂-lactone), 29.0 (CH₂), 25.0 (CH₂), 22.9 (CH₂), 14.1 (CH₃). ESI-HRMS($\text{M}+\text{Na}^+$): 266.1363; found: 266.1364. $[\alpha]^{24}_{\text{D}}$ = -47.3 ($c=0.55$, acetone).



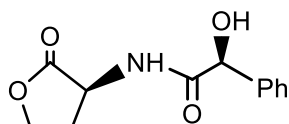
(*R*)-2-hydroxy-*N*-((*S*)-2-oxotetrahydrofuran-3-yl)octanamide (**2f**). ^1H NMR (500 MHz, Chloroform-*d*) δ 7.24 (d, J = 6.4 Hz, 1H, NH), 4.55 (ddd, J = 11.3, 8.8, 6.9 Hz, 1H, CH-NH), 4.49 (td, J = 9.1, 1.4 Hz, 1H, OCHH-lactone), 4.29 (ddd, J = 10.6, 9.2, 6.1 Hz, 1H, OCHH-lactone), 4.14 (ddd, J = 8.7, 5.3, 3.8 Hz, 1H, CH-OH), 3.11 (d, J = 18.2 Hz, 1H, OH), 2.73 (m, 1H, CHH-lactone), 2.27 (m, 1H, CHH-lactone), 1.85 (m, 1H, CH-CHH), 1.65 (m, 1H, CH-CHH), 1.42 (m, 2H, CH₂), 1.36 – 1.22 (m, 6H, 3 \times CH₂), 0.87 (t, J = 6.7 Hz, 3H, CH₃). ^{13}C NMR (126 MHz, Chloroform-*d*) δ 175.4 (CO), 174.9 (CO), 72.2 (CHOH), 66.1 (OCH₂-lactone), 48.8 (CH-NH), 34.5 (CHCH₂), 31.7 (CH₂), 29.6 (CH₂-lactone), 29.0 (CH₂), 24.9 (CH₂), 22.6 (CH₂), 14.1 (CH₃). ESI-HRMS($\text{M}+\text{Na}^+$): 266.1363; found: 266.1364. $[\alpha]^{24}_{\text{D}}$ = +6.2 ($c=0.325$, acetone).



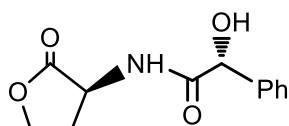
(*S*)-2-hydroxy-*N*-((*S*)-2-oxotetrahydrofuran-3-yl)dodecanamide (**2g**). According to the general procedure G, flash chromatography of the crude product (1:2 EtOAc-pentane) afforded **2g** and **2h** (63%) as a white solid. ^1H NMR (400 MHz, Chloroform-*d*) δ 7.30 (d, J = 7.6 Hz, 1H, NH), 4.75 (dt, J = 11.7, 8.2 Hz, 1H, CH-NH), 4.47 (td, J = 9.0, 1.2 Hz, 1H, OCHH-lactone), 4.29 (ddd, J = 11.2, 9.2, 5.9 Hz, 1H, OCHH-lactone), 4.17 (dd, J = 8.2, 3.7 Hz, 1H, CH-OH), 3.24 (br, 1H, OH), 2.72 (m, 1H, CHH-lactone), 2.22 (m, 1H, CHH-lactone), 1.81 (m, 1H, CH-CHH), 1.61 (m, 1H, CH-CHH), 1.46 – 1.20 (m, 16H, 8 \times CH₂), 0.87 (t, J = 8.0 Hz, 3H, CH₃). ^{13}C NMR (101 MHz, Chloroform-*d*) δ 175.7 (CO), 175.3 (CO), 72.3 (CHOH), 66.0 (OCH₂-lactone), 48.3 (CH-NH), 34.5 (CHCH₂), 31.9 (CH₂), 29.8 (CH₂), 29.6 (CH₂), 29.5 (2 \times CH₂), 29.4 (CH₂), 29.3 (CH₂), 25.1 (CH₂), 22.7 (CH₂), 14.1 (CH₃). ESI-HRMS($\text{M}+\text{Na}$)⁺: 322.1989; found: 322.1976. $[\alpha]^{24}_{\text{D}}$ = -36 (c =0.39, acetone).



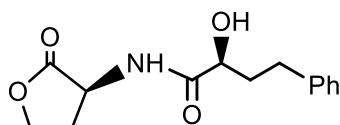
(*R*)-2-hydroxy-*N*-((*S*)-2-oxotetrahydrofuran-3-yl)dodecanamide (**2h**). ^1H NMR (400 MHz, Chloroform-*d*) δ 7.21 (d, J = 6.9 Hz, 1H, NH), 4.49 (ddd, J = 11.4, 8.8, 6.9 Hz, 1H, CH-NH), 4.43 (td, J = 9.1, 1.5 Hz, 1H, OCHH-lactone), 4.29 (ddd, J = 11.0, 9.3, 6.2 Hz, 1H, OCHH-lactone), 4.14 (dd, J = 8.2, 3.8 Hz, 1H, CH-OH), 3.04 (br, 1H, OH), 2.74 (m, 1H, CHH-lactone), 2.26 (m, 1H, CHH-lactone), 1.85 (m, 1H, CH-CHH), 1.64 (m, 1H, CH-CHH), 1.47 – 1.20 (m, 16H, 8 \times CH₂), 0.87 (t, J = 8.0 Hz, 3H, CH₃). ^{13}C NMR (101 MHz, Chloroform-*d*) δ 175.4 (CO), 174.9 (CO), 72.3 (CHOH), 66.1 (OCH₂-lactone), 48.8 (CH-NH), 34.5 (CHCH₂), 31.9 (CH₂), 29.6 (CH₂), 29.6 (2 \times CH₂), 29.5 (CH₂), 29.3 (2 \times CH₂), 25.0 (CH₂), 22.7 (CH₂), 14.1 (CH₃). $[\alpha]^{24}_{\text{D}}$ = 0 (c =0.62, acetone).



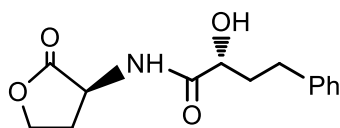
(*S*)-2-hydroxy-*N*-((*S*)-2-oxotetrahydrofuran-3-yl)-2-phenylacetamide (**2i**). From commercial available (*S*)-2-hydroxy-2-phenylacetic acid following general procedure G, flash chromatography of the crude product (4:1 EtOAc-pentane) afforded **2i** (39%) as a white solid. ^1H NMR (300 MHz, Acetone- d_6) δ 7.97 (d, J = 8.0 Hz, 1H, NH), 7.59 – 7.44 (m, 2H, Ph), 7.42 – 7.19 (m, 3H, Ph), 5.40 (d, J = 4.6 Hz, 1H, OH), 5.12 (d, J = 4.4 Hz, 1H, CH-OH), 4.72 (dt, J = 8.7, 8.4 Hz, 1H, CH-NH), 4.40 (td, J = 8.9, 1.8 Hz, 1H, OCHH-lactone), 4.29 (ddd, J = 10.7, 8.9, 6.3 Hz, 1H, OCHH-lactone), 2.53 (m, 1H, CHH-lactone), 2.36 (m, 1H, CHH-lactone). ^{13}C NMR (101 MHz, Acetone- d_6) δ 174.7 (CO), 172.3 (CO), 140.8 (Ph), 128.0 (2C, Ph), 127.6 (Ph), 126.8 (2C, Ph), 73.9 (CHOH), 65.2 (OCH₂-lactone), 48.0 (CH-NH), 28.7 (CH₂-lactone). $[\alpha]^{24}_{\text{D}} = +14$ (c=0.425, acetone).



(*R*)-2-hydroxy-*N*-((*S*)-2-oxotetrahydrofuran-3-yl)-2-phenylacetamide (**2j**). From commercial available (*R*)-2-hydroxy-2-phenylacetic acid following the general procedure G, flash chromatography of the crude product (4:1 EtOAc-pentane) afforded **2j** (45%) as a white solid. ^1H NMR (300 MHz, Acetone- d_6) δ 8.06 (d, J = 8.2 Hz, 1H, NH), 7.57 – 7.46 (m, 2H, Ph), 7.43 – 7.29 (m, 3H, Ph), 5.43 (d, J = 4.5 Hz, 1H, OH), 5.11 (d, J = 4.4 Hz, 1H, CH-OH), 4.71 (ddd, J = 11.1, 9.1, 8.2 Hz, 1H, CH-NH), 4.39 (td, J = 8.9, 1.9 Hz, 1H, OCHH-lactone), 4.28 (ddd, J = 10.6, 8.9, 6.4 Hz, 1H, OCHH-lactone), 2.54 (m, 1H, CHH-lactone), 2.35 (m, 1H, CHH-lactone). ^{13}C NMR (75 MHz, Acetone- d_6) δ 174.7 (CO), 172.4 (CO), 140.8 (Ph), 128.1 (2C, Ph), 127.7 (Ph), 127.0 (2C, Ph), 74.0 (CHOH), 65.2 (OCH₂-lactone), 48.1 (CH-NH), 28.5 (CH₂-lactone). ESI-HRMS($\text{M}+\text{Na}$)⁺: 258.0737; found: 258.0740. $[\alpha]^{24}_{\text{D}} = -59$ (c=0.61, acetone).



(*S*)-2-hydroxy-*N*-((*S*)-2-oxotetrahydrofuran-3-yl)-4-phenylbutanamide (**2k**). From commercial available (*S*)-2-hydroxy-4-phenylbutanoic acid following the general procedure G, flash chromatography of the crude product (5:1 EtOAc-pentane) afforded **2k** (15%) as a white solid. ¹H NMR (300 MHz, Chloroform-*d*) δ 7.34 (d, *J* = 7.9 Hz, 1H, NH), 7.31 – 7.27 (m, 1H, Ph), 7.26 – 7.14 (m, 4H, Ph), 4.75 (ddd, *J* = 11.8, 8.8, 7.9 Hz, 1H, CH-NH), 4.46 (td, *J* = 9.1, 1.3 Hz, 1H, OCHH-lactone), 4.28 (ddd, *J* = 11.2, 9.3, 6.0 Hz, 1H, OCHH-lactone), 4.18 (dt, *J* = 8.0, 3.8 Hz, 1H, CH-OH), 3.72 (d, *J* = 4.3 Hz, 1H, OH), 2.85 – 2.73 (m, 2H, CH₂), 2.73 – 2.60 (m, 1H, CHH-lactone), 2.31 – 2.08 (m, 2H, CHH-lactone, CHCHH), 2.02 – 1.86 (m, 1H, CHCHH). ¹³C NMR (75 MHz, Chloroform-*d*) δ 175.8 (CO), 175.1 (CO), 141.2 (Ph), 128.5 (2C, Ph), 128.5 (2C, Ph), 126.1 (Ph), 71.5 (CHOH), 66.0 (OCH₂-lactone), 48.3 (CH-NH), 36.0 (CH₂), 31.3 (CH₂), 29.7 (CH₂-lactone). [α]_D²⁴ = -35 (c=0.46, acetone).

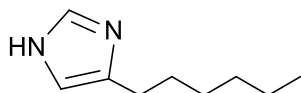


(*R*)-2-hydroxy-*N*-((*S*)-2-oxotetrahydrofuran-3-yl)-4-phenylbutanamide (**2l**). From commercial available (*R*)-2-hydroxy-4-phenylbutanoic acid following the general procedure for route B, flash chromatography of the crude product (5:1 EtOAc-pentane) afforded **2l** (59%) as a white solid. ¹H NMR (300 MHz, Acetone-*d*₆) δ 7.85 (d, *J* = 8.1 Hz, 1H, NH), 7.35 – 7.08 (m, 5H, Ph), 4.88 (s, 1H, OH), 4.71 (ddd, *J* = 11.2, 9.0, 8.2 Hz, 1H, CH-NH), 4.41 (td, *J* = 8.9, 1.8 Hz, 1H, OCHH-lactone), 4.30 (ddd, *J* = 10.6, 8.9, 6.3 Hz, 1H, OCHH-lactone), 4.10 (dd, *J* = 7.7, 4.0 Hz, 1H, CH-OH), 2.83 – 2.70 (m, 2H, CH₂), 2.56 (m, 1H, CHH-lactone), 2.48 – 2.32 (m, 1H, CHH-lactone), 2.17 – 2.07 (m, 1H, CHCHH), 1.98 – 1.79 (m, 1H, CHCHH). ¹³C NMR (75 MHz, Acetone-*d*₆) δ 174.7 (CO), 174.0 (CO), 142.1 (Ph), 128.4 (2C, Ph), 128.3 (2C, Ph), 125.7 (Ph), 70.8 (CHOH), 65.2 (OCH₂-lactone), 47.9 (CH-NH), 36.7 (CH₂), 30.9

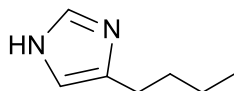
(CH₂), 28.6 (CH₂-lactone). ESI-HRMS(M+Na)⁺: 286.1050; found: 286.1052. $[\alpha]^{24}_D$ = -8.3 (c=0.48, acetone).

General procedure H for the synthesis of 4(5)-substituted imidazole:

To a mixture of olefin (1.0 eq) in acetone/water (10/1) was added DBH (3.0 eq) at rt. The mixture was refluxed at 80°C for 6h. After the reaction, saturated NaHCO₃ was added to neutralize. Acetone was removed to afford the residue. The residue was diluted with EtOAc and washed with brine. The organic extract was collected, dried over anhydrous Na₂SO₄, concentrated and purified by flash chromatography to yield α -bromo ketones as a colorless oil. Formamide (5ml) was preheated at 180°C under N₂ until the solution turned yellow. Then α -bromo ketone (3mmol) was added dropwise at 180°C. The reaction mixture was stirred at 180°C for 2h. After cooling to rt, the mixture was diluted with toluene and washed with aq. NaOH (3M). The organic extract was dried over anhydrous Na₂SO₄, concentrated and purified by flash chromatography to give 4(5)-substituted imidazole.



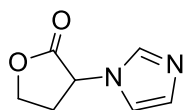
4(5)-hexyl-1*H*-imidazole (**3a**). Following the general procedure H, flash chromatography of the crude product (2:1 EtOAc-Acetone) afforded **3a** (51%) as a yellow oil. ¹H NMR (300 MHz, Chloroform-*d*) δ 10.32 (s, 1H, NH), 7.51 (s, 1H, Imidazole), 6.74 (s, 1H, Imidazole), 2.57 (t, *J* = 7.7 Hz, 2H, CH₂), 1.59 (m, 2H, CH₂), 1.38 – 1.14 (m, 6H, 3 \times CH₂), 0.84 (t, *J* = 6.5 Hz, 3H, CH₃). ¹³C NMR (75 MHz, Chloroform-*d*) δ 136.6 (Imidazole), 134.2 (Imidazole), 117.9 (Imidazole), 31.6 (CH₂), 29.4 (CH₂), 29.0 (CH₂), 26.5 (CH₂), 22.6 (CH₂), 14.0 (CH₃).



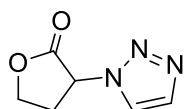
4(5)-butyl-1*H*-imidazole (**3b**). Following the general procedure A, flash chromatography of the crude product (2:1 EtOAc-Acetone) afforded **3b** (45%) as a yellow oil. ¹H NMR (300 MHz, Chloroform-*d*) δ 10.73 (s, 1H, NH), 7.55 (d, *J* = 1.1 Hz, 1H, Imidazole), 6.77 (d, *J* = 1.0 Hz, 1H, Imidazole), 2.61 (t, *J* = 7.2 Hz, 2H, CH₂), 1.62 (m, 2H, CH₂), 1.41 – 1.27 (m, 2H, CH₂), 0.90 (t, *J* = 7.3 Hz, 3H, CH₃). ¹³C NMR (75 MHz, Chloroform-*d*) δ 136.7 (Imidazole), 134.3 (Imidazole), 117.9 (Imidazole), 31.6 (CH₂), 26.2 (CH₂), 22.3 (CH₂), 13.8 (CH₃).

General procedure I for alkylation reaction:

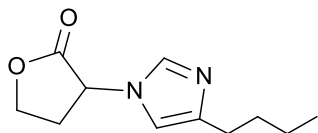
To a mixture of imidazole or their derivatives or triazole (1 mmol) and K₂CO₃ (2 mmol) in MeCN (4 ml) was added α-bromo-γ-butyrolactone (1.4 mmol) or ethyl bromoacetate (1.2 mmol). The mixture was stirred under reflux for 2h. After cooling to rt, the solid was filtered and washed with EtOAc. The solution phase was collected and concentrated. The residue was purified by flash chromatography to give the desired product.



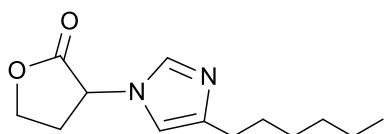
3-(1*H*-imidazol-1-yl)dihydrofuran-2(3*H*)-one (**3r**): Following the general procedure I, flash chromatography of the crude product (9:1 EtOAc-MeOH) afforded a yellow oil (yield 47%). ¹H NMR (300 MHz, Chloroform-*d*) δ 7.56 (s, 1H, Imidazole), 7.06 (t, *J* = 1.2 Hz, 1H, Imidazole), 6.96 (t, *J* = 1.4 Hz, 1H, Imidazole), 5.01 (dd, *J* = 11.5, 8.7 Hz, 1H, CH-lactone), 4.49 (td, *J* = 9.1, 1.8 Hz, 1H, OCHH-lactone), 4.33 (ddd, *J* = 10.6, 9.4, 6.1 Hz, 1H, OCHH-lactone), 2.82 (m, 1H, CHH-lactone), 2.62 – 2.47 (m, 1H, CHH-lactone). ¹³C NMR (75 MHz, Chloroform-*d*) δ 172.2 (CO), 136.8 (Imidazole), 130.1 (Imidazole), 117.7 (Imidazole), 65.4 (OCH₂-lactone), 54.8 (CH-lactone), 30.6 (CH₂-lactone). ESI-HRMS(M+H)⁺: 153.0659; found: 153.0660.



3-(1*H*-1,2,3-triazol-1-yl)dihydrofuran-2(3*H*)-one (**3s**): Following the general procedure I, flash chromatography of the crude product (EtOAc) afforded a colorless oil (yield 37%). ¹H NMR (300 MHz, Chloroform-*d*) δ 7.85 (s, 1H, CH-triazole), 7.77 (s, 1H, CH-triazole), 5.40 (t, *J* = 9.4 Hz, 1H, CH-lactone), 4.68 (ddd, *J* = 9.3, 7.5, 4.1 Hz, 1H, OCHH-lactone), 4.50 (ddd, *J* = 9.4, 8.7, 7.1 Hz, 1H, OCHH-lactone), 3.15 – 2.92 (m, 2H, CH₂-lactone). ¹³C NMR (75 MHz, Chloroform-*d*) δ 171.0 (CO), 134.3 (C-triazole), 123.9 (C-triazole), 66.3 (OCH₂-lactone), 57.5 (CH-lactone), 29.4 (CH₂-lactone). ESI-HRMS(M+Na)⁺: 176.0430; found: 176.0427.

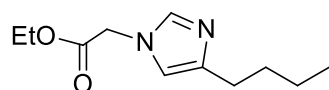


3-(4-Butyl-1*H*-imidazol-1-yl)dihydrofuran-2(3*H*)-one (**3c**): Following the general procedure I, flash chromatography of the crude product (1:1 EtOAc-acetone) afforded **3c** (57%) as a yellow oil. ¹H NMR (400 MHz, Chloroform-*d*) δ 7.43 (d, *J* = 1.5 Hz, 1H, CH=N-Imidazole), 6.62 (d, *J* = 1.2 Hz, 1H, CH=C-Imidazole), 4.92 (dd, *J* = 11.3, 8.7 Hz, 1H, CH-lactone), 4.51 – 4.40 (td, *J* = 9.2, 1.9 Hz, 1H, OCHH-lactone), 4.28 (ddd, *J* = 10.6, 9.4, 6.1 Hz, 1H, OCHH-lactone), 2.76 (m, 1H, CHH-lactone), 2.55 – 2.41 (m, 3H, CHH-lactone, CH₂), 1.61 – 1.47 (m, 2H, CH₂), 1.29 (m, 2H, CH₂), 0.84 (t, *J* = 7.3 Hz, 3H, CH₃). ¹³C NMR (101 MHz, Chloroform-*d*) δ 172.4 (CO), 144.3 (C-N, Imidazole), 136.0 (CH=N, Imidazole), 113.2 (CH=C, Imidazole), 65.4 (OCH₂-lactone), 54.7 (CH-lactone), 31.3 (CH₂), 30.5 (CH₂-lactone), 28.1 (CH₂), 22.4 (CH₂), 13.9 (CH₃). ESI-HRMS(M+H)⁺: 209.1285; found: 209.1284.

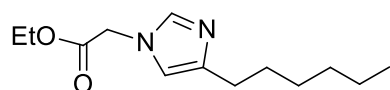


3-(4-Hexyl-1*H*-imidazol-1-yl)dihydrofuran-2(3*H*)-one (**3d**): Following the general

procedure I, flash chromatography of the crude product (2:1 EtOAc-acetone) afforded **3d** (39%) as a yellow syrup. ^1H NMR (400 MHz, Chloroform-*d*) δ 7.54 (d, J = 1.5 Hz, 1H, CH=N-Imidazole), 6.69 (d, J = 1.2 Hz, 1H, CH=C-Imidazole), 4.95 (dd, J = 11.2, 8.7 Hz, 1H, CH-lactone), 4.58 – 4.51 (td, J = 9.2, 2.0 Hz, 1H, OCHH-lactone), 4.38 (ddd, J = 10.5, 9.4, 6.2 Hz, 1H, OCHH-lactone), 2.85 (m, 1H, CHH-lactone), 2.65 – 2.50 (m, 3H, CHH-lactone, CH₂), 1.62 (m, 2H, CH₂), 1.38 – 1.23 (m, 6H, 3 \times CH₂), 0.88 – 0.81 (t, J = 6.8 Hz, 3H, CH₃). ^{13}C NMR (75 MHz, Chloroform-*d*) δ 172.0 (CO), 144.5 (C-N, Imidazole), 135.9 (CH=N, Imidazole), 113.2 (CH=C, Imidazole), 65.3 (OCH₂-lactone), 54.7 (CH-lactone), 31.7 (CH₂), 30.7 (CH₂-lactone), 29.2 (CH₂), 29.1 (CH₂), 28.4 (CH₂), 22.6 (CH₂), 14.1 (CH₃). ESI-HRMS(M+H)⁺: 237.1598; found: 237.1596.



Ethyl 2-(4-butyl-1*H*-imidazol-1-yl)acetate (**3e**): Following the general procedure I, flash chromatography of the crude product (2:1 EtOAc-acetone) afforded **3e** (40%) as a syrup. ^1H NMR (300 MHz, Chloroform-*d*) δ 7.35 (s, 1H, Imidazole), 6.58 (s, 1H, Imidazole), 4.55 (s, 2H, CH₂), 4.17 (q, J = 7.1 Hz, 2H, OCH₂), 2.50 (t, J = 7.3 Hz, 2H, CH₂), 1.56 (m, 2H, CH₂), 1.39 – 1.27 (m, 2H, CH₂), 1.22 (t, J = 7.1 Hz, 3H, CH₃), 0.85 (t, J = 7.3 Hz, 3H, CH₃). ^{13}C NMR (75 MHz, Chloroform-*d*) δ 167.6 (CO), 143.7 (Imidazole), 137.0 (Imidazole), 115.8 (Imidazole), 62.0 (OCH₂), 48.1 (CH₂), 31.4 (CH₂), 28.0 (CH₂), 22.4 (CH₂), 14.1 (CH₃), 13.9 (CH₃). ESI-HRMS(M+H)⁺: 211.1441; found: 211.1445.



Ethyl 2-(4-hexyl-1*H*-imidazol-1-yl)acetate (**3g**): Following the general procedure I, flash chromatography of the crude product (2:1 EtOAc-acetone) afforded **3g** (42%) as

a syrup. ^1H NMR (300 MHz, Chloroform-*d*) δ 7.38 (s, 1H, Imidazole), 6.63 (s, 1H, Imidazole), 4.59 (s, 2H, CH₂), 4.21 (q, J = 7.2 Hz, 2H, OCH₂), 2.54 (t, J = 7.3 Hz, 2H, CH₂), 1.62 (m, 2H, CH₂), 1.41 – 1.21 (m, 9H, 3 \times CH₂, CH₃), 0.86 (t, J = 7.5 Hz, 3H, CH₃). ^{13}C NMR (75 MHz, Chloroform-*d*) δ 167.6 (CO), 143.8 (Imidazole), 137.0 (Imidazole), 115.7 (Imidazole), 62.0 (OCH₂), 48.0 (CH₂), 31.7 (CH₂), 29.2 (CH₂), 29.1 (CH₂), 28.4 (CH₂), 22.6 (CH₂), 14.1 (2 \times CH₃). ESI-HRMS(M+H)⁺: 239.1754; found: 239.1746.

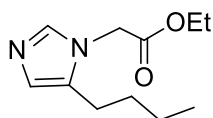
General procedure J for 1,5-disubstituted imidazole:

To a solution of 4(5)-butylimidazole or 4(5)-hexylimidazole (1 mmol) in DCM (5 ml) were added triethylamine (2.5 mmol) and trityl chloride (1.2 mmol). The mixture was stirred at rt for 1h. After the reaction, the mixture was diluted with DCM and washed with saturated NaHCO₃ and brine. The organic phase was dried over anhydrous Na₂SO₄, concentrated and purified by flash chromatography (EtOAc/Pentane 1:1) to give 4-butyl-1-trityl-1*H*-imidazole **3i** or 4-hexyl-1-trityl-1*H*-imidazole **3j**.

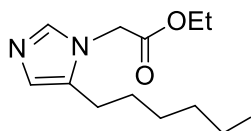
To a solution of compound **3i** or **3j** (0.5 mmol) in DCM (3 ml) was added ethyl bromoacetate (0.6 mmol) and the reaction mixture was stirred under N₂ at 40°C overnight. Then the solvent was evaporated and the resulting product was precipitated from cold Et₂O. The residue solid was dissolved in DCM (2 ml). 20%(v/v) TFA and triethylsilane (0.5 mmol) were added dropwise. The mixture was stirred at rt for 1h. After the reaction, saturated NaHCO₃ was added to neutralize the excess TFA. The mixture was firstly extracted with DCM and followed by extraction with EtOAc. The organic phase was dried over anhydrous Na₂SO₄, concentrated and purified by flash chromatography to give compound **3f** or **3h** as a colorless oil.

To a solution of ethyl ester (0.5 mmol) in 4 ml THF was added LiHMDS (1M in THF, 0.6 ml, 0.6 mmol) dropwise at -78°C. After the reaction mixture was stirred for 40 min at -78°C, the solution of ethylene sulfate (75 mg, 0.6 mmol) in 2ml THF was slowly added. The mixture was warmed to rt for 1 day. After the solvent was

evaporated, dioxane (2 ml) and 4M HCl in dioxane (1 ml) were added. The reaction mixture was stirred at 80°C overnight. After the reaction, the mixture was diluted with DCM and washed with saturated NaHCO₃. The organic phase was dried over anhydrous Na₂SO₄, concentrated and purified by column chromatography (EtOAc/Acetone 2:1) to give the final product **3k** or **3l**.

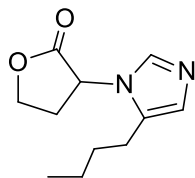


Ethyl 2-(5-butyl-1H-imidazol-1-yl)acetate (**3f**): Following the general procedure J, flash chromatography of the crude product (2:1 EtOAc-acetone) afforded **3f** (50%) as a colorless oil. ¹H NMR (300 MHz, Chloroform-*d*) δ 7.39 (s, 1H, Imidazole), 6.76 (s, 1H, Imidazole), 4.55 (s, 2H, CH₂), 4.19 (q, *J* = 7.1 Hz, 2H, OCH₂), 2.41 (t, *J* = 7.3 Hz, 2H, CH₂), 1.56 (m, 2H, CH₂), 1.49 – 1.29 (m, 2H, CH₂), 1.24 (t, *J* = 7.1 Hz, 3H, CH₃), 0.90 (t, *J* = 7.3 Hz, 3H, CH₃). ¹³C NMR (75 MHz, Chloroform-*d*) δ 167.6 (CO), 137.6 (Imidazole), 132.1 (Imidazole), 126.1 (Imidazole), 62.0 (OCH₂), 45.9 (CH₂), 30.1 (CH₂), 23.4 (CH₂), 22.3 (CH₂), 14.1 (CH₃), 13.8 (CH₃). ESI-HRMS(M+H)⁺: 211.1441; found: 211.1434.

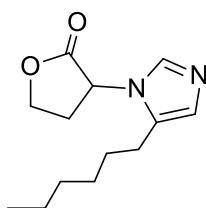


Ethyl 2-(5-hexyl-1H-imidazol-1-yl)acetate (**3h**): Following the general procedure J, flash chromatography of the crude product (2:1 EtOAc-acetone) afforded **3h** (58%) as a colorless oil. ¹H NMR (300 MHz, Chloroform-*d*) δ 7.43 (s, 1H, Imidazole), 6.79 (s, 1H, Imidazole), 4.58 (s, 2H, CH₂), 4.30 – 4.07 (q, *J* = 7.1 Hz, 2H, OCH₂), 2.44 (t, *J* = 7.7 Hz, 2H, CH₂), 1.59 (m, 2H, CH₂), 1.46 – 1.15 (m, 9H, 3×CH₂, CH₃), 0.88 (t, *J* = 6.9 Hz, 3H, CH₃). ¹³C NMR (75 MHz, Chloroform-*d*) δ 167.6 (CO), 137.6 (Imidazole), 132.2 (Imidazole), 126.1 (Imidazole), 62.0 (OCH₂), 46.0 (CH₂), 31.5

(CH₂), 29.0 (CH₂), 28.0 (CH₂), 23.7 (CH₂), 22.5 (CH₂), 14.1 (CH₃), 14.0 (CH₃).
ESI-HRMS(M+H)⁺: 239.1754; found: 239.1753.

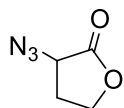


3-(5-butyl-1*H*-imidazol-1-yl)dihydrofuran-2(3*H*)-one (**3k**): Following the general procedure J, flash chromatography of the crude product (2:1 EtOAc-acetone) afforded **3k** (40%) as a colorless oil. ¹H NMR (400 MHz, Chloroform-*d*) δ 7.52 (s, 1H, Imidazole), 6.85 (s, 1H, Imidazole), 4.92 (dd, *J* = 11.4, 8.8 Hz, 1H, CH-lactone), 4.66 – 4.54 (m, 1H, OCHH-lactone), 4.42 (ddd, *J* = 10.5, 9.5, 6.2 Hz, 1H, OCHH-lactone), 2.85 (m, 1H, CHH-lactone), 2.66 – 2.44 (m, 3H, CHH-lactone, CH₂), 1.66 (m, 2H, CH₂), 1.43 (m, 2H, CH₂), 0.95 (t, *J* = 7.4 Hz, 3H, CH₃). ¹³C NMR (101 MHz, Chloroform-*d*) δ 171.9 (CO), 134.9 (Imidazole), 132.4 (Imidazole), 126.3 (Imidazole), 65.2 (OCH₂), 53.0 (CH-lactone), 30.8 (CH₂), 30.1 (CH₂), 23.9 (CH₂), 22.4 (CH₂), 13.8 (CH₃). ESI-HRMS(M+H)⁺: 209.1285; found: 209.1286.



3-(5-hexyl-1*H*-imidazol-1-yl)dihydrofuran-2(3*H*)-one (**3l**): Following the general procedure J, flash chromatography of the crude product (2:1 EtOAc-acetone) afforded **3l** (38%) as a white solid. ¹H NMR (400 MHz, Acetone-*d*₆) δ 7.49 (s, 1H, Imidazole), 6.62 (s, 1H, Imidazole), 5.27 (dd, *J* = 11.8, 8.9 Hz, 1H, CH-lactone), 4.49 (td, *J* = 8.9, 1.5 Hz, 1H, OCHH-lactone), 4.37 (ddd, *J* = 10.8, 9.0, 6.1 Hz, 1H, OCHH-lactone), 2.85 (m, 1H, CHH-lactone), 2.71 – 2.57 (m, 1H, CHH-lactone), 2.49 (m, 2H, CH₂), 1.56 (m, 2H, CH₂), 1.30 (m, 2H, CH₂), 1.26 – 1.10 (m, 4H, 2×CH₂), 0.79 (t, *J* = 6.0 Hz, 3H, CH₃). ¹³C NMR (101 MHz, Acetone-*d*₆) δ 173.0 (CO), 135.3 (Imidazole),

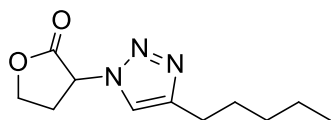
132.3 (Imidazole), 125.7 (Imidazole), 65.3 (OCH₂), 52.7 (CH-lactone), 31.4 (CH₂), 30.4 (CH₂), 28.9 (CH₂), 28.2 (CH₂), 23.6 (CH₂), 22.4 (CH₂), 13.4 (CH₃). ESI-HRMS(M+H)⁺: 237.1598; found: 237.1598. m.p. 60°C.



3-Azidodihydrofuran-2(3*H*)-one (**3m**): to a solution of 3-bromodihydrofuran-2(3*H*)-one (1ml, 10.8mmol) in 20ml acetone was added a solution of sodium azide (1g, 15.2mmol) in 4ml water at rt. The mixture was stirred for 24h at rt. After the reaction, acetone was evaporated. The residue was extracted with DCM. The organic phase was dried over anhydrous Na₂SO₄, concentrated and purified by column chromatography (EtOAc/pentane 1:2) to give the colorless oil 1.3g (yield 94%). ¹H NMR (300 MHz, Chloroform-*d*) δ 4.43 (ddd, *J* = 9.1, 8.5, 3.6 Hz, 1H, OCHH-lactone), 4.36 – 4.20 (m, 2H, OCHH-lactone, CH-lactone), 2.56 (dddd, *J* = 13.1, 8.4, 6.7, 3.6 Hz, 1H, CHH-lactone), 2.26 – 2.10 (m, 1H, CHH-lactone).

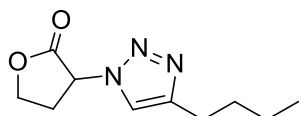
General procedure K for 1,4-disubstituted triazole:

To a solution of azidodihydrofuranone (1 mmol) in THF (3 ml) were added CuI (15 mol%), 1-heptyne or 1-hexyne (1.5 mmol), DIEA (3 mmol) at rt. After the 16h, the solvent was evaporated and the residue was purified by column chromatography to afford the desired product.



3-(4-pentyl-1*H*-1,2,3-triazol-1-yl)dihydrofuran-2(3*H*)-one (**3q**): Following the general procedure K, flash chromatography of the crude product (EtOAc/pentane 3:2) afforded **3q** (72%) as a white solid. ¹H NMR (300 MHz, Chloroform-*d*) δ 7.47 (s, 1H, CH-triazole), 5.26 (t, *J* = 9.3 Hz, 1H, CH-lactone), 4.60 (ddd, *J* = 9.3, 7.9, 3.9 Hz, 1H, OCHH-lactone), 4.42 (td, *J* = 9.0, 6.9 Hz, 1H, OCHH-lactone), 3.03 – 2.86 (m, 2H,

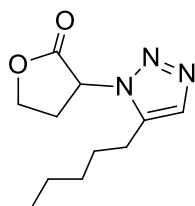
CH₂-lactone), 2.71 – 2.56 (m, 2H, CH₂), 1.72 – 1.53 (m, 2H, CH₂), 1.28 (m, 4H, 2×CH₂), 0.83 (t, *J* = 7.3 Hz, 3H, CH₃). ¹³C NMR (75 MHz, Chloroform-*d*) δ 171.2 (CO), 149.1 (C-triazole), 120.8 (CH-triazole), 66.3 (OCH₂-lactone), 57.5 (CH-lactone), 31.4 (CH₂), 29.3 (CH₂-lactone), 29.0 (CH₂), 25.6 (CH₂), 22.4 (CH₂), 14.0 (CH₃). ESI-HRMS(M+H)⁺: 224.1394; found: 224.1383. m.p. 70°C



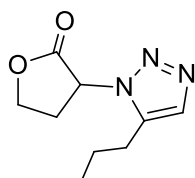
3-(4-butyl-1H-1,2,3-triazol-1-yl)dihydrofuran-2(3H)-one (**3p**): Following the general procedure K, flash chromatography of the crude product (EtOAc/pentane 2:1) afforded **3p** (74%) as a white solid. ¹H NMR (400 MHz, Chloroform-*d*) δ 7.54 (s, 1H, CH-triazole), 5.32 (t, *J* = 9.3 Hz, 1H, CH-lactone), 4.65 (ddd, *J* = 9.3, 8.0, 3.6 Hz, 1H, OCHH-lactone), 4.47 (td, *J* = 9.1, 6.8 Hz, 1H, OCHH-lactone), 3.06 – 2.88 (m, 2H, CH₂-lactone), 2.71 (t, *J* = 7.7 Hz, 2H, CH₂), 1.75 – 1.57 (m, 2H, CH₂), 1.37 (h, *J* = 7.4 Hz, 2H, CH₂), 0.92 (t, *J* = 7.3 Hz, 3H, CH₃). ¹³C NMR (75 MHz, Chloroform-*d*) δ 171.5 (CO), 148.9 (C-triazole), 121.0 (CH-triazole), 66.3 (OCH₂-lactone), 57.5 (CH-lactone), 31.3 (CH₂), 29.3 (CH₂-lactone), 25.3 (CH₂), 22.3 (CH₂), 13.8 (CH₃). ESI-HRMS(M+H)⁺: 210.1237; found: 210.1232. m.p. 68°C.

General procedure L for 1,5-disubstituted triazole:

To a solution of azidodihydrofuranone (1 mmol) in THF (3 ml) were added Cp*RuCl(PPh₃)₂ (6 mol%), 1-heptyne or 1-hexyne (1.5 mmol). The reaction was stirred at 65°C. After 1 day, the solvent was evaporated and the residue was purified by column chromatography to afford the desired product.



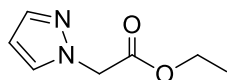
3-(5-pentyl-1*H*-1,2,3-triazol-1-yl)dihydrofuran-2(3*H*)-one (**3o**): Following the general procedure L, flash chromatography of the crude product (EtOAc/pentane 3:2) afforded **3o** (52%) as a white solid. ¹H NMR (300 MHz, Chloroform-*d*) δ 7.50 (s, 1H, CH-triazole), 5.14 (dd, *J* = 9.1, 8.4 Hz, 1H, CH-lactone), 4.77 (ddd, *J* = 9.2, 8.3, 4.4 Hz, 1H, OCHH-lactone), 4.51 (ddd, *J* = 9.1, 7.9, 7.1 Hz, 1H, OCHH-lactone), 3.18 (m, 1H, CHH-lactone), 2.84 (m, 1H, CHH-lactone), 2.77 – 2.54 (m, 2H, CH₂), 1.70 (m, 2H, CH₂), 1.37 (m, 4H, 2×CH₂), 0.94 – 0.87 (t, *J* = 7.5 Hz, 3H, CH₃). ¹³C NMR (75 MHz, Chloroform-*d*) δ 171.0 (CO), 138.7 (C-triazole), 132.4 (CH-triazole), 66.7 (OCH₂-lactone), 55.1 (CH-lactone), 31.3 (CH₂), 28.6 (CH₂-lactone), 27.7 (CH₂), 23.1 (CH₂), 22.3 (CH₂), 13.9 (CH₃). ESI-HRMS(M+H)⁺: 224.1394; found: 224.1384. m.p. 39°C.



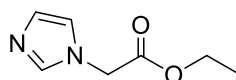
3-(5-butyl-1*H*-1,2,3-triazol-1-yl)dihydrofuran-2(3*H*)-one (**3n**): Following the general procedure K, flash chromatography of the crude product (EtOAc/pentane 2:1) afforded **3n** (53%) as a white solid. ¹H NMR (300 MHz, Chloroform-*d*) δ 7.44 (s, 1H, CH-triazole), 5.08 (dd, *J* = 9.1, 8.4 Hz, 1H, CH-lactone), 4.71 (ddd, *J* = 9.1, 8.3, 4.4 Hz, 1H, OCHH-lactone), 4.45 (ddd, *J* = 9.2, 8.0, 7.2 Hz, 1H, OCHH-lactone), 3.13 (m, 1H, CHH-lactone), 2.79 (m, 1H, CHH-lactone), 2.73 – 2.50 (m, 2H, CH₂), 1.72 – 1.57 (m, 2H, CH₂), 1.46 – 1.28 (m, 2H, CH₂), 0.90 (t, *J* = 7.3 Hz, 3H, CH₃). ¹³C NMR (75 MHz, Chloroform-*d*) δ 171.0 (CO), 138.6 (C-triazole), 132.4 (CH-triazole), 66.7 (OCH₂-lactone), 55.1 (CH-lactone), 30.1 (CH₂), 28.6 (CH₂-lactone), 22.8 (CH₂), 22.3 (CH₂), 13.7 (CH₃). ESI-HRMS(M+H)⁺: 210.1237; found: 210.1230. m.p. 70°C.

General procedure M for the synthesis of ethyl ester:

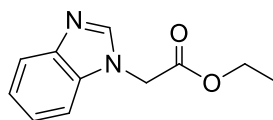
To a solution of imidazole or other substrates (1.0 eq) in CH₃CN were added ethyl bromoacetate (1.0 eq) and K₂CO₃ (2.1 eq). The reaction mixture was heated at reflux for 2 h. Then the yellow mixture was diluted with EtOAc, washed with saturated NH₄Cl, dried over anhydrous Na₂SO₄, concentrated and purified by flash chromatography to get the desired product.



Ethyl-2-(1*H*-pyrazol-1-yl)acetate (**4b**): Following the general procedure M, flash chromatography of the crude product (EtOAc/pentane 1:4) afforded **4b** (84%) as a yellow oil. ¹H NMR (300 MHz, Chloroform-*d*) δ 7.56 (d, *J* = 1.3 Hz, 1H, CH-N), 7.48 (d, *J* = 1.8 Hz, 1H, CH=N), 6.33 (dd, *J* = 2.3, 1.9 Hz, 1H, CH=CH-N), 4.92 (s, 2H, CH₂C=O), 4.24 (q, *J* = 7.1 Hz, 2H, OCH₂), 1.28 (t, *J* = 7.1 Hz, 3H, CH₃).



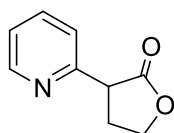
Ethyl-2-(1*H*-imidazol-1-yl)acetate (**4c**): Following the general procedure M, flash chromatography of the crude product (EtOAc/pentane 1:4) afforded **4c** (43%) as a yellow oil. ¹H NMR (300 MHz, Chloroform-*d*) δ 7.51 (s, 1H, N=CH-N), 7.10 (d, *J* = 1.1 Hz, 1H, NCH=CH), 6.96 (d, *J* = 1.4 Hz, 1H, NCH=CH), 4.69 (s, 2H, CH₂C=O), 4.25 (q, *J* = 7.1 Hz, 2H, OCH₂), 1.29 (t, *J* = 7.1 Hz, 3H, CH₃).



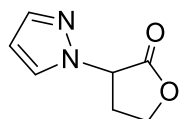
Ethyl-2-(1*H*-benzimidazol-1-yl)acetate (**4d**): Following the general procedure M, flash chromatography of the crude product (EtOAc/pentane 1:4) afforded **4d** (65%) as a yellow solid. ¹H NMR (300 MHz, Chloroform-*d*) δ 7.93 (s, 1H, N=CH-N), 7.87 – 7.76 (m, 1H, Ar), 7.36 – 7.28 (m, 3H, Ar), 4.89 (s, 2H, CH₂C=O), 4.24 (q, *J* = 7.1 Hz, 2H, OCH₂), 1.27 (t, *J* = 7.1 Hz, 3H, CH₃).

General procedure N for the synthesis of lactones:

A solution of 1M LiHMDS in THF (1.2 eq) was diluted in 2 mL anhydrous THF, followed by adding dropwise a solution of various ethyl ester substrates (1 eq) in 2 mL anhydrous THF at -15 °C or -78 °C. After the reaction mixture was stirred at -15 °C or -78 °C for 40 min, a solution of cyclic sulfate (1.2 eq) in 2 mL anhydrous THF was added. The reaction was allowed to warm up to rt. Then THF was evaporated under reduced pressure to give a yellow solid which was subsequently treated with 2 mL 4M HCl in dioxane, additional 4 mL dioxane was added, and the reaction was stirred at 80 °C for 14h. Finally, dioxane was evaporated to give a brown syrup, which was dissolved in 20 mL dichloromethane and washed with water (2x20 mL), the aqueous layer was extracted with dichloromethane (2x20 mL), the organic layers were combined, dried over Na₂SO₄, concentrated, and purified by flash chromatography.

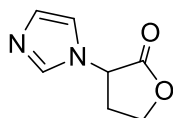


3-(pyridin-2-yl)dihydrofuran-2(3H)-one (**4e**): Following the general procedure N, flash chromatography of the crude product (EtOAc/pentane 1:2) afforded **4e** (62%). ¹H NMR (300 MHz, Chloroform-*d*) δ 8.57 (ddd, *J* = 4.9, 1.9, 1.0 Hz, 1H, Ar), 7.69 (td, *J* = 7.7, 1.9 Hz, 1H, Ar), 7.38 (dt, *J* = 7.9, 1.1 Hz, 1H, Ar), 7.22 (ddd, *J* = 7.6, 4.9, 1.2 Hz, 1H, Ar), 4.58 (ddd, *J* = 8.8, 8.1, 4.9 Hz, 1H, OCHH-lactone), 4.40 (dt, *J* = 8.8, 7.5 Hz, 1H, OCHH-lactone), 3.95 (t, *J* = 9.2 Hz, 1H, CH-lactone), 2.83 (m, 1H, CHH-lactone), 2.68 (m, 1H, CHH-lactone).

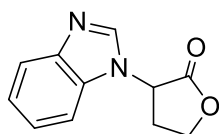


3-(1H-pyrazol-1-yl)dihydrofuran-2(3H)-one (**4f**): Following the general procedure N, flash chromatography of the crude product (EtOAc/pentane 1:3) afforded **4f** (49%). ¹H NMR (300 MHz, Chloroform-*d*) δ 7.59 (t, *J* = 2.3 Hz, 2H, Ar), 6.34 (t, *J* = 2.1 Hz, 1H, Ar), 5.09 (t, *J* = 9.0 Hz, 1H, CH-lactone), 4.65 (ddd, *J* = 9.1, 8.3, 3.8 Hz, 1H,

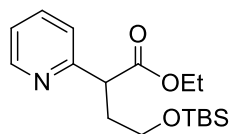
OCHH-lactone), 4.43 (td, $J = 8.9, 7.0$ Hz, 1H, OCHH-lactone), 3.05 – 2.71 (m, 2H, CH₂-lactone). ¹³C NMR (101 MHz, Chloroform-*d*) δ 172.5 (CO), 140.8 (Ar), 130.1 (Ar), 106.5 (Ar), 66.3 (OCH₂), 59.0 (CH), 29.2 (CH₂). ESI-HRMS(M+Na)⁺: 175.0478; found: 175.0470.



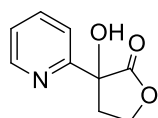
3-(1*H*-imidazol-1-yl)dihydrofuran-2(3*H*)-one (**4g**): Following the general procedure N, flash chromatography of the crude product (EtOAc/MeOH 9:1) afforded **4g** (35%). ¹H NMR (300 MHz, Chloroform-*d*) δ 7.64 (s, 1H, Ar), 7.13 (d, $J = 1.1$ Hz, 1H, Ar), 7.01 (d, $J = 1.5$ Hz, 1H, Ar), 5.03 (dd, $J = 11.3, 8.7$ Hz, 1H, CH-lactone), 4.58 (ddd, $J = 9.6, 8.5, 1.9$ Hz, 1H, OCHH-lactone), 4.40 (m, 1H, OCHH-lactone), 2.96 – 2.83 (m, 1H, CH₂-lactone), 2.61 (m, 1H, CH₂-lactone).



3-(1*H*-benzo[*d*]imidazol-1-yl)dihydrofuran-2(3*H*)-one (**4h**): Following the general procedure N, flash chromatography of the crude product (EtOAc/pentane/MeOH 6:3:1) afforded **4h** (49%). ¹H NMR (400 MHz, Chloroform-*d*) δ 7.97 (s, 1H, Ar), 7.91 – 7.76 (m, 1H, Ar), 7.38 – 7.28 (m, 3H, Ar), 5.29 (dd, $J = 11.5, 8.9$ Hz, 1H, CH-lactone), 4.66 (td, $J = 9.2, 1.7$ Hz, 1H, OCHH-lactone), 4.47 (ddd, $J = 10.7, 9.6, 6.3$ Hz, 1H, OCHH-lactone), 2.89 (m, 1H, CHH-lactone), 2.71 (m, 1H, CHH-lactone). ¹³C NMR (101 MHz, Chloroform-*d*) δ 171.4 (CO), 144.0 (Ar), 141.8 (Ar), 132.6 (Ar), 123.7 (Ar), 122.9 (Ar), 121.0 (Ar), 109.6 (Ar), 65.5 (OCH₂), 53.7 (CH), 29.4 (CH₂). ESI-HRMS(M+H)⁺: 203.0815; found: 203.0818.

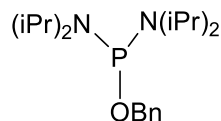


Ethyl 4-((tert-butyldimethylsilyl)oxy)-2-(pyridin-2-yl)butanoate (**4i**): To a solution of 1M LiHMDS (1.2 eq) in THF (4ml) was added dropwise ethyl-2-pyridyl acetate (1.0eq) which was diluted with THF (3ml) at -10 °C. Then the mixture was allowed to warm up to rt. After 16h, the mixture was concentrated to give a residue, which was purified by flash chromatography (EtOAc/pentane 1:1) to afford **4i** (46%). ¹H NMR (300 MHz, Chloroform-*d*) δ 8.55 (ddd, *J* = 4.9, 1.9, 0.9 Hz, 1H, Ar), 7.63 (td, *J* = 7.7, 1.9 Hz, 1H, Ar), 7.28 (dt, *J* = 7.8, 1.1 Hz, 1H, Ar), 7.15 (ddd, *J* = 7.5, 4.9, 1.2 Hz, 1H, Ar), 4.13 (m, 2H, OCH₂CH₃), 4.02 (t, *J* = 7.5 Hz, 1H, CH), 3.64 (ddd, *J* = 10.3, 6.4, 5.7 Hz, 1H, OCH₂), 3.53 (ddd, *J* = 10.3, 6.9, 5.6 Hz, 1H, OCH₂), 2.35 (dddd, *J* = 13.5, 7.8, 6.9, 5.7 Hz, 1H), 2.11 (dddd, *J* = 13.7, 7.2, 6.4, 5.6 Hz, 1H), 1.18 (t, *J* = 7.1 Hz, 3H, OCH₂CH₃), 0.87 (s, 9H, 3×CH₃), -0.01 (s, 6H, 2×CH₃). ¹³C NMR (75 MHz, Chloroform-*d*) δ 172.9 (CO), 158.8, 149.5, 136.5, 123.0, 122.0 (Ar), 60.8 (OCH₂), 60.5 (OCH₂), 50.1 (CH), 34.8 (CH₂), 25.9 (3×CH₃), 18.3 (C), 14.1 (CH₃), -5.4 (CH₃), -5.5 (CH₃).

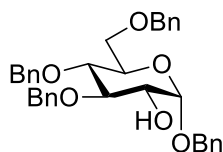


3-Hydroxy-3-(pyridin-2-yl)dihydrofuran-2(3H)-one (**4j**): To a solution of **4i** in THF (2ml) was added 1M TBAF in THF (0.2ml) at reflux for 5h. Then THF was evaporated under reduced pressure to give a residue, which was purified by flash chromatography (EtOAc/pentane 1:1) to afford **4j** (70%). ¹H NMR (500 MHz, Chloroform-*d*) δ 8.56 (ddd, *J* = 4.9, 1.8, 1.0 Hz, 1H, Ar), 7.77 (td, *J* = 7.7, 1.8 Hz, 1H, Ar), 7.50 (dt, *J* = 7.9, 1.1 Hz, 1H, Ar), 7.29 (ddd, *J* = 7.5, 4.9, 1.1 Hz, 1H, Ar), 4.89 (br, 1H, OH), 4.64 – 4.40 (m, 2H, OCH₂-lactone), 2.73 (ddd, *J* = 13.2, 7.0, 5.2 Hz, 1H, CH₂-lactone), 2.65 (ddd, *J* = 13.2, 7.9, 7.3 Hz, 1H, CH₂-lactone). ¹³C NMR (126 MHz, Chloroform-*d*) δ 177.3 (CO), 158.4, 148.5, 137.5, 123.5, 119.6 (Ar), 77.0 (OCH₂), 66.0 (C-OH), 37.7 (CH₂).

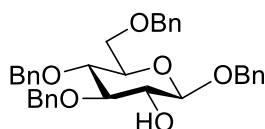
Supporting information (II)



Benzyloxy bis(diisopropylamino)phosphine (**B1**): To a suspension of bis(*N,N*-diisopropylamino) chlorophosphine (5g) in ether (100ml) was added dropwise a solution of benzyl alcohol (2.1ml) and triethylamine (3ml) in ether (2.5ml) at 0 °C. After the reaction mixture was stirred at 0 °C for 2h, the resulting white solid was filtered. The organic phase was collected, concentrated and purified by flash chromatography (pentane/Et₃N 97/3) to afford 4.2g product (67% yield) as a colorless oil. ¹H NMR (300 MHz, Chloroform-*d*) δ 7.36 (m, 5H, Ph), 4.67 (d, *J* = 6.0 Hz, 2H, OCH₂), 3.60 (m, 4H, 4×CH), 1.20 (m, 24H, 8×CH₃).

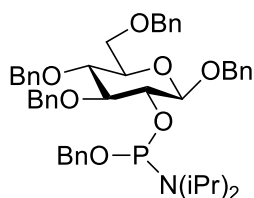


Benzyl 3,4,6-*O*-benzyl- α -D-glucopyranoside (**5c**): To a solution of penta-benzyl glucoside (1g, 1.6mmol) in toluene (10ml) was added dropwise TIBA1 (2.4ml, 19mmol) at rt under N₂ protection. The mixture was stirred at 50°C for 60h. After the reaction was cooled to 0°C, 1M HCl was added slowly to neutralize the excess base. The mixture was extracted with EtOAc and the organic was collected, concentrated and purified by flash chromatography (pentane/EtOAc 4/1) to afford 150mg product (18% yield) as a colorless oil. ¹H NMR (300 MHz, Chloroform-*d*) δ 7.41 – 7.23 (m, 18H, Ph), 7.19 – 7.09 (m, 2H, Ph), 5.02 (d, *J* = 3.3 Hz, 1H, H1), 4.93 (d, *J* = 11.1 Hz, 1H, CHHPh), 4.84 (d, *J* = 2.2 Hz, 1H, CHHPh), 4.80 (d, *J* = 1.8 Hz, 1H, CHHPh), 4.75 (d, *J* = 11.6 Hz, 1H, CHHPh), 4.64 (d, *J* = 12.1 Hz, 1H, CHHPh), 4.58 – 4.46 (m, 3H, CHHPh, CH₂Ph), 3.88 – 3.69 (m, 4H, H5, H2, H3, H6a), 3.69 – 3.56 (m, 2H, H6b, H4), 2.09 (d, *J* = 8.4 Hz, 1H, OH).



Benzyl 3,4,6-*O*-benzyl-β-D-glucopyranoside (5f):

1,2-Anhydro-3,4,6-tri-*O*-benzyl-α-D-glucopyranose was synthesized from commercially available 3,4,6-tri-*O*-benzyl-D-glucal as previously reported^[15]. Without further purification, 1,2-anhydro-3,4,6-tri-*O*-benzyl-α-D-glucopyranose was subjected to the next step. To a solution of 1,2-anhydro-3,4,6-tri-*O*-benzyl-α-D-glucopyranose (1.5g, 1.0 eq) in THF were added benzyl alcohol (1.5 eq), 1M ZnCl₂ in ether (3.5ml) at 0 °C. The reaction was stirred overnight. Then the mixture was diluted with EtOAc, washed with water. The organic phase was dried over Na₂SO₄, concentrated to afford the crude product. The remaining benzyl alcohol was co-evaporated with water. The residue was purified by silica gel chromatography (EtOAc-pentane 1:6) to afford the white solid, the resulting product was recrystallized from EtOH to give the pure product 1.05g as a white solid, yield 55%. ¹H NMR (300 MHz, Benzene-*d*₆) δ 7.39 (d, *J* = 6.7 Hz, 2H, Ph), 7.34 – 7.27 (m, 4H, Ph), 7.24 – 7.04 (m, 14H, Ph), 5.06 (d, *J* = 11.5 Hz, 1H, *CHHPh*), 4.94 – 4.77 (m, 3H, *CHHPh*, CH₂Ph), 4.55 (d, *J* = 11.4 Hz, 1H, *CHHPh*), 4.51 – 4.35 (m, 3H, *CHHPh*, CH₂Ph), 4.25 (d, *J* = 7.7 Hz, 1H, H1), 3.84 – 3.65 (m, 4H, H3, H4, H6a, H6b), 3.59 (t, *J* = 8.8 Hz, 1H, H2), 3.37 (m, 1H, H5), 2.19 (d, *J* = 1.8 Hz, 1H, OH).

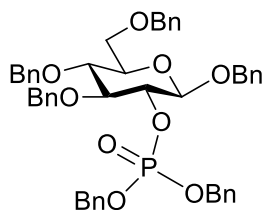


Benzyl ((2*R*,3*R*,4*S*,5*R*,6*R*)-2,4,5-tris(benzyloxy)-6-((benzyloxy)methyl)tetrahydro-2H-pyran-3-yl) diisopropylphosphoramidite (5g): To a solution of diisopropylammonium tetrazolide salt (mixed 1.0 eq tetrazole with 1.2 eq diisopropylamine in DCM, then evaporated the solvent) in 10 ml DCM was added benzyl 3,4,6-tri-*O*-benzyl-β-D-glucopyranoside (1 g) which was dissolved in 10 ml DCM at

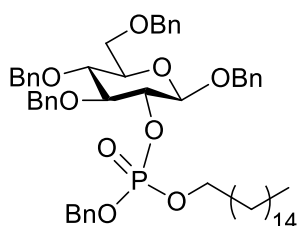
0 °C. Then the mixture was stirred overnight at room temperature. When the starting material was consumed, the solid salt was filtered. The organic phase was collected, concentrated and purified by silica gel chromatography (EtOAc-pentane 1:9 with 1% Et₃N) gave 1.2 g the desired product (yield 81%). R_f=0.56. ¹H NMR (500 MHz, Chloroform-*d*) δ 7.38 – 7.09 (m, 23H, Ph), 7.07 – 7.00 (m, 2H, Ph), 4.93 (m, 1H, CHHPh), 4.84 (m, 1H, CHHPh), 4.74 – 4.43 (m, 8H, 4×CH₂Ph), 4.40 (d, *J* = 7.5 Hz, 1H, H-1), 3.84 (m, 1H, H-2), 3.66–3.51 (m, 6H, H6a, H6b, H-4, H-3, 2×CH), 3.42 (m, 1H, H-5), 1.07 – 0.96 (m, 12H, 4×CH₃). ¹³C NMR (126 MHz, CDCl₃) δ 139.9 (C-Ph), 139.6 (C-Ph), 138.8 (C-Ph), 138.3 (C-Ph), 137.7 (C-Ph), 128.4 (Ph), 128.4 (Ph), 128.4 (Ph), 128.3 (Ph), 128.2 (Ph), 128.2 (Ph), 128.1 (Ph), 128.0 (Ph), 128.0 (Ph), 128.0 (Ph), 127.9 (Ph), 127.8 (Ph), 127.8 (Ph), 127.8 (Ph), 127.7 (Ph), 127.7 (Ph), 127.6 (Ph), 127.6 (Ph), 127.6 (Ph), 127.4 (Ph), 127.3 (Ph), 127.2 (Ph), 127.1 (Ph), 127.0 (Ph), 127.0 (Ph), 102.0 (C1), 101.7 (d, *J*_{C-P} = 2.9 Hz, C1'), 85.5 (d, *J*_{C-P} = 2.8 Hz, C3), 85.4 (C3'), 78.1 (C4), 76.2 (d, *J*_{C-P} = 10.9 Hz, C2'), 75.9 (d, *J*_{C-P} = 5.2 Hz, C2), 75.2 (OCH₂), 75.0 (C5, C5'), 74.9 (OCH₂), 73.5 (OCH₂), 70.8 (OCH₂), 69.2 (C6, C6'), 65.5 (OCH₂), 43.1 (CH), 43.0 (CH), 24.7 (CH₃), 24.6 (CH₃), 24.6 (CH₃), 24.5 (CH₃). ³¹P NMR (122 MHz, CDCl₃) δ 151.44, 150.23. ESI-HRMS(M+H₃O)⁺: 796.3973; found: 796.3976.

General procedure for the synthesis of phosphotriesters:

To a solution of phosphoramidite **5g** (0.2 mmol) in 2 ml DCM were added corresponding alcohol (0.2 mmol) dissolved in 1 ml DCM, 1*H*-tetrazole (0.2 mmol) at rt. Then the mixture was stirred for 5 h at rt. After completion of the reaction, *t*-BuOOH (0.24 mmol) was added at 0 °C. After 1 h at rt, the white solid was filtered. The organic phase was collected, concentrated and purified by silica gel chromatography.

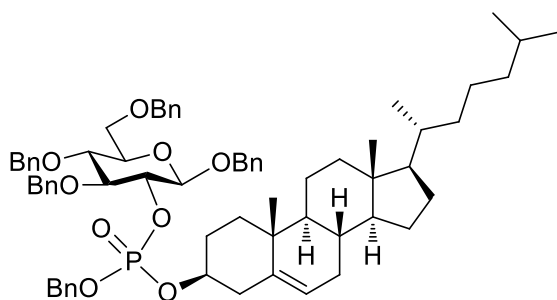


Dibenzy ((2*R*,3*R*,4*S*,5*R*,6*R*)-2,4,5-tris(benzyloxy)-6-((benzyloxy)methyl)tetrahydro-2H-pyran-3-yl) phosphate **5h**: From benzyl alcohol following general procedure, flash chromatography of the crude product (1:3 EtOAc-pentane) afforded **5h** (yield 88%) as a white solid. $R_f=0.43$. ^1H NMR (500 MHz, Chloroform-*d*) δ 7.31 (m, 8H, Ph), 7.25 – 7.13 (m, 16H, Ph), 7.12 – 7.01 (m, 6H, Ph), 4.93 – 4.85 (m, 4H, 2 \times CH₂Ph), 4.82 (m, 1H, CHHPh), 4.79 – 4.68 (m, 3H, CHHPh, CH₂Ph), 4.61 – 4.55 (m, 2H, CH₂Ph), 4.51 (d, J = 10 Hz, 1H, H1), 4.50 – 4.47 (m, 2H, CH₂Ph), 4.45 – 4.39 (m, 1H, H2), 3.70 – 3.62 (m, 4H, H6a, H6b, H3, H4), 3.45 (m, 1H, H5). ^{13}C NMR (126 MHz, Chloroform-*d*) δ 138.3 , 138.1 , 137.9 , 136.9 , 136.2 , 136.1 , 128.4 , 128.4 , 128.4 , 128.4 , 128.3 , 128.2 , 128.2 , 128.0 , 127.9 , 127.8 , 127.8 , 127.7 , 127.7 , 127.7 , 127.6 , 127.5 , 100.1 (d, $J_{\text{C-P}}$ = 3.7 Hz, C1), 83.7 (d, $J_{\text{C-P}}$ = 4.0 Hz, C3), 79.1 (d, $J_{\text{C-P}}$ = 6.9 Hz, C2), 77.8 (C4), 75.2 (C5), 75.1 (OCH₂), 75.0 (OCH₂), 73.6 (OCH₂), 70.8 (OCH₂), 69.2 (d, $J_{\text{C-P}}$ = 5.2 Hz, OCH₂), 69.1 (d, $J_{\text{C-P}}$ = 5.3 Hz, OCH₂), 68.7 (C6). ^{31}P NMR (122 MHz, Chloroform-*d*) δ -1.71. ESI-HRMS($\text{M}+\text{Na}^+$): 823.3006; found: 823.3006.



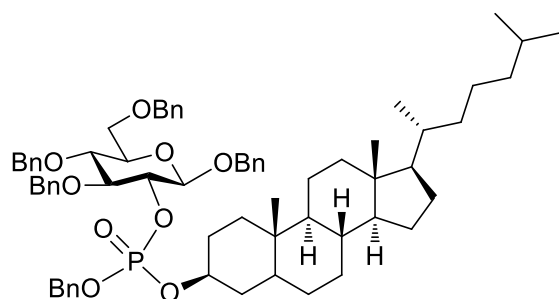
Benzyl hexadecyl ((2*R*,3*R*,4*S*,5*R*,6*R*)-2,4,5-tris(benzyloxy)-6-((benzyloxy)methyl)tetrahydro-2H-pyran-3-yl) phosphate **5i**: From cetearyl alcohol following general procedure, flash chromatography of the crude product (1:1 EtOAc-pentane) afforded **5i** (yield 90%) as a white solid. $R_f=0.4$. ^1H NMR (500 MHz, Chloroform-*d*) δ 7.46 – 7.41 (m, 1H, Ph), 7.41 – 7.12 (m, 24H, Ph), 5.08 – 4.88 (m, 4H, 2 \times CH₂Ph), 4.88 – 4.81 (m, 1H, CHHPh), 4.81 – 4.75 (m, 1H, CHHPh), 4.70 – 4.61 (m, 2H, CH₂Ph),

4.57 (d, $J = 8.3$ Hz, 1H, H1), 4.56 – 4.53 (m, 2H, CH₂Ph), 4.45 (m, 1H, H2), 3.94 – 3.81 (m, 2H, OCH₂), 3.79 – 3.68 (m, 4H, H3, H4, H6a, H6b), 3.51 (m, 1H, H5), 1.51 – 1.37 (m, 2H, CH₂), 1.28 (m, 26H, 13×CH₂), 0.90 (t, $J = 6.9$ Hz, 3H, CH₃). ¹³C NMR (126 MHz, Chloroform-*d*) δ 138.3 , 138.1 , 137.9 , 137.0 , 136.3 , 128.6 , 128.5 , 128.4 , 128.4 , 128.4 , 128.3 , 128.3 , 128.3 , 128.2 , 128.1 , 128.1 , 128.0 , 128.0 , 127.9 , 127.8 , 127.8 , 127.8 , 127.7 , 127.7 , 127.6 , 127.6 , 127.4 , 100.1 (d, $J_{C-P} = 3.6$ Hz, C1, C1'), 83.7 (t, $J_{C-P} = 3.6$ Hz, C3, C3'), 78.9 (t, $J_{C-P} = 7.5$ Hz, C2, C2'), 77.8 (C4, C4'), 75.2 (C5, C5'), 75.0 (OCH₂Ph), 73.5 (OCH₂Ph), 70.8 (OCH₂Ph), 69.2 (d, $J_{C-P} = 8.2$ Hz, OCH₂Ph), 69.1 (d, $J_{C-P} = 5.4$ Hz, OC'H₂Ph), 69.0 (OCH₂Ph), 68.7 (C6, C6'), 68.2 (d, $J_{C-P} = 10.3$ Hz, OCH₂), 68.2 (d, $J_{C-P} = 6.0$ Hz, OC'H₂), 32.0 , 30.1 , 29.8 , 29.7 , 29.7 , 29.7 , 29.6 , 29.5 , 29.4 , 29.1 , 25.4 , 25.3 , 22.7 , 14.2 . ³¹P NMR (122 MHz, Chloroform-*d*) δ -1.55, -1.80. ESI-HRMS(M+Na)⁺: 957.5041; found: 957.5038.



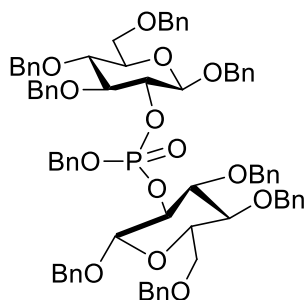
Benzyl cholesteryl ((2*R*,3*R*,4*S*,5*R*,6*R*)-2,4,5-tris(benzyloxy)-6-((benzyloxy)methyl) tetrahydro-2H-pyran-3-yl) phosphate **5j**: From cholesterol following general procedure, flash chromatography of the crude product (1:4 EtOAc-pentane) afforded **5j** (yield 70%) as a white solid. $R_f = 0.56$. ¹H NMR (500 MHz, Chloroform-*d*) δ 7.35 – 7.00 (m, 25H, Ph), 5.12 (m, 1H, C=CH-Cholesterol), 4.98 – 4.79 (m, 4H, 2×CH₂Ph), 4.78 – 4.66 (m, 2H, CH₂Ph), 4.62 – 4.52 (m, 2H, CH₂Ph), 4.47 (d, $J = 6$ Hz, 1H, H1), 4.46 – 4.42 (m, 2H, CH₂Ph), 4.34 (m, 1H, H2), 4.05 (m, 1H, OCH-Chol), 3.69 – 3.57 (m, 4H, H3, H4, H6a, H6b), 3.41 (m, 1H, H5), 2.34 – 2.11 (m, 2H, CH₂-Chol), 1.98 – 1.65 (m, 5H, Chol), 1.63 – 1.12 (m, 12H, Chol), 1.11 – 0.63 (m, 21H, Chol), 0.60 – 0.53 (m, 3H, Chol). ¹³C NMR (126 MHz, Chloroform-*d*) δ 139.5 (C=CH, Chol), 138.4 , 138.1 , 137.9 , 137.1 , 136.4 , 128.6 , 128.4 , 128.3 , 128.2 , 128.1 , 128.0 ,

127.9 , 127.8 , 127.7 , 127.6 , 127.4 , 122.7 (C=CH, Chol), 100.2 (d, J_{C-P} = 3.5 Hz, C1, C1'), 83.7 (d, J_{C-P} = 3.7 Hz, C3), 78.9 (t, J_{C-P} = 6.7 Hz, C2, C2'), 78.6 (d, J_{C-P} = 6.0 Hz, OCH-Chol), 78.5 (d, J_{C-P} = 5.8 Hz, OC'H-Chol), 77.8 (C4, C4'), 75.1 (C5, C5'), 75.0 (OCH₂Ph), 74.9 (OCH₂Ph), 73.5 (OCH₂Ph), 70.8 (OCH₂Ph), 69.0 (d, J_{C-P} = 5.5 Hz, OCH₂Ph), 68.7 (C6, C6'), 56.7 , 56.2 , 49.8 , 42.3 , 39.8 , 39.6 , 36.7 , 36.6 , 36.3 , 36.2 , 35.8 , 31.9 , 31.8 , 29.4 , 29.3 , 28.3 , 28.1 , 24.3 , 23.9 , 22.9 , 22.6 , 21.0 , 19.3 , 19.2 , 18.8 , 11.9 . ³¹P NMR (122 MHz, Chloroform-*d*) δ -2.60, -2.98. ESI-HRMS(M+H)⁺: 1079.6160; found: 1079.6170.

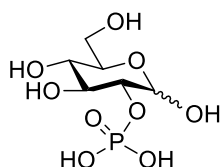


Benzyl cholestanyl ((2*R*,3*R*,4*S*,5*R*,6*R*)-2,4,5-tris(benzyloxy)-6-((benzyloxy)methyl)tetrahydro-2H-pyran-3-yl) phosphate **5k**: From cholesterol following general procedure, flash chromatography of the crude product (1:3 EtOAc-pentane) afforded **5k** (yield 74%) as a white solid. R_f =0.37. ¹H NMR (500 MHz, Chloroform-*d*) δ 7.46 – 7.09 (m, 25H, Ph), 4.97 (m, 3H, CHHPh, CH₂Ph), 4.92 – 4.74 (m, 3H, CHHPh, CH₂Ph), 4.70 – 4.61 (m, 2H, CH₂Ph), 4.57 – 4.56 (m, 2H, CH₂Ph), 4.54 (d, J = 8.3 Hz, 1H, H1), 4.45 – 4.40 (m, 1H, H2), 4.23 – 4.09 (m, 1H, OCH-Chol), 3.81 – 3.66 (m, 4H, H3, H4, H6a, H6b), 3.51 (m, 1H, H5), 1.95 (m, 1H, Chol), 1.86 – 1.73 (m, 2H, Chol), 1.63 – 1.50 (m, 4H, Chol), 1.44 (d, J = 7.4 Hz, 1H, Chol), 1.41 – 0.94 (m, 20H, Chol), 0.93 – 0.84 (m, 9H, Chol), 0.82 – 0.70 (m, 2H, Chol), 0.69 – 0.60 (m, 6H, Chol), 0.55 – 0.39 (m, 1H, Chol). ¹³C NMR (126 MHz, Chloroform-*d*) δ 138.4 , 138.1 , 137.9 , 137.2 , 136.5 , 128.4 , 128.3 , 128.3 , 128.3 , 128.3 , 128.3 , 128.0 , 128.0 , 128.0 , 127.9 , 127.8 , 127.8 , 127.8 , 127.8 , 127.7 , 127.7 , 127.7 , 127.5 , 127.4 , 100.2 (d, J_{C-P} = 1.9 Hz, C1, C1'), 83.7 (d, J_{C-P} = 3.7 Hz, C3, C3'), 78.9 (d, J_{C-P} = 7.2 Hz, C2), 78.8 (d, J_{C-P} = 7.0 Hz, C2'), 78.6 (d, J_{C-P} = 6.0 Hz, OCH-Chol), 77.8

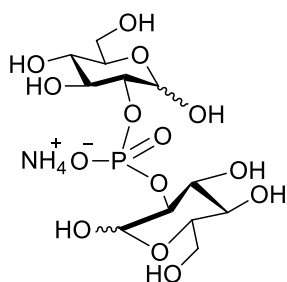
(C4, C4'), 75.1 (C5, C5'), 75.0 (OCH₂Ph), 74.7 (OCH₂Ph), 73.5 (OCH₂Ph), 70.8 (OCH₂Ph), 69.0 (d, J_{C-P} = 5.4 Hz, OCH₂Ph), 68.7 (C6), 56.5, 56.3, 54.0, 44.3, 42.6, 40.0, 39.6, 36.6, 36.2, 35.8, 35.6, 35.1, 32.0, 29.3, 29.1, 28.5, 28.3, 28.1, 24.2, 23.9, 22.9, 22.6, 21.2, 18.7, 12.2, 12.1. ³¹P NMR (122 MHz, Chloroform-*d*) δ -2.47, -2.85. ESI-HRMS(M+H)⁺: 1081.6317; found: 1081.6309.



Benzyl bis((2*R*,3*R*,4*S*,5*R*,6*R*)-2,4,5-tris(benzyloxy)-6-((benzyloxy)methyl)tetrahydro-2*H*-pyran-3-yl) phosphate **5i**: From compounds **5f** following general procedure, flash chromatography of the crude product (1:3 EtOAc-pentane) afforded **5i** (yield 53%) as a white solid. R_f =0.36. ¹H NMR (500 MHz, Chloroform-*d*) δ 7.49 – 7.41 (m, 4H, Ph), 7.37 – 7.27 (m, 26H, Ph), 7.25 – 7.12 (m, 13H, Ph), 7.07 (m, 2H, Ph), 5.01 – 4.84 (m, 6H, 3×CH₂Ph), 4.73 (d, J = 10.8 Hz, 2H, CH₂Ph), 4.71 – 4.66 (m, 2H, CH₂Ph), 4.66 – 4.45 (m, 8H, 4×CH₂Ph), 4.44 – 4.39 (m, 1H, H2), 4.35 (m, 1H, H2'), 4.30 (d, J = 6.9 Hz, 1H, H1), 4.29 (d, J = 6.9 Hz, 1H, H1'), 3.68 (m, 2H, H6), 3.61 (m, 2H, H6'), 3.53 – 3.36 (m, 4H, H4, H4', H3, H3'), 3.35 – 3.26 (m, 2H, H5, H5'). ¹³C NMR (126 MHz, Chloroform-*d*) δ 138.5, 138.2, 138.0, 137.3, 137.3, 128.4, 128.4, 128.3, 128.3, 128.3, 128.2, 128.2, 127.9, 127.9, 127.8, 127.8, 127.8, 127.7, 127.7, 127.7, 127.6, 127.5, 127.5, 127.4, 127.4, 100.2 (d, J_{C-P} = 2.9 Hz, C1'), 99.8 (d, J_{C-P} = 4.2 Hz, C1), 83.6 (d, J_{C-P} = 4.8 Hz, C3'), 83.5 (d, J_{C-P} = 3.6 Hz, C3), 79.1 (d, J_{C-P} = 7.4 Hz, C2'), 78.6 (d, J_{C-P} = 6.8 Hz, C2), 77.7 (C4'), 77.6 (C4), 75.0 (C5), 74.8 (C5'), 74.8 (OCH₂Ph), 74.8 (OCH₂Ph), 74.7 (OCH₂Ph), 74.7 (OCH₂Ph), 73.4 (OCH₂Ph), 73.4 (OCH₂Ph), 70.9 (OCH₂Ph), 70.2 (OCH₂Ph), 69.3 (d, J_{C-P} = 5.0 Hz, OCH₂Ph), 68.7 (C6, C6'). ³¹P NMR (122 MHz, Chloroform-*d*) δ -3.64. ESI-HRMS(M+Na)⁺: 1255.4943; found: 1255.4949.



D-glucose-2-phosphate (**G2P**): To a solution of phosphate **5h** (100 mg, 0.12 mmol) in 5 mL of EtOAc was added 10% Pd/C (60 mg). The mixture was stirred under 1 atm H₂ at rt. After 24 h, Pd/C was filtered with a celite layer. The filtrate was collected and concentrated to gave G2P as a white solid in 90% yield ($\alpha/\beta=5:3$). ¹H NMR (300 MHz, Deuterium Oxide) δ 5.33 (d, $J = 3.3$ Hz, 1H, H1 α), 4.69 (d, $J = 7.6$ Hz, 0.6H, H1 β), 3.98 – 3.88 (m, 1H, H2 α), 3.86 – 3.59 (m, 5.8H, H2 β , H3 α , H5 α , H6 α , H6 β), 3.58 (t, $J = 7.7$ Hz, 0.6H, H3 β), 3.47 – 3.36 (m, 2.2H, H4 α , H4 β , H5 β). NMR data were consistent with the reported [9].



Agrocinosine D: To a solution of phosphate **5l** (100 mg, 0.08 mmol) in 5 ml of methanol was added 10% Pd/C (60 mg). The mixture was stirred under 1 atm H₂ at rt for 1 day. TLC monitoring using DCM, acetone, MeOH, H₂O 4:3:3:1 (vol.) shows the formation of the desired product ($R_f = 0.48$). After filtration with a celite layer, the organic phase was concentrated to afford a white solid, which was further purified by ion-exchange chromatography on a DEAE-Sephadex column pre-washed with water. The column was then eluted with a 5% to 100% gradient 1M ammonium carbonate. Freeze-drying the resulting fractions allows getting agrocinosine D as a white solid in 78% yield. The ratio of α/β is 2/1. ¹H NMR (500 MHz, Deuterium Oxide) δ 5.39 (d, $J = 3.6$ Hz, 1H, H1 α), 4.75 (d, $J = 7.9$ Hz, 0.5H, H1 β), 4.09 – 3.96 (m, 1H, H2 α), 3.93 – 3.60 (m, 6H, H2 β , H3 α , H3 β , H5 α , H6 α , H6 β), 3.51 – 3.43 (m, 2H, H4 α , H4 β , H5 β). ESI-HRMS(M-H)⁻: 421.0753; found: 421.0735. NMR data were consistent with the reported [12].



FOLIO ADMINISTRATIF

THESE DE L'UNIVERSITE DE LYON OPEREE AU SEIN DE L'INSA LYON

NOM : ZHANG

DATE de SOUTENANCE : 23/02/2021

(avec précision du nom de jeune fille, le cas échéant)

Prénoms : Qiang

TITRE : Chimie du quorum sensing bactérien: des analogues d'acyl homosérine lactones chez *Vibrio fischeri* aux carbohydrates phosphodiester chez *Agrobacterium*.

NATURE : Doctorat

Numéro d'ordre : 2021LYSEI015

Ecole doctorale : ED206

Spécialité : Chimie

RESUME :

Le processus utilisé par les bactéries pour coordonner leur comportement en fonction de leur densité de population en communiquant par de petits signaux chimiques (synthèse et détection) est connu sous le nom de Quorum Sensing (QS). Ce processus existe chez de nombreuses bactéries, y compris les pathogènes. Le QS régule diverses expressions de gènes impliqués dans la croissance, la virulence et la production de toxines. Par conséquent, l'inhibition du QS est considérée comme une stratégie prometteuse pour prévenir l'infection bactérienne. Compte tenu de la nécessité de diversifier les stratégies antibactériennes pour faire face à la problématique de la résistance aux antibiotiques des bactéries, cibler le QS peut être une approche complémentaire aux voies biologiques existantes. En se concentrant sur la chimie du quorum sensing bactérien, les travaux de cette thèse visent à étudier deux aspects différents. Dans une première partie, nous avons conçu, synthétisé et testé une série de nouveaux analogues d'AHL, dont des hydrazides, des carbamates ou des thiocarbamates, des analogues 2-OH AHL et des analogues AHL hétérocycliques dérivés de l'imidazole et du triazole. Dans une deuxième partie, afin d'étudier les carbohydrates phosphodiester impliqués dans la pathogénicité de la bactérie *Agrobacterium tumefaciens*, nous avons développé une méthode efficace pour synthétiser une agrocinopine naturelle ainsi que certains analogues. Nous avons donc développé une voie synthétique flexible pour accéder aux structures rares de glucose-2-phosphate, y compris l'agrocinopine D qui a fait l'objet d'une étude biologique approfondie. Les agrocinopines sont capables d'activer la voie du QS chez *Agrobacterium* qui à son tour active le facteur de virulence.

MOTS-CLÉS : quorum sensing, AHL analogues, agrocinopines, G2P, *Agrobacterium*

Laboratoire (s) de recherche : ICBMS

Directeur de thèse: Yves Queneau

Président de jury : Mme Florence Popowycz, Professeure, INSA de Lyon

Composition du jury :

Mme Florence Djedaini-Pilard, Professeure, Université de Picardie	Rapporteuse
M. Yves Blache, Professeur, Université de Toulon	Rapporteur
Mme Florence Popowycz, Professeure, INSA de Lyon	Examinatrice
M. Sébastien Fort, DR CNRS, Université de Grenoble Alpes	Examineur
M. Yves Queneau, DR CNRS, Université de Lyon	Directeur de thèse
M. Laurent Soulère, Maître de conférence HDR, INSA de Lyon	Co-directeur de thèse
M. Mohammed Ahmar, CR CNRS, Université de Lyon	Membre invité